The dynamic behaviour of check valves in pipeline systems

by

A.C.H. Kruisbrink

A Thesis submitted to City University London

for the Degree of Doctor of Philosophy

in Mechanical Engineering

Amsterdam - Delft

The Netherlands

December

1996

TABLE OF CONTENTS

Acknowledgements

The author thanks:

Prof. A.R.D. Thorley for his valuable, sympathetic guidance and encouraging support during the course of the project. For his visits to Delft and contributions during the CVRP meetings. For the contributions within the Large Installations Program. For the hospitality during my stays in London.

Dr. H.L. Fontijn for his accurate reading and critical comments on the CVRP reports. For his valuable suggestions and discussions as supervisor.

Prof. Betamio de Almeida for his ideas and comments during the CVRP meetings and contributions within the Large Installations Program.

Miss L. Thorley for her pioneers work done on the generation of the first dynamic valve characteristics for damped check valves.

Mr. A. Pereira da Silva for his work done on the processing of the experimental data into valve characteristics.

Mr. L.P.D.M. Van Hulst for the numerical work done with respect to the design of the test facility.

Mr. A.M. Boele, T. Ammerlaan and L.F. Lindeboom for their work done on the set up and performance of the experiments.

Dr. A.G.T.J. Heinsbroek for his ideas and the many discussions on the software development.

Mr. C. Kooij for his contribution to the CVWP manual and the distribution of the software to the CVRP participants.

Dr. H.F.P. van den Boogaard for his work done on the interpolation procedures and neural networks.

Mr. J. Teijema for the organisation, guidance and support during the CVRP project.

Dr. A.S. Tijsseling for his friendship and discussions about the theory.

Mr. J. Wijdieks for his interest in my work, his ideas and discussions about the theory.

Mr. C.S.W. Lavooij for his friendship, ideas and critical comments during the CVRP meetings.

Mr. E. Kruisbrink for his ideas with respect to the data representation.

Mr. P. van der Salm for the graphical work.

Mrs. J.M. Haze-van Steenbeek for her typo-graphical work.

The author is grateful to:

Delft Hydraulics for enabling me to graduate, for the financial support within the CVRP project and for the mental support during and after the CVRP project.
The CVRP participants for their sponsoring, which made the project possible, and their steering and guidance during the half-yearly meetings at Delft.

CVRP is sponsored by: (France) Electricité de France, Socla; (Japan) Toyo Engineering Corporation; (The Netherlands) Delft Hydraulics, KEMA, Mokveld Valves, RMI Holland, Waterworks of Friesland, Gelderland, Oost-Brabant, Overijssel and Zuid-Holland; (United Kingdom) Goodwin International.

The experiments were performed within the Large Installations Plan of European researchers, financially supported by the EC, and represented by (United Kingdom) Prof. A.R.D. Thorley, City University, London and (Portugal) Prof. A.B. Betamio de Almeida, Technical University of Lisbon.

Scientific support is given by (The Netherlands) Dr. H.L. Fontijn, Delft University of Technology.

Abstract

A semi-empirical method is developed to describe the dynamic behaviour of check valves in pipeline systems. The method is based on parameterized valve models and dimensionless valve characteristics, which may be obtained from experiments. The check valve is considered as a black box with certain input and output characteristics. The check valve closure and associated pressure surges are the dominant phenomena. Undamped check valves may be considered as a special case of damped check valves.

Much attention is paid to the description of the hydrodynamic (fluid) forces on the internal, moving valve elements. These elements may be considered as translating or rotating bodies with (at least) one plane of symmetry. The equations of motion for the constrained, unsteady motion of such a body in an unconfined, unsteady fluid flow are based on the dynamical theory of Kirchhoff, extended to an unsteady fluid flow. The equivalent equations for a body in a confined fluid are based on Lagrange's method of generalized coordinates.

A general (dimensionless) valve equation of motion is developed, which is valid for most of the existing check valve types.

Basic differential equations are derived for the transient flow in a pipe with constant initial flow deceleration. The equations are applied to describe the check valve closure under reflection free and reflecting boundary conditions in the form of dimensionless, analytical equations. The theory is based on conventional waterhammer theory.

The pipe and valve equations are coupled via the integral form of the momentum equation.

The uncoupled and coupled, (dimensionless) pipe and valve equations show formally which (dimensionless) variables and valve, system and fluid parameters are relevant to the dynamic behaviour of check valves in pipeline systems. In that sense they are used in a dimensional analysis to develop (dimensionless) valve characteristics and dynamic scale laws.

Based on the dimensionless valve characteristics, models for undamped and damped check valves are developed and implemented in the waterhammer computer code CVWP (Check Valve Waterhammer Program).

Experiments are performed in the test facility at Delft Hydraulics to measure several valve characteristics of weakly and strongly damped check valves.

The dynamic scale laws are validated by means of numerical simulations. The valve models are validated against experimental data.

The study has been performed within the Check Valve Research Project (CVRP).

Nomenclature

A	area	[m^2]
Ac	acceleration number	[-]
B	body force	[N/m^3]
c	pressure wave speed	[m/s]
C	coefficient	[-]
c_1	constant which accounts for the effects of support conditions of the pipe on the pressure wave speed	[-]
d	distance, characteristic diameter of damping device	[m]
D	characteristic diameter	[m]
$(dv/dt)_-$	(mean) initial flow deceleration at check valve	[m/s^2]
$(dv/dt)_+$	(mean) reverse flow deceleration at check valve	[m/s^2]
e	eccentricity, pipe wall thickness	[m]
E	modulus of elasticity	[N/m^2]
Eu	Euler number	[-]
f	Darcy-Weisbach friction coefficient	[-]
f	frequency	[Hz]
F	force	[N]
g	gravitational acceleration	[m/s^2]
H	pressure head	[m]
I	mass moment of inertia	[kgm^2]
k	radius of gyration	[m]
K	geometrical parameter	[-]
K	bulk modulus of elasticity	[N/m^2]
L	pipe length	[m]
L	Lagrangian	[J]
m	mass	[kg]
Ma	Mach number	[-]
n	unit-normal	[-]
p	pressure	[N/m^2]
q	generalized coordinate	[m or rad]
Q	flow rate, volumetric discharge	[m^3/s]
R	radius	[m]
Re	Reynolds number	[-]
S	surface of control volume	[m^2]
S	Strouhal number	[-]
t	time	[s]
T	kinetic energy	[J]
T	torque	[Nm]
T	time shift	[s]

v	linear velocity, fluid velocity	[m/s]
v_o	critical velocity of check valve	[m/s]
V	volume	[m^3]
V	potential function	[J]
x	linear position; distance along pipe	[m]
Y	hysteresis factor	[-]
z	elevation of pipe centreline above datum	[m]

α	angular position, angle of incidence	[rad]
β	parameter characterizing the velocity-time function	[-]
γ	inclination angle of pipe and valve	[rad]
ΔH	pressure head difference or variation	[m]
Δp	pressure difference or variation	[N/m^2]
η	slope in dimensionless valve characteristic	[-]
θ	angular position	[rad]
λ	wave-length	[m]
M	pseudo-torque	[Nm]
μ	dynamic fluid viscosity	[Ns/m^2]
μ	bearing friction coefficient	[-]
ν	Poisson's ratio	[-]
ξ	loss coefficient	[-]
ρ	mass density	[kg/m^3]
σ	normal stress	[N/m^2]
τ	dimensionless time	[-]
τ	shear stress	[N/m^2]
τ_o	shear stress between fluid and pipe wall	[N/m^2]
υ	dimensionless fluid velocity	[-]
ϕ	velocity potential	[m_2/s]
ϕ	closure phase	[-]
χ	pseudo-force (component)	[N]
ψ	pseudo-force (component)	[N]
ω	angular velocity, circular frequency	[rad/s]
ω	relaxation factor	[-]

Subscripts

A	added mass, area
abs	absolute
b	body, begin, bearing
B	Basset
B	buoyancy

bnd	boundary
bp	bypass
c	valve is just closed
cg	centre of gravity
cb	centre of buoyancy
d,D	damping (becomes active or effective), damping fluid
d/D	downstream/downstream pressure tap location
D	drag
e	eccentricity
eff	effective
f	fluid
f,F	friction
G	gravitational
h	hose
H	hydrodynamic
i	initial
I	inertia
m	moving valve element(s)
o	valve is just fully open
p	pipe, packing
P	pressure
pn	piston
refl	reflection
R	maximum reverse flow
S	spring(s)
th	throttle valve
u/U	upstream/upstream pressure tap location
V	volume
τ	shear

1 Introduction

1.1 General

Check valves - recoil, reflux or non-return valves - are older than human life and could already be found in the hearts of mammals to enable the pumping of blood through the body (figure 1.1). In the Ancient Roman time check valves were used at the suction and discharge side of piston pumps (figure 1.2). Even today they are found in pumps and compressors of the reciprocating type. With the development of hydrodynamic engines of the rotating type (centrifugal pumps, turbines) in the last century the necessity for built-in check valves faded. Nowadays they are commonly used components in pump stations and pipeline systems.

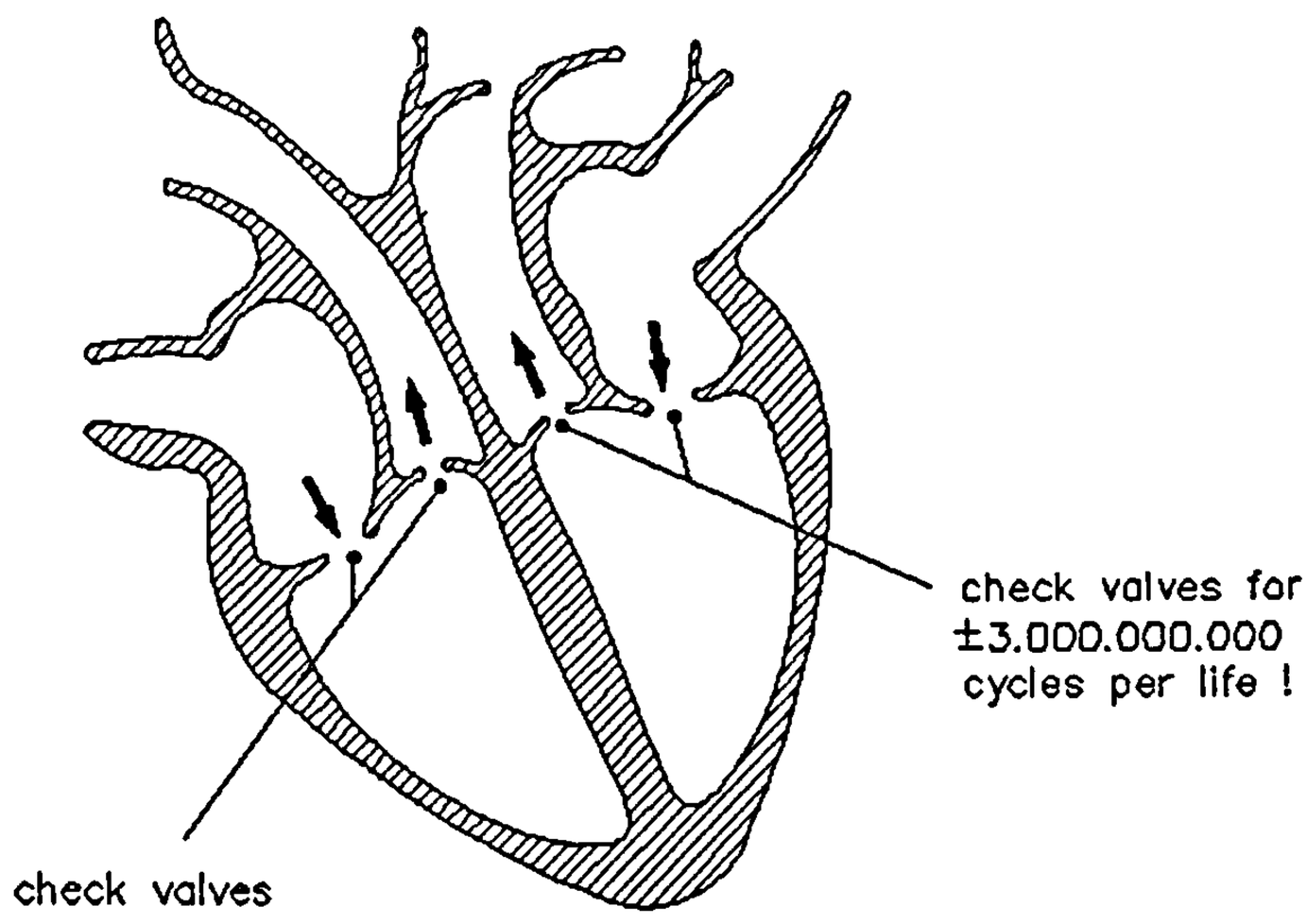

Figure 1.1 Check valves in the human heart

The function of check valves in fluid circuits is to allow flow in one direction and to prevent flow in the reverse direction. They are used in pipelines in order to prevent the lines draining backwards when pumps stop running, to prevent downstream reservoirs from emptying, to prevent reverse flow through non-operating parallel pumps and booster pumps, to prevent emptying of the line in case of pipe rupture and to prevent reverse rotation of pumps, thereby avoiding damage to seals and to the brush gear of the driving motors.

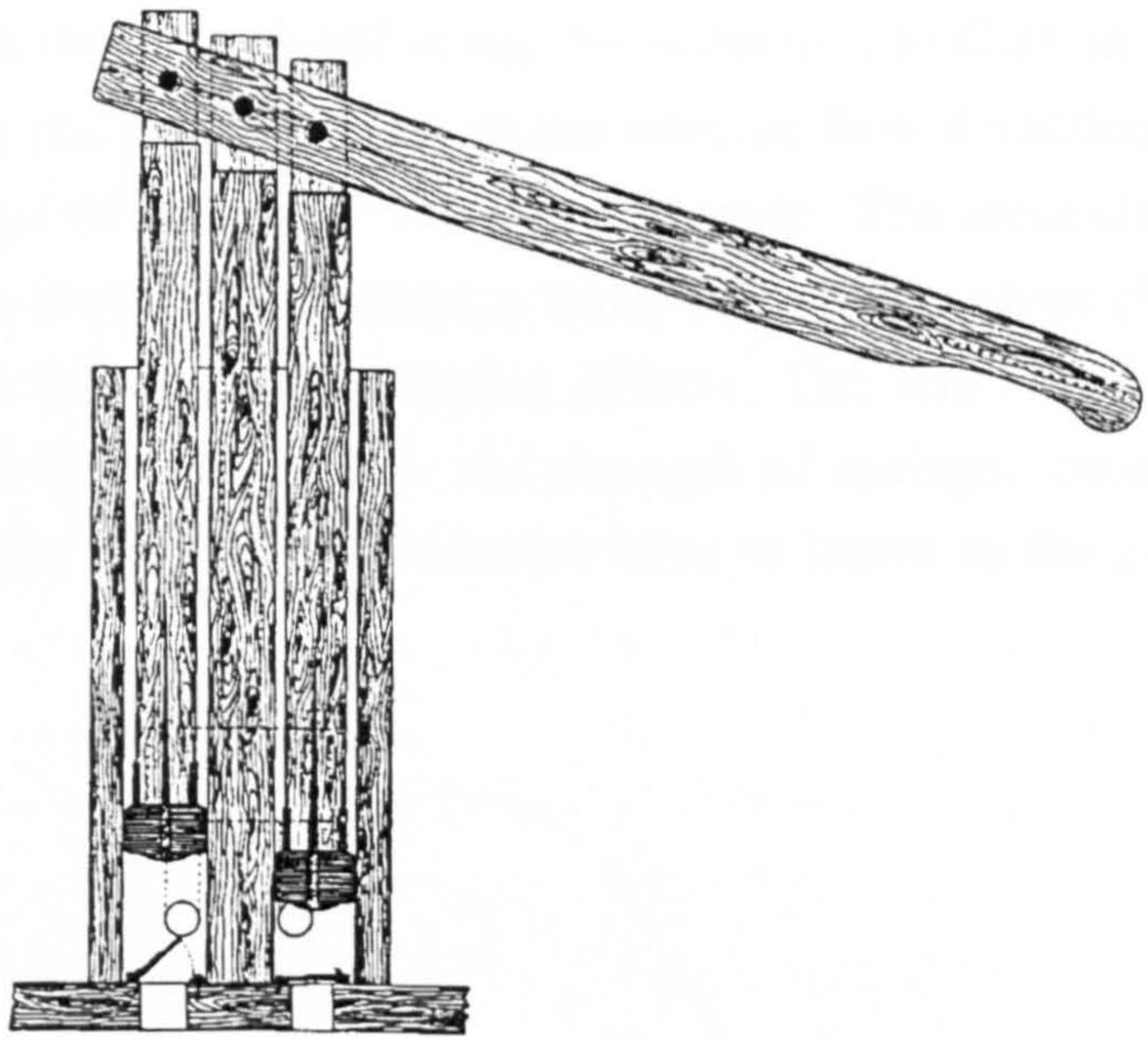

Figure 1.2 Ancient Roman piston pump (Rop, 1987)

Check valves are simple devices consisting of a casing around one or more translating or rotating elements. The position of the element(s) is primarily controlled by the fluid passing through (figure 1.3). The position may secondarily be influenced by springs, a counterweight and/or a damping device, which slows down the motion of the element(s), in general only during the last part of closure. As distinct from *undamped check valves*, check valves with a damping device are denoted as *damped check valves*.

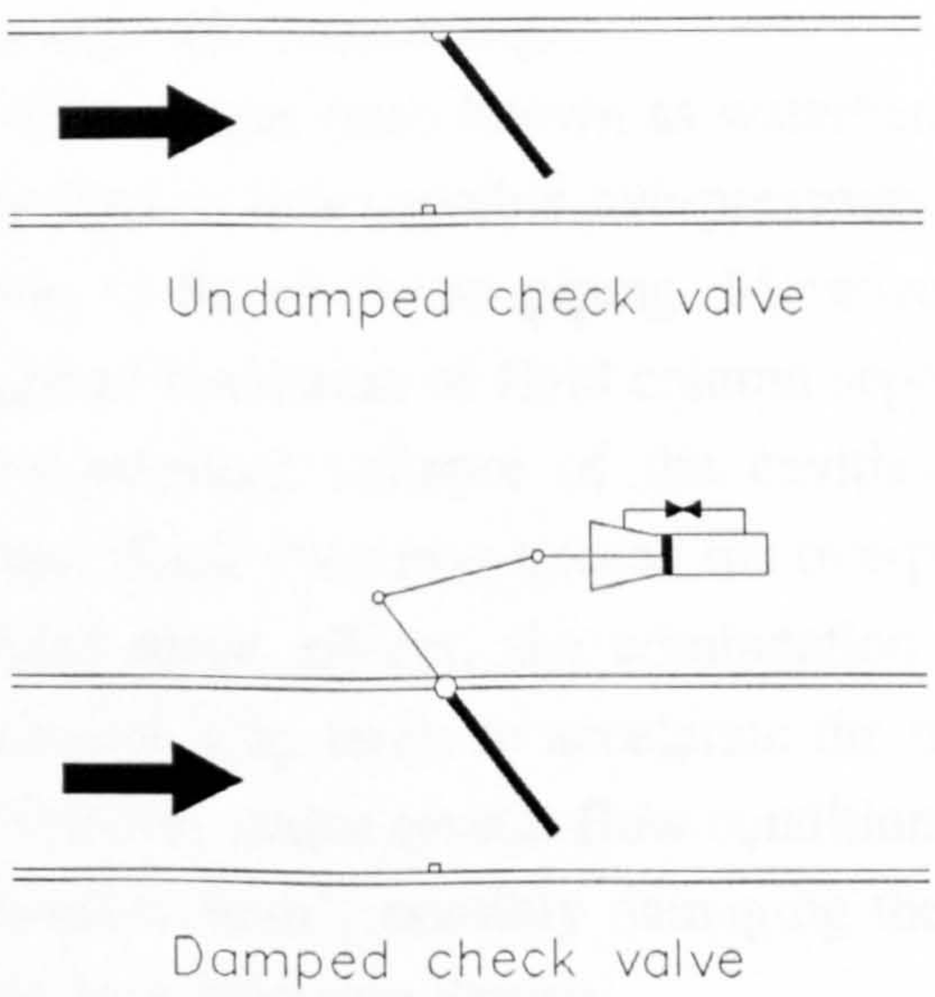

Figure 1.3 Undamped and damped check valves

The ideal check valve has no resistance to flow in the normal flow direction and infinite resistance to flow in the reverse flow direction. In this respect the electrical analogue of the check valve is the diode. The ideal check valve closes at the instant of flow reversal. In practice however, check valves close after flow reversal due to inertia, friction and damping effects. The amount of reverse flow depends on the (initial) flow conditions, the strength of springs, counterweights, and the stroke or angle that the valve element(s) have to move to the closed position.

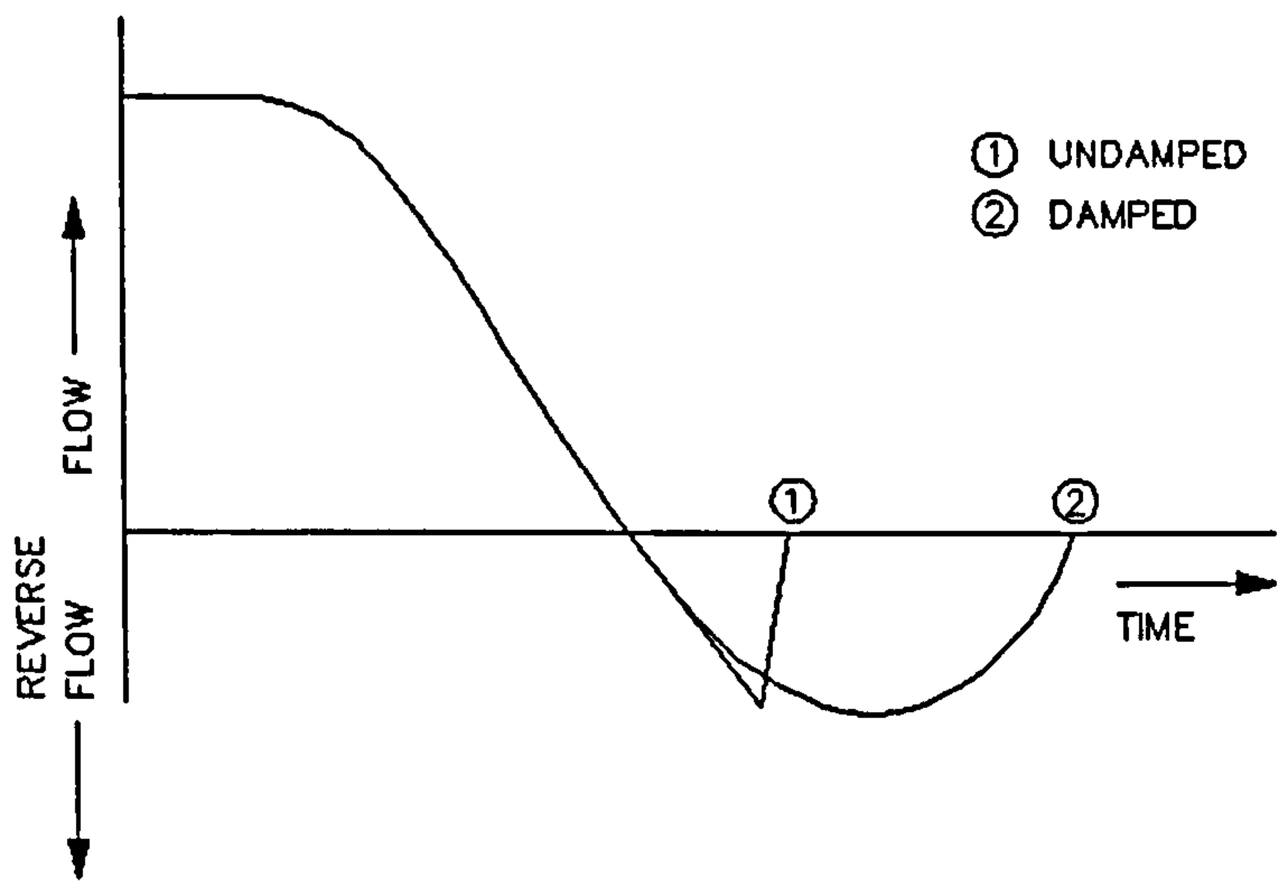

Figure 1.4 Flow behaviour of check valves

The reduction of the reverse flow to zero (valve closed) may take place instantaneously (undamped check valves) or gradually (damped check valves; figure 1.4), and is accompanied with pressure surges in the pipeline system, a possible occurrence of cavitation and valve slamming.

The pressure surges (also known as waterhammer), induced by the check valve closure, may lead to unacceptable overpressures in the downstream piping, and/or underpressures in the upstream piping. Moreover, the underpressures may lead to the occurrence of cavitation or fluid column separation when the vapour pressure is reached. The eventual collapse of the cavities in the upstream piping leads to overpressures, which even may exceed the overpressures in the downstream piping.

Apart from surge effects, the combination of downstream pressure rise and upstream pressure drop tends to accelerate the motion of the valve element(s) onto the seat. Therefore, under certain flow conditions, the closure may be accompanied with "check valve slam", possibly damaging the valve seat element(s). This effect is suppressed by a damping device.

The pressure difference across the valve, particularly at the instant of closure, introduces hydrodynamic forces on the valve which are transmitted to the supports of the pipeline system. With respect to the anchoring of these supports it is important to know the magnitude of these forces.

The above-mentioned phenomena illustrate that a wrong selection of check valves may permit damage to the valve and the associated pipeline system with the risk of damage to people, plant and environment.

With the evolution of high capacity and multi-pump systems, there is a need for larger pumps and pump heads. At the same time there is a tendency to design low-inertia pumps. Surge protection devices such as air vessels become more common. These developments lead to an increasing number of problems with check valves.

Billington et al. (1985) describe a comprehensive statistical analysis of valve problems within BP. The analysis comprises nearly a quarter of a million valves and shows that 6% of the valves are check valves. Among the check valves 6.3 % give rise to problems varying from erosion, material failure and jamming to leakage.

1.2 State-of-the-Art

From the sixties on the closure behaviour of undamped check valves is studied in detail by means of valve response models, on-site and laboratory tests.

The models are based on a one-dimensional valve equation of motion. The equations are solved numerically. In the stand-alone models the fluid velocity-time history is used as boundary condition. As a next step the valve models are coupled to waterhammer computer codes, which enables to simulate the interaction between valve and pipeline system. In fluid-structure analyses the valve model is coupled to waterhammer and/or structural dynamics computer codes, which enables detailed studies into e.g. the thermal and stress behaviour of check valves under extreme conditions.

In general these research activities are restricted to case studies, to investigate in how far a specific check valve operates in a specific application.

Researchers like Provoost, Collier and Thorley recognize that there is a need to identify scale laws to help generalizing the application of experimental data, that have been generated (private communication with prof. A.R.D. Thorley).

The behaviour of check valves under steady flow conditions is described by steady-state characteristics. The characteristics provide information on the opening pressure, flow capacity and energy losses.

The closure behaviour of *undamped* check valves is described by so-called "dynamic" characteristics. These characteristics provide information on the maximum reverse flow velocity and pressure surges due to valve closure.

Delft Hydraulics developed an internationally adopted method to describe the dynamic behaviour of undamped check valves in specific applications (Provoost, 1982; Koetzier, Kruisbrink and Lavooij, 1986; Kruisbrink, 1988). The method can be used for the selection of valves and is based on system-independent (dimensionless) dynamic characteristics.

The hydrodynamic behaviour of undamped check valves is well described in the steady-state and dynamic characteristics. The characteristics are *system independent* and can be used in the selection of undamped check valves for any pipeline system.

With respect to the dynamic behaviour of *damped* check valves there is a lack of knowledge. Contrary to undamped check valves the motion of damped check valves may be influenced by reflections of pressure waves, particularly during the stage of active damping. For this reason the behaviour of damped check valves is much more complicated and *system dependent*.

Thus far no general approach, dynamic valve characteristics or valve models are available. The selection of damped check valves and the adjustment of damping devices often takes place by *trial and error* under operating conditions.

1.3 Objectives and preview of study

The objective of the present study is to develop a semi-empirical method to describe the hydrodynamic behaviour of check valves in pipeline systems. For this purpose (dimensionless) valve characteristics should be introduced, which are defined in such a way that they can be applied to all types of check valves. The valve characteristics are intended as tool in the valve selection and pipeline design, to judge the hydrodynamic behaviour of check valves in specific applications. This can be done by means of quick estimates or more detailed computer surge analyses. For the latter purpose numerical valve models should be developed.

The scope of the present study is limited to self-actuating check valves (i.e. valves operating without power supply), with or without damping device.

A survey of literature reveals that within the research into the dynamic behaviour of check valves mainly a *direct* approach is followed with a deterministic character (chapter 2). The valves are described by numerical models, which are based on conservation laws (mass, momentum) in the form of one or more, ordinary or partial differential equations. Within the enormous variety of check valve types, many so-called "valve response models" have been developed. These models are used in uncoupled or coupled mode with waterhammer computer codes. Although these models form a sound basis, their accuracy is limited due to uncertainties in the model

formulation and coefficients used. Therefore, often additional series of experiments are needed to quantify e.g. the flow and damping coefficients used in the model, and to tune and validate the model. As such both the development and the implementation of these models takes a lot of effort and is time consuming.

For the above reasons, within the present study a more global, "*parameterized*" approach is chosen, which has a more non-deterministic character. The method is based on valve characteristics, which describe the overall behaviour of the valve. The characteristics are determined from experiments, whereby the check valve is considered as a *black box* with certain input and output characteristics.

Although a more global approach is chosen, much attention is paid to:

- the development of a general valve response model (valve equations),
- the description of the pressure surge effects of a valve closure (pipe equations),
- the interaction between check valve and pipeline system (coupling of equations).

The main purpose of this qualitative study is to identify which parameters are relevant to the check valve dynamics in pipeline systems. In that sense they form the basis for the development of "parameterized" models.

Within the development of a general valve model, the concept of conservation of (kinetic) energy is chosen, rather than of momentum conservation laws, for the following reasons:

- Momentum equations (like the Euler and Navier-Stokes equations) are succesfully applied to describe the fluid forces on translating bodies (in rather slow motion). However, no results are obtained for rotating bodies yet.
- The (kinetic) energy concept allows a general treatment of the fluid forces and torques on a body, whereby details about the geometry, other than in the form of coefficients, are not required. It can thus be applied to most of the existing check valve types.
- The qualitative approach of the (kinetic) energy concept is consistent with the more global, "parameterized" approach to be followed here.

An overview of check valve types (chapter 3) shows that the moving elements of check valves are generally characterized by translating or rotating bodies, with at least one plane of symmetry. This important geometrical condition is used to describe the hydrodynamic forces on the moving valve elements.

From a hydrodynamic point of view the check valve closure is a typical confined flow problem around a moving body. The problem is rather complicated due to the facts that: 1) the geometry of the valve body, including the moving elements, is rather complex, 2) the body moves in a confined space, which implies that the overall geometry changes in time, 3) the body may rotate, 4) the motion of the body is flow

controlled, and 5) the motion of the body as well as the fluid is unsteady. The check valve closure is accompanied with and influenced by pressure surges, which may interact with the pipeline system.

In this respect much more is known about: 1) simple geometries (e.g. cylinders, spheres), 2) bodies moving in an unconfined or semi-infinite space (e.g. aircraft, submarines, ships and small particles), 3) translating bodies, 4) controlled motion (e.g. control valves), and 5) steady motion.

Due to the complexity of the confined, viscous fluid flow problem sketched above, a stepwise approach is chosen, starting with the relatively simple case of the unconfined, inviscid fluid as a basis for further developments.

The motion of a body in an *unconfined, inviscid fluid* is described by the dynamical theory of Kirchhoff (chapter 4). This potential flow theory enables us to derive general equations of motion for a body, moving in a stagnant fluid due to external forces and torques.

The general equations are very complex, when applied to an arbitrary body in arbitrary motion. However, the equations become more tractable by imposing constraints to the geometry and motion of the body. By analogy with the internal, moving elements of check valves, the body is assumed to have a plane of symmetry. The motion of the body is constrained to a motion in this plane of symmetry.

Kirchhoff's equations are derived for the motion of a body in a stagnant fluid. Within the present study the theory is extended to the motion of a body in an unsteady fluid flow. For this purpose a non-inertial reference frame is introduced, which moves with the unsteady fluid flow. Moreover, by the special positioning of the body frame (i.e. the coordinate system which is fixed to the body) an eccentricity arises, which reveals an analogy with fluid viscosity.

In the Lagrangian approach of Kirchhoff's theory the coefficients in the kinetic energy equations are constants, determined by the geometry of the rigid body. Note that for confined flows this no longer holds, since the geometry of the confined space, as seen from the moving body, changes. This enables the development of analytical expressions for the fluid force terms and coefficients. It thus offers opportunities to study and to describe the properties of these quantities.

The motion of a body in an *unconfined, viscous fluid* is described in chapter 5. Fluid viscosity generally causes a move of the hydrodynamic centre, due to boundary layers and flow separation, which is analogous to the effect of an eccentricity. This analogy is used to make the step from unconfined, inviscid to unconfined, viscous fluids. As distinct from unconfined, inviscid fluids, the fluid force and torque equations generally become fully coupled now (i.e. all fluid terms appear in both the force and the torque equations).

For unconfined, viscous fluids most experimental data are available in the form of empirical relations for both the steady and unsteady, fluid force terms. These relations give a further insight into the properties of the fluid force coefficients, which to some extent may be applied to confined fluids.

The motion of a body in a *confined, inviscid fluid* is described by Lagrange's method of generalized coordinates (chapter 6). The basic concept is similar to that of the dynamical theory of Kirchhoff. In the Eulerian approach of Lagrange's method, however, the coefficients in the kinetic energy equations are no longer constants, but functions of the generalized coordinates. This allows the development of equations of motion for rigid as well as non-rigid bodies in a confined space. Nevertheless, analytical expressions for the fluid force terms can only be developed if the above functional relations are known. In practice, these expressions are known for a few academic cases only. As for unconfined, viscous fluids, the fluid forces and torques are fully coupled here. This property is used to make the step from confined, inviscid fluids to *confined, viscous fluids*. The known empirical relations for the fluid force coefficients in unconfined, viscous fluids, form the basis for those in confined fluids.

The fluid force terms which play a role in a viscous, unsteady fluid flow, such as the drag, added mass, pressure and history terms, cannot always be quantified, either by theory or by experiment. For this reason, in some flow problems a more global approach is followed, whereby the fluid force is described in the form of a conventional drag term. For this purpose a global force coefficient is introduced, to account for all (steady and unsteady) effects of the fluid motion. The properties and form of the global fluid force (and torque) coefficients are studied (chapter 7) by using the results of the previous chapters. The concept of the global fluid force coefficients is used in the development of valve characteristics and computer models.

The theory dealt with in the chapters 4 through 7 is primarily used to describe the check valve dynamics. It should be emphasized, however, that the theory holds for bodies in general (provided that they have at least one plane of symmetry). The stepwise approach of the study reveals the similarities and differences between unconfined and confined, inviscid and viscous, unsteady fluid flows. Such a systematic approach is not available in literature yet (as far as the author knows). At the same time relatively less is known about rotating bodies in unsteady fluid flows. In that sense the author hopes that the results of the present study are useful in a wider sense, i.e. beyond that of check valves.

Nevertheless, the rest of the study deals only with check valves.

A general valve equation of motion is developed, which is valid for most of the existing check valve types (chapter 8). The equation is based on the equations of motion for a body in a confined, viscous fluid. It is written in a dimensionless form. For this purpose the critical velocity and valve diameter are introduced to define a velocity and a time scale.

The hydrodynamic effects of a (check) valve closure on the pipeline system are studied in chapter 9. The phenomenon of unsteady (instead of the usual steady) initial flow conditions in pipeline systems is studied. Basic differential equations are derived for the transient flow in a pipe with a constant initial flow deceleration, based on conventional waterhammer theory. The equations are applied to describe a check valve closure under reflection-free and reflecting boundary conditions. The equations are written in a dimensionless form. For this purpose the fluid velocity at which the damping becomes active, and the pipeline period or reflection time are introduced to define a (second) velocity and time scale.

So far the check valve and pipeline system are considered separately. To describe the interaction between check valve and pipeline system, a momentum equation is derived for the check valve as a short-length component (chapter 10). The (dimensionless) pipe and valve equations are coupled via this momentum equation. This results in an additional "coupling" parameter.

The uncoupled and coupled, pipe and valve equations formally show which valve, system and fluid parameters are relevant to the check valve dynamics in a pipeline system. In that sense they are used in a dimensional analysis to develop *dimensionless* parameter groups (chapter 11). Note that the results of this dimensional analysis are not so self-evident, since several velocity and time scales are involved. The latter justifies a thorough study into the valve and the pipe equations.

The parameter groups in their turn, are used to develop valve characteristics and *dynamic* scale laws. Two theoretical approaches are followed. In the first approach the check valve behaviour is described in terms of (dimensionless) fluid velocity and pressure head characteristics. The second approach is based on the concept of global fluid force coefficients, in terms of dynamic valve loss coefficients.

Based on the valve characteristics, semi-empirical, parameterized valve models are developed to simulate the dynamic behaviour of check valves in waterhammer computer codes (chapter 12). Here, the above two approaches are applied to undamped and damped check valves, respectively. The models are implemented in the computer code CVWP (Check Valve Waterhammer Program).

A test facility is described, for the dynamic testing of check valves at Delft Hydraulics. Experiments are described, as performed on weakly and strongly damped check valves, in order to measure the valve characteristics of approach 1 and 2, and other valve characteristics (chapter 13 and 14).

The dynamic scale laws are validated by means of numerical simulations. The experimental data are used to validate the valve models as implemented in the computer code CVWP (chapter 15).

The study is completed with some final conclusions and recommendations for further research (chapter 16).

2 Survey of literature

In this chapter a survey of literature about check valves is presented. The themes which pass in review (printed in bold type) are listed in an order, which corresponds with the chronological order of the relevant publications. After the introduction of a theme, the associated work of other researchers is treated under the same heading.

2.1 Survey of literature

Pioneers Studies into the hydrodynamic behaviour of check valves begin in the early fifties. Livingston (1954) describes steady-state characteristics, measured for a wide variety of check valves. The first dynamic tests are performed in 1951 in a 3" test loop (Pool et al, 1962).

Esleeck and Rosser (1959) are the first-ones that describe the phenomenon of check valve closure in detail. They recognize the occurrence of reverse flow and associated pressure surges due to a delayed valve closure.

A one-dimensional (1D) valve equation of motion is developed for a swing type check valve. The equation is based on the second law of Newton, taking into account gravitational, inertia, spring and hydrodynamic effects. In the "stand-alone" valve model the fluid velocity-time history is used as a boundary condition, and derived from a separate surge analysis in which the check valve is kept fully open. The surge analysis is restricted to positive flows. After flow reversal the fluid velocity-time history is assumed to be linear.

The valve model is used to calculate the valve disc position in time and the maximum reverse flow at the instant of closure. Assuming that the reduction of the reverse flow to zero takes place instantaneously, the pressure surges due to check valve closure are calculated from the Joukowsky equation.

Stand-alone valve models Following Esleeck and Rosser (1959) many researchers develop stand-alone valve models based on a 1D valve equation of motion (e.g. Worster, 1959 and 1960; Pool et al., 1962; Lewinsky-Kesslitz, 1965; Douglas, 1969; Gwinn, 1974; Deich and Jörgl, 1981; Koch, 1981; Thorley and Oei, 1981; Ellis and Mualla, 1983; Provoost, 1983a and 1983b; Valibouse and Verry, 1983; Gronau and Zwink, 1984; Schneider, 1985).

In general the inertia of the moving elements and the gravitational, buoyancy and spring effects are described in an unambigious and straightforward way.

Added mass effects are taken into account by Worster (1959), Thorley and Oei (1981) and Schneider (1985) as the mass of a sphere of fluid with diameter equal to the disc diameter.

Friction effects are described in several ways by Worster (1960), Pool et al. (1962), Deich and Jörgl (1981), Thorley and Oei (1981), Gronau and Zwink (1984).

However, most of the differences are found in the description and determination of the hydrodynamic effects. Worster (1959), Pool et al. (1962) and Koch (1981) base the hydrodynamic torque on relative velocities between the fluid and the disc. Provoost (1983a) bases the hydrodynamic torque on the relative flow between the fluid and the disc. Thorley and Oei (1981) and Ellis and Mualla (1983) derive the hydrodynamic torque from closure characteristics measured under stagnant flow conditions in water. Worster (1959) and Valibouse and Verry (1983) obtain the hydrodynamic forces from steady flow measurements. Valibouse and Verry (1983) describe hydrodynamic forces taking into account the effect of a moving disc and an accelerating fluid. Schneider (1985) derives the hydrodynamic forces and torques from potential flow theory, modelling the valve as a source in a parallel (pipe) flow.

Damping effects are not considered by the above-mentioned researchers.

On-site tests Whiteman and Pearsall (1959) describe on-site tests to study the closure behaviour of swing type check valves in a sewage multi-pump station. During pump shut down the pressure drop across a partly opened valve is used as a measure for the flow rate.

Following Whiteman and Pearsal (1959) on-site tests are described by e.g. Douglas (1969), Fox (1980), Erdödy and Bökemeier (1981), Koch (1981), Hsu and Ramey (1988).

Laboratory tests Worster (1959) describes a laboratory test facility for the "dynamic" testing of 2" check valves. The flow rate in time is measured from the change of the water level in an air vessel.

Pool et al. (1962) describe a 10" test loop, which is designed after experiences with 3" and 6" loops. The first experiments in the 3" loop are performed in 1951.

Provoost (1980) describes a test facility for the dynamic testing of check valves up to diameters of 12" in horizontal and vertical position, using an electro-magnetic flowmeter.

Collier and Hoerner (1982) describe a test facility for the dynamic testing of check valves in horizontal (12") and vertical (6") position, using a velocity probe as flowmeter.

Pake (1983) describes a test facility for the dynamic testing of check valves up to diameters of 12" in horizontal and vertical position, using an electro-magnetic

flowmeter.

Valibouse and Verry (1983) describe a test facility for the simulation of the check valve closure, starting from stagnant flow conditions, whereby the valve is kept fully open.

Koetzier, Kruisbrink and Lavooij (1986) describe a test facility for the dynamic testing of check valves up to diameters of 32", using an electro-magnetic flowmeter.

Standards In 1959 the Dutch standard comes out for check valves in water up to diameters of 50 mm (Standard, 1959). In the standard the general demands with respect to materials, dimensions, flanges, etc. are described. With respect to the hydrodynamic behaviour the minimum flow capacity is specified at pressure losses of 5 and 100 kPa. Leakage, opening pressure and durability tests are prescribed. The first revision of this standard appears in 1975 (Standard, 1975a).

In 1963 the German equivalent of the above-mentioned Dutch standard appears with a first revision in 1975 (Standard, 1975b). With respect to the hydrodynamic behaviour here also energy loss tests are prescribed.

In 1977 the second edition of the API standard for wafer-type check valves comes out (Standard, 1977). In the standard the general demands with respect to design, materials, dimensions and warranty are described. With respect to the hydrodynamic behaviour leakage tests are prescribed.

In 1990 the Dutch standard appears for check valves up to diameters of 1200 mm (Standard, 1990). This is the equivalent of the above-mentioned Dutch standard (Standard, 1959). With respect to the hydrodynamic behaviour leakage tests are prescribed. With respect to energy losses the valve loss coefficient is specified within certain limits as function of the fluid velocity. Although pressure surges due to valve closure are recognized and surge control devices are mentioned, no "dynamic" demands are described.

Analytical valve models Worster (1960) linearizes the valve equation of motion and assumes a cosines-shaped velocity-time function. Analytical expressions are derived for the valve disc position and the time lag between flow reversal and valve closure.

Combes (1982) and Provoost (1983b) describe a simple analytical method to estimate the reverse flow velocity, based on the assumption that the valve displaced volume is equal to the fluid displaced volume during closure. Inertia effects are neglected.

Valve slamming Gwinn (1974) uses a simplified 1D valve model to calculate the impact speed of the valve disc on its seat, simulating the event of pipe rupture at different initial valve disc positions and line pressures. A threshold impact speed, corresponding to visible fracture of the disc, is used to judge under which conditions

the valve will survive an event.

Collier (1983) studies the phenomenon of check valve hammer in triplex reciprocating pumps.

Kim (1989) studies the chatter behaviour of check valves during the changeover of the feedwater pumps in a boiling water reactor.

Valve design O'Keefe (1976) describes design features for several types of check valves with respect to sealing, wear, disc support and hingeing, opening angle (stroke), temperature effects and applications.

Thorley (1983), Föllmer (1987) and Weisshaupl et al. (1989) describe (sometimes conflicting) design features to improve the check valve response.

Föllmer (1987) introduces the "natural closing time" (i.e. the valve closure time under stagnant flow conditions, e.g. in air) as a measure for the valve response. Based on dynamic tests the natural closing time of a tilting disc check valve is related to the maximum reverse flow velocity. The semi-empirical method is used to improve check valve response.

Special applications Steenhoven and Dongen (1979) study the closure behaviour of the aorta valve in the human heart.

Sauren et al. (1981) investigate the operation of aorta valves for the benefit of the design of artificial heart valves.

Horsten (1990) develops a numerical fluid-structure interaction model of heart valves.

Cleijne and Smulders (1987) study the behaviour of a piston type check valve in a windmill-driven water pump.

Fluid-structure analysis Cho and Kane (1980) combine a fluid and structure analysis to investigate the thermal stress behaviour of tilting disc check valves with dashpot in the primary sodium loops of a power plant. The computer code used for the fluid analysis provides the 2D (axi-symmetrical) flow distribution, heat transfer coefficients and liquid temperatures for specified transient conditions. The temperature data are used in a thermal stress analysis to investigate the ability of the valve to withstand thermal cycles.

Dooley and Mosby (1983) perform a fluid-structure analysis to study the event of pipe rupture in the feedwater loop of a steam reactor (HDR-Heiβdampfreaktor), with a plug type check valve with internal piston damper. The flow conditions are obtained from a transient computer code and used in a structural analysis as boundary condition.

Müller (1987) studies the pipe rupture in the HDR using computer codes for a 3D structural analysis and 1D fluid transient analysis (with two-phase flow and valve model) in coupled and uncoupled mode.

Valve wear Collier (1980) studies the wear of check valves. Relative wear rates are given for valves with upstream flow disturbances like reducers and elbows.

Other wear studies are described by Collier et al. (1983) and Jeanmougin (1986).

Pipe rupture tests Kirik and Gradle (1980) describe a test facility for the dynamic testing of 6" check valves in water. An upstream rupture disc is used to simulate the event of pipe rupture from initial, stagnant flow conditions with an artificially opened valve.

Dooley and Mosby (1983), Travis and Torrey (1985) and Müller (1987) perform tests in a feedwater loop of a steam reactor with a plug type check valve with internal piston damper. The event of pipe rupture is simulated from initial, steady flow conditions using a rupture disc. The experiments, performed in a former 100 MW nuclear power plant in Germany, are used as benchmark problem (German standard problem 4A) with respect to the safety of nuclear power plants.

Rommel et al. (1984), Huet et al. (1987), Panet and Martin (1988) and Henry et al. (1989) describe test facilities in the USA and France for the simulation of pipe rupture from initial, stagnant flow conditions using rupture discs.

Yamada and Imao (1987) describe a test facility for the dynamic testing of 4" check valves, simulating pump trip and pipe rupture. Pipe rupture is simulated from initial, steady flow conditions by a sudden drop of the upstream pressure to atmospheric conditions. The downstream length of the measuring section can be varied from 5 to 50 m.

Valve models coupled to pipe equations Provoost (1980) proposes to couple valve models to the equations for transient flow in pipeline systems.

This approach is followed by several researchers like Ellis (1980), Kirik and Gradle (1980), Erdödy and Bökemeier (1981), Koch (1981), Kubie (1982), Ellis and Mualla (1983), Provoost (1983a), Siikonen (1983), Valibouse and Verry (1983), Rommel et al. (1984), Travis and Torrey (1985), Ellis and Mualla (1986), Henry et al. (1989), Kim (1989), and Suzuki et al. (1991).

The combination of valve model and pipeline model offers opportunities to study the interaction between valve and pipeline, which is essential in the behaviour of damped check valves.

Kirik and Gradle (1980) develop a model of a piston type check valve with an internal dashpot.

Kubie (1982) develops a model of a plug type check valve with damping holes and air cushion.

Provoost (1983a) models a check valve used in the cooling water circuit of a power plant to adjust its external hydraulic damper.

Rommel et al. (1984) develop a model for a tilting disc check valve, and couple it to a 1D computer code for thermal hydraulic analysis (without pipe elasticity effects).

Travis and Torrey (1985) model a plug type check valve with internal piston damper. The valve model is coupled to a computer code for two-phase transient flow.

Ellis and Mualla (1986) model a swing check valve with counterweight and dashpot in a simple pipeline system. It is concluded that counterweights only slightly improve the valve response. Further it is shown that an increase of the dashpot contact angle reduces pressure surges.

Henry et al. (1989) study three types of damped check valves during pipe rupture in a high pressure reactor coolant system of a nuclear power plant.

Scale laws Collier and Hoerner (1981) describe scale laws for check valves in terms of steady flow, head loss and torque coefficients.

Koetzier, Kruisbrink and Lavooij (1986) derive scale laws for unsteady flow conditions. Based on a parameter study and a dimensional analysis the dimensionless "dynamic" characteristic for undamped check valves is introduced.

Thorley (1989) extends the number of parameters which are involved in valve closure and derives a more general form of the dimensionless dynamic characteristic for undamped check valves.

Added mass effects Thorley and Oei (1981) perform oscillation tests on a swing type check valve to determine the added mass, which seems to be approximated by the liquid mass of a sphere having the same diameter and centre as the valve disc.

Valibouse and Verry (1983) relate the added mass of a piston type check valve to the dimensions of the translating disc and valve chamber.

Schneider (1985) concludes from differences between measured and calculated dynamic characteristics, that the added mass of a split disc check valve increases with increasing reverse flow velocity.

Valve characteristics Provoost (1982) introduces the "dynamic" characteristic for undamped check valves. In this characteristic the maximum reverse flow velocity is plotted against a characteristic flow deceleration. The dynamic characteristic is composed out of a series of dynamic tests at different flow decelerations.

In the application of the dynamic characteristics for surge analyses, in first approximation the flow deceleration is obtained from rigid column theory, neglecting pipe friction and pump inertia effects. The pressure surges and anchor forces are assumed to be proportional to the maximum reverse flow velocity and calculated from the Joukowsky equation.

Collier and Hoerner (1982) present a dynamic characteristic in which the pressure surges due to valve closure are represented versus the flow deceleration.

Kruisbrink (1988) proposes to standardize the procedures for the dynamic testing of undamped check valves and the procedures for the data processing into dynamic characteristics. A semi-empirical valve model, based on (dimensionless) dynamic

characteristics, is presented to simulate the closure of undamped check valves in waterhammer computer codes.

Statistics Billington et al. (1985) describe a comprehensive statistical analysis of valve problems within BP. The analysis comprises nearly a quarter of a million valves and shows that 6% of the valves are check valves. Among the check valves 6.3 % give rise to problems varying from erosion, material failure and jamming to leakage.

Non-intrusive monitoring Jeanmougin (1986) explores to what extent a non-intrusive monitoring technique based on acoustic emission, can be used to determine the valve condition with respect to loosened internals.

Charbonneau (1988) uses non-intrusive monitoring, which is based on ultrasonic techniques, to determine the operational status (stable or unstable) of valves with respect to flow induced vibrations.

Haynes (1991) describes non-intrusive monitoring techniques, based on the magnetic flux (using magnets or wire coils), to determine the operational status of a check valve.

Selection criteria Rop (1987) gives an overview of the general demands and selection criteria for check valves.

Working groups A special group which should be mentioned is the Nuclear Industry Check valve group (NIC), representing all 48 utilities (about 100 plants) of the nuclear power industry in the USA. Within NIC working groups are involved with subjects like diagnostics of check valves, check valve performance data, development of instructions and standards for maintenance, all on a continuous basis.

2.2 Review and conclusions

Studies into the hydrodynamic behaviour of check valves begin in the fifties and are restricted to steady flow considerations.

In the sixties studies into the closure behaviour of undamped check valves begin. Many researchers develop stand-alone valve response models based on the valve equation of motion. Within the hydrodynamic effects differences are found in the description and determination of the fluid forces on the disc, added mass and damping effects. The equations are solved numerically, whereby the fluid velocity-time history is prescribed as boundary condition.

A small number of researchers perform on-site measurements. A few small-diameter test facilities come available for the "dynamic" testing of check valves under laboratory conditions.

In the eighties researchers start to couple the valve models to computer codes for transient flow in pipeline systems. Thus the interaction between check valve and pipeline system can be simulated, which enables to study the dynamic behaviour of damped check valves. A few fluid-structure analyses are performed for the sake of more detailed studies, e.g. into the thermal and stress behaviour of check valves under extreme conditions.

The number and the size of test facilities for the dynamic testing of check valves are further enlarged. Several test facilities appear for the simulation of check valve behaviour under the event of pipe rupture.

Scale laws for steady flow conditions are described (1981). The "dynamic" characteristic for undamped check valves is introduced (1982). The first scale laws for unsteady flow conditions appear, together with the dimensionless dynamic characteristic for undamped check valves (1986).

Summarizing it can be stated that the majority of the researchers have studied the dynamic behaviour of check valves in pipeline systems by following a "deterministic" approach. For many different types valve response models have been developed, whereby the description of the hydrodynamic effects is subject to some speculation. The models are used in uncoupled or coupled mode with waterhammer computer codes. The research is restricted to case studies. No attempts are made to generalize, non-dimensionalize or standardize the application of these tools. From the mid-eighties on a few researchers work on the development of dynamic scale laws for undamped check valves.

Note: The survey of literature has tended to be descriptive, rather than provided with critical comments. This is because the "direct" approach of most research discussed above differs from the "parameterized" approach, which is followed within the present study. In that respect a qualitative analysis of the applied methods is more useful than a detailed and comparative, quantitative analysis. The latter may even be regarded as inconsistent with the more global, non-deterministic approach.

3 Check valve types

The development of check valves dates from the second century B.C. It is therefore somewhat remarkable that under the U.S. Patent Class 137, which covers fluid devices, approximately 100 improvement patents on check valves continue to be issued each year (Collier, 1980).

A comprehensive survey of more than fifty types of check valves is presented by Obering et al. (1966). A selection of the most commonly used valve types is given in figure 3.1. The swing type, butterfly and tilting disc valve (with rotating elements), and the sinking ball valve typically close due to gravitational effects. The closure of the piston, plug and ring types (with translating elements), and the split disc valve is spring assisted. The membrane check valve closes due to the elastic effects of the flexible membrane. The response of check valves with translating elements is, generally speaking, faster. On the other hand these valve types have a relatively small, cross sectional flow area, which results in higher energy losses and makes them less suited to dirty fluids (e.g. sewage water).

Check valves may be categorized according to their built-in configuration, principle of operation or valve disc configuration. Further some specials can be mentioned.

Within the **built-in configuration** a distinction is made between:

- flanged (figure 3.1.a, b, c, e, g, h and i)
- threaded (figure 3.1.f)
- wafer (figure 3.1.d)

Within the **principle of operation** a distinction is made between:

- undamped check valves (figure 3.1.a, d, e, g and i)
- damped check valves (figure 3.1.b, c, f and h)
    * hydraulic damper (external; fig 3.1.b)
    * dashpot (internal or external; fig 3.1.c)
    * piston damper (internal; figure 3.1.f)
    * membrane (internal; figure 3.1.h)

Within the **valve disc configuration** a distinction is made between:

- rotating element(s)
  - * swing type (figure 3.1.a)
  - * butterfly (figure 3.1.b)
  - * tilting disc (figure 3.1.c)
  - * split or double disc, dual plate (figure 3.1.d)
- translating element(s)
  - * piston type (straight bonnets; figure 3.e)
  - * plug type (Y-bonnets[1]; figure 3.1.f)
  - * ring type (figure 3.1.g)
- miscellaneous
  - * membrane type (figure 3.1.h)
  - * (sinking) ball type (figure 3.1.i)

The group of check valves comprising the piston, ring and membrane types is also denoted as nozzle type.

Within the **specials** can be mentioned:

- swing type with secondary subvalve (Yamada and Imao, 1987)
- multi-door or multi-disc type
- multi-ring type

In general the internal geometry of check valves (i.e. that of the outer and inner valve body inclusive the moving elements) is characterized by at least one *plane of symmetry*. Check valves with translating elements may be axi-symmetrical, while check valves with rotating elements usually have one plane of symmetry.

These features are used as geometrical condition in the next chapters, to describe the hydrodynamic forces on the moving valve elements.

[1] O'Keefe (1976)

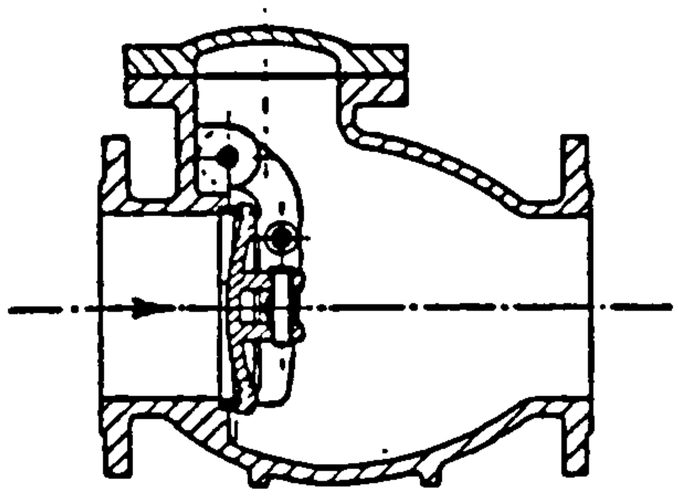

a) Swing type

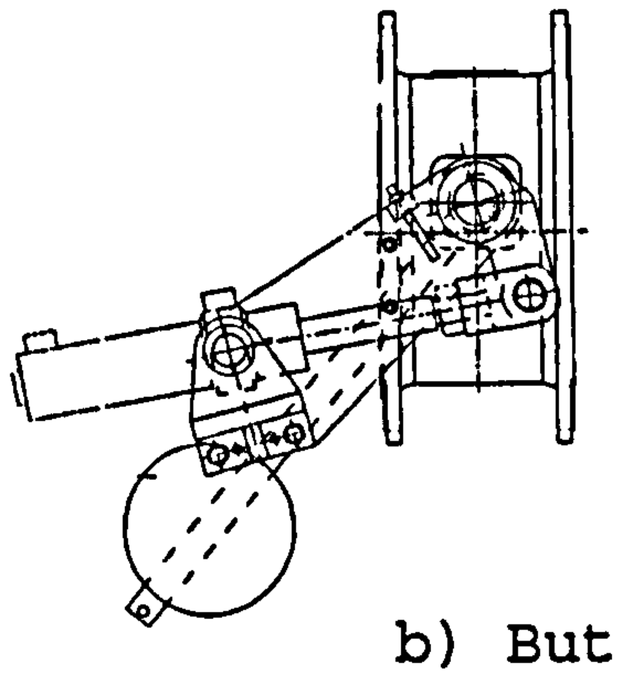

b) Butterfly

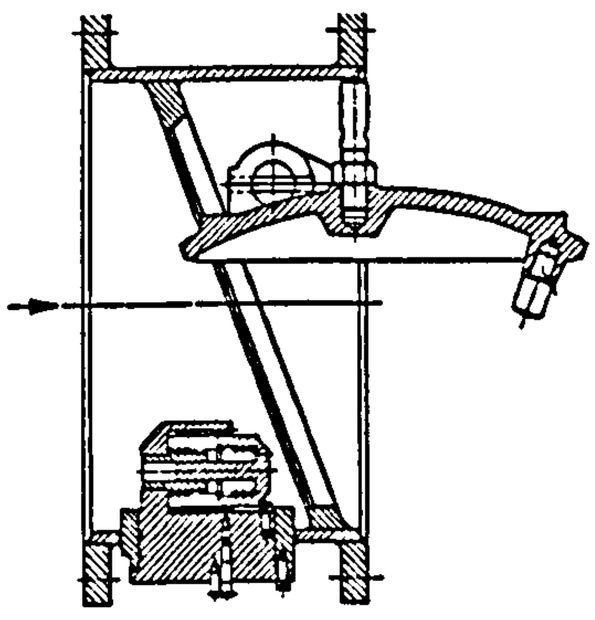

c) Tilting disc

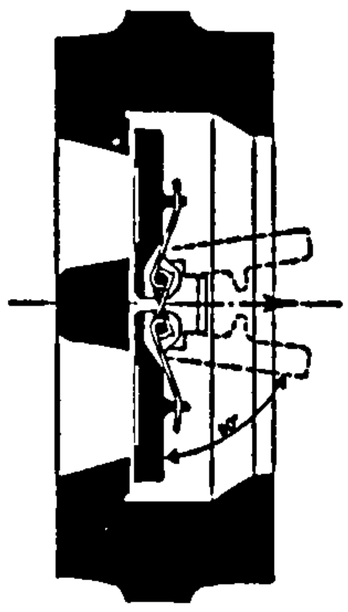

d) Split disc

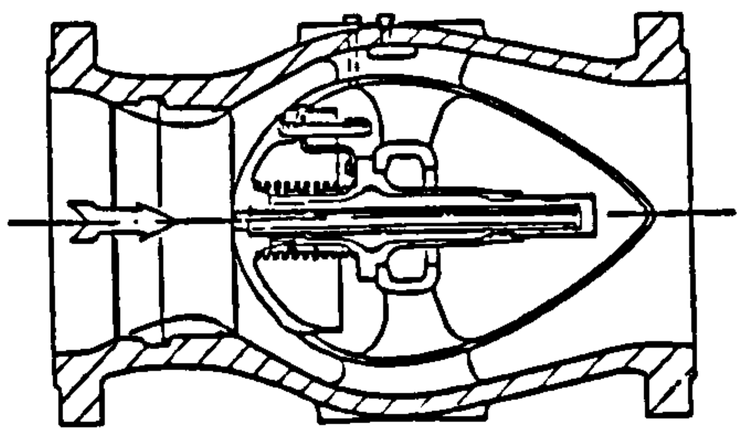

e) Piston type

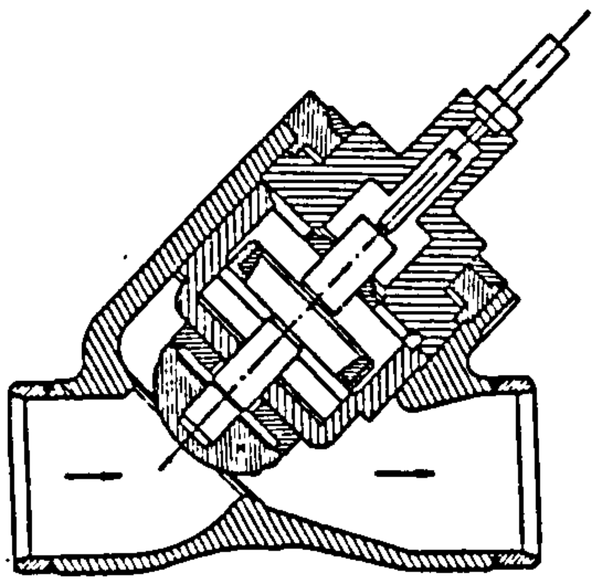

f) Plug type

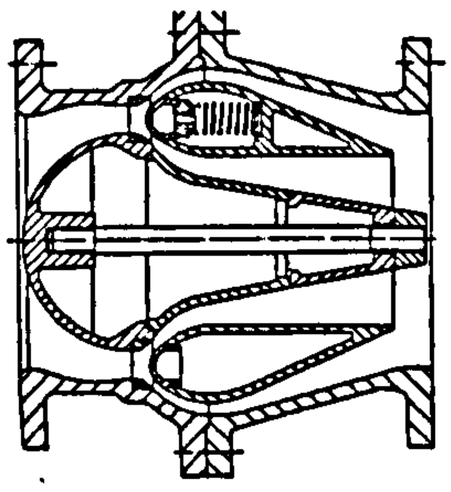

g) Ring type

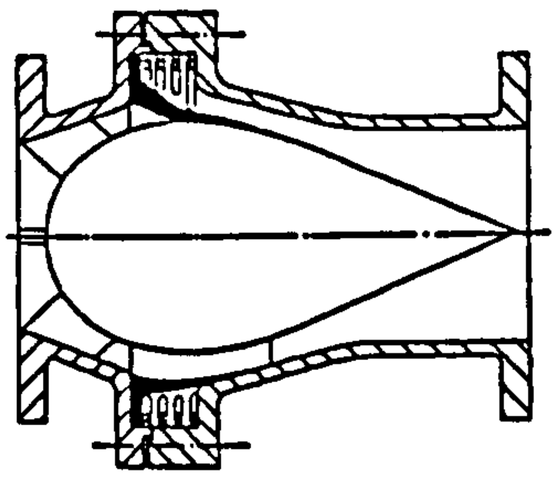

h) Membrane

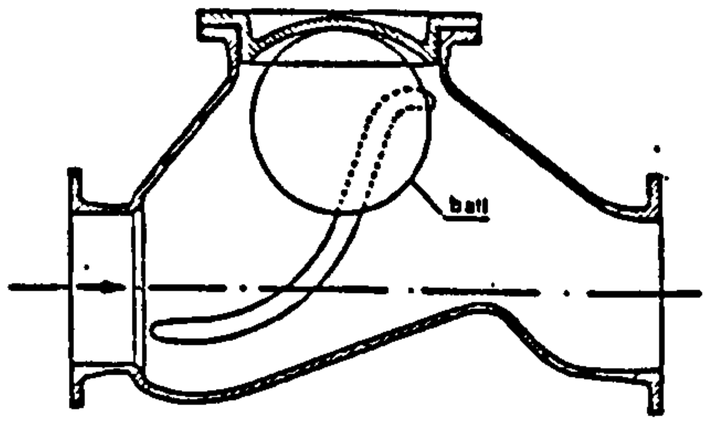

i) Sinking ball

Figure 3.1 Check valve types

4 Motion of a body in an unconfined, inviscid fluid

In this chapter the motion of a body in an unconfined, inviscid fluid is studied. This chapter is not directly relevant to the confined flow problem of check valves. However, as stated in section 1.3, the theory about unconfined, inviscid fluids forms a strong basis for the study into confined fluid flows and thus may be considered as a pre-investigation. Analytical expressions for the fluid force terms and coefficients give a better insight into the basic properties of these quantities.

General equations of motion are described, based on the dynamical theory of Kirchhoff. This potential flow theory, based on a (kinetic) energy concept, enables the treatment of, in particular, *rotating* bodies in an *unsteady* fluid flow, which cannot be achieved easily by the application of (linear and angular) momentum equations. On the analogy of check valves the motion is constrained to a motion in the plane of symmetry. In the first instance the motion of the fluid is entirely due to that of the body. Within this study the theory is extended to the motion of a body in an unsteady fluid flow. Equations of motion are derived for translating and rotating bodies. Some physical aspects of the fluid force terms and coefficients are discussed.

4.1 General equations of motion

Consider the motion of a body in an inviscid and unconfined fluid. The motion of the fluid is entirely due to that of the body, and is therefore irrotational and acyclic (theorem of Helmholz).

The geometry of the body is described in a Cartesian coordinate system x'-y'-z', which is fixed to the body and moves with it. This system is denoted as *body frame*. The motion of the body is described by a translation of the origin O', with linear[1] velocity components v_1, v_2, v_3 parallel to the instantaneous positions of the x'-, y'- and z'-axes, and a rotation, with angular velocity components ω_1, ω_2, ω_3 about the instantaneous positions of these axes (i.e. six degrees of freedom). The motion of the body frame is described relative to a *reference frame*, which is fixed in space.

---

[1] The term "linear" is introduced here in the sense of "translational".

After Kirchhoff, the motion of the fluid is characterized by the existence of a single-valued velocity potential (Lamb, 1932):

$$\phi = v_1\phi_1 + v_2\phi_2 + v_3\phi_3 + \omega_1\chi_1 + \omega_2\chi_2 + \omega_3\chi_3 \qquad \textbf{(4.1)}$$

where ϕ_1, ϕ_2, ϕ_3, χ_1, χ_2, χ_3 are functions of x', y', z', determined only by the configuration of the surface of the body, relative to the coordinate axes.

The kinetic energy of the fluid T_f may be described by:

$$2T_f = \int\int\int_V \rho_f \left[\left(\frac{\partial\phi}{\partial x'} \right)^2 + \left(\frac{\partial\phi}{\partial y'} \right)^2 + \left(\frac{\partial\phi}{\partial z'} \right)^2 \right] dV \qquad \textbf{(4.2)}$$

where V is the volume occupied by the fluid.

With the introduction of the nabla vector operator:

$$\vec{\nabla} = \vec{i}\frac{\partial}{\partial x'} + \vec{j}\frac{\partial}{\partial y'} + \vec{k}\frac{\partial}{\partial z'} \qquad \textbf{(4.3)}$$

Equation (4.2) may be written as:

$$2T_f = \int\int\int_V \rho_f \, \vec{\nabla}\phi \,.\vec{\nabla}\phi \; dV = \int\int\int_V \rho_f \left[\vec{\nabla}.(\phi\vec{\nabla}\phi) - \phi\,\nabla^2\phi \right] dV \qquad \textbf{(4.4)}$$

It is assumed that the fluid is *incompressible*, so that the continuity equation may be written in the form of the Laplace equation:

$$\nabla^2\phi = 0 \qquad \textbf{(4.5)}$$

Applying the Gauss theorem gives:

$$\int\int\int_V \vec{\nabla}.(\phi\vec{\nabla}\phi)\; dV = -\int\int_S \vec{n}.(\phi\vec{\nabla}\phi)\; dS \qquad \textbf{(4.6)}$$

Substitution of the Equations (4.5) and (4.6) in Equation (4.4) yields:

$$2T_f = -\rho_f \int\int_S \vec{n}.(\phi\vec{\nabla}\phi)\; dS \qquad \textbf{(4.7)}$$

so that the kinetic energy of the fluid may be written as:

$$2T_f = -\rho_f \int\int \phi \frac{\partial \phi}{\partial n}\, dS \tag{4.8}$$

The fluid volume V around the body may be chosen such that the fluid velocity at the outer boundary of the volume is at rest. In that case the integration extends over the surface of the body only.

The kinematic condition at the surface of the body is given by:

$$-\frac{\partial \phi}{\partial n} = l\left(v_1 + \omega_2 z' - \omega_3 y'\right) + m\left(v_2 + \omega_3 x' - \omega_1 z'\right) + n\left(v_3 + \omega_1 y' - \omega_2 x'\right) \tag{4.9}$$

where l, m, n are the direction-cosines of the normal (pointed towards the fluid) at any point of this surface.

Substitution of the Equations (4.1) and (4.9) into Equation (4.8) yields the form:

$$\begin{aligned} 2T_f = {} & C'_1 v_1^2 + C'_2 v_2^2 + C'_3 v_3^2 + 2C'_4 v_2 v_3 + 2C'_5 v_3 v_1 + 2C'_6 v_1 v_2 + \\ & + C'_7 \omega_1^2 + C'_8 \omega_2^2 + C'_9 \omega_3^2 + 2C'_{10} \omega_2 \omega_3 + 2C'_{11} \omega_3 \omega_1 + 2C'_{12} \omega_1 \omega_2 + \\ & + 2\omega_1\left(C'_{13} v_1 + C'_{14} v_2 + C'_{15} v_3\right) + 2\omega_2\left(C'_{16} v_1 + C'_{17} v_2 + C'_{18} v_3\right) + 2\omega_3\left(C'_{19} v_1 + C'_{20} v_2 + C'_{21} v_3\right) \end{aligned} \tag{4.10}$$

The twenty-one terms in this equation represent all possible combinations of v_1, v_2, v_3, ω_1, ω_2 and ω_3. The coefficients are constants determined by the form and position of the surface, relative to the body frame. For example:

$$C'_1 = -\rho_f \int\int \phi_1 \frac{\partial \phi_1}{\partial n}\, dS = \rho_f \int\int \phi_1 l\, dS \tag{4.11}$$

The kinetic energy of the body T_b can be written in a similar form, although strictly speaking only fifteen terms are needed, so that Equation (4.10) also holds for the body and for the system of body and fluid.

Kirchhoff derives equations of motion, based on the supposition that the increment of kinetic energy of the system is equal to the work done by the external forces and torques on the body. The work done by the force X' is for example:

$$\int X' v_1 \, dt \tag{4.12}$$

After Kirchhoff, the equations of motion are:

$$\begin{aligned}
\frac{d}{dt}\frac{\partial T}{\partial v_1} &= \omega_3 \frac{\partial T}{\partial v_2} - \omega_2 \frac{\partial T}{\partial v_3} + \sum X' \\
\frac{d}{dt}\frac{\partial T}{\partial v_2} &= \omega_1 \frac{\partial T}{\partial v_3} - \omega_3 \frac{\partial T}{\partial v_1} + \sum Y' \\
\frac{d}{dt}\frac{\partial T}{\partial v_3} &= \omega_2 \frac{\partial T}{\partial v_1} - \omega_1 \frac{\partial T}{\partial v_2} + \sum Z'
\end{aligned} \tag{4.13}$$

and:

$$\begin{aligned}
\frac{d}{dt}\frac{\partial T}{\partial \omega_1} &= v_3 \frac{\partial T}{\partial v_2} - v_2 \frac{\partial T}{\partial v_3} + \omega_3 \frac{\partial T}{\partial \omega_2} - \omega_2 \frac{\partial T}{\partial \omega_3} + \sum K' \\
\frac{d}{dt}\frac{\partial T}{\partial \omega_2} &= v_1 \frac{\partial T}{\partial v_3} - v_3 \frac{\partial T}{\partial v_1} + \omega_1 \frac{\partial T}{\partial \omega_3} - \omega_3 \frac{\partial T}{\partial \omega_1} + \sum L' \\
\frac{d}{dt}\frac{\partial T}{\partial \omega_3} &= v_2 \frac{\partial T}{\partial v_1} - v_1 \frac{\partial T}{\partial v_2} + \omega_2 \frac{\partial T}{\partial \omega_1} - \omega_1 \frac{\partial T}{\partial \omega_2} + \sum M'
\end{aligned} \tag{4.14}$$

where T is the kinetic energy of the system of body and fluid. $\Sigma X'$, $\Sigma Y'$, $\Sigma Z'$ are the external forces on the body in the x', y' and z'-directions, respectively, and $\Sigma K'$, $\Sigma L'$, $\Sigma M'$ are the external torques about the x', y' and z'-directions, respectively.

For a derivation of the Kirchhoff equations it is referred to Lamb (1932).

4.2 Constrained motion in the plane of symmetry

The general equations of motion described in the previous section, are valid for an arbitrary body in arbitrary motion. In this section some constraints are imposed on the geometry as well as on the motion of the body.

On the analogy of the internal, moving elements of check valves, the body is assumed to have a *plane of symmetry*. Let this plane be the x'-y'-plane. Now the kinetic energy of the motion must remain unaltered if the sign of v_3, ω_1 and ω_2 is reversed. Consequently several terms vanish in Equation (4.10). The kinetic energy of the system of body and fluid is then described by:

$$2T = C_1 v_1^2 + C_2 v_2^2 + C_3 v_3^2 + 2 C_6 v_1 v_2 + C_7 \omega_1^2 + C_8 \omega_2^2 + C_9 \omega_3^2 + \\ + 2 C_{12} \omega_1 \omega_2 + 2 C_{15} \omega_1 v_3 + 2 C_{18} \omega_2 v_3 + 2 \omega_3 (C_{19} v_1 + C_{20} v_2) \tag{4.15}$$

The coefficients in this equation refer to the system of body and fluid. For a rigid body solely the coefficients C_1, C_2 and C_3 are equal and represent the mass of the body; C_7, C_8 and C_9 represent moments of inertia, while C_6 and C_{12} are zero.

The motion of the body is constrained to a motion in the plane of symmetry. The constrained motion is described by a translation parallel to this plane, with linear velocity components $v_1 \neq 0$, $v_2 \neq 0$ and $v_3 = 0$, and a rotation about an axis normal to the plane, with angular velocity components $\omega_1 = 0$, $\omega_2 = 0$ and $\omega_3 \neq 0$. Thus the motion has three degrees of freedom.

Now Equation (4.15) reduces to:

$$2T = C_1 v_1^2 + C_2 v_2^2 + 2 C_6 v_1 v_2 + C_9 \omega_3^2 + 2 \omega_3 (C_{19} v_1 + C_{20} v_2) \tag{4.16}$$

Note that this result also holds if the body has no plane of symmetry.

With the above constraints the Equations (4.13) and (4.14) reduce to:

$$\frac{d}{dt}\frac{\partial T}{\partial v_1} = \omega_3 \frac{\partial T}{\partial v_2} + \sum X'$$

$$\frac{d}{dt}\frac{\partial T}{\partial v_2} = -\omega_3 \frac{\partial T}{\partial v_1} + \sum Y' \tag{4.17}$$

$$\frac{d}{dt}\frac{\partial T}{\partial v_3} = \sum Z'$$

and:

$$\frac{d}{dt}\frac{\partial T}{\partial \omega_1} = -\nu_2\frac{\partial T}{\partial \nu_3} + \omega_3\frac{\partial T}{\partial \omega_2} + \sum K'$$

$$\frac{d}{dt}\frac{\partial T}{\partial \omega_2} = \nu_1\frac{\partial T}{\partial \nu_3} - \omega_3\frac{\partial T}{\partial \omega_1} + \sum L' \qquad \textbf{(4.18)}$$

$$\frac{d}{dt}\frac{\partial T}{\partial \omega_3} = \nu_2\frac{\partial T}{\partial \nu_1} - \nu_1\frac{\partial T}{\partial \nu_2} + \sum M'$$

Due to the motion in the plane of symmetry the fluid force in the z' direction and the fluid torques about the x'- and y'-axis are zero. Consequently the sum of the external forces Z', and the sum of the external torques K', L' must be zero. These so-called *forces of constraint* are not of interest and further ignored.

Substitution of Equation (4.16) in the Equations (4.17) and (4.18) yields after some manipulation:

$$C_1\frac{d\nu_1}{dt} + C_6\frac{d\nu_2}{dt} + C_{19}\frac{d\omega_3}{dt} = \omega_3\left(C_6\nu_1 + C_2\nu_2 + C_{20}\omega_3\right) + \sum X'$$

$$C_6\frac{d\nu_1}{dt} + C_2\frac{d\nu_2}{dt} + C_{20}\frac{d\omega_3}{dt} = -\omega_3\left(C_1\nu_1 + C_6\nu_2 + C_{19}\omega_3\right) + \sum Y' \qquad \textbf{(4.19)}$$

$$C_{19}\frac{d\nu_1}{dt} + C_{20}\frac{d\nu_2}{dt} + C_9\frac{d\omega_3}{dt} = \nu_2\left(C_1\nu_1 + C_6\nu_2 + C_{19}\omega_3\right) +$$

$$-\nu_1\left(C_6\nu_1 + C_2\nu_2 + C_{20}\omega_3\right) + \sum M'$$

About a second and third plane of symmetry .....

If the body has a second plane of symmetry, e.g. the y'-z'-plane, then the terms $\nu_1\ \nu_2$ and $\nu_2\ \omega_3$ vanish in Equation (4.15). This can easily be seen, since the kinetic energy of the motion must remain unaltered if the signs of ν_1, ω_2 and ω_3 are reversed. Consequently C_6 and C_{20} must be zero.

If the body has a third plane of symmetry, e.g. the x'-z'-plane, then also the term $\nu_1\ \omega_3$ vanishes in Equation (4.15). Now the kinetic energy of the motion must remain unaltered if the signs of ν_2, ω_1 and ω_3 are reversed. In that case C_6, C_{19} and C_{20} must be zero.

As a next step the linear motion of the body in the plane of symmetry is further constrained to a translation along a straight line. This constraint enables the step to fluid flows (section 4.4) and enables to describe the motion of translating bodies

(section 4.6).

To describe the constrained motion a second coordinate system x-y-z is introduced, which is fixed in space. The x-y-plane of this reference frame is chosen parallel to the x'-y'-plane, so that the z- and z'-axis are also parallel (figure 4.1).

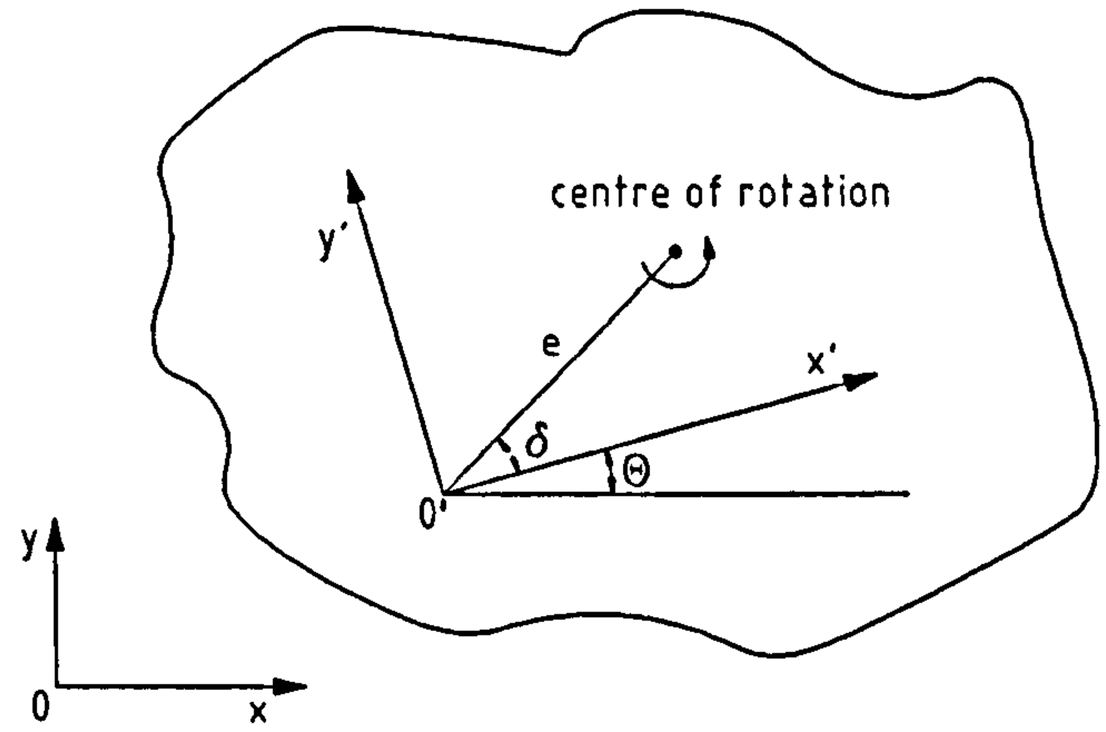

Figure 4.1 Constrained motion in the plane of symmetry

Consider the case that a certain point of the body translates parallel to the x-axis with a linear velocity $\dot{x}$. Meanwhile the body rotates about this point with an angular velocity $\dot{\theta}$. This system point is further denoted as the *centre of rotation* with fixed coordinates $(x', y', 0) = (e\cos\delta, e\sin\delta, 0)$. The motion of the origin O', relative to the reference frame, is now described by:

$$\begin{aligned} v_1 &= \dot{x}\cos\theta + e\dot{\theta}\sin\delta \\ v_2 &= -\dot{x}\sin\theta - e\dot{\theta}\cos\delta \\ \omega_3 &= \dot{\theta} \end{aligned} \tag{4.20}$$

so that:

$$\begin{aligned} \frac{dv_1}{dt} &= \frac{d\dot{x}}{dt}\cos\theta - \dot{x}\dot{\theta}\sin\theta + e\sin\delta\frac{d\dot{\theta}}{dt} \\ \frac{dv_2}{dt} &= -\frac{d\dot{x}}{dt}\sin\theta - \dot{x}\dot{\theta}\cos\theta - e\cos\delta\frac{d\dot{\theta}}{dt} \\ \frac{d\omega_3}{dt} &= \frac{d\dot{\theta}}{dt} \end{aligned} \tag{4.21}$$

Substitution of the Equations (4.20) and (4.21) in Equation (4.19) yields:

$$\sum X' = \left(C_1\cos\theta - C_6\sin\theta\right)\frac{d\dot{x}}{dt} + \left((C_2 - C_1)\sin\theta - 2C_6\cos\theta\right)\dot{x}\dot{\theta} +$$

$$+\left(C_1 e\sin\delta - C_6 e\cos\delta + C_{19}\right)\frac{d\dot{\theta}}{dt} + \left(C_2 e\cos\delta - C_6 e\sin\delta - C_{20}\right)\dot{\theta}^2$$

$$\sum Y' = \left(C_6\cos\theta - C_2\sin\theta\right)\frac{d\dot{x}}{dt} + \left((C_1 - C_2)\cos\theta - 2C_6\sin\theta\right)\dot{x}\dot{\theta} +$$

$$+\left(C_6 e\sin\delta - C_2 e\cos\delta + C_{20}\right)\frac{d\dot{\theta}}{dt} + \left(C_1 e\sin\delta - C_6 e\cos\delta + C_{19}\right)\dot{\theta}^2 \qquad \textbf{(4.22)}$$

$$\sum M' = \left(C_{19}\cos\theta - C_{20}\sin\theta\right)\frac{d\dot{x}}{dt} + \left(C_9 + C_{19}e\sin\delta - C_{20}e\cos\delta\right)\frac{d\dot{\theta}}{dt} +$$

$$+\left((C_1 - C_2)(\cos\delta\cos\theta + \sin\delta\sin\theta) + 2C_6(\sin\delta\cos\theta - \cos\delta\sin\theta)\right)e\dot{x}\dot{\theta} +$$

$$+\left((C_1 - C_2)\sin\theta\cos\theta + C_6(\cos^2\theta - \sin^2\theta)\right)\dot{x}^2 +$$

$$+\left((C_1 - C_2)e\cos\delta\sin\delta + C_6 e(\sin^2\delta - \cos^2\delta^2) + C_{19}\cos\delta + C_{20}\sin\delta\right)e\dot{\theta}^2$$

The equations may be written in a general form as:

$$A\frac{d\dot{x}}{dt} + B\dot{x}\dot{\theta} + C\frac{d\dot{\theta}}{dt} + D\dot{\theta}^2 = \sum X'$$

$$A'\frac{d\dot{x}}{dt} + B'\dot{x}\dot{\theta} + C'\frac{d\dot{\theta}}{dt} + D'\dot{\theta}^2 = \sum Y' \qquad \textbf{(4.23)}$$

$$A''\frac{d\dot{x}}{dt} + B''e\dot{x}\dot{\theta} + C''\frac{d\dot{\theta}}{dt} + D''e\dot{\theta}^2 + E''\dot{x}^2 = \sum M'$$

The coefficients A, B, .., A', ... are dependent on the configuration of the surface of the body, the angular position θ of the body and the position of the center of rotation, relative to the origin O'.

Note that some terms vanish in the torque equation, if the origin O' is moved to the center of rotation ($e \rightarrow 0$). In that case the forces and torques about the center of rotation are considered. Nevertheless, the present result is of interest, since due to the eccentricity e an analogy with viscous fluids arises. More about this analogy in section 4.4.

If the body has three planes of symmetry ($C_6 = 0$, $C_{19} = 0$, $C_{20} = 0$), then the general form of Equation (4.23) changes. With $A'' = 0$ the torque equation becomes:

$$B''e\dot{x}\dot{\theta} + C''\frac{d\dot{\theta}}{dt} + D'''e^2\dot{\theta}^2 + E''\dot{x}^2 = \sum M' \tag{4.24}$$

In section 4.5.2 the equivalent equation is developed for a rotating body in a fluid flow.

4.3 Separation of body and fluid

Thus far the body and fluid are considered as one system, which moves due to external forces on the body. In terms of (kinetic) energy and work, the body and fluid may also be considered separately.

In section 4.1 it is illustrated that the kinetic energy of the body T_b and the kinetic energy of the fluid T_f can be described in similar terms, although strictly speaking fewer terms are needed for the kinetic energy of the body. Thus, the kinetic energy of the system T, as given in Equation (4.16), may be divided into similar equations for the body and fluid. The (external) forces on the system $\Sigma X'$, $\Sigma Y'$, ... in the Equations (4.17) and (4.18) may be divided into (internal and external) forces on the body and (internal) forces on the fluid. Consequently, the equations of motion for body and fluid may be treated separately and in the same manner.

4.3.1 Equations of motion for the body

The equations of motion for the body can be obtained by separation of the body and fluid terms in the general equations of motion as described above.

However, they can also be derived in a direct way. Equation (4.23) describes the motion of a body in a stagnant fluid, due to external forces on the body. It may also be applied to the body solely, if the fluid forces on the body are considered as additional *external* forces. Let the fluid forces and torques on the body be described by X_f', Y_f', M_f'. Thus follows:

$$A_b \frac{d\dot{x}}{dt} + B_b \dot{x}\dot{\theta} + C_b \frac{d\dot{\theta}}{dt} + D_b \dot{\theta}^2 = X_f' + \sum X'$$

$$A_b' \frac{d\dot{x}}{dt} + B_b' \dot{x}\dot{\theta} + C_b' \frac{d\dot{\theta}}{dt} + D_b' \dot{\theta}^2 = Y_f' + \sum Y'$$

$$A_b'' \frac{d\dot{x}}{dt} + B_b'' e\dot{x}\dot{\theta} + C_b'' \frac{d\dot{\theta}}{dt} + D_b'' e\dot{\theta}^2 + E_b'' \dot{x}^2 = M_f' + \sum M' \qquad (4.25)$$

The body coefficients A_b, B_b, .., A_b', ... are dependent on the geometry and angular position of the body. For a rigid body the coefficient E_b" is zero. This can be easily seen from Equation (4.22), since for the body solely $C_1 = C_2$, while $C_6 = 0$.

The equations illustrate which terms are relevant to the motion of a body in a stagnant fluid, which moves in its plane of symmetry due to external forces and torques. The equations also hold if there is no fluid. For $e \rightarrow 0$ the forces and torques about the center of rotation are obtained.

4.3.2 Equations of motion for the fluid

The equations of motion for the fluid are obtained by separation of the body and fluid terms in the general equations of motion as described above.

The motion of the fluid is entirely due to that of the body, so that no external forces and torques act on the fluid. The only forces on the fluid are exerted by the body via normal surface stresses. These forces are equal in magnitude, but opposite of sign to the fluid forces X_f', Y_f', M_f' on the body, exerted via normal fluid stresses (i.e. pressure). Separation of the terms in Equation (4.23) gives:

$$A_f \frac{d\dot{x}}{dt} + B_f \dot{x}\dot{\theta} + C_f \frac{d\dot{\theta}}{dt} + D_f \dot{\theta}^2 = -X_f'$$

$$A_f' \frac{d\dot{x}}{dt} + B_f' \dot{x}\dot{\theta} + C_f' \frac{d\dot{\theta}}{dt} + D_f' \dot{\theta}^2 = -Y_f' \qquad (4.26)$$

$$A_f'' \frac{d\dot{x}}{dt} + B_f'' e\dot{x}\dot{\theta} + C_f'' \frac{d\dot{\theta}}{dt} + D_f'' e\dot{\theta}^2 + E_f'' \dot{x}^2 = -M_f'$$

The fluid coefficients A_f, B_f, .., A_f', ... are dependent on the configuration of the surface of the body, the angular position θ of the body and the position of the centre

of rotation relative to the origin O'.

The equations illustrate which terms are relevant to the forces and torques on the body, due to an inviscid fluid.

The *complete equations of motion for a body in a stagnant, inviscid fluid* can be obtained by the summation of Equation (4.25) and Equation (4.26). As a result the coefficients A, B, ... in Equation (4.23) are divided into body coefficients and fluid coefficients, such that $A = (A_b + A_f)$, $B = (B_b + B_f)$, ... Thus, it is demonstrated in a qualitative sense that the whole effect of the fluid may be represented by an addition to the "inertia" of the body, if the term inertia is used in a somewhat extended sense.

4.4 Motion of a body in a fluid flow

The theory of Kirchhoff (section 4.1) is developed for the motion of a body in a stagnant fluid. The question arises in how far the theory may be applied to the motion of a body in a *fluid flow*.

The equations of motion are derived under the condition that the motion of the fluid is entirely due to that of the body. This implies that: 1) the motion of the fluid is irrotational, 2) the change of kinetic energy of the fluid is effected by the motion of the body only, so that 3) no external forces work on the fluid.

The fluid flow is restricted to the *uniform parallel flow* of an ideal, frictionless fluid, so that: 1) the motion of the fluid remains irrotational. The flow direction is assumed to be parallel to the plane of symmetry, with velocity components $V_1 \neq 0$, $V_2 \neq 0$ and $V_3 = 0$, parallel to the instantaneous positions of the x'-, y'- and z'-axes, and relative to the fixed reference frame.

Thus far the motion of the body is described relative to a reference frame, which is fixed in space. It may also be considered as a frame which "moves" with the stagnant fluid at zero velocity. The latter principle is hold in the following.

To describe the motion of the body in a fluid flow, a reference frame is used which *moves* with the fluid. This reference frame is a so-called *inertial frame* or *inertial system*, as long as it moves at a uniform velocity. To such systems the classical mechanics (Newton's laws) may be applied. In other cases it is a *non-inertial system*, to which the classical mechanics may only be applied, if the Newtonian forces are replaced by so-called *pseudo-forces* (e.g. Halliday and Resnick, 1966).

About non-inertial systems and pseudo-forces .....

Consider the linear motion of a body with velocity v_1, parallel to the flow direction with velocity V_1.

The kinetic energy of the system, relative to a moving reference frame, is:

$$2T' = C_1(v_1 - V_1)^2 \tag{4.27}$$

So that:

$$\frac{dT'}{dt} = C_1(v_1 - V_1)\frac{d(v_1 - V_1)}{dt} \tag{4.28}$$

The kinetic energy is described in terms of relative velocities. Note that the coefficient C_1, as introduced in section 4.1, remains unchanged, since it is only determined by the form and position of the body surface relative to the body frame.

The increment of kinetic energy of the system due to the work done by the pseudo-force χ is:

$$dT' = \chi(v_1 - V_1)\,dt \tag{4.29}$$

From the Equations (4.28) and (4.29) follows:

$$\chi = C_1\frac{d(v_1 - V_1)}{dt} \tag{4.30}$$

This example illustrates the following: a) The kinetic energy T', relative to the moving reference frame, is only equal to the kinetic energy T, relative to a fixed reference frame, if $V_1 = 0$. The kinetic energy is a relative concept; b) The change of kinetic energy dT'/dt is only equal to dT/dt, if both $V_1 = 0$ and $dV_1/dt = 0$; c). The pseudo-force χ is only the equal to the "real" force X if $dV_1/dt = 0$. In that case the reference frame is an inertial frame.

Inertial frames with "real" forces, and non-inertial frames with "pseudo" forces are equivalent. The choice of one or the other is a matter of convenience.

The motion of the body, relative to the moving reference frame, is now described by the linear velocity components $(v_1 - V_1)$ and $(v_2 - V_2)$ and the angular velocity component ω_3, which remains unchanged.

The fluid velocity and kinetic energy far from the body are zero now, so that: 2) the change of (relative) kinetic energy of the fluid is effected by the (relative) motion of the body only.

In the equations in section 4.2 the velocity components v_1 and v_2 may now be replaced by relative velocities (v_1 - V_1) and (v_2 - V_2), while ω_3 remains unchanged. The kinetic energy is replaced by a relative value T', while the forces and torques are replaced by the pseudo-forces and -torques $\Sigma\chi'$, $\Sigma\psi'$, $\Sigma M'$.

Let the uniform parallel flow be described by a fluid velocity v parallel to the x-axis of the fixed coordinate system x-y-z. The velocity components, parallel to the x'-, y'- and z'-axes are then given by $V_1 = v \cos\theta$ and $V_2 = -v \sin\theta$. The motion of the origin O', relative to the moving reference frame is now described by:

$$\begin{aligned} v_1 - V_1 &= (\dot{x} - v)\cos\theta + e\dot{\theta}\sin\delta \\ v_2 - V_2 &= -(\dot{x} - v)\sin\theta - e\dot{\theta}\cos\delta \\ \omega_3 &= \dot{\theta} \end{aligned} \qquad (4.31)$$

In Equation (4.20) the linear velocity of the body $\dot{x}$ is now replaced by a relative velocity ($\dot{x}$ - v). The coefficients A_f, B_f, ... ,A_f',... remain unaltered, since they are only determined by the geometry and angular position of the body, relative to the body frame.

Just like Kirchhoff assumed that no external forces act on the fluid, it is here assumed that: 3) no external pseudo-forces act on the fluid. However, the latter does not necessarily mean that the "real" external forces on the fluid are zero.

In the case of an unsteady flow "real" external forces bring the fluid in unsteady motion. In the case of an inviscid, incompressible, uniform parallel flow, the external forces on the fluid are proportional to the fluid velocity gradient dv/dt only (as will be treated in section 4.6.4). This may described by:

$$X' = F_f \frac{dv}{dt} \quad ; \quad Y' = F_f' \frac{dv}{dt} \quad ; \quad M' = F_f'' \frac{dv}{dt} \qquad (4.32)$$

The fact that the magnitude of the pseudo-forces is unknown is fully accepted here, since we are only interested in the terms, which are relevant to the fluid forces and torques.

After replacing the term $\dot{x}$ in Equation (4.26) by the term ($\dot{x}$ - v), and returning to "real" forces by adding the real force terms described in Equation (4.32), the equations of motion for the fluid become:

$$A_f \frac{d(\dot{x}-v)}{dt} + B_f(\dot{x}-v)\dot{\theta} + C_f \frac{d\dot{\theta}}{dt} + D_f \dot{\theta}^2 = F_f \frac{dv}{dt} - X_f'$$

$$A_f' \frac{d(\dot{x}-v)}{dt} + B_f'(\dot{x}-v)\dot{\theta} + C_f' \frac{d\dot{\theta}}{dt} + D_f' \dot{\theta}^2 = F_f' \frac{dv}{dt} - Y_f'$$

$$A_f'' \frac{d(\dot{x}-v)}{dt} + B_f'' e(\dot{x}-v)\dot{\theta} + C_f'' \frac{d\dot{\theta}}{dt} + D_f'' e\dot{\theta}^2 +$$

$$+ E_f'' (\dot{x}-v)^2 = F_f'' \frac{dv}{dt} - M_f' \qquad \textbf{(4.33)}$$

The equations show which fluid terms are relevant to the motion of a body in a uniform parallel flow. For $e \rightarrow 0$ the forces and torques about the center of rotation are obtained.

About hydrodynamic center .....

For a steady motion follows ($d\dot{x}/dt = 0$; $d\dot{\theta}/dt = 0$; $dv/dt = 0$):

$$X_f' = B_f(v-\dot{x})\dot{\theta} - D_f\dot{\theta}^2$$

$$Y_f' = B_f'(v-\dot{x})\dot{\theta} - D_f'\dot{\theta}^2 \qquad \textbf{(4.34)}$$

$$M_f' = B_f''e(v-\dot{x})\dot{\theta} - D_f''e\dot{\theta}^2 - E_f''(v-\dot{x})^2$$

The terms $(v - \dot{x})\,\dot{\theta}$ and $\dot{\theta}^2$ appear in the force as well as in the torque equations. However, the terms in the torque equation vanish if the origin O' is moved to the center of rotation ($e \rightarrow 0$). Apparently the fluid forces which arise due to the *motion* of body and fluid act along a line through the center of rotation. This holds for any θ, so that the center of rotation may be considered as the hydrodynamic center (figure 4.2). As a result the terms in the force and torque equations become *uncoupled*.

On the other hand, the term $(v - \dot{x})^2$ appears in the torque equation but not in the force equations. Apparently this term gives no resulting force but only a fluid couple.

About an analogy between eccentricity and fluid viscosity .....

The above case is of interest, since due to the eccentricity e, additional terms appear in the torque equation. Common practice learns that these terms are also found in the torque equation for viscous fluids, which is illustrated by means of two examples.

Example 1: Although the fluid torque on a steady rotating body in an inviscid, stagnant fluid is zero, the torque is proportional to $\dot{\theta}^2$ in a viscous, stagnant fluid.

Example 2: The term $(v - \dot{x})\,\dot{\theta}$ in the force equations does not arise from circulation, but from the kinematic boundary (surface) conditions. In an irrotational, inviscid and incompressible fluid no circulation can be generated (theorem of Kelvin). Nevertheless, in the case of a viscous flow indeed circulation is generated in the boundary layer. Here a fluid force arises normal to the flow direction, which is proportional to the linear velocity of the body and the circulation around the body (theorem of Kutta-Joukowsky), e.g. the top spin of a tennis ball. In general the effects of this lift force, which contributes to the above force term, are also found in the fluid torque.

Apparently the effect of an eccentricity is analogous to that of fluid viscosity. The analogy must be found in the fact that viscous flows are generally characterized by boundary layers and separation points, which move the hydrodynamic center from the center of rotation (figure 4.2).

On the other hand: Although the fluid force on a steady, translating body in an inviscid fluid is zero, the force is proportional to $(v - \dot{x})^2$ in a viscous fluid.

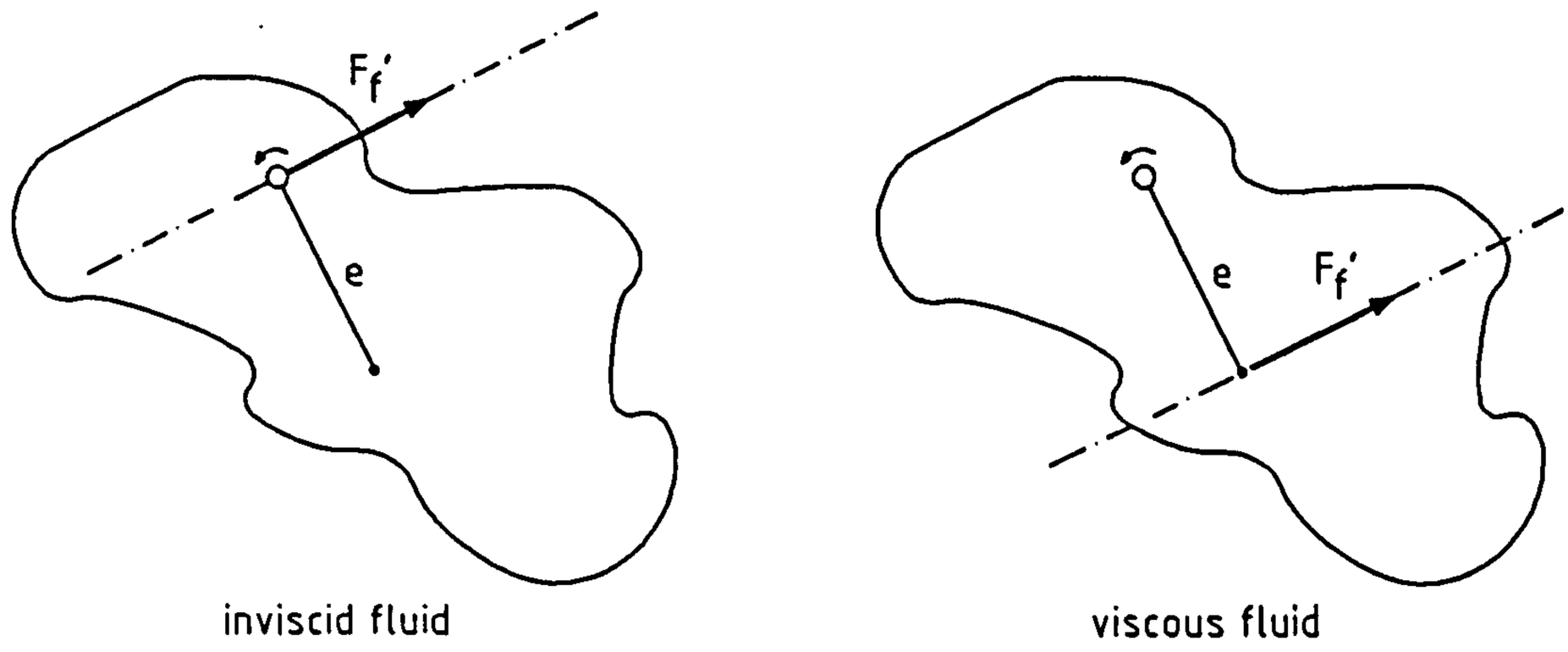

Figure 4.2 Analogy between an eccentricity and viscosity

The equations of motion for a body in a fluid flow are the same as those for a body in a stagnant fluid (section 4.3.1), since all effects of the fluid flow are accounted for in the fluid forces and torques on the body.

The *complete equations of motion for a body in an inviscid, fluid flow* can be obtained by the summation of the Equations (4.25) and (4.33).

4.5 Translating and rotating bodies

The equations of motion, as developed for a body in a fluid flow (section 4.4), are applied to translating or rotating bodies, moving in an inviscid, uniform, parallel flow. The bodies are assumed to have at least one plane of symmetry, in the sense as described in section 4.2. The equations of motion in the constrained directions are not of interest and further ignored.

4.5.1 Linear motion

Consider a body that translates in the x-direction, so that $\dot{x} \neq 0$ and $\dot{\theta} = 0$, the fluid velocity v is parallel to the x-direction, while the x'-axis is chosen to be parallel to the x-axis.

The equation of motion for the body directly follows from Equation (4.25):

$$m_b \frac{d\dot{x}}{dt} = X_f + \sum X \tag{4.35}$$

where $m_b = \rho_b V_b$ is the mass of the body.

The equation of motion for the fluid directly follows from Equation (4.33)[2]:

$$\boxed{X_f = m_f \frac{d(v-\dot{x})}{dt} + \rho_f V_b \frac{dv}{dt}} \tag{4.36}$$

where:

$$m_f = C_A \rho_f V_b \tag{4.37}$$

The equation consists of an added mass term, where m_f is the added mass of the body, and a pressure term due to the pressure gradient over the accelerating fluid (section 4.6). C_A is the added mass coefficient. Note that the flow direction ($v > 0$ or $v < 0$) is not relevant here.

Substitution of Equation (4.36) in Equation (4.35) yields the complete equation of motion for *translating* bodies in an inviscid fluid flow:

[2] For the conversion of A_f, B_f, ... into physical quantities it is referred to section 4.6.

$$\left(m_b + m_f\right)\frac{d\dot{x}}{dt} = \left(C_A + 1\right)\rho_f V_b \frac{dv}{dt} + \sum X \tag{4.38}$$

The term $(m_b + m_f)$ is known as the virtual mass of the body.

More about the physical meaning of the fluid terms and coefficients in the sections 4.6 and 4.7.

4.5.2 Angular motion

Consider a body that rotates about the z-axis, so that $\dot{x} = 0$ and $\dot{\theta} \neq 0$, the fluid velocity v is parallel to the x-direction, while the z'-axis is chosen to be parallel to the z-axis.

The equation of motion for the body directly follows from Equation (4.25) ($e \rightarrow 0$):

$$I_b \frac{d\dot{\theta}}{dt} = M_f + \sum M \tag{4.39}$$

where $I_b = \rho_b V_b k^2$ is the mass moment of inertia of the body (section 4.6.3).

The equation of motion for the fluid directly follows from Equation (4.33)[2] ($e \rightarrow 0$):

$$\boxed{M_f = C_D \frac{1}{2}\rho_f v^2 D^3 + \left(C_{A_1} + K_P\right)\rho_f V_b \frac{dv}{dt} D - I_f \frac{d\dot{\theta}}{dt}} \tag{4.40}$$

where:

$$I_f = C_{A_2}\, \rho_f V_b k^2 \tag{4.41}$$

The equation consists of a drag term, two added mass terms, where I_f is the added mass moment of inertia of the body, and a pressure term (section 4.6). The nature of the drag term is that of a form drag. Therefore C_D is introduced here (in an unusual way) as torque coefficient, while D is a characteristic dimension of the body. The coefficients $C_{A..}$ are added mass coefficients, due to the linear motion of the fluid (subscript 1) and angular motion of the body (subscript 2), while K_P is a pressure coefficient.

The "viscous" equivalent follows from Equation (4.33):

$$M_f = \left(A_f'' + F_f''\right)\frac{dv}{dt} + B_f'' e v\dot{\theta} - C_f''\frac{d\dot{\theta}}{dt} - D_f'' e\dot{\theta}^2 - E_f'' v^2 \qquad (4.42)$$

If the body has three planes of symmetry then $A_f'' = 0$, D_f'' may be replaced by $D_f'' e$ (section 4.2), and F_f'' may be replaced by $F_f'' e$ since the center of gravity lies in the origin O'. Thus follows:

$$M_f = B_f'' e v\dot{\theta} - C_f''\frac{d\theta}{dt} - D_f'' e^2\dot{\theta}^2 - E_f'' v^2 + F_f'' e\frac{dv}{dt} \qquad (4.43)$$

This equation is of interest, since it shows some analogy with the global form of the fluid torque on rotating bodies (section 7.3.4).

Substitution of Equation (4.40) in Equation (4.39) yields the complete equation of motion for *rotating* bodies in an inviscid fluid flow:

$$\left(I_b + I_f\right)\frac{d\dot{\theta}}{dt} = C_D\ \frac{1}{2}\rho_f v^2 D^3 + \left(C_{A_1} + K_P\right)\rho_f V_b\frac{dv}{dt}D + \sum M \qquad (4.44)$$

The term $(I_b + I_f)$ is introduced as the virtual mass moment of inertia of the body.

More about the physical meaning of the fluid terms and coefficients in the sections 4.6 and 4.7.

4.6 Physical aspects

In this section the physical meaning of the terms and coefficients in the fluid equations of motion (section 4.4) is studied in more detail. Special attention is paid to translating and rotating bodies (section 4.5).

4.6.1 General

In the fluid equations of motion, given in Equation (4.33), three classes of force terms can be recognized:

1) Terms that arise from the (relative) motion of the body. These terms are described by $(\dot{x} - v)$ and $\dot{\theta}$, and may be seen as *drag terms*, if the term "drag" is used in a somewhat extended sense (usually drag forces are defined in the direction of motion only). For inviscid fluids these forces are exerted via normal surface

stresses (pressure) only. In that sense they may be considered as form drags.

2) Terms that arise from the (relative) change of motion of the body. These terms are described by $d(\dot{x} - v)/dt$ and $d\dot{\theta}/dt$, and may be considered as an addition to the inertia of the body. In that sense they are so-called *added mass terms*.
3) Terms that arise from the external forces on the fluid. These terms are described by dv/dt, and are proportional to the pressure gradient over the fluid. In that sense they are denoted as *pressure terms*.

For inviscid fluids two basic principles are available to quantify the fluid force terms and coefficients:

1) The fluid coefficients C_1', C_2', ... can directly be obtained from the *velocity potential*. In that case integrals in the form of Equation (4.11) must be solved. The conversion into the coefficients A_f, B_f, .., A_f', ... is then easily made.
2) The fluid coefficients can indirectly be obtained from the *superposition principle*. The coefficients A_f, B_f, .., A_f', ... are only dependent on the fluid density (section 4.1) and the geometry and angular position of the body (section 4.3.2). Therefore the terms in the fluid equations of motion may be considered separately and superimposed. The fluid terms may be isolated by imposing constraints to the motion of the body. The isolated fluid terms can then be obtained from a) the pressure distribution around the body, or b) the change of kinetic energy of the fluid (dynamical theory of Kirchhoff).

The principles are essentially the same. Nevertheless, the combination of these principles may lead to a simplified velocity potential, which adopts a more tractable form.

In the next sections the superposition principle is applied to isolate the drag and added mass terms.

4.6.2 Drag terms

The drag terms are isolated by considering the steady motion of a body in a steady, uniform parallel flow. Now Equation (4.33) reduces to ($e \rightarrow 0$):

$$X_f' = B_f(v-\dot{x})\dot{\theta} - D_f\dot{\theta}^2$$

$$Y_f' = B_f'(v-\dot{x})\dot{\theta} - D_f'\dot{\theta}^2 \qquad (4.45)$$

$$M_f' = -E_f''(v-\dot{x})^2$$

For the translating and rotating bodies considered in section 4.5 these equations reduce to:

linear motion:

$$X_f = 0 \tag{4.46}$$

angular motion:

$$M_f = -E_f'' v^2 \tag{4.47}$$

The fluid force on a steady translating body in an inviscid, stagnant or steady, uniform parallel flow is zero (although the fluid torque differs from zero). Apparently, the sum of the normal stresses (pressure) over the surface of the body is zero. This phenomenon is discovered by Euler in 1745 and rediscovered by D'Alembert in 1752, and known as the paradox of Euler-D'Alembert. The paradox must be found in the fact that the statement conflicts with our daily experience (see viscous fluids).

The fluid torque on a steady rotating body in an inviscid, stagnant flow is zero (although the fluid force differs from zero). The fluid torque on a stationary body in a steady flow differs from zero (although the fluid force is zero). Apparently, a reverse-symmetry in the pressure distribution may give rise to a fluid couple.

After dimensional reasoning the above equation may be written as:

angular motion:

$$M_f = C_D \tfrac{1}{2}\rho_f v^2 D^3 \tag{4.48}$$

In this equation C_D is introduced as a drag coefficient for angular motion. Usually the drag coefficient C_D is only used as force coefficient in flow direction. The fluid couple is assumed to be proportional to the dynamic pressure ½ $\rho_f v^2$ and the volume of the body, represented by D^3, where D is a characteristic length. The nature of the fluid couple is that of a form "drag" (see definition in section 4.6.1), which arises from the normal stress (pressure) distribution only, since in an inviscid fluid shear stresses do not exist.

4.6.3 Added mass terms

The added mass terms cannot be isolated from the other fluid terms, which is illustrated by Equation (4.33). However, some of the fluid terms vanish if the motion of a body in a stagnant fluid is considered. Then Equation (4.33) reduces to ($e \to 0$):

$$A_f \frac{d\dot{x}}{dt} + B_f \dot{x}\dot{\theta} + C_f \frac{d\dot{\theta}}{dt} + D_f \dot{\theta}^2 = -X_f'$$

$$A_f' \frac{d\dot{x}}{dt} + B_f' \dot{x}\dot{\theta} + C_f' \frac{d\dot{\theta}}{dt} + D_f' \dot{\theta}^2 = -Y_f' \qquad \textbf{(4.49)}$$

$$A_f'' \frac{d\dot{x}}{dt} + C_f'' \frac{d\dot{\theta}}{dt} + E_f'' \dot{x}^2 = -M_f'$$

For the translating or rotating bodies considered in section 4.5 this leads to:

linear motion:

$$X_f = -A_f \frac{d\dot{x}}{dt} = -m_f \frac{d\dot{x}}{dt} \qquad \textbf{(4.50)}$$

angular motion:

$$M_f = -C_f'' \frac{d\dot{\theta}}{dt} = -I_f \frac{d\dot{\theta}}{dt} \qquad \textbf{(4.51)}$$

The physical meaning of the coefficients A_f and C_f" is that of an *added mass* and *added mass moment of inertia* of the body, respectively. In this form the added mass appears as a lumped, virtual amount of fluid, which moves with the body at the same acceleration.

The force needed to accelerate a body in a stagnant fluid is larger than the force needed to accelerate it in vacuum. The extra force, needed to accelerate the fluid around the body, is known as the *added mass force* (Campbell, 1982).

According to this definition the added mass force is an external force, which is equal in magnitude but opposite of sign to the fluid force, which arises due to the unsteady motion of the body.

The added mass force may be obtained from the dynamical theory of Kirchhoff (section 4.1) under the condition that the increment of kinetic energy of the fluid is equal to the work done by the added mass force or torque. This can only be achieved if no other forces or torques contribute to the work. The forces of constraint do not contribute to the (virtual) work.

According to the Equations (4.50) and (4.51) these condtions are satisfied for a translating or rotating body in a stagnant flow. The added mass force may now be calculated from Equation (4.12) as:

linear motion:

$$X_A \dot{x} = \frac{d}{dt} \int\int\int_{V_f} \frac{1}{2} \rho_f v^2 \, dV \tag{4.52}$$

In a similar way the added mass torque may be calculated from:

angular motion:

$$M_A \dot{\theta} = \frac{d}{dt} \int\int\int_{V_f} \frac{1}{2} \rho_f v^2 \, dV \tag{4.53}$$

Thus follows:

$$X_A = \int\int\int_{V_f} \rho_f \frac{v}{\dot{x}} \frac{\partial v}{\partial t} \, dV \tag{4.54}$$

$$M_A = \int\int\int_{V_f} \rho_f \frac{v}{\dot{\theta}} \frac{\partial v}{\partial t} \, dV \tag{4.55}$$

Note that in the above equations v is not anymore the fluid velocity of the undisturbed flow far from the body, but a *local* fluid velocity. The added mass force or torque can be calculated if the velocity distribution in the entire flow field is known.

The added mass is usually related to the volume of the body by the so-called added mass coefficient C_A (e.g. Steetzel, 1984). The mass and the added mass of the body are now described as:

linear motion:

$$m_b = \int_{V_b} \rho_b \, dV = \rho_b V_b \tag{4.56}$$

$$m_f = C_A \int_{V_b} \rho_f \, dV = C_A \, \rho_f V_b \tag{4.57}$$

The equivalent equations for the mass moment of inertia and the added mass moment of inertia are here introduced as:

angular motion:

$$I_b = \int_{V_b} \rho_b r^2 \, dV = \rho_b V_b \, k^2 \tag{4.58}$$

$$I_f = C_{A_2} \int_{V_b} \rho_f r^2 \, dV = C_{A_2} \, \rho_f V_b \, k^2 \tag{4.59}$$

Where k is known as the *radius of gyration* (e.g. Alonso and Finn, 1976). In these equations the density of the body and fluid is assumed to be constant in space.

About the added mass of a sphere ...

The added mass of a sphere in an inviscid, uniform parallel flow is: $m_f = \frac{1}{2} \rho_f V_b$, where V_b is the volume of the sphere (Merk, 1982), so that the added mass coefficient $C_A = \frac{1}{2}$.

The added mass term $A_f'' \, d(\dot{x} - v)/dt$ in Equation (4.33) accounts for the fluid torque due to the linear, (relative) unsteady motion of the body (without the effect of the pressure gradient). The term cannot be isolated from the other terms. However, for a translating body in a stagnant fluid the term appears with the drag term only. The effect is found in the pressure distribution, and assumed to be proportional to the volume of the body. After dimensional reasoning this may be written as:

angular motion:

$$M_{A_1} = C_{A_1} \rho_f V_b \frac{dv}{dt} D \tag{4.60}$$

4.6.4 Pressure terms

The pressure terms appear at the right hand side of Equation (4.33) as external forces on the fluid. As such they are treated differently from the drag and added mass terms.

An unsteady fluid flow is driven by external forces, which is revealed by the existence of a pressure gradient over the fluid. For an inviscid fluid with velocity v parallel to the x-axis, the pressure gradient is described by the Euler equation (without distributed forces per unit volume):

$$-\frac{1}{\rho_f} \frac{\partial p}{\partial x} = \frac{\partial v}{\partial t} + v \frac{\partial v}{\partial x} \tag{4.61}$$

For an incompressible, uniform parallel flow the convective term vanishes. The force due to the pressure gradient, in the absence of the body, is now given by:

$$X_P = \int\int_{V_b}\int -\frac{\partial p}{\partial x}\, dx\,dy\,dz = \int\int_{V_b}\int \rho_f \frac{\partial v}{\partial t}\, dV = \rho_f V_b \frac{dv}{dt} \qquad (4.62)$$

The force works along a line through the center of gravity of the body. Therefore, the torque due to the pressure gradient may be written as:

$$M_P = \rho_f V_b \frac{dv}{dt}\, e_{cg} \sin(\theta + \delta_{cg}) = K_P \rho_f V_b \frac{dv}{dt} D \qquad (4.63)$$

The position of the center of gravity is, analogous to the origin O' in figure 4.1, described by an eccentricity e_{cg} of the center of gravity from the center of rotation and an angle δ_{cg}, relative to the body frame. Thus K_P is introduced as a pressure coefficient, which is determined by the geometry and position of the body only.

The above equations hold for any body, no matter what the motion is.

4.7 Fluid force and torque coefficients

The coefficients C_1', C_2', ... in the kinetic energy equation of the fluid are constants, determined by the form and position of the body surface (representing its geometry), relative to the body frame and the density of the incompressible fluid only (section 4.1):

$$C_1',\ C_2',\ \ldots = f(\rho_f, x', y', z') \qquad (4.64)$$

The coordinates are further omitted.

The coefficients A_f, B_f, ... , A_f', B_f', ... in the fluid equations of motion are derived from the above coefficients (section 4.3). For a body which moves in its plane of symmetry (section 4.2) is for example:

$$\begin{aligned} A_f &= C_1' \cos\theta - C_6' \sin\theta \\ A_f' &= C_6' \cos\theta - C_2' \sin\theta \end{aligned} \qquad (4.65)$$

The coefficients are thus described in an analytical form, and dependent on the angular position of the body:

$$A_f, B_f, \ldots, A_f', \ldots = f(\rho_f, \theta) \tag{4.66}$$

Note that the forces and force coefficients are defined relative to the body frame (section 4.1). The transformation from the body frame to the fixed reference frame gives e.g. for the x- and y-components of the force term $d\dot{x}/dt$ (figure 4.1):

$$\begin{aligned} A_f &= A_f \cos\theta - A_f' \sin\theta \\ A_f' &= A_f \sin\theta + A_f' \cos\theta \end{aligned} \tag{4.67}$$

The drag and added mass coefficients, introduced in the drag and added mass terms of the fluid equations of motion (section 4.6), are proportional to the above coefficients. However, in the coefficients the dimensions of the body and the density of the fluid are excluded now. Thus, the dimensionless fluid force and torque coefficients are determined by the geometry and angular position of the body only:

$$C_{D,A} = f(\theta) \tag{4.68}$$

The pressure coefficient, introduced in the pressure term of the fluid equations of motion (section 4.6) is also only dependent on the angular position of the body:

$$K_P = f(\theta) \tag{4.69}$$

4.8 Review and conclusions

Equations of motion are developed for a body in an inviscid, unconfined and stagnant fluid. The equations are based on the dynamical theory of Kirchhoff and applied to the constrained motion of a body in its plane of symmetry. The equations of motion for the body and fluid are treated separately. The theory of Kirchhoff is extended to the motion of a body in an unsteady fluid flow. For this purpose the relative motion of body and fluid in a non-inertial system is considered. In the fluid equations of motion additional external forces arise, after the conversion from pseudo-forces to real forces, due to the pressure gradient over the fluid.

The equations of motion are applied to translating and rotating bodies. The terms in the fluid equations are subdivided into drag, added mass and pressure terms, which

are used in a somewhat extended sense. For these terms fluid force and torque coefficients are introduced, which are only dependent on the angular position of the body.

The equations of motion for inviscid fluids and the properties of the fluid force and torque coefficients form the basis for the development of equivalent equations for viscous fluids. To some extent the effects of an eccentricity (of the origin of the body frame relative to the center of rotation) are analogous to that of fluid viscosity. This analogy is used in the next chapter to make the step from inviscid to viscous fluids.

5 Motion of a body in an unconfined, viscous fluid

Following the theory for inviscid fluids, the motion of a body in an unconfined, viscous fluid is now studied. Although this chapter is not directly relevant to the confined flow problem of check valves, it may be considered as a pre-investigation for further developments (see section 1.3).

As in the previous chapter the body is assumed to have at least one plane of symmetry, while the motion is constrained to this plane.

The analogy between an eccentricity and fluid viscosity is used to make the step from inviscid to viscous fluids. General fluid equations of motion are developed from the equivalent equations for inviscid fluids with eccentricity. The equations are applied to translating and rotating bodies.

For unconfined (viscous) fluids most experimental data are available in the form of empirical relations for both the steady and the unsteady fluid force terms. These relations give a further insight into the properties of the fluid force coefficients, which to some extent may be applied to confined fluids.

5.1 General fluid equations of motion

In the previous chapter it is demonstrated that the hydrodynamic centre of a steady moving body in an inviscid fluid, coincides with the centre of rotation (section 4.4). Thus, the steady fluid forces and torque about this centre are uncoupled. Due to viscous effects the hydrodynamic centre moves from the centre of rotation. Consequently, in general the fluid forces and torque become fully coupled now, i.e. *all* fluid terms appear in the force as well as in the torque equations.

The effect of the move of the hydrodynamic centre is analogous to that of an eccentricity (section 4.4). This analogy is used here to make the step from inviscid to viscous fluids. The torque equation with eccentricity, given in Equation (4.33), now serves to supply all terms that are relevant to viscous fluids. This coupling of terms leads to:

$$A_f \frac{d(\dot{x}-v)}{dt} + B_f(\dot{x}-v)\dot{\theta} + C_f \frac{d\dot{\theta}}{dt} + D_f\dot{\theta}^2 + E_f(\dot{x}-v)^2 = F_f \frac{dv}{dt} - X'_f$$

$$A'_f \frac{d(\dot{x}-v)}{dt} + B'_f(\dot{x}-v)\dot{\theta} + C'_f \frac{d\dot{\theta}}{dt} + D'_f\dot{\theta}^2 + E'_f(\dot{x}-v)^2 = F'_f \frac{dv}{dt} - Y'_f$$

$$A''_f \frac{d(\dot{x}-v)}{dt} + B''_f e(\dot{x}-v)\dot{\theta} + C''_f \frac{d\dot{\theta}}{dt} + D''_f e\dot{\theta}^2 + E''_f(\dot{x}-v)^2 = F''_f \frac{dv}{dt} - M'_f \qquad (5.1)$$

The equations of motion for the body are similar to those for inviscid fluids (section 4.3.1), since all the effects of the fluid are accounted for in the fluid forces and torques on the body.

5.2 Translating and rotating bodies

The equations of motion for a body in a viscous fluid flow (section 5.1) are applied to translating and rotating bodies, in the sense described in section 4.5.

5.2.1 Linear motion

The fluid equation of motion directly follows from Equation (5.1)[1]:

linear motion:

$$X_f = C_D \frac{1}{2}\rho_f(v-\dot{x})^2 A + m_f \frac{d(v-\dot{x})}{dt} + \rho_f V_b \frac{dv}{dt} \qquad (5.2)$$

The fluid force consists of a drag, added mass and pressure term (section 5.3), where $m_f = C_A \rho_f V_b$ is the added mass of the body. The coefficients C_D and C_A are drag and added mass coefficients, respectively. The added mass and pressure terms are similar to those for inviscid fluids (section 4.5.1), although the added mass coefficient will differ in magnitude.

More about the physical meaning of the fluid terms and coefficients in the sections 5.3 and 5.4.

[1] For the conversion of A_f, B_f, ... into physical quantities it is referred to section 5.3.

About history effects .....

Boussinesq (1885), Basset (1888) and Oseen (1927) derive an equation of motion for a (small) sphere in a viscous, stagnant fluid. Tchen (1947) extends the equation to an accelerating flow. In this equation the fluid force on the sphere with diameter D is described by:

linear motion:

$$X_f = 3\pi\mu_f D(v-\dot{x}) + \tfrac{1}{2}\rho_f\tfrac{\pi}{6}D^3\frac{d(v-\dot{x})}{dt} + \rho_f\tfrac{\pi}{6}D^3\frac{dv}{dt}$$

$$+ \tfrac{3}{2}D^2\sqrt{\pi\rho_f\mu_f}\int_0^t \frac{d(v-\dot{x})}{dt'}\frac{1}{\sqrt{t-t'}}\,dt' \qquad (5.3)$$

This equation is derived from the Navier-Stokes equations and valid for small relative velocities ($Re < 1$) and accelerations. With a drag coefficient $C_D = 24/Re$ (Stokes equation; section 5.4.2), a volume of the sphere $V_b = \pi/6\ D^3$, an added mass $m_f = \frac{1}{2}\ \rho_f\ \pi/6\ D^3$ (section 4.6.3), and a Basset coefficient $C_B = 6$ (section 5.4.3). Equation (5.3) may be written in a general form as:

$$X_f = C_D\tfrac{1}{2}\rho_f(v-\dot{x})^2A + C_A\rho_f V_b\frac{d(v-\dot{x})}{dt} + \rho_f V_b\frac{dv}{dt} +$$

$$+ C_B A\sqrt{\frac{\rho_f\mu_f}{\pi}}\int_0^t \frac{d(v-\dot{x})}{dt'}\frac{1}{\sqrt{t-t'}}\,dt' \qquad (5.4)$$

In this form the equation is valid for a wider range of relative velocities (Reynolds numbers) and accelerations. This equation is identical to Equation (5.2), except from the last term.

This fourth term is the so-called *history or Basset term*, which represents the effect of the entire history of the unsteady motion of the sphere ($0 \le t' \le t$). At the instant $t = 0$ the velocities of fluid and particle are the same ($v = \dot{x}$). A theoretical derivation of this term is given by Landau and Lifshitz (1987), who give an explanation for the convolution integral on the analogy of the thermal conduction in a semi-infinite medium.

Hughes and Gilliland (1952) demonstrate by means of calculations that the history term may exceed the steady fluid force many times in the first stage of motion of a falling sphere. Maxey and Riley (1982) and Steetzel (1984) confirm this. Hereafter the motion becomes steady and the history term fades out.

Odar and Hamilton (1964) use Equation (5.4) to describe the fluid forces on an oscillating sphere in a stagnant fluid ($v = 0$) for Reynolds numbers up to 62. In that case the history term can be described in an analytical form and related to the oscillation frequency (Steetzel, 1984).

The added mass and history term may be described by dimensionless variables if the unsteady flow field can be characterized by some characteristic velocity. Let this velocity be $(v - \dot{x})^*$. Then the following dimensionless variables may be introduced:

$$\tau = \frac{t\,(v-\dot{x})^*}{D} \quad ; \quad \upsilon = \frac{v-\dot{x}}{(v-\dot{x})^*} \tag{5.5}$$

The history term may now be rewritten as:

$$\frac{C_B A}{\sqrt{\pi}}\,\rho_f (v-\dot{x})^{*2}\sqrt{\frac{\mu_f}{\rho_f (v-\dot{x})^* D}}\int_0^{\frac{D\tau}{(v-\dot{x})^*}} \frac{d\upsilon}{d\tau'}\frac{1}{\sqrt{\tau-\tau'}}\,d\tau' \tag{5.6}$$

and the added mass term as:

$$\frac{C_A V_b}{D}\,\rho_f (v-\dot{x})^{*2}\,\frac{d\upsilon}{d\tau} \tag{5.7}$$

To get an idea about the relative importance of the history term the following dimensionless number, defined as the ratio of the history term and added mass term, may now be introduced as:

$$\frac{\frac{C_B A}{\sqrt{\pi}}\sqrt{\frac{1}{Re^*}}\int_0^{\frac{D\tau}{(v-\dot{x})^*}} \frac{d\upsilon}{d\tau'}\frac{1}{\sqrt{\tau-\tau'}}\,d\tau'}{\frac{C_A V_b}{D}\,\frac{d\upsilon}{d\tau}} \tag{5.8}$$

Suppose that $dv/d\tau'$ is constant, this expression reduces to:

$$\frac{2}{\sqrt{\pi}}\,\frac{C_B A\,D}{C_A V_b}\sqrt{\frac{\tau}{Re^*}}\left(1-\sqrt{1-\frac{D}{(v-\dot{x})^*}}\right) \tag{5.9}$$

In this case the relative importance of the history term increases in time and decreases with increasing Reynolds number. For small time scales and higher Reynolds numbers the ratio is much smaller than unity. Under these conditions the history term may be neglected.

The history term is also used for turbulent flows (e.g. Maxey and Riley, 1982). If the turbulence scale is small relative to the size of the particle, the main effect of the turbulence is found as an increase of the flow resistance. If the turbulence scale is relatively large, the particles will tend to follow the turbulence components (Hinze, 1975).

Mei et al (1991) investigate the influence of the history term on the dispersion of small spherical particles due to isotropic turbulence. In the statistical analysis the ratio of the turbulence time scale and the particle response time is varied strongly. It is concluded that the history term has very little effect on the macroscopic behaviour of the particle motion. This conclusion also holds if the turbulence time scale is one order higher than the response time of the particle.

Although history effects do not exist in inviscid, incompressible fluids, they do exist in inviscid, compressible fluids, due to a finite pressure wave speed!

The importance of the history term for the present study must be attributed to the the fact that it demonstrates that the unsteady fluid force is not only dependent of instantaneous values, but also dependent on the history of the flow field.

5.2.2 Angular motion

The fluid equation of motion directly follows from Equation (5.1)[2]:

angular motion:

$$M_f = C_{D_1}\,\frac{1}{2}\rho_f v^2\,D^3 + C_{D_{12}}\,\frac{1}{2}\rho_f v\dot{\theta}\,D^4 - C_{D_2}\,\frac{1}{2}\rho_f \dot{\theta}^2\,D^5 + \\ + \left(C_{A_1} + K_P\right)\rho_f V_b \frac{dv}{dt} D - I_f \frac{d\dot{\theta}}{dt} \qquad \textbf{(5.10)}$$

The fluid torque consists of three drag, two added mass and one pressure term (section 5.3), where $I_f = C_{A2}\,\rho_f\,V_b\,k^2$ is the added mass moment of inertia of the body. The coefficients $C_{D..}$ and $C_{A..}$ are drag and added mass coefficients, due to the linear motion of the fluid (subscript 1), the angular motion of the body (subscript 2), and combined motion (subscript 12). The added mass and pressure terms are similar to those for inviscid fluids (section 4.5.2), although the added mass coefficients will differ in magnitude.

More about the physical meaning of the fluid terms and coefficients in the sections 5.3 and 5.4.

About history effects .....

The history term for angular motion is unknown.

[2] For the conversion of A_f, B_f, ... into physical quantities it is referred to section 5.3.

5.3 Physical aspects

For incompressible, inviscid fluids the coefficients in the equations of motion can be derived directly from the velocity potential or indirectly from the superposition principle (section 4.6.1). Thus all fluid terms can be considered separately and described in an analytical form (section 4.7).

For viscous fluids the dynamical theory of Kirchhoff and the superposition principle no longer hold, due to the dissipation of energy. The fluid terms are correlated now and should be considered together. In practice, however, the superposition principle is still applied, since there is no good alternative. Consequently, an inaccuracy arises in the determination and application of the fluid terms and coefficients, in particular for unsteady flow conditions, which magnitude is not known exactly. In a strict sense the terms can no longer be described in an analytical form.

5.3.1 Drag terms

The (steady) drag terms are isolated by considering the steady motion of a body in a steady, uniform parallel flow. Now Equation (5.1) reduces to:

$$X'_f = B_f(v-\dot{x})\dot{\theta} - D_f\dot{\theta}^2 - E_f(v-\dot{x})^2$$

$$Y'_f = B'_f(v-\dot{x})\dot{\theta} - D'_f\dot{\theta}^2 - E'_f(v-\dot{x})^2 \qquad \textbf{(5.11)}$$

$$M'_f = B''_f e(v-\dot{x})\dot{\theta} - D''_f e\dot{\theta}^2 - E''_f(v-\dot{x})^2$$

For the translating and rotating bodies considered in section 5.2, these equations reduce to:

linear motion:

$$X_f = -E_f(v-\dot{x})^2 \qquad \textbf{(5.12)}$$

angular motion:

$$M_f = B''_f ev\dot{\theta} - D''_f e\dot{\theta}^2 - E''_f v^2 \qquad \textbf{(5.13)}$$

After dimensional reasoning the equations may be rewritten as:

linear motion:

$$X_f = C_D \frac{1}{2}\rho_f (v - \dot{x})^2 A \tag{5.14}$$

angular motion:

$$M_f = C_{D_1} \frac{1}{2}\rho_f v^2 D^3 + C_{D_{12}} \frac{1}{2}\rho_f v\dot{\theta} D^4 - C_{D_2} \frac{1}{2}\rho_f \dot{\theta}^2 D^5 \tag{5.15}$$

The drag force and torque are assumed to be proportional to the dynamic pressure used in a somewhat extended sense (see below), and a characteristic area (e.g. the frontal area) or volume of the body (represented by D^3), respectively.

About dynamic pressure .....

The dynamic pressure $\frac{1}{2}\rho_f v^2$, defined as the difference between the total pressure (at the stagnation point upstream of the body) and the static pressure (in the wake downstream of the body), is a direct measure for the pressure difference across a body in a viscous fluid flow.

The effect of a parallel flow (v) is the same as that of a translating body ($-\dot{x}$). For rotating bodies similar considerations hold. Thus the characteristic fluid velocity v may be replaced by $-\dot{x}$ or $-\dot{\theta} D$. In this way several forms arise for the dynamic pressure which are found in the above equations.

Within the drag usually a distinction is made between *form* drag, due to normal stresses (pressure), and *friction* drag due to shear stresses. In a strict sense the dynamic pressure is a measure for the form drag only.

The fluid torque in Equation (5.15) consists of three drag terms. For a rotating body in an inviscid fluid flow only the drag term with v^2 appears (Equation (4.40)). Apparently the other two terms arise due to viscous effects. The equation is similar to its inviscid, steady equivalent with eccentricity (Equation (4.42)).

Although the motion of the body and that of the fluid far from the body is steady, the flow pattern around the steady rotating body is periodical.

5.3.2 Added mass terms

The added mass terms for a body in a viscous fluid are basically the same as those for a body in an inviscid fluid (section 4.6.3). However, Equation (5.1) illustrates that the terms can no longer be isolated from the other terms, e.g. the drag terms are always involved. The added mass terms can no longer be determined exactly, but only be estimated.

5.3.3 Pressure terms

For an incompressible, Newtonian fluid with velocity v parallel to the x-axis, the pressure gradient is described by the Navier-Stokes equations (without distributed

forces, per unit volume):

$$-\frac{\partial p}{\partial x} = \rho_f \left[\frac{\partial v}{\partial t} + v \frac{\partial v}{\partial x} \right] - \mu_f \left[\frac{\partial^2 v}{\partial x^2} + \frac{\partial^2 v}{\partial y^2} + \frac{\partial^2 v}{\partial z^2} \right] \qquad \textbf{(5.16)}$$

In the case of a laminar, uniform parallel flow, both the convective and viscous terms vanish. In the case of a turbulent flow, the effects of turbulence on the pressure gradient are assumed to be neglectable. Consequently, the pressure terms are proportional to $\partial v/\partial t$ and the same as those for inviscid fluids (see further section 4.6.4).

5.4 Fluid force and torque coefficients

5.4.1 General

For incompressible, inviscid fluids the fluid force and torque coefficients are determined by the geometry and the angular position of the body only (section 4.7). For viscous fluids these coefficients are also determined by:

1) the deviation of the viscous, steady flow pattern from the inviscid, steady flow pattern. This leads to a change of the form drag, due to the development of boundary layers and flow separation, and the introduction of friction drag.
2) the deviation of the viscous, unsteady flow pattern from the inviscid, unsteady flow pattern. This leads to a change of the added mass terms and the introduction of the history term.

According to the (dimensionless) Navier-Stokes equations the pressure field around a body is dependent on the Reynolds, Mach (e.g. Schlichting, 1979) and Acceleration number (e.g. Odar and Hamilton, 1964). These effects are found in all terms of the fluid equations of motion. Therefore the force and torque coefficients formally must be written as:

$$C_{D,A,B} = f\left(\theta,\ Re,\ Ma,\ Ac\right) \qquad \textbf{(5.17)}$$

For the *incompressible* or *slightly compressible* fluids considered here, the compressibility effects, represented by the Mach number, are further ignored.

In general the Reynolds and Acceleration number are introduced as a measure for the relative importance of viscous and unsteady flow effects, respectively. At the same time they serve to specify the (instantaneous) flow conditions around the body.

For a body which moves in its plane of symmetry in a uniform parallel flow, the following Reynolds and Acceleration numbers are introduced:

$$Re_1 = \frac{\rho_f (v-\dot{x}) D}{\mu_f} \quad \Lambda \quad Re_2 = \frac{\rho_f \dot{\theta} D^2}{\mu_f} \tag{5.18}$$

$$Ac_1^{-1} = \frac{D}{(v-\dot{x})^2} \frac{d(v-\dot{x})}{dt} \quad \Lambda \quad Ac_2^{-1} = \frac{1}{\dot{\theta}^2} \frac{d\dot{\theta}}{dt}$$

The general form of these numbers is consistent with the terms in the general equations of motion (section 5.1). Note that the unsteady flow conditions (in terms of *dv/dt*) and the history of the flow field are not specified by these numbers.

5.4.2 Drag coefficients

The (steady and unsteady) drag coefficients are generally dependent on the angular position of the body (angle of incidence), the Reynolds and Acceleration numbers. Viscous effects are assumed to be first order effects, which dominate second order, unsteady flow effects.

For the body of consideration this may be written as[3]:

$$C_D = f\left(\theta\,,\ Re_{1,2}\,,\ Ac_{1,2}\right) \tag{5.19}$$

Stokes (1851) derives for the drag coefficient of a **sphere** in a laminar, uniform parallel flow ($Re_d < 1$; based on diameter *d*):

linear motion:

$$C_D = \frac{24}{Re_d} \tag{5.20}$$

Torobin and Gauvin (1961) extend Stokes expression to ($1 < Re_d < 100$):

$$C_D = \frac{24}{Re_d}\left(1 + 0.197\, Re_d^{0.63} + 0.0026\, Re_d^{1.38}\right) \tag{5.21}$$

Many more examples exist (e.g. Schlichting, 1979).

---

[3] First order effects are printed in bold type.

The above cases demonstrate that the drag coefficient generally may be described or approximated by a *power law* as:

$$C_D = \frac{C}{Re^k} \tag{5.22}$$

The coefficient C and power k are functions of the angular position of the body, and valid for a range of **Reynolds** and Acceleration numbers. The power characterizes the flow in terms of laminar ($0.5 \leq k \leq 1$) or turbulent ($0 \leq k < 0.5$) (see also the examples in section 6.8.2). The power k is in principle a function of the angular position, which is illustrated by the following example: The flow around an aerofoil may be laminar at zero incidence and (partly) turbulent at stalled conditions at the same range of Reynolds numbers.

Note that the drag coefficient $C_D \rightarrow \infty$ for $Re \rightarrow 0$ if the power $k \neq 0$. This is allowed, since the drag force vanishes for small velocities, due to the presence of the quadratic velocity in the dynamic pressure.

About the power law ...

The power law is a general formulation, which allows to describe increasing or decreasing tendencies. Such a tendency is described by the combination of a coefficient C and power k, which are constants within a certain range (here of Reynolds numbers). As an example: The decreasing tendency in Equation (5.21) may be approximated by $C = 29$ and $k = 0.7$ in the range $1 < Re_d < 100$.

For the determination of the drag coefficients both experimental and theoretical approaches are used.

The drag coefficients are usually measured under steady flow conditions, so that $Re_1 \neq 0$ and $Ac_1^{-1} = 0$ or $Re_2 \neq 0$ and $Ac_2^{-1} = 0$. In practice these conditions are realized by a stationary body in a steady flow (e.g. wind tunnel tests), a steady translating body in a stagnant fluid (e.g. the test flight of an airplane) or a rotating body in a stagnant fluid.

Under laboratory conditions the drag terms are usually obtained from force or pressure measurements. Alternatively the terms may be obtained from the change of momentum per time unit, which is calculated from the velocity profile in the wake of the body. Under confined flow conditions a correction (e.g. for tunnel wall effects) may be necessary.

Under unsteady flow conditions the drag terms cannot be isolated anymore from the other terms. For this reason the unsteady drag coefficient is commonly assumed to be equal to the steady-state value. Note that the Reynolds numbers now have instantaneous values.

The drag coefficients may also be obtained in a theoretical way. Within the wide field of computational fluid dynamics (CFD), the numerical treatment of the Navier-Stokes equations gains interest. However, this approach is still less accurate than the experimental approach, due to amongst others numerical dispersion and limitations in the turbulence modelling.

More about the physical meaning of the Reynolds number in section 11.8.

5.4.3 Added mass and Basset coefficients

The added mass and Basset coefficients are generally dependent of the angular position of the body, the Reynolds and Acceleration numbers. For these coefficients the unsteady flow effects are assumed to be first order effects, which dominate second order, viscous effects.

For the body of consideration this may be written as[4]:

$$C_{A,B} = f\left(\theta\,,\ Re_{1,2}\,,\ Ac_{1,2}\right) \tag{5.23}$$

Boussinesq (1885), Basset (1888), Oseen (1927) and Tchen (1947) take the added mass and Basset coefficient of a **sphere** as (see Equation (5.3) and (5.4)):

linear motion:

$$C_A = \tfrac{1}{2} \quad \Lambda \quad C_B = 6 \tag{5.24}$$

The coefficients are valid for small relative velocities ($Re < 1$) and accelerations. The added mass coefficient is the same as that for inviscid fluids (section 4.6.3), since in both cases flow separation and turbulence play no role.

Hardly anything is known about these coefficients at higher Reynolds numbers and accelerations (Torobin and Gauvin, 1959; Schöneborn, 1974).

Odar and Hamilton (1964) give the following empirical relations for higher Reynolds numbers ($Re < 62$, $Ac < 5$), derived from oscillation tests of a sphere in a stagnant fluid:

linear motion:

$$C_A = 1.05 - \frac{0.066}{Ac^2 + 0.12} \quad \Lambda \quad C_B = 2.88 + \frac{3.12}{(Ac+1)^2} \tag{5.25}$$

[4] First order effects are printed in bold type.

so that:

$$\frac{dC_A}{dAc} = \frac{0.132\,Ac}{(Ac^2+0.12)^2} \quad \wedge \quad \frac{dC_B}{dAc} = -\frac{6.24}{(Ac+1)^3} \tag{5.26}$$

The added mass coefficient increases and the Basset coefficient decreases with increasing acceleration (figure 5.1). For $Ac \to 0$ the values in Equation (5.24) are obtained. For $Ac > 1$ the added mass coefficient is about equal to unity and doubled, which is due to viscous effects. Note that $dC_A/dAc \to 0$ for $Ac \to 0$ and for $Ac \to \infty$.

The added mass and Basset coefficients are also dependent on the Reynolds number, which is revealed by the fact that the validity range of the equations is restricted to $Re < 62$. In that sense the Reynolds effect may be seen as a second order effect.

Nothing is known about added mass and Basset coefficients for *angular motion*.

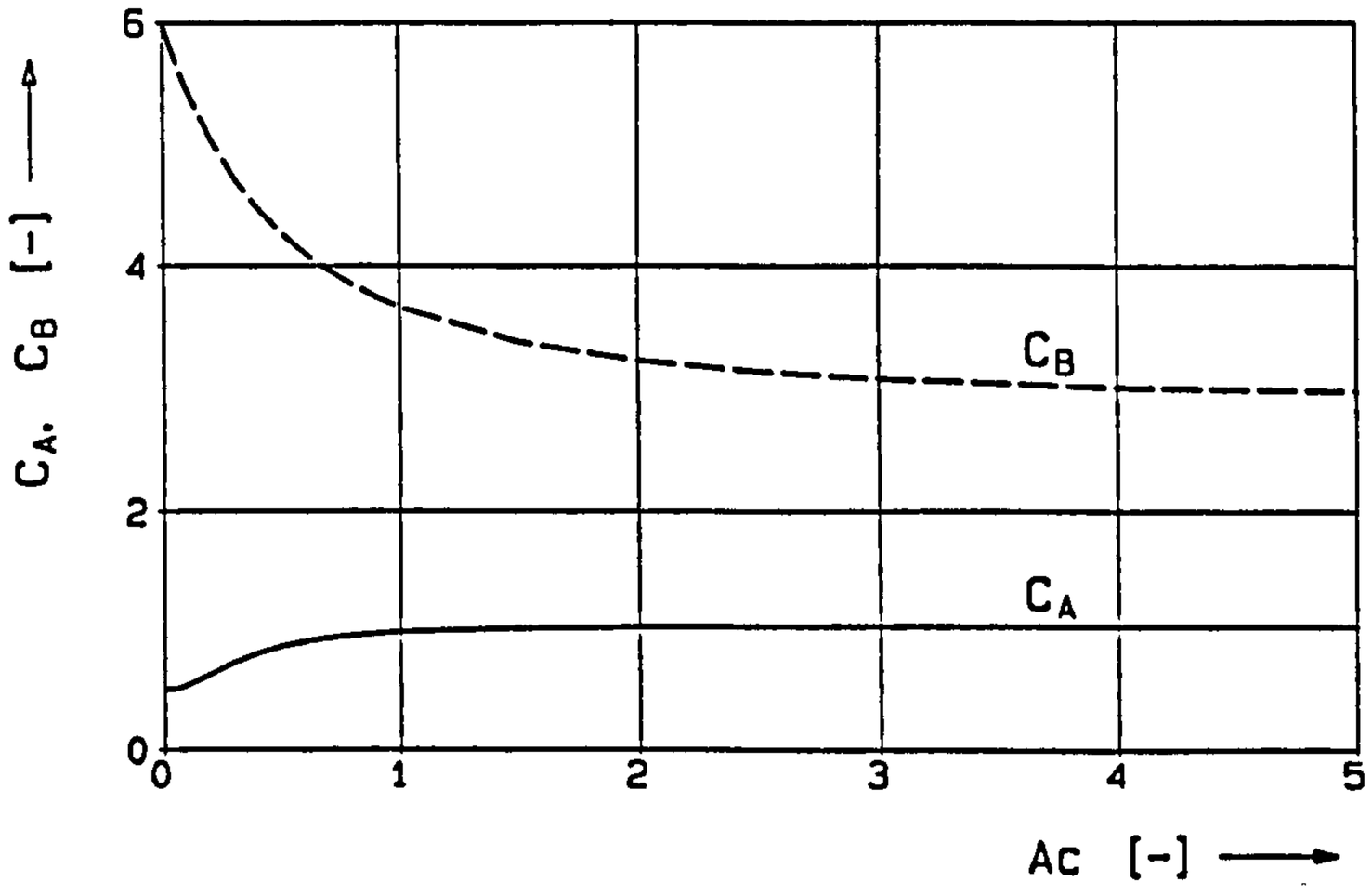

Figure 5.1 Added mass and Basset coefficients of a sphere (Re < 62)
(Odar and Hamilton, 1964)

On the analogy of the drag coefficient, also here a *power law* is introduced for the added mass and Basset (history) coefficients:

$$C_{A,B} = \frac{C}{Ac^n} \tag{5.27}$$

The coefficient C and power n are functions of the angular position of the body, and valid for a range of **Acceleration** and Reynolds numbers. Here the power may be positive (in a range of decreasing coefficients) as well as negative (in a range of increasing coefficients).

Note that in the above equation the added mass coefficient $C_A \to \infty$ for $Ac \to 0$ and $C_A \to 0$ for $Ac \to \infty$, if the power $n \neq 0$. The added mass coefficient, however, must have a finite value for small accelerations, to ensure that the added mass force vanishes. This finite value must differ from zero, which follows from the dynamical theory of Kirchhoff for inviscid fluids. Thus the power is preconditioned by $n \to 0$ if $Ac \to 0$ and for similar reasons if $Ac \to \infty$. This is in agreement with the empirical relation given in Equation (5.25).

The Basset coefficient in Equation (5.25) may be approximated by a power law with $C = 3.81$ and $n = 0.156$ in the range $0.1 < Ac < 5$.

In the literature both experimental and theoretical approaches are found to determine the added mass and Basset coefficients of a body in a viscous, unconfined fluid. Within the experimental approach two principles are applied:

1. *Non-periodical flow tests*. Tests may be performed on an accelerating body in a stagnant fluid (e.g. the falling of a small sphere), or on a stationary body in an accelerating flow. However, in practice, an unconfined, accelerating flow can hardly be realized. The added mass and history terms may be derived from force or torque measurements, after correction for the drag and pressure terms. Hereby the unsteady drag coefficients are usually assumed to be equal to the steady values (superposition principle). Alternatively, the fluid forces may be derived from the trajectory which is followed by the body (e.g. Talman, 1994).
2. *Periodical flow tests*. Oscillation tests are performed, whereby the oscillation frequency of the system (i.e. body and fluid) is chosen as a non-imposed (natural) frequency or an imposed (excitation) frequency. The motion of the body may be constrained to small displacement amplitudes, so that the drag terms can be ignored (e.g. Odar and Hamilton, 1964).

The theoretical approaches are based on potential flow theory and applied to cases where flow separation and turbulence play a role of minor importance. History effects are absent here.

More about the physical meaning of the Acceleration number in section 11.8.

5.4.4 Pressure coefficients

The pressure coefficients are similar to those for inviscid fluids (section 4.6.4).

5.5 Review and conclusions

Equations of motion for a body in an unconfined, viscous fluid are developed. The equations are obtained by coupling the terms in the force and torque equations for inviscid fluids. The equations are applied to translating and rotating bodies. History effects are described for (small) translating bodies under special initial conditions. The history terms for other initial conditions and rotating bodies are unknown.

In the description of the fluid force and torque coefficients separate Reynolds and Acceleration numbers are introduced for the relative, linear motion of the body, and for its angular motion. The drag coefficients in the fluid equations are assumed to be dominated by viscous effects. Based on the few empirical relations which are available in the literature, the added mass and Basset coefficients are assumed to be dominated by inertia effects. The coefficients are described in the form of power laws. The properties of the drag, added mass and Basset coefficients form the basis for the development of equivalent coefficients for confined fluids in the next chapter. The power law formulation for the drag coefficients enables a distinction between laminar and turbulent flows. For this purpose it is further used in the development of (dimensionless) equations of motion for check valves (chapter 8).

6 Motion of a body in a confined fluid

The previous chapters deal with the motion of a body in an unconfined fluid. The unconfined flow problem is treated by the dynamical theory of Kirchhoff. Although this theory allows no geometrical changes, it may be considered as a pre-investigation for the confined flow problem of check valves. In this chapter the motion of a body in a confined fluid is studied. In the case of more than one moving body, or when the fluid is confined by fixed walls (wholly or in part), Lagrange's method of generalized coordinates may be applied (Lamb, 1932).

General equations of motion are developed, based on Lagrange's method of generalized coordinates. The basic concept is similar to that of the dynamical theory of Kirchhoff, which allows no geometrical changes. On the analogy of check valves, the motion is constrained to a motion in the plane of symmetry. In the first instance the motion of the fluid is entirely due to that of the body. Within this study the theory is extended to the motion of a body in an unsteady fluid flow. Equations of motion are derived for translating and rotating bodies. Some physical aspects of the fluid force terms and coefficients are discussed. The theory is applied to check valves, in order to develop a valve equation of motion (chapter 8).

6.1 Method of generalized coordinates

Consider the motion of a body in an inviscid and confined fluid. The motion of the fluid is entirely due to that of the body, and is therefore irrotational and acyclic.

Let q_1, q_2, ..., q_n, be a system of generalized coordinates, which serve to specify the configuration of the body. The velocity potential at any instant will be of the form:

$$\phi = \dot{q}_1\phi_1 + \dot{q}_2\phi_2 + \ldots\ldots + \dot{q}_n\phi_n + \ldots\ldots \tag{6.1}$$

where ϕ_1, ϕ_2, ..., ϕ_n are determined in a manner analogous to that in section 4.1.

The kinetic energy of the fluid may be described by:

$$2T_f = -\rho_f \int_S \int \phi \frac{\partial \phi}{\partial n}\, dS \tag{6.2}$$

Substitution of Equation (6.1) into Equation (6.2) now gives:

$$2T_f = C_1' \dot{q}_1^2 + C_2' \dot{q}_2^2 + \ldots\ldots + 2C_6' \dot{q}_1 \dot{q}_2 + \ldots\ldots \qquad (6.3)$$

The kinetic energy of the body T_b can be written in a similar form, so that the energy of the system of body and fluid is described by:

$$2T = C_1 \dot{q}_1^2 + C_2 \dot{q}_2^2 + \ldots\ldots + 2C_6 \dot{q}_1 \dot{q}_2 + \ldots\ldots \qquad (6.4)$$

The major difference with the dynamical theory of Kirchhoff (chapter 4) is that the coefficients are no longer constants, determined by the geometry of the body only, but functions of the coordinates $q_1, q_2, \ldots, q_n$.

The equations of motion in generalized coordinates, derived from the *principle of virtual work* and *D'Alembert's principle*, and often referred to as Lagrange equations, are given by (e.g. Goldstein, 1980):

$$\frac{d}{dt}\left[\frac{\partial T}{\partial \dot{q}_j}\right] - \frac{\partial T}{\partial q_j} = F_{q_j} \qquad (j = 1,2,\ldots\ldots,n) \qquad (6.5)$$

The components of the generalized force are defined as:

$$F_{q_j} = \sum_i F_i \cdot \frac{\partial r_i}{\partial q_j} \qquad (6.6)$$

Where r_i are the coordinates and F_i the components of the forces on the system. The components of the generalized force do not need to have the dimension of a force, as long as $F_q\, \partial q$ has the dimensions of work.

The limitation in the application of the method of generalized coordinates lies in the fact that the functional relations for the coefficients C_1, C_2, ... may become very complex. In the next sections the equations are used in a qualitative sense only.

About the Lagrangian .....

The forces on a system can often be derived from a scalar potential function V. In that case the generalized force can be written as:

$$F_{q_j} = -\frac{\partial V}{\partial q_j} \qquad (6.7)$$

The potential function V does not depend on the generalized velocities, so that $\partial V/\partial \dot{q}_j = 0$.

Thus Equation (6.5) may be rewritten as:

$$\frac{d}{dt}\left(\frac{\partial L}{\partial \dot{q}_j}\right) - \frac{\partial L}{\partial q_j} = 0 \tag{6.8}$$

where:

$$L = T - V \tag{6.9}$$

The term *Lagrange equations* is usually reserved for the more general form given in Equation (6.8), where L is known as the *Lagrangian*. The equations may also be derived from *Hamilton's principle*, also known as *variational principle* (Goldstein, 1980).

In the classical mechanics of rigid bodies the Lagrange equations are often applied to conservative systems. In that case the potential function V is no explicit function of time, so that the terms $\partial T/\partial q_j$ may be derived from V and described in terms of q_j. However, the equations are not necessarily restricted to conservative systems, but may also be applied if V is an explicit function of time.

The Lagrange equations may be considered as the basic postulate, rather than Newton's laws of motion, since they also may be applied to non-mechanical systems, as in the theory of fields.

The Lagrangian is not suited to check valves, since e.g. damping and friction effects are not easily described by potential functions.

6.2 Constrained motion in the plane of symmetry

The equations of motion in generalized coordinates (section 6.1) are applied to a body, which moves in its plane of symmetry, in the sense described in section 4.2.

The body is assumed to have a *plane of symmetry*. Let this plane be the x-y-plane. The constrained motion is described by a translation parallel to the plane, with linear velocity components $\dot{x} \neq 0$, $\dot{y} \neq 0$, and a rotation about an axis normal to this plane, with angular velocity component $\dot{\theta} \neq 0$.

The generalized coordinates are chosen as: $q_1 = x$, $q_2 = y$ and $q_3 = \theta$. This coordinate system may be considered as a reference frame, which is fixed in space.

The kinetic energy of the system is now described by:

$$2T = C_1\dot{x}^2 + C_2\dot{y}^2 + 2C_6\dot{x}\dot{y} + C_9\dot{\theta}^2 + 2\dot{\theta}\left(C_{19}\dot{x} + C_{20}\dot{y}\right) \tag{6.10}$$

where C_1, C_2, ... $= f(x, y, \theta)$. Note that in the dynamical theory of Kirchhoff the coefficients are defined relative to the body frame (section 4.1).

Substitution of Equation (6.10) in Equation (6.5) yields:

$$\frac{dC_1\dot{x}}{dt} + \frac{dC_6\dot{y}}{dt} + \frac{dC_{19}\dot{\theta}}{dt} - \frac{\partial T}{\partial x} = \sum X$$

$$\frac{dC_6\dot{x}}{dt} + \frac{dC_2\dot{y}}{dt} + \frac{dC_{20}\dot{\theta}}{dt} - \frac{\partial T}{\partial y} = \sum Y \qquad \textbf{(6.11)}$$

$$\frac{dC_{19}\dot{x}}{dt} + \frac{dC_{20}\dot{y}}{dt} + \frac{dC_9\dot{\theta}}{dt} - \frac{\partial T}{\partial \theta} = \sum M$$

The motion of the body is now further constrained to a translation along the x-axis ($\dot{y} = 0$) and a rotation about the z-axis (section 4.2). After some manipulation the above equations become:

$$C_1\frac{d\dot{x}}{dt} + C_{19}\frac{d\dot{\theta}}{dt} + \frac{\partial C_1}{\partial x}\dot{x}^2 + \left[\frac{\partial C_1}{\partial \theta} + \frac{\partial C_{19}}{\partial x}\right]\dot{x}\dot{\theta} + \frac{\partial C_{19}}{\partial \theta}\dot{\theta}^2 - \frac{\partial T}{\partial x} = \sum X$$

$$C_6\frac{d\dot{x}}{dt} + C_{20}\frac{d\dot{\theta}}{dt} + \frac{\partial C_6}{\partial x}\dot{x}^2 + \left[\frac{\partial C_6}{\partial \theta} + \frac{\partial C_{20}}{\partial x}\right]\dot{x}\dot{\theta} + \frac{\partial C_{20}}{\partial \theta}\dot{\theta}^2 - \frac{\partial T}{\partial y} = \sum Y$$

$$C_{19}\frac{d\dot{x}}{dt} + C_9\frac{d\dot{\theta}}{dt} + \frac{\partial C_{19}}{\partial x}\dot{x}^2 + \left[\frac{\partial C_{19}}{\partial \theta} + \frac{\partial C_9}{\partial x}\right]\dot{x}\dot{\theta} + \frac{\partial C_9}{\partial \theta}\dot{\theta}^2 - \frac{\partial T}{\partial \theta} = \sum M \qquad \textbf{(6.12)}$$

where:

$$\frac{\partial T}{\partial x} = \frac{1}{2}\frac{\partial C_1}{\partial x}\dot{x}^2 + \frac{1}{2}\frac{\partial C_9}{\partial x}\dot{\theta}^2 + \frac{\partial C_{19}}{\partial x}\dot{x}\dot{\theta}$$

$$\frac{\partial T}{\partial y} = \frac{1}{2}\frac{\partial C_1}{\partial y}\dot{x}^2 + \frac{1}{2}\frac{\partial C_9}{\partial y}\dot{\theta}^2 + \frac{\partial C_{19}}{\partial y}\dot{x}\dot{\theta} \qquad \textbf{(6.13)}$$

$$\frac{\partial T}{\partial \theta} = \frac{1}{2}\frac{\partial C_1}{\partial \theta}\dot{x}^2 + \frac{1}{2}\frac{\partial C_9}{\partial \theta}\dot{\theta}^2 + \frac{\partial C_{19}}{\partial \theta}\dot{x}\dot{\theta}$$

For a rigid body the change of kinetic energy with the position of the body refers to the fluid only.

About a sphere .....

Consider the one-dimensional motion of a sphere normal to an infinite plane wall. Let x be the distance from the wall. The kinetic energy of the system is:

$$2T = C_1 \dot{x}^2 \tag{6.14}$$

The coefficient C_1, as originally derived by Stokes, is given by (Lamb, 1932):

$$C_1 = m_b + \tfrac{1}{2} \rho_f V_b \left(1 + \tfrac{3}{8} \frac{R^3}{x^3}\right) \qquad (x > R) \tag{6.15}$$

Where m_b is the mass, V_b is the volume and R is the radius of the sphere.

The equation of motion becomes:

$$C_1 \frac{d\dot{x}}{dt} + \tfrac{1}{2} \frac{\partial C_1}{\partial x} \dot{x}^2 = \sum X \tag{6.16}$$

About unconfined fluids .....

The kinetic energy of the fluid in an unconfined space is independent of the linear position of the body. Consequently the terms $\partial T/\partial x$ and $\partial T/\partial y$ must be zero. This must hold for any velocity, so that also $\partial C_1/\partial x$, $\partial C_2/\partial x$, ... , $\partial C_1/\partial y$, ... must be zero. Furthermore, the kinetic energy in terms of $\dot{\theta}^2$ is independent of the angular position of the body, so that also the term $\partial C_9/\partial \theta$ must be zero. This can easily be seen from the rotational symmetry which arises due to a pure rotation. Equation (6.12) now reduces to:

$$C_1 \frac{d\dot{x}}{dt} + C_{19} \frac{d\dot{\theta}}{dt} + \frac{\partial C_1}{\partial \theta} \dot{x}\dot{\theta} + \frac{\partial C_{19}}{\partial \theta} \dot{\theta}^2 = \sum X$$

$$C_6 \frac{d\dot{x}}{dt} + C_{20} \frac{d\dot{\theta}}{dt} + \frac{\partial C_6}{\partial \theta} \dot{x}\dot{\theta} + \frac{\partial C_{20}}{\partial \theta} \dot{\theta}^2 = \sum Y \tag{6.17}$$

$$C_{19} \frac{d\dot{x}}{dt} + C_9 \frac{d\dot{\theta}}{dt} - \tfrac{1}{2} \frac{\partial C_1}{\partial \theta} \dot{x}^2 = \sum M$$

This form of the Lagrange equations is similar to that of the Kirchhoff equations for unconfined fluids, as given in Equation (4.23) for $e \to 0$.

Equation (6.12) may be written in a general form as:

$$A\frac{d\dot{x}}{dt} + B\dot{x}\dot{\theta} + C\frac{d\dot{\theta}}{dt} + D\dot{\theta}^2 + E\dot{x}^2 = \sum X$$

$$A'\frac{d\dot{x}}{dt} + B'\dot{x}\dot{\theta} + C'\frac{d\dot{\theta}}{dt} + D'\dot{\theta}^2 + E'\dot{x}^2 = \sum Y \qquad \textbf{(6.18)}$$

$$A''\frac{d\dot{x}}{dt} + B''\dot{x}\dot{\theta} + C''\frac{d\dot{\theta}}{dt} + D''\dot{\theta}^2 + E''\dot{x}^2 = \sum M$$

The coefficients A, B, .., A', ... are dependent on the geometry of body and confined space, and the position of the body within the confined space, described by x and θ.

6.3 Separation of body and fluid

In this section separate equations of motion for the body and fluid are developed, just as is done in section 4.3.

6.3.1 Equations of motion for the body

The equations of motion for the body are similar to those for unconfined fluids. All effects of the fluid are accounted for in the fluid forces X_f, Y_f, ... on the body. The equations are given by (section 4.3.1; $e \to 0$):

$$A_b\frac{d\dot{x}}{dt} + B_b\dot{x}\dot{\theta} + C_b\frac{d\dot{\theta}}{dt} + D_b\dot{\theta}^2 = X_f + \sum X$$

$$A_b'\frac{d\dot{x}}{dt} + B_b'\dot{x}\dot{\theta} + C_b'\frac{d\dot{\theta}}{dt} + D_b'\dot{\theta}^2 = Y_f + \sum Y$$

$$A_b''\frac{d\dot{x}}{dt} + C_b''\frac{d\dot{\theta}}{dt} + E_b''\dot{x}^2 = M_f + \sum M \qquad \textbf{(6.19)}$$

The coefficients A_b, B_b, .., A_b', ... are dependent on the geometry and angular position of the body only (section 4.3.1). The equations also hold if there is no fluid.

6.3.2 Equations of motion for the fluid

The equations of motion for the fluid are obtained by the separation of the body and fluid terms in the general equations of motion, as described in section 4.3.

Separation of the terms in Equation (6.18) gives:

$$A_f \frac{d\dot{x}}{dt} + B_f \dot{x}\dot{\theta} + C_f \frac{d\dot{\theta}}{dt} + D_f \dot{\theta}^2 + E_f \dot{x}^2 = -X_f$$

$$A_f' \frac{d\dot{x}}{dt} + B_f' \dot{x}\dot{\theta} + C_f' \frac{d\dot{\theta}}{dt} + D_f' \dot{\theta}^2 + E' \dot{x}^2 = -Y_f \qquad \textbf{(6.20)}$$

$$A_f'' \frac{d\dot{x}}{dt} + B_f'' \dot{x}\dot{\theta} + C_f'' \frac{d\dot{\theta}}{dt} + D_f'' \dot{\theta}^2 + E_f'' \dot{x}^2 = -M_f$$

The coefficients A_f, B_f, .., A_f', .. are dependent of the geometry of body and confined space, and the *angular* and *linear* (spatial) position of the body in the confined space.

The equations illustrate which terms are relevant to the forces and torques on the body due to a confined, inviscid fluid. A comparison of Equation (4.26) ($e \rightarrow 0$) and Equation (6.20) illustrates that extra terms arise in the force and torque equations, due to the fact that the fluid is confined now.

6.4 Motion of a body in a fluid flow

Just like the Kirchhoff equations, the Lagrange equations may be applied to the motion of a body in a *fluid flow*. Hereto the motion is described in a *non-inertial* reference frame, which moves with the fluid (section 4.4). The confined space around the body must now be considered as a second moving "body".

The confined fluid flow is restricted to a *non-uniform parallel flow*, so that the motion of the fluid remains irrotational. The flow direction is assumed to be parallel to the x-axis, with a fluid velocity v, relative to the fixed reference frame.

Now, in a manner analogous to that in section 4.4, the term $\dot{x}$ in Equation (6.20) may be replaced by the term $(\dot{x} - v)$. The fluid velocity must be specified now, e.g. as the mean velocity $v = Q/A$. Further "real" force terms must be added due to the pressure gradient over the fluid. For a parallel pipe flow this term is proportional to dv/dt (section 6.7.3). This leads to the following equations of motion for the fluid:

$$A_f \frac{d(\dot{x}-v)}{dt} + B_f(\dot{x}-v)\dot{\theta} + C_f \frac{d\dot{\theta}}{dt} + D_f \dot{\theta}^2 + E_f(\dot{x}-v)^2 = F_f \frac{dv}{dt} - X_f$$

$$A_f' \frac{d(\dot{x}-v)}{dt} + B_f'(\dot{x}-v)\dot{\theta} + C_f' \frac{d\dot{\theta}}{dt} + D_f' \dot{\theta}^2 + E_f'(\dot{x}-v)^2 = F_f' \frac{dv}{dt} - Y_f$$

$$A_f'' \frac{d(\dot{x}-v)}{dt} + B_f''(\dot{x}-v)\dot{\theta} + C_f'' \frac{d\dot{\theta}}{dt} + D_f'' \dot{\theta}^2 + E_f''(\dot{x}-v)^2 = F_f'' \frac{dv}{dt} - M_f$$

(6.21)

The equations show which fluid terms are relevant to the motion of a body in a confined, fluid flow. The *complete equations of motion for body and fluid* can be obtained by the summation of the Equations (6.19) and (6.21).

6.5 Translating and rotating bodies

The equations of motion, as developed for a body in a fluid flow (section 6.4), are applied to translating or rotating bodies, moving in an inviscid, non-uniform, parallel flow. The bodies are assumed to have at least one plane of symmetry, in the sense as described in section 4.2. The equations of motion in the constrained directions are further ignored.

6.5.1 Linear motion

Consider a body which moves in the x-direction, so that $\dot{x} \neq 0$ and $\dot{\theta} = 0$, while the fluid velocity v is parallel to the x-direction.

The equation of motion for the body directly follows from Equation (6.19):

$$m_b \frac{d\dot{x}}{dt} = X_f + \sum X \qquad \textbf{(6.22)}$$

where $m_b = \rho_b V_b$ is the mass of the body.

The equation of motion for the fluid directly follows from Equation (6.21)[1]:

$$X_f = C_D \frac{1}{2}\rho_f (v-\dot{x})^2 A + m_f \frac{d(v-\dot{x})}{dt} + \rho_f V_b \frac{dv}{dt} \qquad (6.23)$$

The equation consists of a drag, added mass and pressure term (section 6.7), where $m_f = C_A \rho_f V_b$ is the added mass of the body. This equation of motion for confined, inviscid fluids is similar to that for unconfined, viscous fluids (section 5.2.1).

Although the fluid force on a steady translating body in an unconfined, inviscid, steady, uniform parallel flow is zero (section 4.6.2), the fluid force is proportional to $(v - \dot{x})^2$ here. According to the Equations (6.12) and (6.13) the term vanishes if $\partial T/\partial x$ is zero, e.g. for any body moving in a prismatic tube.

Substitution of Equation (6.23) in Equation (6.22) yields the complete equation of motion for translating bodies in an inviscid, confined, fluid flow:

$$(m_b + m_f)\frac{d\dot{x}}{dt} = C_D \frac{1}{2}\rho_f (v-\dot{x})^2 A + (C_A + 1)\rho_f V_b \frac{dv}{dt} + \sum X \qquad (6.24)$$

The term $(m_b + m_f)$ is the virtual mass of the body.

Valibouse and Verry (1983) use a similar expression for the fluid force on the translating disc of a piston type check valve. However, in the pressure term the volume of the valve chamber is used instead of the volume of the body, which is incorrect.

More about the physical meaning of the fluid terms and coefficients in the sections 6.7 and 6.8.

6.5.2 Angular motion

Consider a body which rotates about the z-axis, so that $\dot{x} = 0$ and $\dot{\theta} \neq 0$, while the fluid velocity v is parallel to the x-direction.

[1] For the conversion of A_f, B_f, ... into physical quantities it is referred to section 6.7.

The equation of motion for the body directly follows from Equation (6.19):

$$I_b \frac{d\dot{\theta}}{dt} = M_f + \sum M \tag{6.25}$$

where $I_b = \rho_b V_b k^2$ is the mass moment of inertia of the body (section 4.6.3).

The equation of motion for the fluid directly follows from Equation (6.21)[2]:

$$M_f = C_{D_1} \tfrac{1}{2}\rho_f v^2 D^3 + C_{D_{12}} \tfrac{1}{2}\rho_f v\dot{\theta} D^4 - C_{D_2} \tfrac{1}{2}\rho_f \dot{\theta}^2 D^5 + \left(C_{A_1} + K_P\right)\rho_f V_b \frac{dv}{dt} D - I_f \frac{d\dot{\theta}}{dt} \tag{6.26}$$

The equation consists of three drag terms, two added mass terms and one pressure term, where $I_f = C_{A2}\, \rho_f\, V_b\, k^2$ is the added mass moment of inertia of the body (section 4.6.3). This equation of motion for confined, inviscid fluids is similar to that for unconfined, viscous fluids (section 5.2.2).

Substitution of Equation (6.26) in Equation (6.25) yields the complete equation of motion for rotating bodies in an inviscid, confined, fluid flow:

$$\left(I_m + I_f\right)\frac{d\dot{\theta}}{dt} = C_{D_1} \tfrac{1}{2}\rho_f v^2 D^3 + C_{D_{12}} \tfrac{1}{2}\rho_f v\dot{\theta} D^4 - C_{D_2} \tfrac{1}{2}\rho_f \dot{\theta}^2 D^5 + \left(C_{A_1} + K_P\right)\rho_f V_b \frac{dv}{dt} D + \sum M \tag{6.27}$$

The term $(I_b + I_f)$ is the virtual mass moment of inertia of the body.

More about the physical meaning of the fluid terms and coefficients in the sections 6.7 and 6.8.

[2] For the conversion of A_f, B_f, ... into physical quantities it is referred to section 6.7.

6.6 Step to viscous fluids ...

The equations of motion for a body in an inviscid, confined fluid (section 6.4) are similar to those for a viscous, unconfined fluid (section 5.1). In both cases the fluid forces and torques are fully coupled. It is assumed that the general form of these equations remains unchanged for a body in a *confined, viscous flow*, although the force and torque coefficients will differ in magnitude. Thus the equations of motion for translating and rotating bodies (section 6.5) also hold for viscous fluids. History effects are not taken into account.

About history effects .....

In section 5.2.1 the history term is described for a translating body in an unconfined accelerating flow, with initial condition $(v - \dot{x}) = 0$. It is demonstrated that the relative importance of the history term increases in time and decreases with increasing Reynolds number, if the relative flow acceleration is constant in time.

For confined flows the history term is unknown. However, it is expected that the history effect is smaller here, since the development of upstream disturbances and downstream wakes is more or less suppressed by the presence of a confined space. Therefore the author believes that, in a qualitative sense, the above-mentioned tendencies also hold for confined flows.

Note that for check valves with translating elements the initial condition $(v - \dot{x}) = 0$ is not satisfied, since under steady flow conditions $v \neq 0$ and $\dot{x} = 0$. Dependent on the valve type, the turbulence scale of eddies may vary from small to large, relative to the size of the body. On the other hand, in the dimensionless history and added mass terms in Equation (5.8) the critical velocity may be chosen as characteristic velocity. For check valves and liquids the dimensionless time scale and critical Reynolds number are usually in the order of 10 and 10^5 - 10^6, respectively.

6.7 Physical aspects

The terms in the fluid equations of motion in section 6.4 are similar to those for unconfined, viscous fluids (section 5.1). The major difference is that the coefficients are now also dependent on the linear (spatial) position of the body.

For confined, inviscid fluids the fluid terms may be determined from the velocity potential or by applying the superposition principle, although the isolation of terms, apart from some drag terms, can no longer be realized. These principles are already discussed in section 4.6.1.

For confined, viscous fluids the concept of generalized coordinates and the superposition principle no longer hold, due to the dissipation of energy. However, just like for unconfined viscous fluids, the superposition principle is still applied. Also here the fluid terms can no longer be described in an analytical form.

6.7.1 Drag terms

The drag terms are similar to those for unconfined, viscous fluids (section 5.3.1).

6.7.2 Added mass terms

For confined, inviscid fluids the added mass effects may be determined directly from the velocity potential. However, this approach is restricted due to the complexity of the potential function and hardly used in practice.

The added mass of a **sphere**, which moves normal to an infinite plane wall (section 6.1), follows from the coefficient C_1 in Equation (6.15) as:

linear motion:

$$m_f = \frac{1}{2}\rho_f V_b \left(1 + \frac{3}{8}\frac{R^3}{x^3}\right) \qquad (6.28)$$

For $x \rightarrow \infty$ the added mass is equal to the value in an unconfined space (section 4.6.3).

For **check valves** a different approach is found in the literature. Valibouse and Verry (1983) approximate the added mass of the **translating disc** of a piston type check valve by:

linear motion:

$$m_f = \rho_f \left(\frac{A_{disc}}{A_{cham} - A_{disc}}\right) V_{cham} \qquad (6.29)$$

where A_{disc} and A_{cham} represent the area of the valve disc and chamber, respectively. Note that $m_f \rightarrow \infty$, if $A_{disc} = A_{cham}$.

Worster (1959) and Schneider (1985) take the added mass of the **rotating disc** of a swing type check valve as the mass of a fluid sphere with the same diameter as the valve disc ($C_A > 1$):

angular motion:

$$m_f = \rho_f \frac{1}{6}\pi D_{disc}^3 \qquad (6.30)$$

In the above equations the added mass is described in an analytical form, which is typical for inviscid fluids. Note that the dependency on the (linear or angular) disc position is not described.

For the estimation of added mass effects in confined, viscous fluids experimental approaches are found in the literature, which are based on periodical flow tests. This is already discussed in section 5.4.3. Non-periodical flow tests are absent here.

Thorley and Oei (1981) determine the added mass effect of the **rotating disc** of a swing type check valve from oscillation tests. The mass moment of inertia of the disc is obtained from the natural frequency in air. The virtual mass moment of inertia is obtained from the natural frequency in stagnant water. In order to minimize bearing friction the disc is supported by knife-edges. The drag term is assumed to be of minor importance by allowing small displacement angles only. They confirm the above-mentioned results of Worster (1959) and Schneider (1985).

Kruisbrink (1990) determines the added mass effect of a spring loaded **pressure relief valve** from excitation tests. Tests without spring are performed at different (average) disc positions and excitation frequencies. From the displacement amplitude, force amplitude, excitation frequency and phase shift (between displacement and excitation force), the virtual mass and viscous damping are derived. A small tendency of decreasing added mass could be noticed with increasing (average) disc position. The added mass is approximated by an average value as:

linear motion:

$$m_f = 1.4\ \rho_f\ D_{disc}^3 \tag{6.31}$$

6.7.3 Pressure terms

For a viscous, non-uniform, parallel flow in a pipe, the pressure gradient over the fluid is described by the pipe equation of motion (section 9.1.2):

$$-\frac{1}{\rho_f}\frac{\partial p}{\partial x} = \frac{\partial v}{\partial t} + v\frac{\partial v}{\partial x} + \frac{f\ v|v|}{2D} \tag{6.32}$$

For the transient flow in a pipe the convective terms are neglected (section 9.1). Further, the transient flow is assumed to be dominated by fluid inertia effects, so that friction effects may be neglected (section 9.3). As a result the pressure gradient is only proportional to the fluid velocity gradient $\partial v/\partial t$, just like the pressure gradient in an inviscid or viscous, uniform, parallel flow. For the description of the pressure terms it is referred to section 4.6.4.

6.8 Fluid force and torque coefficients

6.8.1 General

For confined, inviscid fluids the coefficients C_1', C_2', ... in the kinetic energy equation of the fluid are determined by the geometry, the (linear and angular) position

of the body in the confined space, and the density of the incompressible fluid (see section 6.1).

In a manner, analogous to that for unconfined, inviscid fluids (section 4.7), the fluid force and torque coefficients may now be written as:

$$C_{D,A} = f\left(x,\ \theta\right) \tag{6.33}$$

Just like for unconfined, inviscid fluids the coefficients may be described in an analytical form. However, due to the complexity of these expressions, this can hardly be realized in practice.

For viscous fluids the force and torque coefficients are also dependent on the Reynolds, Mach and Acceleration number (section 5.4.1):

$$C_{D,A,B} = f\left(x,\ \theta,\ Re,\ Ma,\ Ac\right) \tag{6.34}$$

For the *incompressible* or *slightly compressible* fluids considered here, compressibility effects, represented by the Mach number, are further ignored.

For a body in a confined space, which moves in its plane of symmetry, the following Reynolds and Acceleration numbers are introduced:

$$Re_1 = \frac{\rho_f v D}{\mu_f} \quad \wedge \quad Re_2 = \frac{\rho_f \dot{x} D}{\mu_f} \quad \wedge \quad Re_3 = \frac{\rho_f \dot{\theta} D^2}{\mu_f}$$

$$Ac_1^{-1} = \frac{D}{v^2}\frac{dv}{dt} \quad \wedge \quad Ac_2^{-1} = \frac{D}{\dot{x}^2}\frac{d\dot{x}}{dt} \quad \wedge \quad Ac_3^{-1} = \frac{1}{\dot{\theta}^2}\frac{d\dot{\theta}}{dt} \tag{6.35}$$

Here two Reynolds and Acceleration numbers are introduced for the linear motion, since the effect of a translating body in a confined space is no longer the same as that of a (non-uniform) parallel flow. Three Reynolds and Acceleration numbers are necessary and sufficient to describe the (instantaneous) flow conditions around the body, apart from the history of the flow field.

For the translating and rotating bodies considered in section 6.5 one of the Reynolds and one of the Acceleration numbers is not relevant.

About the necessity of two Reynolds and two Acceleration numbers .....

For unconfined fluids the Reynolds and Acceleration numbers are based on the relative motion between body and fluid (see section 5.4.1):

$$Re = \frac{\rho_f (v - \dot{x}) D}{\mu_f} \quad \wedge \quad Ac^{-1} = \frac{D}{(v - \dot{x})^2} \frac{d(v - \dot{x})}{dt} \tag{6.36}$$

This definition is based on the supposition that the effect of a moving body and moving fluid on the flow pattern is the same, which is correct for unconfined, viscous fluids, but no longer holds for confined, viscous fluids. A confined, stagnant flow is characterized by a uniform (zero) velocity distribution, whereas a confined, parallel flow is characterized by a non-uniform velocity distribution, due to boundary effects (no slip conditions) at the wall. Therefore the flow patterns differ in these cases.

Moreover, in a confined space a steady flow (constant v) gives a steady flow pattern, while a steady moving body (constant $\dot{x}$) gives an unsteady flow pattern. The latter case is characterized by history effects. These effects are ignored in the above definition of the Reynolds number, which suggests that, at a certain position of the body, the flow pattern due to a moving body is the same as that due to a moving fluid (this only holds for inviscid fluids).

For the above-mentioned reasons two Reynolds and two Acceleration numbers are introduced for the linear motion.

6.8.2 Drag coefficients

The (steady and unsteady) drag coefficients are generally dependent on the linear and angular position of the body, and on the Reynolds and Acceleration numbers. Just like for unconfined fluids, the viscous effects are assumed to be first order effects, which dominate the second order, unsteady flow effects.

For the body of consideration this may be written as[3]:

$$C_D = f\left(x\,,\ \theta\,,\ \mathbf{Re_{1,2,3}}\,,\ \mathbf{Ac_{1,2,3}}\right) \tag{6.37}$$

Blasius (1913) derives an empirical expression for the friction coefficient of smooth pipes with circular cross section. The expression is obtained from available experimental data and valid for turbulent flows ($Re_D < 10^5$):

$$\lambda = \frac{0.3164}{Re_D^{0.25}} \tag{6.38}$$

[3] First order effects are printed in bold type.

Colebrook and White (Colebrook, 1939) describe the pipe friction coefficient as:

$$\frac{1}{\sqrt{\lambda}} = 1.74 - 2 \log\left(\frac{k_S}{R} + \frac{18.7}{Re_D\sqrt{\lambda}}\right) \qquad (6.39)$$

The implicit equation is valid for the whole transition region from hydraulically smooth to rough pipes. When the relative wall roughness is small ($k_S/R \rightarrow 0$), the equation gives the same values as Blasius' equation in the range $5000 < Re_D < 10^5$. For high Reynolds numbers the pipe friction coefficient is constant, and only dependent on the relative wall roughness k_S/R.

Schultz-Grunow (1935) describes the torque coefficient of a **rotating disc** in a housing, in a stagnant, laminar flow as ($Re_{\dot{\theta}R} < 2 \times 10^5$):

angular motion:

$$C_M = \frac{2.67}{Re_{\dot{\theta}R}^{0.5}} \qquad (6.40)$$

and for turbulent flow ($Re_{\dot{\theta}R} > 3 \times 10^5$):

$$C_M = \frac{0.0622}{Re_{\dot{\theta}R}^{0.2}} \qquad (6.41)$$

Collier and Hoerner (1981) show that the drag or loss coefficient of a split disc **check valve**, measured at fixed valve disc positions, is about constant at high Reynolds numbers ($Re_D > 10^5$).

Many more examples exist (e.g. Schlichting, 1979).

The above presented cases demonstrate that, just like for unconfined fluids, the drag coefficients generally may be described or approximated by a *Power law* as:

$$\boxed{C_D = \frac{C}{Re^k}} \qquad (6.42)$$

However, the coefficient C and power k are now functions of the linear and angular position of the body. Also here the power is valid for a range of **Reynolds** and Acceleration numbers, characterizing the flow in terms of laminar ($0.5 \leq k \leq 1$) or turbulent ($0 \leq k < 0.5$).

In practice the drag coefficients are measured under steady flow conditions. For confined flows this can only be realized on a stationary body in a steady flow and no longer on a steady translating or rotating body in a stagnant flow.

Under unsteady conditions the drag terms cannot be isolated anymore. For this reason the unsteady drag coefficient is commonly assumed to be equal to the steady value. Note that the Reynolds numbers now have instantaneous values.

More about the physical meaning of the Reynolds number in section 11.8.

6.8.3 Added mass and Basset coefficients

The added mass and Basset coefficients are generally dependent on the linear and angular position of the body, and on the Reynolds and Acceleration numbers. For these coefficients the unsteady flow effects are assumed to be first order effects, which dominate the second order viscous effects.

For the body of consideration follows[4]:

$$C_{A,B} = f\left(x\,,\ \theta\,,\ Re_{1,2,3}\,,\ Ac_{1,2,3}\right) \tag{6.43}$$

The added mass coefficient of a **sphere** in a semi-infinite space (section 6.7.2) follows from Equation (6.28):

linear motion:

$$C_A = \frac{1}{2} + \frac{3}{16}\frac{R^3}{x^3} \tag{6.44}$$

Also for the other cases described in section 6.7.2 the added mass coefficients can be quantified, if the volume of the body is known.

Nothing is known about added mass and Basset coefficients in confined fluids.

On the analogy of the added mass and Basset (history) coefficients for unconfined fluids, here also the general *power law* formulation is used:

$$\boxed{C_{A,B} = \frac{C}{Ac^{\,n}}} \tag{6.45}$$

[4] First order effects are printed in bold type.

The coefficient C and power n are now functions of the linear and angular position of the body. The power is valid for a range of **Acceleration** and Reynolds numbers.

The determination of the added mass and Basset coeffcients is essentially the same as in the case of unconfined fluids (section 5.4.3). However, the situation is much more complicated, since the coefficients are now also dependent on the linear (spatial) position of the body. Note that the added mass and history effects hardly can be separated, since the analytical form of the history term is unknown.

6.8.4 Pressure coefficients

The pressure coefficients are similar to those for inviscid, unconfined fluids (see further section 4.6.4).

6.9 Review and conclusions

Equations of motion are developed for a body in a confined, inviscid fluid. The equations are based on Lagrange's method of generalized coordinates and applied to the constrained motion of a body in its plane of symmetry. Just like for unconfined fluids the theory is extended to the motion of a body in an unsteady fluid flow. For a parallel pipe flow the external forces are similar to those for an unconfined, uniform parallel flow. The equations of motion for a body in an inviscid, confined fluid are similar to those for a body in a viscous, unconfined fluid. In both cases the fluid forces and torques are fully coupled. Based on this analogy the step from confined, inviscid fluids to confined, viscous fluids is made.

The equations of motion are applied to translating and rotating bodies. The drag, added mass and pressure terms are similar to those for unconfined, viscous fluids. The history terms are unknown, although it is expected that the history effects are reduced due to the presence of a confined space.

In the description of the fluid force and torque coefficients separate Reynolds and Acceleration numbers are introduced for the linear and angular motion of the body, and the linear motion of the fluid. Just like for unconfined fluids the drag coefficients in the fluid equations are assumed to be dominated by viscous effects, while the added mass and history coefficients are assumed to be dominated by inertia effects. Also here the coefficients are approximated by power laws. The fluid force and torque coefficients are now dependent on the linear and angular position of the body.

The equations of motion for the body and fluid are used in chapter 8 to develop (dimensionless) equations of motion for check valves.

7 Global form of fluid equations

In the previous chapters the fluid forces on a body are described by separate terms like drag, added mass, pressure and history terms. For some flow problems, in particular confined flow problems, these fluid terms cannot always be quantified, either by theory or by experiment. For this reason in the literature another, more global approach is also found (e.g. Steetzel, 1984). The fluid force is then described in a rather simple form, analogous to that of the conventional drag term. All steady and unsteady effects of the fluid on the body are accounted for in one single fluid force coefficient. This principle is studied here and applied to translating as well as to rotating bodies, including check valves. The results of the previous chapters are used to describe the properties of these global force and torque coefficients.

The concept of the global fluid force coefficients is used in the development of valve characteristics (chapter 11) and computer models (chapter 12).

7.1 General fluid equations of motion

In the global form of the fluid equations, the fluid force is described in terms of a conventional drag term. Instead of the drag coefficient, a global force coefficient is introduced, which accounts for *all* effects of the motion and the change of motion of body and fluid, including added mass, pressure and history effects.

For a body which moves in its plane of symmetry, the drag terms appear in several forms (section 4.6.2, 5.3.1, and 6.7.1). From the combination of these forms the following global form of the fluid equations may be composed:

$$X_f = C_X \tfrac{1}{2}\rho_f \left[(v-\dot{x}) - d\dot{\theta}\right]^2 A$$

$$Y_f = C_Y \tfrac{1}{2}\rho_f \left[(v-\dot{x}) - d\dot{\theta}\right]^2 A \qquad (7.1)$$

$$M_f = C_M \tfrac{1}{2}\rho_f \left[(v-\dot{x}) - d\dot{\theta}\right]^2 D^3$$

where d is a parameter that links the linear and angular velocity terms. In the next sections it is demonstrated that this theoretical form has no practical value, although it contains all relevant drag terms.

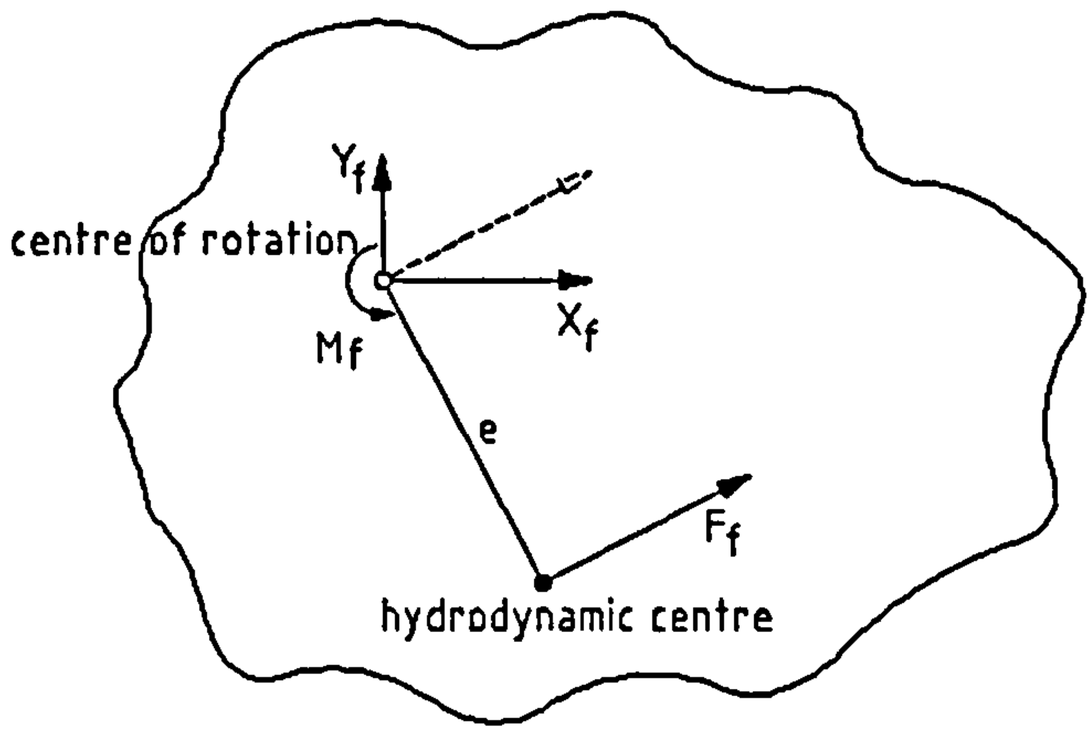

Figure 7.1 Link between fluid forces and torque

The link between the fluid forces and torque is (figure 7.1):

$$M_f = X_f\, e_y + Y_f\, e_x \qquad (7.2)$$

where e_x and e_y are the components of the eccentricity e.

7.2 Fluid force and torque coefficients

The equations of motion for unconfined and confined, inviscid and viscous fluids (sections 4.4, 5.1, 6.4 and 6.6) are considered together now. The terms that appear in these equations are:

$$\frac{d(v-\dot{x})}{dt} \;;\; (v-\dot{x})\dot{\theta} \;;\; \frac{d\dot{\theta}}{dt} \;;\; \dot{\theta}^2 \;;\; (v-\dot{x})^2 \;;\; \frac{dv}{dt} \qquad (7.3)$$

All terms appear in the fluid force and torque equations, except for unconfined, inviscid fluids, where less terms are needed. History terms are absent here.

It can easily be seen that Equation (7.1) is inconsistent with the fluid equations developed in the previous chapters, even for a steady motion (see also section 7.3.4). Moreover, the form does not match with the Reynolds and Acceleration numbers, introduced in the previous chapters. Therefore Equation (7.1) is reduced to a more simple form. More sensible options for the dynamic pressure may be:

$$\frac{1}{2}\rho_f(v-\dot{x})^2 \qquad \mathsf{V} \qquad \frac{1}{2}\rho_f(d\dot{\theta})^2 \tag{7.4}$$

$$\frac{1}{2}\rho_f v^2 \qquad \mathsf{V} \qquad \frac{1}{2}\rho_f \dot{x}^2 \tag{7.5}$$

Let the dynamic pressure in Equation (7.1) be described by the two options in Equation (7.4). A comparison with Equation (7.3) gives, after dimensional reasoning whereby the parameter d is replaced by a characteristic dimension D, respectively:

$$C_{X,Y,M} = f\left[\frac{D}{(v-\dot{x})^2}\frac{d(v-\dot{x})}{dt}\ ,\ \frac{D\dot{\theta}}{(v-\dot{x})}\ ,\ \frac{D^2}{(v-\dot{x})^2}\frac{d\dot{\theta}}{dt}\ ,\ \frac{D}{(v-\dot{x})^2}\frac{dv}{dt}\right] \tag{7.6}$$

$$C_{X,Y,M} = f\left[\frac{1}{\dot{\theta}^2 D}\frac{d(v-\dot{x})}{dt}\ ,\ \frac{(v-\dot{x})}{D\dot{\theta}}\ ,\ \frac{1}{\dot{\theta}^2}\frac{d\dot{\theta}}{dt}\ ,\ \frac{1}{\dot{\theta}^2 D}\frac{dv}{dt}\right] \tag{7.7}$$

Both equations are equivalent with:

$$C_{X,Y,M} = f\left[\frac{D\dot{\theta}}{(v-\dot{x})}\ ,\ \frac{D}{(v-\dot{x})^2}\frac{d(v-\dot{x})}{dt}\ ,\ \frac{\mathbf{1}}{\dot{\theta}^2}\frac{d\dot{\theta}}{dt}\ ,\ \frac{D}{(v-\dot{x})^2}\frac{dv}{dt}\right] \tag{7.8}$$

In this equation the Acceleration number appears in two forms (printed in bold), which are typical for *unconfined fluids* (section 5.4.1).

Let the dynamic pressure be described by the two options in Equation (7.5). A comparison with the terms in Equation (7.3) then gives, respectively:

$$C_{X,Y,M} = f\left[\frac{D}{v^2}\frac{d(v-\dot{x})}{dt}\ ,\ \frac{v-\dot{x}}{v}\ ,\ \frac{D\dot{\theta}}{v}\ ,\ \frac{D^2}{v^2}\frac{d\dot{\theta}}{dt}\ ,\ \frac{D}{v^2}\frac{dv}{dt}\right] \tag{7.9}$$

$$C_{X,Y,M} = f\left[\frac{D}{\dot{x}^2}\frac{d(v-\dot{x})}{dt}\ ,\ \frac{v-\dot{x}}{\dot{x}}\ ,\ \frac{D\dot{\theta}}{\dot{x}}\ ,\ \frac{D^2}{\dot{x}^2}\frac{d\dot{\theta}}{dt}\ ,\ \frac{D}{\dot{x}^2}\frac{dv}{dt}\right] \tag{7.10}$$

Both equations are equivalent with:

$$C_{X,Y,M} = f\left[\frac{\dot{x}}{v}\ ,\ \frac{D\dot{\theta}}{v}\ ,\ \frac{D}{v^2}\frac{dv}{dt}\ ,\ \frac{D}{\dot{x}^2}\frac{d\dot{x}}{dt}\ ,\ \frac{\mathbf{1}}{\dot{\theta}^2}\frac{d\dot{\theta}}{dt}\right] \tag{7.11}$$

In this equation the Acceleration number appears in three forms (printed in bold), which are typical for *confined fluids* (section 6.8.1).

From these results it is concluded that the options in Equation (7.4) are more suited to unconfined fluids, whereas the options in Equation (7.5) are more suited to confined fluids.

For unconfined, inviscid fluids the drag and added mass coefficients are only dependent on the angular position of the body (section 4.7). In that case follows with Equation (7.8):

unconfined, inviscid fluids:

$$C_{X,Y,M} = f\left[\theta\,,\ \frac{D\dot{\theta}}{(v-\dot{x})}\,,\ \frac{D}{(v-\dot{x})^2}\frac{d(v-\dot{x})}{dt}\,,\ \frac{1}{\dot{\theta}^2}\frac{d\dot{\theta}}{dt}\,,\ \frac{D}{(v-\dot{x})^2}\frac{dv}{dt}\right] \qquad \textbf{(7.12)}$$

For unconfined, viscous fluids the drag, added mass and Basset coefficients are also dependent on two Reynolds and two Acceleration numbers (section 5.4.1). In that case follows with Equation (7.8):

unconfined, viscous fluids:

$$C_{X,Y,M} = f\left[\theta\,,\ \frac{\rho_f(v-\dot{x})D}{\mu_f}\,,\ \frac{\rho_f\dot{\theta}\,D^2}{\mu_f}\,,\ \frac{D}{(v-\dot{x})^2}\frac{d(v-\dot{x})}{dt}\,,\ \frac{1}{\dot{\theta}^2}\frac{d\dot{\theta}}{dt}\,,\ \frac{D}{(v-\dot{x})^2}\frac{dv}{dt}\right] \qquad \textbf{(7.13)}$$

The first group in Equation (7.8) is covered now by the Reynolds numbers.

For confined, inviscid fluids the coefficients are only dependent on the linear and angular position of the body (section 6.2). In that case follows with Equation (7.11):

confined, inviscid fluids:

$$C_{X,Y,M} = f\left[x\,,\ \theta\,,\ \frac{\dot{x}}{v}\,,\ \frac{D\dot{\theta}}{v}\,,\ \frac{D}{v^2}\frac{dv}{dt}\,,\ \frac{D}{\dot{x}^2}\frac{d\dot{x}}{dt}\,,\ \frac{1}{\dot{\theta}^2}\frac{d\dot{\theta}}{dt}\right] \qquad \textbf{(7.14)}$$

For confined, viscous fluids the drag, added mass and Basset coefficients are also dependent on three Reynolds and three Acceleration numbers (section 6.8.1). In that case follows with Equation (7.11):

confined, viscous fluids:

$$C_{X,Y,M} = f\left[x\,,\ \theta\,,\ \frac{\rho_f v D}{\mu_f}\,,\ \frac{\rho_f\dot{x}\,D}{\mu_f}\,,\ \frac{\rho_f\dot{\theta}\,D^2}{\mu_f}\,,\ \frac{D}{v^2}\frac{dv}{dt}\,,\ \frac{D}{\dot{x}^2}\frac{d\dot{x}}{dt}\,,\ \frac{1}{\dot{\theta}^2}\frac{d\dot{\theta}}{dt}\right] \qquad \textbf{(7.15)}$$

The first and second group in Equation (7.11) are covered by the Reynolds numbers.

The definition of the global fluid forces and torques allows to link the global force and torque coefficients. From the Equations (7.1) and (7.2) follows:

$$C_M D^3 = \left(C_X e_y + C_Y e_x\right) A \tag{7.16}$$

This equation links the torque coefficient to the force coefficients via the eccentricity of the hydrodynamic center. This link holds, no matter what the definition of the global fluid forces and torques is. From Equation (7.16) it directly follows that the above-mentioned functional relationships for the global force and torque coefficients also hold for the eccentricities e_x and e_y. In that case they describe the move of the hydrodynamic centre.

The theoretical as well as the experimental determination of the global fluid force coefficients is a problem. Various attempts are made to solve the Navier-Stokes equations, however without quantitative results (Steetzel, 1984).

7.3 Translating and rotating bodies

In this section the global form of the fluid equations is applied to translating and rotating bodies, moving in an unconfined or confined, *viscous* fluid. The equations in the constrained directions of motion are further ignored.

7.3.1 Translating body in unconfined fluid

The fluid force on a translating body in an unconfined, viscous fluid may be described by (section 7.1 and 7.2):

$$\boxed{X_f = C_X \tfrac{1}{2}\rho_f (v-\dot{x})^2 A} \tag{7.17}$$

A comparison with Equation (5.2) gives:

linear motion:

$$C_X = C_D + C_A \frac{2V_b}{AD} \frac{D}{(v-\dot{x})^2}\frac{d(v-\dot{x})}{dt} + \frac{2V_b}{AD} \frac{D}{(v-\dot{x})^2}\frac{dv}{dt} \tag{7.18}$$

where (section 5.4.1):

$$C_{D,A} = f\left[\frac{\rho_f(v-\dot{x})D}{\mu_f}\ ,\ \frac{D}{(v-\dot{x})^2}\frac{d(v-\dot{x})}{dt}\right] \qquad \textbf{(7.19)}$$

In this global force coefficient history effects are ignored.

Houghton (1963) and Sellgren (1983) describe the fluid force on a small particle in a stagnant flow in the form of Equation (7.17). They assume in first approximation that the global force coefficient is equal to the drag coefficient, which is obtained from steady flow measurements. The effects of un unsteady motion are accounted for by an instantaneous Reynolds number, based on the relative motion of the particle, so that C_X = f (Re (t)).

Tchen (1947) also describes the fluid force on a (small) sphere in a stagnant fluid in the form of Equation (7.17). He proposes to describe the global force coefficient in the form of a series as:

linear motion:

$$C_X = f_1\,(Re) + Ac^{-1}\,f_2\,(Re) \qquad \textbf{(7.20)}$$

This equation is similar to Equation (7.18), since in a stagnant fluid the pressure term is absent. The equation suggests that the added mass coefficient is a function of the Reynolds number only. The dependency on the Acceleration number, as suggested in Equation (5.23) and illustrated in Equation (5.25), is not described. In that sense the function f_2 (Re) is better described by f_2 (Re, Ac).

Some thoughts about history effects and time series .....

For laminar flow the fluid force is proportional to the instantaneous velocity (drag term) and velocity gradient (added mass term), which is demonstrated by Equation (5.3):

linear motion:

$$X_f = f\left(\ (v-\dot{x})\ ,\ \frac{d(v-\dot{x})}{dt}\ \right) \qquad \textbf{(7.21)}$$

The question arises if history effects may be taken into account by higher order terms:

$$X_f = f\left(\ (v-\dot{x})\ ,\ \frac{d(v-\dot{x})}{dt}\ ,\ \frac{d^2(v-\dot{x})}{dt^2}\ ,\ .....\ \right) \qquad \textbf{(7.22)}$$

If so, then the fluid force is described by the history of the (relative) fluid velocity in the form of a Taylor series, which is mathematically correct.

The force coefficient, defined in Equation (7.17), may then be written as:

$$C_X = f\left(\frac{1}{(v-\dot{x})} , \frac{1}{(v-\dot{x})^2} \frac{d(v-\dot{x})}{dt} , \frac{1}{(v-\dot{x})^2} \frac{d^2(v-\dot{x})}{dt^2} , ... \right) \qquad (7.23)$$

After dimensional reasoning this may be written as:

$$C_X = f\left(\frac{\mu_f}{\rho_f (v-\dot{x}) D} , \frac{D}{(v-\dot{x})^2} \frac{d(v-\dot{x})}{dt} , \frac{D^2}{(v-\dot{x})^3} \frac{d^2(v-\dot{x})}{dt^2} , ... \right) \qquad (7.24)$$

In this equation the inverse Reynolds number and Acceleration number appear as the first and second term of a series. Let the third term be the inverse of some History number *Hi*.

Equation (7.20) may now possibly be extended as:

$$C_X = f_1 (Re) + Ac^{-1} f_2 (Re, Ac) + Hi^{-1} f_3 (Re, Ac) + ... \qquad (7.25)$$

The global force coefficient in Equation (7.18) may now be developed in a series as:

$$C_X = C_D + C_A' \frac{D}{(v-\dot{x})^2} \frac{d(v-\dot{x})}{dt} + K_P' \frac{D}{(v-\dot{x})^2} \frac{dv}{dt} + C_B' \frac{D^2}{(v-\dot{x})^3} \frac{d^2(v-\dot{x})}{dt^2} + ... \qquad (7.26)$$

Note that the pressure term needs no development in higher order terms.

7.3.2 Translating body in confined fluid

For translating bodies in confined, viscous fluids (section 6.5.1) the fluid equations are the same as those for unconfined, viscous fluids (section 5.2.1). The Reynolds and Acceleration numbers, however, differ. The fluid force may now be described by:

$$X_f = C_X \frac{1}{2} \rho_f v^2 A \qquad (7.27)$$

A comparison with Equation (6.23) gives after some manipulation:

$$C_X = C_D \left[1 - \frac{\dot{x}}{v} \right]^2 + (C_A + 1) \frac{2V_b}{AD} \frac{D}{v^2} \frac{dv}{dt} - C_A \frac{2V_b}{AD} \left[\frac{\dot{x}}{v} \right]^2 \frac{D}{\dot{x}^2} \frac{d\dot{x}}{dt} \qquad (7.28)$$

where (section 6.8.1):

$$C_{D,A} = f\left[\frac{x}{D}\ ,\ \frac{\rho_f v D}{\mu_f}\ ,\ \frac{\rho_f \dot{x} D}{\mu_f}\ ,\ \frac{D}{v^2}\frac{dv}{dt}\ ,\ \frac{D}{\dot{x}^2}\frac{d\dot{x}}{dt}\right] \qquad (7.29)$$

7.3.3 Rotating body in unconfined fluid

The fluid torque on a rotating body in an unconfined, viscous fluid may be described by (section 7.2):

$$\boxed{M_f = C_M \tfrac{1}{2}\rho_f v^2 D^3} \qquad (7.30)$$

A comparison with Equation (5.10) gives:

$$C_M = C_{D_1} + C_{D_{12}}\left[\frac{D\dot{\theta}}{v}\right] - C_{D_2}\left[\frac{D\dot{\theta}}{v}\right]^2 +$$

$$+ \left(C_{A_1} + K_P\right)\frac{2V_b}{D^3}\frac{D}{v^2}\frac{dv}{dt} - C_{A_2}\frac{2V_b k^2}{D^5}\left[\frac{D\dot{\theta}}{v}\right]^2\frac{1}{\dot{\theta}^2}\frac{d\dot{\theta}}{dt} \qquad (7.31)$$

where (section 5.4.1):

$$C_{D,A} = f\left[\theta\ ,\ \frac{\rho_f v D}{\mu_f}\ ,\ \frac{\rho_f \dot{\theta} D^2}{\mu_f}\ ,\ \frac{D}{v^2}\frac{dv}{dt}\ ,\ \frac{1}{\dot{\theta}^2}\frac{d\dot{\theta}}{dt}\right] \qquad (7.32)$$

In the global torque coefficient history effects are ignored.

About history effects .....

If history effects may be taken into account by higher order terms (section 7.3.1), this gives the form:

$$C_M = C_{D_1} + C_{D_{12}}\frac{D\dot{\theta}}{v} - C_{D_2}\left(\frac{D\dot{\theta}}{v}\right)^2 + C_{A_1}'\frac{D}{v^2}\frac{dv}{dt} +$$

$$- C_{A_2}'\left(\frac{D\dot{\theta}}{v}\right)^2\frac{1}{\dot{\theta}^2}\frac{d\dot{\theta}}{dt} + C_{B_1}'\frac{D^2}{v^3}\frac{d^2v}{dt^2} - C_{B_2}'\left(\frac{D\dot{\theta}}{v}\right)^3\frac{1}{\dot{\theta}^3}\frac{d^2\dot{\theta}}{dt^2} + \ .....$$

(7.33)

7.3.4 Rotating body in confined fluid

For rotating bodies in confined, viscous fluids (section 6.6) the fluid equations, Reynolds and Acceleration numbers are the same as those for unconfined, viscous fluids (section 5.2.2). The fluid torque may be described according to Equation (7.30) (see section 7.2). Therefore the equations in the previous section also hold for confined, viscous fluids.

About relative motion .....

Several researchers like Worster (1960), Pool et al. (1962), Ellis (1980), Koch (1981) and Provoost (1983a) describe the hydrodynamic torque on the rotating disc of a check valve in the form:

$$M_f = C_M \frac{1}{2} \rho_f \left[v - e \dot{\theta} \right]^2 D^3 \qquad (7.34)$$

The eccentricity e, however, which links the linear flow and the angular valve motion, is interpreted in different, more or less conflicting ways, as illustrated below.

Worster (1960) and Provoost (1983a) base the relative motion on the flow volume displaced by the rotating disc. They assume that the radial component of the displaced flow is directed into the axial (flow) direction of the confined space. This leads to the relative flow term (Q - $A_{disc}\ e_{cg}\ \dot{\theta}$), where e_{cg} is the eccentricity of the center of gravity from the center of rotation. With $Q = v\ A_{pipe}$, this leads to the above form, where C_M is assumed to be a function of the angular position of the valve disc. The equation contains properties of both inviscid and viscous fluids:

a) The equation actually consists of three terms, which are similar to the drag terms for confined, inviscid or viscous fluids.

b) The velocity terms in the above equation are only linked by geometrical dimensions of the body. In terms of the eccentricty e an analogy arises with the steady version of the torque equation given in Equation (4.43), as developed for a body with three planes of symmetry in an unconfined, inviscid flow. However, an essential difference is that the terms in Equation (4.43) are linked via B_f, D_f and E_f. The link is thus dependent on the angular position of the body.

c) For viscous fluids the terms are not linked by hard geometrical dimensions only, but also by more soft dimensions, due to boundary layer effects and flow separation. For instance: Due to boundary layer effects the displaced flow volume is enlarged in a viscous flow, leading to a larger effective value of the eccentricity e.

d) The equation gives a zero torque if $v = e\ \dot{\theta}$, independent of the angular position of the body, which is incorrect for both inviscid and viscous fluids. Also for a centrical body ($e = 0$) in a stagnant fluid ($v = 0$), the equation gives a zero torque, which is only correct for a steady rotating body in an unconfined, inviscid fluid.

Koch (1981) describes the relative motion of a tilting disc check valve in terms of $(v - r\dot{\theta}/\cos\theta)$. The reference radius r is chosen such that the closure time in numerical valve model and experiment is the same. Koch recognizes that the angular disc position plays a role in the relative motion and introduces $\cos\theta$. However, this term leads to infinite values for $\theta = \pi/2$, which is incorrect. A better approach would be $(v - r\,\dot{\theta}\cos\theta)$, so that the influence of the disc motion vanishes for $\theta = \pi/2$.

It is concluded that the parameter e cannot be defined in such a way that Equation (7.34) is consistent with the fluid terms, which are developed for a rotating body in a confined, inviscid or viscous fluid (section 6.5.2), and only gives approximated values. Preference is given to the global form given in Equation (7.30), which is valid for unconfined and confined fluids.

7.4 Review and conclusions

The fluid force and torque equations are described in a global form, based on the conventional drag term. The properties of the global force and torque coefficients are studied by comparing the global fluid equations with the fluid equations, which are described by separate terms, as developed in the previous chapters. Hereby several forms of the dynamic pressure in the global force terms are explored. The properties of the coefficients are thus described in functional relations, in which the Acceleration numbers appear in different forms. It is demonstrated that some of these forms are consistent with and more suited to unconfined fluids, while others are consistent with and more suited to confined fluids. The properties of the global force and torque coefficients also hold for the eccentricity of the hydrodynamic centre relative to the centre of rotation.

The global fluid equations of motion are applied to translating and rotating bodies.

The global form of the equations of motion suited to confined fluids, is applied to check valves (chapter 8) and used to define the valve loss coefficient (chapter 10).

8 Valve equations

In chapter 6 the equations of motion are described for a body in a confined flow. These equations are used here to develop a general equation of motion for check valves with rotating elements. For this purpose the external torques on the valve disc due to a counterweight, spring(s), a damper, etc. are described in detail.

The valve equation of motion is written in a dimensionless form, in which the critical velocity is introduced as a measure for the valve response. In the valve closure a distinction is made between the passive and active stages of damping. During the stage of passive damping (the first event of closure) the flow is assumed to be dominated by the system. During the stage of active damping (the second event of closure) the flow is imposed by the combination of valve and system.

The (dimensionless) valve equation shows in a formal way which (dimensionless) variables and parameters are relevant to the valve behaviour. In that sense the results are used in a dimensional analysis to develop valve characteristics (chapter 11) and parameterized valve models (chapter 12).

8.1 General equation of motion

The equation of motion for a rotating body in a confined flow (section 6.5.2) is applied to check valves with rotating elements. The principle of operation of such valve types is given in figure 1.3. Examples are given in the figures 3.1.a to d.

To avoid confusion with the term "valve body", the term "body" (*b*), is replaced by "moving elements" (*m*). Further the term "moment" (*M*) is replaced by "torque" (*T*), commonly used in mechanical engineering. This leads to:

$$I_m \ddot{\theta} = T_H + \sum T \tag{8.1}$$

where:

$$\sum T = T_G + T_B + T_S + T_D + T_F \tag{8.2}$$

In this equation I_m is the mass moment of inertia of the moving elements about the centre of rotation, T_H is the torque on the valve disc due to *H*ydrodynamics, while ΣT are the external torques on the valve disc due to *G*ravitation, *B*uoyancy, *S*pring(s),

*D*amping and *F*riction, respectively (the italic capitals are used as subscripts). In the next section these torques are described in detail.

8.2 Torques on valve disc

In this section the (internal and external) torques acting on the valve disc are described due to *I*nertia, *H*ydrodynamics, *G*ravitation, *B*uoyancy, *S*pring(s), *F*riction and *D*amping, respectively.

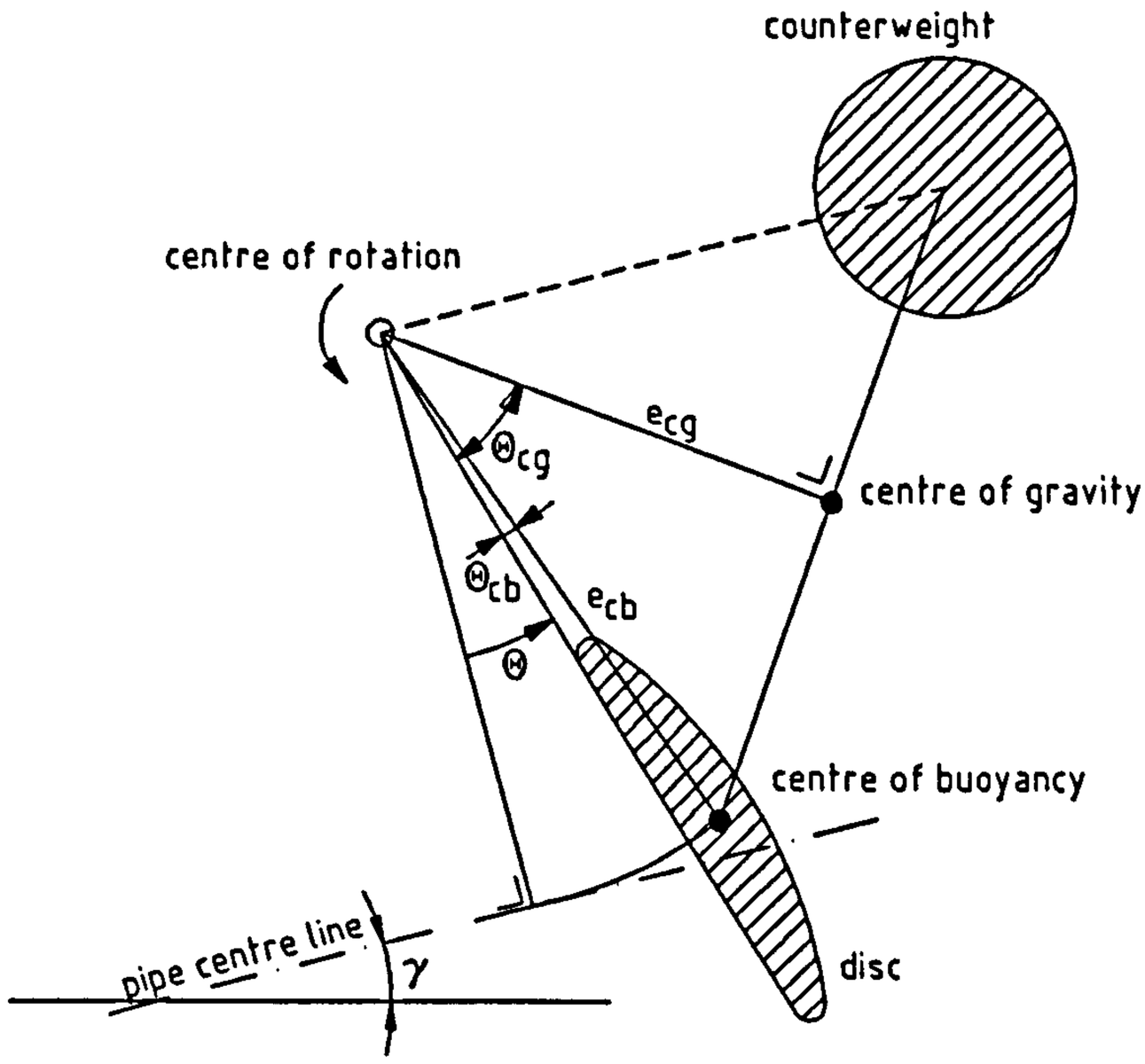

Figure 8.1 Rotating valve disc with counterweight; definition sketch

Inertia The torque due to the inertia of the moving elements may be described by (section 4.6.3):

$$T_I = I_m \ddot{\theta} = \rho_m V_m k^2 \ddot{\theta} \qquad (8.3)$$

where I_m is the moment of inertia, V_m the volume and k the gyration radius of the moving elements (inclusive counterweight, damper, spring(s), etc.).

Introduce dimensionless, geometrical parameters K which relate the volume and gyration radius of the moving elements to the valve diameter D:

$$V_m = K_{V_m} D^3 \quad ; \quad k^2 = K_k D^2 \quad ; \quad K_I = K_{V_m} K_k \qquad (8.4)$$

Substitution of Equation (8.4) in Equation (8.3) results in:

$$T_I = \rho_m K_I D^5 \ddot{\theta} \tag{8.5}$$

Hydrodynamics The fluid torque on the internal, rotating elements of a check valve is described by Equation (6.26). With the substitution of Equation (8.4) the equation may be written in the form:

angular motion:

$$T_H = C_{D_1} \tfrac{1}{2} \rho_f v^2 D^3 + C_{D_{12}} \tfrac{1}{2} \rho_f v \dot{\theta} D^4 - C_{D_2} \tfrac{1}{2} \rho_f \dot{\theta}^2 D^5 + \\ + K_{V_m} \left(C_{A_1} + K_P \right) \rho_f D^4 \frac{dv}{dt} - K_I C_{A_2} \rho_f D^5 \frac{d\dot{\theta}}{dt} \tag{8.6}$$

where in general terms (section 6.8):

$$C_D = f\left(\theta\,,\ Re\,,\ Ac\right)$$
$$C_A = f\left(\theta\,,\ Re\,,\ Ac\right) \tag{8.7}$$

Also here the first order effects are printed in bold type.

The above drag and added mass coefficients are approximated by power laws (see section 5.4 and 6.8) as:

$$C_{D_1} = \frac{C_1}{Re_1^{\,k}} \quad ; \quad C_{D_{12}} = \frac{C_{12}}{Re_{12}^{\,l}} \quad ; \quad C_{D_2} = \frac{C_2}{Re_2^{\,m}}$$
$$C_{A_1} = \frac{C_{11}}{Ac_1^{\,n}} \quad ; \quad C_{A_2} = \frac{C_{22}}{Ac_2^{\,o}} \tag{8.8}$$

where:

$$Re_1 = \frac{\rho_f v D}{\mu_f} \quad ; \quad Re_{12} = \frac{\rho_f v^{1/2} \dot{\theta}^{1/2} D^{3/2}}{\mu_f} \quad ; \quad Re_2 = \frac{\rho_f \dot{\theta} D^2}{\mu_f}$$

$$Ac_1^{-1} = \frac{D}{v^2}\frac{dv}{dt} \quad ; \quad Ac_2^{-1} = \frac{1}{\dot{\theta}^2}\frac{d\dot{\theta}}{dt} \tag{8.9}$$

The coefficients C and powers k, l, ... are functions of the valve disc position θ. For a certain valve disc position C and k, l, ... are assumed to be constants within a certain range of Reynolds or Acceleration numbers. The Reynolds powers characterize the flow in terms of laminar ($0.5 \leq k, .. \leq 1$) or turbulent ($0 \leq k, .. < 0.5$). The Reynolds number Re_{12} is a theoretical number, used to describe the combined motion. Contrary to the "hard" geometrical parameters $K_{..}$, the coefficients C_D and C_A are "soft" dynamic parameters.

History effects are ignored here, since no analytical expressions are available.

Gravitation The torque due to gravitation is described by (figure 8.1):

$$T_G = -\rho_m V_m g \; e_{cg} \sin\left(\theta + \theta_{cg} + \gamma\right) \tag{8.10}$$

where V_m is the volume of the moving elements and e_{cg} is the eccentricity of the center of gravity (cg) relative to the centre of rotation.

Introduce dimensionless geometrical parameters which relate the volume and the eccentricity of the moving elements to the valve diameter:

$$V_m = K_{V_m} D^3 \quad ; \quad e_{cg} = K_{e_{cg}} D \quad ; \quad K_G = K_{V_m} K_{e_{cg}} \tag{8.11}$$

Note that K_{ecg} may be a function of the valve disc position, e.g. if the centre of rotation of counterweight or damping device and valve disc differ. Substitution of Equation (8.11) in Equation (8.10) results in:

$$\boxed{T_G = -K_G \rho_m g D^4 \sin\left(\theta + \theta_{cg} + \gamma\right)} \tag{8.12}$$

Buoyancy The torque due to buoyancy is (figure 8.1):

$$T_B = \rho_f V_b g \; e_{cb} \sin\left(\theta + \theta_{cb} + \gamma\right) \tag{8.13}$$

where V_b is the volume of the submerged moving elements, and e_{cb} is the eccentricity of the centre of buoyancy (*cb*) relative to the centre of rotation.

Introduce geometrical parameters:

$$V_b = K_{V_b} D^3 \quad ; \quad e_{cb} = K_{e_{cb}} D \quad ; \quad K_B = K_{V_b} K_{e_{cb}} \tag{8.14}$$

Substitution of Equation (8.14) in Equation (8.13) yields:

$$\boxed{T_B = K_B \rho_f g D^4 \sin(\theta + \theta_{cb} + \gamma)} \tag{8.15}$$

For check valves which operate in a free surface flow K_B and θ_{cb} are functions of the angular valve disc position.

Spring(s) It is assumed that the spring(s) are mounted to the pivot (centre of rotation). The spring torque may now be described by:

$$\boxed{T_S = -\left(K_{S_c} + K_S (\theta - \theta_c)\right)} \tag{8.16}$$

where K_{Sc} is the preset spring torque in the closed position ($\theta = \theta_c$). Note that K_{Sc} and K_S may be considered as geometrical parameters.

Friction The following general friction model is applied (Appendix A.1):

$$\boxed{T_F = -\sum K_f r_f F_n \, sign\dot{\theta}} \tag{8.17}$$

where K_f is a friction coefficient, r_f the moment arm of the friction force (e.g. radius of spindle, shaft or pin), and F_n the normal force on the friction surface(s). The friction torque is the sum of all friction effects in both valve and damper.

The friction coefficient K_f represents both static and sliding friction. In the case of static friction ($\dot{\theta} = 0$) the sign of $\dot{\theta}$ is determined by the sum of the other torques ($\dot{\theta} = 0^+$ or 0^-). When the static friction torque exceeds a threshold value, the valve

starts moving and sliding friction becomes relevant. In most practical cases the static friction coefficient exceeds the sliding friction coefficient. The friction coefficient may be considered as a geometrical parameter since it is determined by surface roughness.

Damping To describe (external or internal) damping devices such as hydraulic, piston and dashpot dampers (figures 3.1.b, c and f) the following general damping model is applied (Appendix A.2):

$$\boxed{T_D = -\left[C_{D_3} \frac{1}{2} \rho_d \dot{\theta}^2 D^5 + C_{A_3} \rho_d \frac{d\dot{\theta}}{dt} D^5 \right]} \qquad (8.18)$$

where:

$$C_{D_3} = \frac{C_3}{Re_3^p} \quad \wedge \quad C_{A_3} = \frac{C_{33}}{Ac_3^q} \qquad (8.19)$$

and:

$$Re_3 = \frac{\rho_d \dot{\theta} D^2}{\mu_d} \quad \wedge \quad Ac_3^{-1} = \frac{1}{\dot{\theta}^2} \frac{d\dot{\theta}}{dt} \qquad (8.20)$$

The density ρ_d and viscosity μ_d refer to the damping fluid. The damping coefficients are described in a similar way as the hydrodynamic coefficients of the internal, moving valve elements (see above).

About turbulent and laminar damping .....

For turbulent damping ($p = 0$) and higher accelerations ($q = 0$) follows:

$$T_D = C_3 \frac{1}{2} \rho_d \dot{\theta}^2 D^5 + C_{33} \rho_d \frac{d\dot{\theta}}{dt} D^5 \qquad (8.21)$$

For laminar (viscous) damping ($p = 1$) and small accelerations ($\ddot{\theta} \approx 0$) follows:

$$T_D = C_3 \frac{1}{2} \mu_d \dot{\theta} D^3 \qquad (8.22)$$

In literature the damping is described in several ways.

Rommel et al. (1984) assume that the damping torque of a tilting disc check valve is proportional to the disc velocity squared, while the damping coefficient is taken as a constant, independent of the valve disc position.

Travis and Torrey (1985) assume that the damping force of a plug-type check valve (Y-bonnet) with internal piston damper is proportional to the valve disc velocity squared. The damping coefficient

is a function of the valve disc position and obtained from tuning with experiments.

Henry et al. (1989) assume that the damping force of a plug-type check valve with internal piston damper is proportional to the valve disc velocity.

Kim (1989) assumes that the damping torque of a swing check valve with internal dashpot damper is proportional to the valve disc velocity, while the damping coefficient is taken as a constant.

Slegers and Wölk (year unknown) assume that the damping force of a plug-type check valve with piston damper is proportional to the disc velocity squared. The damping coefficient is taken as a constant, although experiments show that it strongly varies during the first stage of valve closure.

Note that the above researchers use a quasi-steady approach, in which the damping effects due to the unsteady disc motion are ignored.

8.3 Valve equation for angular motion

Substitution of the torques on the valve disc (section 8.2) in the general valve equation of motion (section 8.1) yields:

$$\left(K_I \rho_m + K_I C_{A_2} \rho_f + C_{A_3} \rho_d\right) D^5 \frac{d\dot{\theta}}{dt} =$$

$$C_{D_1} \frac{1}{2} \rho_f v^2 D^3 + C_{D_{12}} \frac{1}{2} \rho_f v \dot{\theta} D^4 - C_{D_2} \frac{1}{2} \rho_f \dot{\theta}^2 D^5 + K_{V_m} \left(C_{A_1} + K_P\right) \rho_f D^4 \frac{dv}{dt} +$$

$$- K_G \rho_m g D^4 \sin\left(\theta + \theta_{cg} + \gamma\right) + K_B \rho_f g D^4 \sin\left(\theta + \theta_{cb} + \gamma\right) +$$

$$- \left(K_{S_c} + K_S \left(\theta - \theta_c\right)\right) - C_{D_3} \frac{1}{2} \rho_d \dot{\theta}^2 D^5 - \sum K_f r_f F_n sign\dot{\theta} \qquad \textbf{(8.23)}$$

The subscripts 1, 2 and 3 refer to the motion of the (pipe) fluid, valve elements and damping fluid, respectively. All coefficients K are hard, geometrical parameters which may be a function of the angular valve disc position. The hydrodynamic and damping coefficients C_D and C_A are soft, dynamic parameters, which are a function of the angular valve disc position, and the Reynolds and Acceleration numbers. This makes the equation implicit. The valve equation of motion is a higher order, ordinary, non-linear differential equation, valid for $\theta_c \leq \theta \leq \theta_o$ (the subscript o refers to the fully open position).

8.4 Hysteresis

The motion of the valve disc may be influenced by hysteresis effects. In order to quantify these effects, quasi-steady state versions of the valve equation of motion are considered. For check valves these quasi-steady state versions only exist for the normal flow direction ($v \geq 0$). The steady drag coefficient is described by a power law (section 8.2). Two limit cases are considered.

Consider an *increasing flow* described by $\theta \uparrow \theta_1$, $\theta \downarrow 0$, $v \uparrow v_1$, $dv/dt \downarrow 0$, The valve equation of motion (8.23) then becomes:

Case 1:

$$\frac{C_1}{Re_1^k}\ \frac{1}{2}\rho_f v_1^2 D^3 = K_{G_1}\rho_m g D^4\ \sin\left(\theta_1+\theta_{cg}+\gamma\right) + \tag{8.24}$$

$$- K_{B_1}\rho_f g D^4\ \sin\left(\theta_1+\theta_{cb}+\gamma\right) + \left(K_{S_c} + K_S\left(\theta_1 - \theta_c\right)\right) + \Sigma K_f r_f F_{n_1}$$

Friction tends to delay the valve opening.

Consider a *decreasing flow* described by $\theta \downarrow \theta_2$, $\dot{\theta} \uparrow 0$, $v \downarrow v_2$, $dv/dt \uparrow 0$. The valve equation of motion (8.23) becomes:

Case 2:

$$\frac{C_2}{Re_2^k}\ \frac{1}{2}\rho_f v_2^2 D^3 = K_{G_2}\rho_m g D^4\ \sin\left(\theta_2+\theta_{cg}+\gamma\right) + \tag{8.25}$$

$$- K_{B_2}\rho_f g D^4\ \sin\left(\theta_2+\theta_{cb}+\gamma\right) + \left(K_{S_c} + K_S\left(\theta_2 - \theta_c\right)\right) - \Sigma K_f r_f F_{n_2}$$

Friction tends to delay the valve closure.

Now the case is considered that the angular disc position of the valve in the increasing flow is the same as that in the decreasing flow ($\theta_1 = \theta_2 = \theta$). Then the geometrical parameters $K_{G1} = K_{G2} = K_G$ and $K_{B1} = K_{B2} = K_B$. According to the power law formula, the coefficients $C_1 = C_2 = C$, if the Reynolds numbers Re_1 and Re_2 are in the same range. Due to hysteresis effects the hydrodynamic torques in the Equations (8.24) and (8.25) differ, which is revealed by the fact that $v_1 \neq v_2$. Consequently the friction torques differ, which is denoted by $F_{n1} \neq F_{n2}$. If it is assumed that $F_{n1} \approx F_{n2} = F_n$ the latter two equations yield after some manipulation:

Case 3:

$$C\,\mu^{k}\,\frac{1}{2}\,\rho_f^{1-k}\left[\frac{v\uparrow^{2-k}+v\downarrow^{2-k}}{2}\right]D^{3-k}=K_G\,\rho_m\,g\,D^4\,\sin\left(\theta+\theta_{cg}+\gamma\right)+ \tag{8.26}$$

$$-K_B\,\rho_f\,g\,D^4\,\sin\left(\theta+\theta_{cb}+\gamma\right)+\left(K_{S_c}+K_S\left(\theta-\theta_c\right)\right)$$

and:

$$C\,\mu^{k}\,\frac{1}{2}\,\rho_f^{1-k}\left[\frac{v\uparrow^{2-k}-v\downarrow^{2-k}}{2}\right]D^{3-k}=\sum K_f\,r_f\,F_n \tag{8.27}$$

In these equations v_1 is replaced by a fluid velocity in an *increasing flow*, introduced as $v\uparrow$, and v_2 is replaced by a fluid velocity in a *decreasing flow*, introduced as $v\downarrow$. In Equation (8.26) the effects of gravitation, buoyancy and springs are represented by a *weighted* or *averaged* fluid velocity, as if there is no friction:

$$v^{2-k}=\frac{v\uparrow^{2-k}+v\downarrow^{2-k}}{2} \tag{8.28}$$

The hysteresis may now be quantified by a *hysteresis factor*, introduced as the ratio of the friction torque and the sum of the gravitational, buoyancy and spring torques, which are balanced with the (frictionless) hydrodynamic torque:

$$Y(\theta)=\frac{v\uparrow^{2-k}-v\downarrow^{2-k}}{v\uparrow^{2-k}+v\downarrow^{2-k}} \tag{8.29}$$

This equation enables to estimate the friction torque as function of the valve disc position, if $v\uparrow$ and $v\downarrow$ are known from e.g. steady flow tests. In most practical cases the flow in the check valve is turbulent ($k = 0$).

According to the Equations (8.26) and (8.27) the hysteresis factor is dependent on the valve disc position and valve diameter. In general the relative roughness of sliding surfaces decreases with increasing valve size. Therefore this factor is expected to decrease with increasing valve size, which may be described by ($h < 0$):

$$Y(\theta)=y_1(\theta)+y_2(\theta)\,D^{h} \tag{8.30}$$

8.5 Critical velocity and Reynolds number

8.5.1 Critical velocity

The critical velocity is introduced as a fluid velocity at which the *check valve is just fully open* ($\theta = \theta_o$). Since the hydrodynamic and damping coefficients are soft, dynamic parameters, the critical velocity is also a soft, dynamic parameter. In principle the critical velocity is dependent on the Reynolds and Acceleration numbers (or in a more general sense: on the history of the flow field). It thus is not easily defined or determined in an unambiguous way. This problem is further discussed in section 8.7.2. For practical reasons the critical velocity is defined as a *steady- state* fluid velocity ($\theta = \theta_o$, $\dot{\theta} = 0$, $\ddot{\theta} = 0$, etc).

Due to hysteresis effects three different critical velocities may be distinguished:

1) The *critical velocity in an increasing flow*, denoted as $v_o\uparrow$:
2) The *critical velocity in a decreasing flow*, denoted as $v_o\downarrow$:
3) An *averaged critical velocity*, denoted as v_o:

These three cases are described by the Equations (8.24) to (8.26), applied to the fully opened valve. The latter case gives:

Case 3:

$$C_o \mu_f^k \frac{1}{2} \rho_f^{1-k} \left[\frac{v_o\uparrow^{2-k} + v_o\downarrow^{2-k}}{2} \right] D^{3-k} = K_{G_o} \rho_m g D^4 \sin(\theta_o + \theta_{cg} + \gamma)$$

$$- K_{B_o} \rho_f g D^4 \sin(\theta_o + \theta_{cb} + \gamma) + \left(K_{S_c} + K_S (\theta_o - \theta_c) \right) \qquad \textbf{(8.31)}$$

The *average critical velocity* is now introduced as:

$$\boxed{v_o^{2-k} = \frac{v_o\uparrow^{2-k} + v_o\downarrow^{2-k}}{2}} \qquad \textbf{(8.32)}$$

The average critical velocity is thus defined as the fluid velocity at which the check valve is *just fully open* under *steady flow* and *frictionless, valve conditions*. In that sense it fully represents the net effect of gravitation, buoyancy and spring(s), and may be considered as a measure for the valve response.

Scaling the critical velocity The average critical velocity v_o can be used for scaling to e.g. other valve diameters or spring configurations, since friction effects are eliminated. A general expression for the relationship between the critical velocities of two geometrically similar check valves can be obtained from Equation (8.31). For many check valve types the gravitational, buoyancy and spring effects do not appear together. In those cases simpler relations can be found, as illustrated below.

If spring effects play no role (e.g. swing type check valve) the critical velocity represents the *gravitational* and *buoyancy* effects only. In that case the relationship between the critical velocities of two geometrically similar check valves 1 and 2 is given by:

$$\left[\frac{\mu_{f_1}}{\mu_{f_2}}\right]^k \left[\frac{\rho_{f_1}}{\rho_{f_2}}\right]^{1-k} \left[\frac{v_{o_1}}{v_{o_2}}\right]^{2-k} \left[\frac{D_1}{D_2}\right]^{3-k} = \frac{K_{G_o}\rho_{m_1} g D_1^4 \sin(\theta_o+\theta_{cg}+\gamma) - K_{B_o}\rho_{f_1} g D_1^4 \sin(\theta_o+\theta_{cb}+\gamma)}{K_{G_o}\rho_{m_2} g D_2^4 \sin(\theta_o+\theta_{cg}+\gamma) - K_{B_o}\rho_{f_2} g D_2^4 \sin(\theta_o+\theta_{cb}+\gamma)} \tag{8.33}$$

If all the moving valve elements are submerged (e.g. sinking ball valve), the above equation simplifies to ($K_G = K_B$; $\theta_{cg} = \theta_{cb}$ if homogeneous mass distribution):

$$\left[\frac{v_{o_1}}{v_{o_2}}\right]^{2-k} = \left[\frac{\mu_{f_1}}{\mu_{f_2}}\right]^{-k} \left[\frac{\rho_{f_1}}{\rho_{f_2}}\right]^{k} \left[\frac{\rho_{m_1}/\rho_{f_1}-1}{\rho_{m_2}/\rho_{f_2}-1}\right] \left[\frac{D_1}{D_2}\right]^{1+k} \tag{8.34}$$

If gravitational and buoyancy effects play no role, the critical velocity represents the *spring* effects only. Now the relationship between the critical velocities of two geometrically similar check valves 1 and 2 is:

$$\left[\frac{v_{o_1}}{v_{o_2}}\right]^{2-k} = \left[\frac{\mu_{f_1}}{\mu_{f_2}}\right]^{-k} \left[\frac{\rho_{f_1}}{\rho_{f_2}}\right]^{k-1} \left[\frac{D_1}{D_2}\right]^{k-3} \left[\frac{K_{S_{c1}} + K_{S_1}(\theta_o - \theta_c)}{K_{S_{c2}} + K_{S_2}(\theta_o - \theta_c)}\right] \tag{8.35}$$

If the preset spring torque is relatively small this may be approximated by:

$$\left[\frac{v_{o_1}}{v_{o_2}}\right]^{2-k} \approx \left[\frac{\mu_{f_1}}{\mu_{f_2}}\right]^{-k} \left[\frac{\rho_{f_1}}{\rho_{f_2}}\right]^{k-1} \left[\frac{D_1}{D_2}\right]^{k-3} \left[\frac{K_{S_1}}{K_{S_2}}\right] \tag{8.36}$$

When the (scaled) average critical velocity is known, the actual critical velocities in an increasing flow and decreasing flow can be determined by using the hysteresis factor (section 8.4). Substitution of Equation (8.32) in Equation (8.29) yields after some manipulation:

$$\begin{aligned} v_o\uparrow^{2-k} &= v_o^{2-k}\,(1 + Y_o) \\ v_o\downarrow^{2-k} &= v_o^{2-k}\,(1 - Y_o) \end{aligned} \tag{8.37}$$

8.5.2 Critical Reynolds number

Based on the critical velocity, the critical Reynolds number is introduced as:

$$Re_o = \frac{\rho_f v_o D}{\mu_f} \tag{8.38}$$

Similarity of the critical Reynolds number is satisfied if:

$$\left[\frac{\mu_{f_1}}{\mu_{f_2}}\right]^{-1} \left[\frac{\rho_{f_1}}{\rho_{f_2}}\right] \left[\frac{v_{o_1}}{v_{o_2}}\right] \left[\frac{D_1}{D_2}\right] = 1 \tag{8.39}$$

For several valve types the ratio of the critical velocities is given in the Equations (8.33) to (8.36). These equations illustrate that similarity of the critical Reynolds number is not easily satisfied and can only be realized under exceptional conditions, e.g. with different fluids.

In most practical applications the critical Reynolds number is of the order of 10^5 or higher order, so that the critical flow is turbulent ($k = 0$).

8.6 Dimensionless valve equation of motion

In the development of a dimensionless valve equation of motion, *average* fluid velocities are considered, so that hysteresis effects can be excluded (section 8.4). Then the valve equation for angular motion (section 8.3) reduces to:

$$\left(K_I \rho_m + K_I C_{A_2} \rho_f + C_{A_3} \rho_d\right) D^5 \ddot{\theta} =$$

$$C_{D_1} \frac{1}{2} \rho_f v^2 D^3 + C_{D_{12}} \frac{1}{2} \rho_f v \dot{\theta} D^4 - C_{D_2} \frac{1}{2} \rho_f \dot{\theta}^2 D^5 + K_{V_m} \left(C_{A_1} + K_P\right) \rho_f D^4 \frac{dv}{dt} +$$

$$- K_G \rho_m g D^4 \sin\left(\theta + \theta_{cg} + \gamma\right) + K_B \rho_f g D^4 \sin\left(\theta + \theta_{cb} + \gamma\right) +$$

$$- \left(K_{S_c} + K_S \left(\theta - \theta_c\right)\right) - C_{D_3} \frac{1}{2} \rho_d \dot{\theta}^2 D^5 \qquad \textbf{(8.40)}$$

The critical velocity becomes ($\theta = \theta_o$, $\dot{\theta} = 0$, $\ddot{\theta} = 0$, $v = v_o$, $dv/dt = 0$):

$$C_{D_o} \frac{1}{2} \rho_f v_o^2 D^3 = K_{G_o} \rho_m g D^4 \sin\left(\theta_o + \theta_{cg} + \gamma\right) - K_{B_o} \rho_f g D^4 \sin\left(\theta_o + \theta_{cb} + \gamma\right) + T_{S_o} \qquad \textbf{(8.41)}$$

Elimination of the term gD^4 from the Equations (8.40) and (8.41) and division by $\frac{1}{2} \rho_f v_o^2 D^3$ yields after some manipulation:

$$2 \left[K_I \frac{\rho_m}{\rho_f} + K_I C_{A_2} + C_{A_3} \frac{\rho_d}{\rho_f} \right] \frac{D^2 \ddot{\theta}}{v_o^2} =$$

$$C_{D_1} \left[\frac{v}{v_o} \right]^2 + C_{D_{12}} \left[\frac{v}{v_o} \right] \frac{D \dot{\theta}}{v_o} - C_{D_2} \left[\frac{D \dot{\theta}}{v_o} \right]^2 + 2 K_{V_m} \left(C_{A_1} + K_P\right) \frac{D}{v_o^2} \frac{dv}{dt} +$$

$$- \left[C_{D_o} - \frac{T_{S_o}}{\frac{1}{2} \rho_f v_o^2 D^3} \right] \frac{K_G \rho_m \sin\left(\theta + \theta_{cg} + \gamma\right) - K_B \rho_f \sin\left(\theta + \theta_{cb} + \gamma\right)}{K_{G_o} \rho_m \sin\left(\theta_o + \theta_{cg} + \gamma\right) - K_{B_o} \rho_f \sin\left(\theta_o + \theta_{cb} + \gamma\right)} +$$

$$- \frac{\left(K_{S_c} + K_S \left(\theta - \theta_c\right)\right)}{\frac{1}{2} \rho_f v_o^2 D^3} - C_{D_3} \frac{\rho_d}{\rho_f} \left[\frac{D \dot{\theta}}{v_o} \right]^2 \qquad \textbf{(8.42)}$$

Now the following dimensionless variables may be introduced:

$$\alpha_1 = \theta \quad ; \quad v_1 = \frac{v}{v_o} \quad ; \quad \tau_1 = \frac{t\, v_o}{D} \tag{8.43}$$

so that:

$$\frac{d\alpha_1}{d\tau_1} \left(= \dot{\alpha}_1\right) = \frac{D\,\dot{\theta}}{v_o} \quad ; \quad \frac{d^2\alpha_1}{d\tau_1{}^2} \left(= \ddot{\alpha}_1\right) = \frac{D^2\,\ddot{\theta}}{v_o^2} \quad ; \quad \frac{dv_1}{d\tau_1} = \frac{D}{v_o^2}\frac{dv}{dt} \tag{8.44}$$

The critical velocity, as measure for the valve response, and the valve diameter are now used to define a velocity and a time scale.

As a next step the drag and added mass coefficients are replaced by power laws according to the Equations (8.8) and (8.19). The Reynolds numbers in these equations are converted to the critical Reynolds number, defined in Equation (8.38). With the dimensionless variables in Equation (8.43) this gives after some manipulation:

$$\begin{aligned}
&2\left[K_I\frac{\rho_m}{\rho_f} + K_I C_{22}\left[\frac{1}{\dot{\alpha}_1^2}\frac{d\dot{\alpha}_1}{d\tau_1}\right]^o + C_{33}\frac{\rho_d}{\rho_f}\left[\frac{1}{\dot{\alpha}_1^2}\frac{d\dot{\alpha}_1}{d\tau_1}\right]^q\right]\frac{d\dot{\alpha}_1}{d\tau_1} = \\
&\qquad \frac{C_1}{Re_o^k}\,v_1^{2-k} + \frac{C_{12}}{Re_o^l}\,v_1^{1-\frac{1}{2}l}\,\dot{\alpha}_1^{1-\frac{1}{2}l} - \frac{C_2}{Re_o^m}\,\dot{\alpha}_1^{2-m} + \\
&\qquad + 2\,C_{11}\,K_{V_m}\,v_1^{-2n}\left[\frac{dv_1}{d\tau_1}\right]^{1+n} + 2\,K_P\,K_{V_m}\left[\frac{dv_1}{d\tau_1}\right] + \\
&- \left[\frac{C_o}{Re_o^k} - \frac{T_{S_o}}{\frac{1}{2}\rho_f v_o^2 D^3}\right]\frac{K_G\rho_m\sin\left(\alpha_1+\alpha_{cg}+\gamma\right) - K_B\rho_f\sin\left(\alpha_1+\alpha_{cb}+\gamma\right)}{K_{G_o}\rho_m\sin\left(\alpha_o+\alpha_{cg}+\gamma\right) - K_{B_o}\rho_f\sin\left(\alpha_o+\alpha_{cb}+\gamma\right)} + \\
&- \frac{\left(K_{S_c} + K_S\left(\alpha_1 - \alpha_c\right)\right)}{\frac{1}{2}\rho_f v_o^2 D^3} - \frac{C_3}{Re_o^p}\left[\frac{\mu_d}{\mu_f}\right]^p\left[\frac{\rho_d}{\rho_f}\right]^{1-p}\dot{\alpha}_1^{2-p}
\end{aligned} \tag{8.45}$$

In this higher order, ordinary, non-linear differential equation the dimensionless angular valve disc position is described as function of a dimensionless time, with the dimensionless fluid velocity as boundary condition. The coefficients and powers are functions of the valve disc position. This dimensionless valve equation of motion is valid for $\alpha_c \leq \alpha_1 \leq \alpha_o$.

In general the Reynolds powers k, l, m and p in this equation may differ from zero. In that case the critical Reynolds number Re_o as well as the ratios of the fluid viscosities μ_d/μ_f and fluid densities ρ_d/ρ_f must be similar, in order to ensure physical similarity. (Note that this condition for physical similarity is not equivalent with Reynolds similarity of the flow in the valve and damper.) Only under these conditions the flow in the valve and damper can be considered apart, i.e. the flow in the valve may be turbulent, while the flow in the damper may be laminar or vice versa. However, as mentioned before, in common practice similarity of Re_o is hardly or not satisfied (section 8.5.2).

A more general application of the dimensionless valve equation is enabled by one or more relaxations. The ratio of the fluid viscosities μ_d/μ_f vanishes, if the power p is zero. This implies that the flow in the damper is turbulent. The critical Reynolds number Re_o vanishes, if the powers k, l, m (valve) and p (damping) are zero. This implies that the flow in both the valve and damper is turbulent.

The powers are relevant during all stages of closure and may be a function of the angular valve disc position. Therefore the flow should be turbulent at all valve disc positions, also when the fluid velocity is about zero (i.e. during flow reversal). The transition from a turbulent to a laminar pipe flow is not very likely here, since the time scale of closure is rather small. The stage of (active or effective) damping may be initiated from a stagnant damping fluid. In that case a transition from a laminar to a turbulent (damping) flow must take place.

The above relaxations do not require that the Acceleration powers n, o and q are zero. However, if viscous effects play a role of minor importance (e.g. at higher fluid velocities and fluid accelerations), then these powers are expected to be zero too (see examples in section 5.4.3).

If all powers are zero, then Equation (8.45) reduces to:

$$2\left[K_I\frac{\rho_m}{\rho_f}+K_I C_{22}+C_{33}\frac{\rho_d}{\rho_f}\right]\frac{d\dot{\alpha}_1}{d\tau_1}=$$

$$C_1 v_1^2+C_{12}v_1\dot{\alpha}_1-C_2\dot{\alpha}_1^2+2K_{V_m}(C_{11}+K_P)\left[\frac{dv_1}{d\tau_1}\right]+$$

$$-\left[C_o-\frac{T_{S_o}}{\frac{1}{2}\rho_f v_o^2 D^3}\right]\frac{K_G\rho_m\sin(\alpha_1+\alpha_{cg}+\gamma)-K_B\rho_f\sin(\alpha_1+\alpha_{cb}+\gamma)}{K_{G_o}\rho_m\sin(\alpha_o+\alpha_{cg}+\gamma)-K_{B_o}\rho_f\sin(\alpha_o+\alpha_{cb}+\gamma)}+$$

$$-\frac{\left(K_{S_c}+K_S(\alpha_1-\alpha_c)\right)}{\frac{1}{2}\rho_f v_o^2 D^3}-C_3\left[\frac{\rho_d}{\rho_f}\right]\dot{\alpha}_1^2 \qquad (8.46)$$

About other time and velocity scales .....

The time and velocity scales which are introduced in Equation (8.43) are based on the critical velocity and valve diameter. In principle other time and velocity scales can be used to develop dimensionless valve equations.

A typical time scale of the stage of active damping is the damping time. The damping time, however, is not a direct measure for the valve response and not relevant to undamped check valves.

8.7 Initial and boundary conditions

Self-actuating check valves operate without power supply and are primarily controlled by the fluid passing through. Therefore the initial and boundary conditions are determined by and may be fully described in terms of flow conditions.

8.7.1 Boundary conditions $(t_b < t \leq t_c)$

In the (dimensionless) valve equation of motion the fluid velocity appears as boundary condition. In general this boundary condition is described by:

$$v = f(t) \qquad (8.47)$$

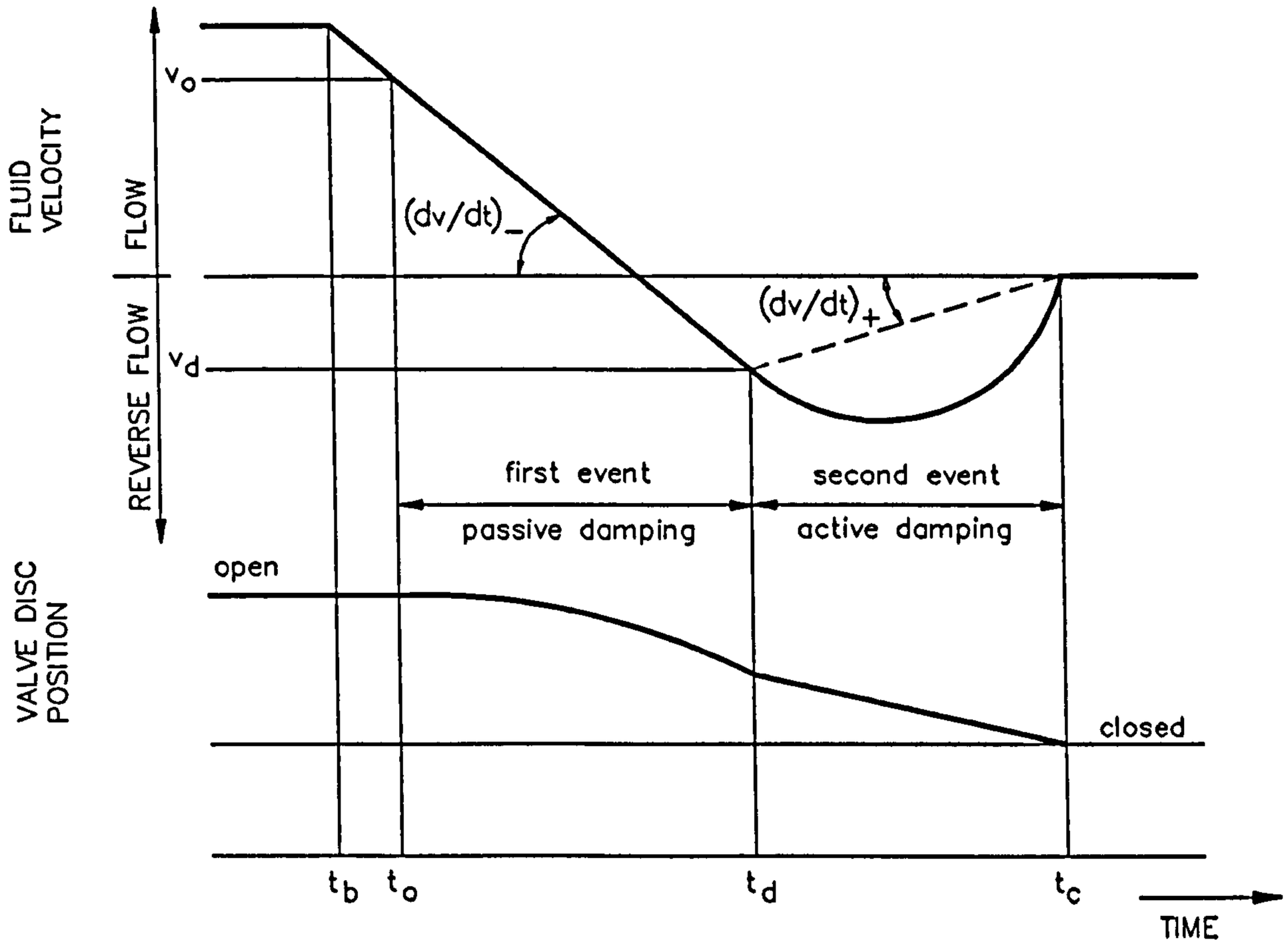

t_o = start of valve closure
t_d = damping becomes active
t_b = start at transient
t_c = instant of valve closure

Figure 8.2 Closure behaviour of damped check valves

Or in a dimensionless form:

$$v_1 = f(\tau_1) \tag{8.48}$$

Here the boundary conditions are described in a global form. The valve closure is assumed to be preceded by steady flow conditions. During closure two events are distinguished: 1) a stage of passive damping, denoted as the *first event*, and 2) a stage of active damping, denoted as the *second event* (figure 8.2).

First event During the stage of passive damping ($t_b < t \leq t_d$; $\theta_d < \theta \leq \theta_b$) the check valve is assumed to have a minor influence on the fluid flow. The valve closure is a result of flow changes which are imposed by the system. The system conditions are described in terms of pipeline configuration and transient conditions like pump trip, pump failure, etc. In first approximation the fluid velocity is assumed to change linearly in time:

$$v = v_b + \left[\frac{dv}{dt}\right]_- (t - t_b) \tag{8.49}$$

Or in a dimensionless form:

$$v_1 = \frac{v_b}{v_o} + \frac{D}{v_o^2}\left[\frac{dv}{dt}\right]_- (\tau_1 - \tau_b) \tag{8.50}$$

Where the *(mean) initial flow deceleration* is defined as:

$$\left[\frac{dv}{dt}\right]_- = \frac{1}{t_d - t_o}\int_{t_o}^{t_d} \frac{dv}{dt}\,dt = \frac{v_d - v_o}{t_d - t_o} \tag{8.51}$$

The subscript - refers to the sign of the mean initial flow deceleration, which is negative during the first event of closure ($v_o > v_d$).

Second event During the stage of active damping ($t_d \leq t < t_c$; $\theta_c < \theta \leq \theta_d$) the flow is imposed by the combination of the valve and system. The damping time (type of damping) and system reflection time play an important role here. At the beginning of the second event the fluid velocity is per definition equal to v_d. At the end of this event the valve is closed, so that the fluid velocity is zero. This leads to the following conditions (figure 8.2):

$$\begin{aligned} t = t_d: &\quad v = v_d \quad \wedge \quad \frac{dv}{dt} = \left[\frac{dv}{dt}\right]_- \\ t = t_c: &\quad v = 0 \end{aligned} \tag{8.52}$$

Analogous to the (mean) initial flow deceleration, as flow characteristic for the first event, the *(mean) reverse flow deceleration* may now be introduced for the second event:

$$\left[\frac{dv}{dt}\right]_+ = \frac{1}{t_c - t_d}\int_{t_d}^{t_c} \frac{dv}{dt}\,dt = -\frac{v_d}{t_c - t_d} \tag{8.53}$$

The subscript + refers to the sign of the mean reverse flow deceleration, which is generally positive during the second event (if $v_d < 0$). The parameter gives global information about the damping time, but no details about the velocity-time history.

This leads to the following dimensionless boundary conditions:

$$\tau_1 = \tau_d : \quad v_1 = \frac{v_d}{v_o} \quad ; \quad \frac{dv_1}{d\tau_1} = \frac{D}{v_o^2} \left[\frac{dv}{dt}\right]_- \tag{8.54}$$

$$\tau_1 = \tau_c : \quad v_1 = 0$$

and:

$$\left[\frac{dv_1}{d\tau_1}\right]_+ = \frac{D}{v_o^2} \left[\frac{dv}{dt}\right]_+ \tag{8.55}$$

The undamped check valve has no stage of active damping. Nevertheless, the motion of the valve disc against the seat may be seen as damped motion. In that sense the second event of closure may be considered as a limit case with infinitesimal damping time, so that $(dv/dt)_+ \rightarrow \infty$.

About alternative descriptions of the boundary conditions ...

The velocity-time history may be described in several forms, e.g. by polynomials:

$$v_1(\tau_1) = a_0 + a_1 \tau_1 + a_2 \tau_1^2 + \ldots \tag{8.56}$$

Or by the time derivatives in a Taylor series:

$$v_1(\tau_1) = f\left(v_1 , \frac{dv_1}{d\tau_1} , \frac{d^2v_1}{d\tau_1^2} , \frac{d^3v_1}{d\tau_1^3} , \ldots\ldots \right) \tag{8.57}$$

However, in general an infinite number of terms are needed.

Alternatively the velocity-time history may be described by a set of combinations of the fluid velocity and velocity gradient, which forms a *trajectory* in the *v-dv/dt*-plane:

$$\Phi\left(v_1 , \frac{dv_1}{d\tau_1} \right) = 0 \tag{8.58}$$

The latter approach is used in the valve model for damped check valves (section 12.2).

8.7.2 Initial conditions

The valve closure is assumed to be preceded by steady flow conditions, so that:

$$\tau_1 \uparrow \tau_b : \quad v_1 = \frac{v_b}{v_o} \quad \wedge \quad \frac{dv_1}{d\tau_1} = 0 \tag{8.59}$$

The initial fluid velocity v_b may be smaller or greater than the critical velocity v_o. Therefore two cases must be distinguished:

$$\tau_1 \uparrow \tau_b :$$

$$v_1 < 1 : \quad \alpha_1 = \alpha_b \quad ; \quad \dot{\alpha}_1 = 0 \quad ; \quad \frac{d\dot{\alpha}_1}{d\tau_1} = 0 \qquad \textbf{(a)}$$

$$v_1 \geq 1 : \quad \alpha_1 = \alpha_o \quad ; \quad \dot{\alpha}_1 = 0 \quad ; \quad \frac{d\dot{\alpha}_1}{d\tau_1} = 0 \qquad \textbf{(b)}$$

(8.60)

If the valve is initially, partly open ($v_1 < 1$), the hydrodynamic torque balances the sum of the gravitational, buoyancy and spring torque, while there is no damping torque. Under these conditions Equation (8.45) holds. If the valve is initially, fully open ($v_1 \geq 1$) the hydrodynamic torque additionally balances the torque, exerted by the mechanical stop that restricts further opening.

After the steady flow period, according to Equation (8.50), the initial unsteady flow conditions are described by:

$$\tau_1 \downarrow \tau_b : \quad v_1 = \frac{v_b}{v_o} \quad ; \quad \frac{dv_1}{d\tau_1} = \frac{D}{v_o^2} \left[\frac{dv}{dt}\right]_- \tag{8.61}$$

So that:

$$\tau_1 \downarrow \tau_b :$$

$$v_1 < 1 : \quad \alpha_1 = \alpha_b \quad ; \quad \dot{\alpha}_1 = 0 \quad ; \quad \frac{d\dot{\alpha}_1}{d\tau_1} \neq 0 \qquad \textbf{(a)}$$

$$v_1 \geq 1 : \quad \alpha_1 = \alpha_o \quad ; \quad \dot{\alpha}_1 = 0 \quad ; \quad \frac{d\dot{\alpha}_1}{d\tau_1} = 0 \qquad \textbf{(b)}$$

(8.62)

Consider the case that the valve is initially partly open ($v_1 < 1$). Substitution of Equation (8.62.a) in Equation (8.45) leads to ($o = 0$):

$$\frac{d\dot{\alpha}_1}{d\tau_1} = \frac{C_{11} K_{V_m} \left[\frac{v_b}{v_o}\right]^{-2n} \left[\frac{D}{v_o^2} \left[\frac{dv}{dt}\right]_-\right]^{1+n} + K_P K_{V_m} \left[\frac{D}{v_o^2} \left[\frac{dv}{dt}\right]_-\right]}{K_I \left[\frac{\rho_m}{\rho_f} + C_{22}\right]} \tag{8.63}$$

The four above-mentioned torques are absent here, since they are balanced, while the damping is assumed to be passive ($C_{33} = 0$). The power o must be zero, in order to obtain a finite value for the added mass coefficient C_{A2} if $Ac_2 \rightarrow 0$ (section 5.4.3). Formally another solution exists: if the power $o \neq 0$ then $d\dot{\alpha}_1/d\tau_1 = 0$.

Now consider the case that the valve is initially fully open ($v_1 \geq 1$). Under these conditions the valve does not begin to close immediately, but at the instant that the fluid velocity equals the critical velocity:

$$\begin{aligned} & v_1 \downarrow \frac{v_o^*}{v_o} \quad ; \quad \frac{dv_1}{d\tau_1} = \frac{D}{v_o^2} \left[\frac{dv}{dt}\right]_- \\ \tau_1 \uparrow \tau_o^* : & \\ & \alpha_1 = \alpha_o \quad ; \quad \dot{\alpha}_1 = 0 \quad ; \quad \frac{d\dot{\alpha}_1}{d\tau_1} \neq 0 \end{aligned} \tag{8.64}$$

The critical velocity v_o^* is introduced here as a dynamic value, at which the valve starts closing. This parameter should be distinguished from the steady-state value v_o, which is introduced in section 8.5. The question arises to what extent these two critical velocities coincide.

About the steady-state and dynamic critical velocity ...

Considering the valve equation of motion, it can be concluded that theoretically v_o^* must be greater than v_o, since additional forces arise proportional to dv/dt (< 0), which tend to close the valve.

For the measurement of the dynamic critical velocity the valve disc position must be known. The determination of v_o^* is complicated, due to the fact that $d\theta/dv$ is zero when the valve starts closing, while fluctuations in the disc position signal and strong hysteresis effects (butterfly valve) may play a role. For these reasons the accuracy of v_o^* is rather limited. Thus far no reliable, quantitative results are obtained, although it can be seen that v_o^* is dependent on the Acceleration number. Further research is needed here.

The influence of the initial fluid velocity on the valve response is assumed to be small for fluid velocities greater than the critical velocity. In other words: history effects are assumed to be neglectable. In that case the initial fluid velocity may be replaced by, and is fully equivalent with the initial valve disc position. Thus either of these parameters may be used.

Kruisbrink (1988) investigates the influence of the initial fluid velocity on the valve response for initial fluid velocities above the critical velocity. Experiments are performed with a piston check valve with initial fluid velocities, varying from once to twice the critical velocity. After the steady flow period the flow deceleration is about constant until valve closure. The test results are presented in dynamic characteristics and show that the valve response is hardly influenced by the initial fluid velocity. Only for small initial flow decelerations up to 2.5 m/s^2 a small influence is observed.

About history effects .....
In the research of Kruisbrink (1988) history effects are indirectly taken into account. They appear in the experiments but do not seem to have a significant effect on the motion of the valve disc.

The kink in the fluid velocity-time history at the instant $t = t_b$ (figure 8.2) is not very realistic. In practice the transition from the steady flow conditions to the unsteady flow conditions takes place gradually.

8.8 Fluid force and torque coefficients

In this section the properties of the fluid force and torque coefficients in the valve equation of motion are studied.

For this purpose the drag and added mass coefficients are considered in the general sense beyond that of the power law formulation. According to Equation (8.7):

$$C_{D_{\cdot\cdot}},\ C_{A_{\cdot\cdot}} = f\left(\theta,\ Re,\ Ac\right) \qquad \textbf{(8.65)}$$

The Reynolds and Acceleration numbers of the flow in the valve and damper are given in Equation (8.9) and (8.20), respectively. These numbers may be converted to the dimensionless variables in the Equations (8.43) and (8.44), and the critical Reynolds number. This leads to:

valve:

$$C_{D_{\cdot\cdot}}, C_{A_{\cdot\cdot}} = f\left[\theta, \frac{v}{v_o}, \frac{\rho_f v_o D}{\mu_f}, \frac{D\dot{\theta}}{v_o}, \frac{D}{v_o^2}\frac{dv}{dt}, \frac{D^2\ddot{\theta}}{v_o^2}\right] \tag{8.66}$$

damping:

$$C_{D_{\cdot\cdot}}, C_{A_{\cdot\cdot}} = f\left[\theta, \frac{\mu_d}{\mu_f}, \frac{\rho_d}{\rho_f}, \frac{\rho_f v_o D}{\mu_f}, \frac{D\dot{\theta}}{v_o}, \frac{D^2\ddot{\theta}}{v_o^2}\right] \tag{8.67}$$

In practice the valve disc position and motion cannot always be determined (e.g. in the case of membrane check valves, multi-disc and multi-ring check valves). The check valve is primarily controlled by the fluid passing through. Therefore it may be assumed that at a certain instant of time the position and the motion of the disc are fully determined by the history of the flow field.

Consider the dimensionless valve equation of motion given in Equation (8.42). This implicit equation describes the dimensionless valve disc position as a function of time with the dimensionless fluid velocity as boundary condition. Let the boundary conditions be described by the Taylor series given in Equation (8.57). Then the following functional relationship holds:

$$\theta(t) = f\left[C_{D_{\cdot\cdot}}, C_{A_{\cdot\cdot}}, \cdots, \frac{v}{v_o}, \frac{D}{v_o^2}\frac{dv}{dt}, \frac{D^2}{v_o^3}\frac{d^2v}{dt^2}, \cdots\right] \tag{8.68}$$

From the combination of the Equations (8.65) to (8.68) it now follows:

$$\theta, \frac{D\dot{\theta}}{v_o}, \frac{D^2\ddot{\theta}}{v_o^2} = f\left[\frac{\mu_d}{\mu_f}, \frac{\rho_d}{\rho_f}, Re_o, \ldots, \frac{v}{v_o}, \frac{D}{v_o^2}\frac{dv}{dt}, \frac{D^2}{v_o^3}\frac{d^2v}{dt^2}, \cdots\right] \tag{8.69}$$

Thus the Equations (8.66) and (8.67) may both be rewritten as:

$$C_{D_{\cdot\cdot}}, C_{A_{\cdot\cdot}} = f\left[\frac{\mu_d}{\mu_f}, \frac{\rho_d}{\rho_f}, Re_o, \ldots, \frac{v}{v_o}, \frac{D}{v_o^2}\frac{dv}{dt}, \frac{D^2}{v_o^3}\frac{d^2v}{dt^2}, \cdots\right] \tag{8.70}$$

In this relation the drag and added mass coefficients are written as implicit functions of the fluid parameters and flow variables.

Finally the step to the global force and torque coefficients is made. Hereto the hydrodynamic forces on the valve elements are written as (section 7.1 and 7.3):

$$X_H = C_X \frac{1}{2} \rho_f v^2 D^2$$

$$Y_H = C_Y \frac{1}{2} \rho_f v^2 D^2$$

$$T_H = C_T \frac{1}{2} \rho_f v^2 D^3$$

(8.71)

A comparison with Equation (8.6) gives after some manipulation:

angular motion:

$$C_T \left[\frac{v}{v_o}\right]^2 = C_{D_1} \left[\frac{v}{v_o}\right]^2 + C_{D_{12}} \left[\frac{v}{v_o}\right]\left[\frac{D\dot{\theta}}{v_o}\right] - C_{D_2} \left[\frac{D\dot{\theta}}{v_o}\right]^2 + \tag{8.72}$$

$$+ 2 K_{V_m}\left(C_{A_1} + K_P\right) \frac{D}{v_o^2}\frac{dv}{dt} - 2 K_I C_{A_2} \frac{D^2 \ddot{\theta}}{v_o^2}$$

With the Equations (8.69) and (8.70) follows directly:

$$C_T = f\left[\frac{\mu_d}{\mu_f}, \frac{\rho_d}{\rho_f}, Re_o, \ldots, \frac{v}{v_o}, \frac{D}{v_o^2}\frac{dv}{dt}, \frac{D^2}{v_o^3}\frac{d^2v}{dt^2}, \ldots\right] \tag{8.73}$$

For confined fluids the fluid forces and torque are fully coupled (section 6.4). Therefore the above result also holds for the global force coefficients C_X and C_Y.

The above result should be considered together with the (other) coefficients and parameter groups in the dimensionless valve equation of motion. In that sense the fluid parameters μ_d/μ_f, ρ_d/ρ_f and Re_o may be excluded from the above functional relation and added to the parameter list.

The latter two steps lead to:

$$C_{X,Y,T} = f\left[\frac{v}{v_o}\ ,\ \frac{D}{v_o^2}\frac{dv}{dt}\ ,\ \frac{D^2}{v_o^3}\frac{d^2v}{dt^2}\ ,\ .....\right] \qquad (8.74)$$

In this expression the global force and torque coefficients are described in the form of series.

About history effects .....

The above result is similar to Equation (7.26), which is developed from the idea that the history term may be represented by higher order terms (section 7.3.1). Although the history term is absent in the valve equation of motion, the history of the flow field is described here by the boundary conditions and in the form of a Taylor series.

As alternative, the boundary conditions may be described by trajectories in the *v-dv/dt*-plane, as introduced in Equation (8.58). In that case holds along a trajectory, which is followed during closure:

$$\boxed{C_{X,Y,T} = f\left[\frac{v}{v_o}\ ,\ \frac{D}{v_o^2}\frac{dv}{dt}\right]} \qquad (8.75)$$

This result is further used in the development of valve characteristics (chapter 11).

About conservative systems .....

Consider a check valve in a pipe with an inviscid, *stagnant fluid*. This system is a conservative system (section 6.1), if friction effects in the valve and in the damping fluid are absent too. In that case history effects play no role. The fluid force and torque coefficients are now a function of the angular valve disc position only (section 6.2). Under such conditions only the instantaneous state of the system is relevant, and not the path (i.e. the history) which is followed from one state to the other.

The question arises if the above still holds for an *inviscid, fluid flow*. Consider the check valve, now in a pipe with an inviscid, non-uniform parallel flow. The external force, which acts on this system due to the pressure gradient across the fluid, is proportional to the fluid velocity gradient *dv/dt* (section 6.7.3). Let this force be described by:

$$X_p = \rho_f (V_b + V_f)\frac{dv}{dt} \qquad (8.76)$$

where V_m and V_f are the volumina of the moving elements and the pipe fluid, respectively.

The energy ΔE which is added to this system in the time interval $[t_1, t_2]$ is:

$$\Delta E = \int_{t_1}^{t_2} X_P v \, dt = \rho_f (V_m + V_f) \int_{t_1}^{t_2} \frac{dv}{dt} v \, dt = \frac{1}{2} \rho_f (V_m + V_f) \left(v_2^2 - v_1^2\right) \qquad (8.77)$$

The equation illustrates that the path which is followed in the v-dv/dt-plane from state 1 to 2 is not relevant. As a next step it should be investigated, if the above also holds for the valve disc position. The latter is hard to prove, seen the implicit and non-linear character of the valve equation of motion. If so, then Equation (8.75) is not only valid along a trajectory, but more generally applicable. If friction and fluid viscosity play a role of minor importance, this inviscid fluid flow concept may even be applied to viscous fluid flows. In practice, however, most damped check valves are non-conservative systems, due to a strong dissipation of energy in the damping device.

8.9 Physical similarity

In this section the conditions for physical similarity between two check valves are summarized.

In the dimensionless valve equation of motion (section 8.6) the dimensionless valve disc position is described as function of a dimensionless time:

$$\alpha_1 = f(\tau_1) \qquad (8.78)$$

A necessary condition for physical similarity is that all coefficients (i.e. dimensionless parameters or parameter groups, powers, Reynolds and Acceleration numbers) in the valve equation of motion are similar functions of the angular valve disc position or constants. Further the initial and boundary conditions must be similar. Usually a distinction is made between geometric, kinematic and dynamic similarity.

Geometric similarity The following parameters ensure geometric similarity of both valve, counterweight, damper and free surface (involves [L] only):

$$K_I \; ; \; K_{V_m} \; ; \; K_P \; ; \; K_G \; ; \; K_B \; ; \; \alpha_o \; ; \; \alpha_{cg} \; ; \; \alpha_{cb} \; ; \; \gamma \qquad (8.79)$$

The geometrical parameters K may be a function of the angular disc position only. Note that geometric similarity is a necessary condition for similarity of the drag and added mass coefficients.

Kinematic similarity Two flows are kinematically similar (i.e similarity of motion), if the ratios of corresponding velocities and accelerations are the same throughout the flow field at corresponding times (e.g. Massey, 1971; Vennard and Street, 1982).

To ensure kinematic similarity for the motion of the valve disc the boundary conditions, in terms of dimensionless fluid velocities, must be similar:

$$v_1 = f(\tau_1) \tag{8.80}$$

The following parameter groups help ensure kinematic similarity for the first event (involves [L, T] only):

$$\frac{v_b}{v_o} \quad ; \quad \frac{D}{v_o^2}\left[\frac{dv}{dt}\right]_- \tag{8.81}$$

The first group in this expression is equivalent with α_b/α_o.

The following parameter groups help ensure kinematic similarity for the second event:

$$\frac{v_d}{v_o} \quad ; \quad \frac{D}{v_o^2}\left[\frac{dv}{dt}\right]_- \quad ; \quad \frac{D}{v_o^2}\left[\frac{dv}{dt}\right]_+ \tag{8.82}$$

Dynamic similarity The following parameter groups help ensure dynamic similarity (i.e. similarity of forces and torques) (involves [M, L, T] only):

$$C_{D_{..}} ; C_{A_{..}} ; \frac{\rho_m}{\rho_f} ; \frac{\rho_d}{\rho_f} ; Re_o ; \frac{\mu_d}{\mu_f} ; \frac{T_{S_o}}{\rho_f v_o^2 D^3} ; \frac{T_{S_c}}{\rho_f v_o^2 D^3} \tag{8.83}$$

The preset spring torque K_{Sc} is represented by T_{Sc} since $T_{Sc} = -K_{Sc}$. The spring constant K_S is fully represented by T_{So}, T_{Sc} and α_o. The fifth group in this expression vanishes, if the flow in the valve and damper is turbulent. The sixth group vanishes if the flow in the damper is turbulent.

8.10 Review and conclusions

A general valve equation of motion is developed for check valves with rotating elements, including inertia, hydrodynamic, gravitational, buoyancy, spring, friction and damping effects. The equation is based on the equation of motion for a rotating body in a confined, viscous fluid. The drag and added mass coefficients in the hydrodynamic torque on the valve disc are described by power laws. History effects are ignored. The hysteresis factor is introduced to represent friction effects. The critical velocity is introduced to represent gravitational, buoyancy and spring effects. In order to enable scaling, a weighted or averaged value of the critical velocity is introduced, such that hysteresis effects are eliminated.

The valve equation for angular motion is described in a dimensionless form, whereby the critical velocity and valve diameter are used to define a velocity and a time scale. The (dimensionless) velocity-time history is used as boundary condition, and described in terms of global flow conditions, defined for the stages of passive and active damping.

The (dimensionless) valve equation of motion shows, together with the initial and boundary conditions, which (dimensionless) variables, parameters and parameter groups are relevant to the check valve closure. In that sense they are used in a dimensional analysis (chapter 11). The dimensionless quantities show under which conditions physical similarity is ensured. A more general application of the dimensionless valve equation of motion is enabled, if the flow in the damper or the flow in both the valve and damper is turbulent.

A dimensionless valve equation for check valves with translating elements can be derived in a similar way. For this purpose the equation of motion for a translating body in a confined, viscous fluid should be used. It can be shown that the results obtained for rotating type check valves are also valid for translating type check valves. Here the torques should be replaced by forces, while the angular position should be replaced by a linear one.

9 Pipe equations

In this chapter the hydrodynamic effects of a (check) valve closure on the pipeline system are studied. The valve is considered as a system component without physical dimensions, and is described in terms of fluid velocities and pressure heads.

The transient flow in the pipes is described by conventional waterhammer theory. It is assumed that the transient flow is dominated by fluid inertia, so that effects such as pipe friction may be ignored. The phenomenon of *unsteady*, initial flow conditions in pipeline systems is studied. Basic differential equations are derived for the transient flow in a pipe with a uniform flow deceleration as initial condition. The differential equations are used to describe the pressure head changes due to a valve closure under reflection free and reflecting boundary conditions. The theory is extended to pipe junctions and varying head boundaries.

As a result (dimensionless) pipe equations are developed which describe the event of a (check) valve closure under unsteady, initial flow conditions. The equations show which (dimensionless) variables and parameters are relevant to the valve closure. As in the previous chapter, the results are used in a dimensional analysis to develop valve characteristics (chapter 11) and parameterized valve models (chapter 12).

9.1 Basic differential equations for transient flow

9.1.1 Continuity equation

Consider the unsteady flow of a fluid in a tube. Due to the pressure surges associated with flow changes the tube wall may stretch and expand. The tube is assumed to be slender so that pressure and density variations over the cross section may be neglected (long wave-length approximation, $\lambda \gg D$). By considering mean values of the fluid velocities over the cross sectional area of the tube the flow may be treated as a one-dimensional flow.

The differential form of the one-dimensional continuity equation is:

$$\frac{\partial \rho_f A}{\partial t} + \frac{\partial \rho_f A v}{\partial x} = 0 \qquad (9.1)$$

In terms of total derivatives, defined with respect to the motion of a fluid particle, this equation may be rewritten as:

$$\frac{1}{\rho_f}\frac{d\rho_f}{dt} + \frac{1}{A}\frac{dA}{dt} + v_x = 0 \qquad \textbf{(9.2)}$$

No restrictions are made with respect to the shape of the cross sectional area, so that the Equations (9.1) and (9.2) hold for converging or diverging tubes.

The first term in Equation (9.2) accounts for the compressibility effects of the fluid. The term may be related to the pressure by the *equation of state*:

$$\frac{\Delta\rho_f}{\Delta p} = \frac{\rho_f}{K} \qquad \textbf{(9.3)}$$

Or, in terms of total derivatives:

$$\frac{1}{\rho_f}\frac{d\rho_f}{dt} = \frac{1}{K}\frac{dp}{dt} \qquad \textbf{(9.4)}$$

The bulk modulus of elasticity K is a function of the pressure and temperature.

K may be approximated by a constant value if the temperature variations are small (isothermal conditions) and the pressure is much smaller than the bulk modulus of elasticity ($p \ll K$). In that case the use of the bulk modulus is limited to slightly compressible fluids.

The second term in Equation (9.2) deals with the elasticity of the tube. The deformation of a tube is dependent on the pressure, wall thickness and elasticity, cross sectional shape and the support conditions of the tube. For *prismatic* tubes the cross sectional area is a function of the pressure only (Wylie and Streeter, 1993):

$$\frac{dA}{dt} = \frac{dA}{dp}\frac{dp}{dt} \qquad \textbf{(9.5)}$$

Substitution of the Equations (9.4) and (9.5) in Equation (9.2) yields:

$$\frac{1}{K}\frac{dp}{dt}\left[1 + \frac{K}{A}\frac{dA}{dp}\right] + v_x = 0 \qquad \textbf{(9.6)}$$

The pressure wave speed can be derived to be (e.g. Wylie and Streeter, 1993):

$$c^2 = \frac{\frac{K}{\rho_f}}{1 + \frac{K}{A}\frac{\Delta A}{\Delta p}} \tag{9.7}$$

For linear elastic fluids and pipe wall materials the pressure wave speed is constant (only if K is a constant). The term $\Delta A/\Delta p$ makes the pressure wave speed dependent of the support conditions of the pipe (section 14.2).

Substitution of Equation (9.7) in Equation (9.6) yields after some manipulation:

$$\frac{dp}{dt} + \rho_f c^2 v_x = 0 \tag{9.8}$$

Introduce now the piezometric head or pressure head H as:

$$p = \rho_f g(H - z) \tag{9.9}$$

With $\partial z/\partial x = \sin\gamma$ Equation (9.8) becomes:

$$\boxed{H_t + \left[v H_x - v \sin\gamma\right] + \frac{c^2}{g} v_x = 0} \tag{9.10}$$

This is the one-dimensional *continuity equation* for slightly compressible fluids in prismatic tubes at any slope. The equation may be simplified under the assumption that the fluid velocity is much smaller than the pressure wave speed ($v \ll c$), known as the acoustic approximation. In that case the convective terms (between square brackets) may be neglected.

Note that cross sectional area changes are usually not considered under steady flow conditions ($H_t = 0$; $v_x = 0$). In that case the steady flow in sloped tubes, with or without friction is not correctly described. This inconsistency disappears, when the convective terms are neglected.

9.1.2 Pipe equation of motion

Consider an unsteady fluid flow in a tube, which is inclined with the horizontal at an angle γ. The forces on the fluid are surface forces (pressure and shear) and body forces (gravitation).

The one-dimensional equation of motion is:

$$p_x A + \tau_o \pi D + \rho_f g A \sin\gamma + \rho_f A \frac{dv}{dt} = 0 \qquad \textbf{(9.11)}$$

The shear stress τ_o is assumed to be the same as if the flow were steady. It thus can be related to the mean fluid velocity by introducing the Darcy-Weisbach friction coefficient f:

$$\tau_o = \rho_f \frac{f v|v|}{8} \qquad \textbf{(9.12)}$$

The equation is obtained from the Darcy-Weisbach equation $\Delta p = f\,(L/D)\,½\rho_f v^2$ and a steady flow force balance, described by $\Delta p\ ¼\pi D^2 = \tau_o\,\pi DL$, as applied to a horizontal pipe of length L and diameter D.

Substitution of the Equations (9.9) and (9.12) in Equation (9.11) yields after some manipulation the one-dimensional *equation of motion*:

$$\boxed{gH_x + v_t + [v\,v_x] + \frac{f\,v|v|}{2D} = 0} \qquad \textbf{(9.13)}$$

The equation is valid for the fluid flow in converging or diverging tubes at any slope. This equation is also commonly used in a simplified form, where the convective term (between square brackets) is neglected (see section 9.2).

9.2 Method of characteristics

The basic differential equations for the transient flow in a pipe are the equations of motion and continuity (section 9.1). These equations form a pair of quasi-linear, hyperbolic, partial differential equations in terms of two dependent variables, the fluid velocity and pressure head, and two independent variables, the distance along the pipe and time. The equations can be transformed into four ordinary differential equations

by applying the method of characteristics. The equations, grouped and identified as C^+-and C^--equations, are:

$$C^+\text{-equations:} \quad \begin{cases} \dfrac{g}{c}\dfrac{dH}{dt} + \dfrac{dv}{dt} - \left[\dfrac{g}{c} v \sin\alpha\right] + \dfrac{f\, v|v|}{2D} = 0 \\ \dfrac{dx}{dt} = [v] + c \end{cases} \tag{9.14}$$

$$C^-\text{-equations:} \quad \begin{cases} -\dfrac{g}{c}\dfrac{dH}{dt} + \dfrac{dv}{dt} + \left[\dfrac{g}{c} v \sin\alpha\right] + \dfrac{f\, v|v|}{2D} = 0 \\ \dfrac{dx}{dt} = [v] - c \end{cases} \tag{9.15}$$

The terms between square brackets vanish if the simplified forms of the respective equations of motion and continuity are used. This will be done from now on.

Multiplying by $c\,dt/g$ and integration of the simplified Equations (9.14) and (9.15) along the characteristic $dx/dt = +c$ (from point A to P), and $dx/dt = -c$ (from point B to P) yields, respectively:

$$H_P + \frac{c}{gA} Q_P = H_A + \frac{c}{gA} Q_A - f \frac{\Delta L_{AP}}{D} \frac{Q_P|Q_A|}{2gA^2} \tag{9.16}$$

$$H_P - \frac{c}{gA} Q_P = H_B - \frac{c}{gA} Q_B + f \frac{\Delta L_{PB}}{D} \frac{Q_P|Q_B|}{2gA^2} \tag{9.17}$$

These two compatibility equations are the basic algebraic relations that describe the transient propagation of pressure and flow along the characteristics $dx/dt = \pm c$. In these equations the friction term is used in the form, as proposed by Wylie (1983). The equations are commonly used in waterhammer computer codes.

9.3 Fluid inertia and pipe friction effects

According to the simplified Equation of motion (9.13) the pressure head gradient along the pipe is determined by a linear fluid inertia effect and a non-linear friction effect. It is assumed that the transient flow is dominated by fluid inertia and that friction may be neglected:

$$\frac{f\,v^2}{2D} \ll |v_t| \qquad \textbf{(9.18)}$$

In most practical cases f is of the order $O(10^{-2})$, v is $O(1)$ and D is $O(10^{-1})$ or of higher order, so that the friction term at the left hand side is of the order $O(10^{-1})$. Thus, the inertia term at the right hand side should be $O(1)$ or higher. If friction may not be neglected and the fluid inertia and friction term are of the same order, then the fluid deceleration will generally be small. In that case the pressure surges induced by the check valve closure play no significant role, with the exception of long pipelines, where line packing and fluid inertia effects may become significant.

Neglecting pipe friction, the Equations (9.16) and (9.17) reduce to ($f = 0$):

$$H + \frac{c}{g}\,v = \text{constant} \qquad \text{along: } \frac{dx}{dt} = +c \qquad \textbf{(9.19)}$$

$$H - \frac{c}{g}\,v = \text{constant} \qquad \text{along: } \frac{dx}{dt} = -c \qquad \textbf{(9.20)}$$

These linear compatibility equations describe the relationship between the pressure head and fluid velocity along the characteristic lines $dx/dt = \pm c$. The constants are determined by the initial and boundary conditions.

The frictionless form of the compatibility equations enables the development of scale laws for unsteady flow conditions since all terms are linear.

9.4 Initial and boundary conditions

Check valves operate in pipeline systems under typical conditions like pump trip, pump shut-off, pump failure, the closure of control valves or pipe rupture. The unsteady flow conditions are determined by system parameters like pipe lengths, pump inertia, the presence of air vessels, surge towers, etc. These conditions may be considered as the initial and boundary conditions of the valve closure.

9.4.1 Initial conditions

In general the following condition holds along any path between two constant head boundaries *bnd i* and *bnd j*:

$$\int_{bnd\,i}^{bnd\,j} \frac{\partial H}{\partial x}\, dx = \text{constant} \tag{9.21}$$

To ensure a continuous function $H(x)$, it is assumed that components along the path like control valves, etc. are not fully closed. Differentiation in time yields:

$$\frac{\partial}{\partial t} \int_{bnd\,i}^{bnd\,j} \frac{\partial H}{\partial x}\, dx = 0 \tag{9.22}$$

As initial condition it is assumed that the tube does not stretch or expand ($\partial L/\partial t = 0$ and $\partial A/\partial t = 0$). In that case the integral and differential operator in Equation (9.22) may be exchanged:

$$\int_{bnd\,i}^{bnd\,j} \frac{\partial}{\partial t}\frac{\partial H}{\partial x}\, dx = 0 \tag{9.23}$$

A solution which satisfies the above equation is:

$$H_{xt} = 0 \tag{9.24}$$

This condition is further used as general *initial condition*.

The equation states that $\partial H/\partial x$ is constant in time, so that with constant head boundaries follows:

$$\boxed{H_t = 0} \tag{9.25}$$

This condition not only represents steady flow conditions, as will be shown later.

The above pressure head conditions may be related to flow conditions via the basic differential equations for transient flow (section 9.1), since the initial conditions form a special solution of these equations.

Converging or diverging tubes Consider a branched pipeline system consisting of converging and diverging tubes with constant head boundaries. Check valves or other system components may be regarded as short tubes as long as they are not fully closed.

If the pressure head is constant in time then, according to Equation (9.3), also the fluid density is constant in time. With $\partial A/\partial t = 0$, Equation (9.1) becomes:

$$\frac{\partial \rho_f Q}{\partial x} = 0 \tag{9.26}$$

Note that Equation (9.10) may not be used, since it is valid for prismatic tubes only.

With $\partial \rho_f/\partial t = 0$ and $\partial p/\partial t = 0$, Equation (9.4) becomes after the substitution of Equation (9.9):

$$\frac{\partial \rho_f}{\partial x} = \frac{\rho_f}{K}\frac{\partial p}{\partial x} = \frac{\rho_f^2 g}{K}\left[\frac{\partial H}{\partial x} - \sin\gamma\right] \tag{9.27}$$

The velocity gradient v_t may be O(10) in relatively short tubes, so that according to Equation (9.13) the pressure head gradient H_x is O(1). For slightly compressible fluids like water ρ_f is $O(10^3)$ while K is $O(10^9)$, so that $\partial \rho_f/\partial x$ is $O(10^{-2})$. For pipes shorter than 1000 m the variation in the density is smaller than 1% and neglectable. In that case Equation (9.26) reduces to:

$$\boxed{\frac{\partial Q}{\partial x} = 0} \tag{9.28}$$

With the introduction of $v = Q/A$ Equation (9.13) may be rewritten as:

$$\frac{\partial H}{\partial x} = -\frac{1}{g}\left[\frac{1}{A}\frac{\partial Q}{\partial t} - \frac{Q}{A^2}\frac{\partial A}{\partial t} + \left[\frac{Q}{A^2}\frac{\partial Q}{\partial x} - \frac{Q^2}{A^3}\frac{\partial A}{\partial x}\right] + \frac{f}{2D}\frac{Q|Q|}{A^2}\right] \tag{9.29}$$

A system component may be described here by a loss coefficient, which is related to the (net) pressure difference across the component by (section 10.2.3):

$$\Delta p = \xi \tfrac{1}{2}\rho_f v^2 \tag{9.30}$$

This equation is similar to the Darcy-Weisbach equation (section 9.1.2) if ξ is replaced by $f_{eff}\,L/D$. In that sense check valves or other system components may be described by an *equivalent* or *effective* pipe friction coefficient. Thus pipes and components can be treated in the same way.

According to Equation (9.24) follows with $\partial A/\partial t = 0$ and $\partial Q/\partial x = 0$:

$$\frac{\partial Q}{\partial t} + \left[-\frac{Q^2}{A^3}\frac{\partial A}{\partial x} \right] + \frac{f}{2D}\frac{Q|Q|}{A} = c_2 \qquad (9.31)$$

where c_2 is an integration constant.

An approximate solution of the above equation is ($f = 0$):

$$\boxed{\frac{\partial Q}{\partial t} = \text{constant}} \qquad (9.32)$$

About other solutions .....

A trivial solution, known as the steady-state condition, is:

$$\frac{\partial Q}{\partial t} = 0 \quad \wedge \quad c_2 = \frac{f}{2D}\frac{Q|Q|}{A} - \left[\frac{Q^2}{A^2}\frac{\partial Q}{\partial x} \right] \qquad (9.33)$$

Other solutions exist for $f \neq 0$. Hereby a disctinction can be made between $c_2 < 0$ (tangential functions), $c_2 = 0$ (reciproke functions), and $c_2 > 0$ (exponential functions). The solutions for $Q(t)$ show in how far $\partial Q/\partial t$ varies in time, and may be approximated by a constant.

Neglecting the convective term and assuming that friction effects in the pipes and components are relatively small, the initial conditions become:

$$\boxed{\frac{\partial Q}{\partial t} = \text{constant} \; ; \; \frac{\partial H}{\partial x} = -\frac{1}{gA}\frac{\partial Q}{\partial t} \; ; \; \frac{\partial H}{\partial t} = 0 \; ; \; \frac{\partial Q}{\partial x} = 0} \qquad (9.34)$$

These unsteady, initial flow conditions are valid for an arbitrary pipeline system with *converging or diverging* tubes, including system components like check valves, etc. Note that pump inertia effects caused by e.g. pump trip are not described.

Prismatic pipes If cross-sectional area variations due to the initial pressure head gradient along the pipe are not considered, the initial conditions for prismatic pipes directly follow from Equation (9.34) as:

$$\frac{\partial v}{\partial t} = \text{constant} \; ; \; \frac{\partial H}{\partial x} = -\frac{1}{g}\frac{\partial v}{\partial t} \; ; \; \frac{\partial H}{\partial t} = 0 \; ; \; \frac{\partial v}{\partial x} = 0 \qquad (9.35)$$

These initial conditions are consistent with the simplified form of the transient equations as given in Equations (9.10) and (9.13), if pipe friction effects are ignored.

9.4.2 Boundary conditions

Typical boundary conditions under which check valves operate are:

- upstream reservoirs and pumps
- downstream reservoirs, air vessels, surge towers
- parallel pumps

Although the pressure head at these boundaries may vary, in the first instance the boundary conditions are simplified to (upstream and downstream) constant head boundaries. Pipe junctions and varying head boundaries are treated in section (9.7).

Within the boundary conditions two cases are distinguished: *reflection free boundary conditions* and *reflecting boundary conditions*.

Reflection free boundary conditions In general a (check) valve may induce pressure waves, which may reflect at e.g. reservoirs, air vessels or pipe junctions. If these reflected pressure waves arrive at the valve after closure ($t_{refl} \geq t_c$), the motion of the valve disc is not influenced by reflections of pressure waves.

Let the reflection time of pressure waves or pipeline period $2L/c$ be introduced as the time increment between the initiation of a pressure wave (at instant t_d) and the arrival of the reflection wave (at instant t_{refl}), so that $t_{refl} - t_d = 2L/c$.

The reflection free boundary conditions are now described by:

$$t_c - t_d \leq \frac{2L_u}{c_u} \quad \wedge \quad t_c - t_d \leq \frac{2L_d}{c_d} \qquad (9.36)$$

Reflecting boundary conditions If the reflected pressure waves arrive at the valve before closure ($t_{refl} < t_c$), the motion of the valve disc is influenced by reflections of pressure waves.

The reflecting boundary conditions are described by:

$$t_c - t_d > \frac{2L_u}{c_u} \quad \vee \quad t_c - t_d > \frac{2L_d}{c_d} \tag{9.37}$$

9.5 Valve closure under reflection free boundary conditions

Consider the closure of a (check) valve in a flow with a uniform flow deceleration as initial condition, and under reflection free boundary conditions. For these flow conditions basic differential equations are derived in Appendix B.1. The relationship between pressure head and fluid velocity at any point along the prismatic pipe is:

$$\boxed{H_{tt} \pm \frac{c}{g} v_{tt} = 0} \tag{9.38}$$

The positive and negative signs in this equation are valid at the initial, upstream and downstream side of the valve, respectively.

About the sign convention ...

The sign convention introduced here is:

upper sign = valid at upstream side

lower sign = valid at downstream side (9.39)

Integration of Equation (9.38) yields:

$$\frac{\partial H}{\partial t} - \left[\frac{\partial H}{\partial t}\right]_i = \mp \frac{c}{g} \left[\frac{\partial v}{\partial t} - \left[\frac{\partial v}{\partial t}\right]_i\right] \tag{9.40}$$

Note that $(\partial H/\partial t)_i = 0$ as initial condition (section 9.4.1).

The pressure head changes are now described by:

$$\Delta H(t) = \int_{t_d}^{t} \frac{\partial H}{\partial t}\, dt$$

$$= \mp \frac{c}{g} \int_{t_d}^{t} \left[\frac{\partial v}{\partial t} - \left[\frac{\partial v}{\partial t} \right]_{t=t_d} \right] dt \qquad \textbf{(9.41)}$$

$$= \mp \frac{c}{g} \left[v(t) - v(t_d) - \left[\frac{\partial v}{\partial t} \right]_{t=t_d} (t - t_d) \right]$$

The equation describes the changes of the pressure head due to changes of the fluid velocity gradient. The fluid velocity $v(t_d)$ represents the value at the instant t_d, at which the flow deceleration $\partial v/\partial t$ starts to deviate from its initial value. Due to the fact that the pressure wave speed has a finite value, the instant t_d and the fluid velocity $v(t_d)$ will vary along the pipe.

About other relations ...

The relationship between the pressure heads in two points along the pipe is given in Appendix B.1.2. The relationship between the fluid velocities in two points along the pipe is given in Appendix B.1.3. The equations are of interest for experiments, since they relate measured pressure heads or fluid velocities (at some distance from the valve) to the pressure heads or fluid velocities at the valve.

Thus far the equations are valid at any point along the (infinite) pipe. Hereafter only the pressure head changes at the valve will be considered. For this purpose v_d is introduced as the fluid velocity $v(t_d)$ at the valve. The value may now also be regarded as the fluid velocity at which the damping of a check valve becomes active or effective. In most cases this takes place after flow reversal, so that $v_d < 0$ and may be introduced as a *reverse flow* velocity.

Since variations along the pipe (x-direction) are no longer considered, the partial derivatives are replaced by total derivatives. The initial fluid velocity gradient at the valve may now be replaced by the (mean) initial flow deceleration, which is already introduced for check valves in section 8.7:

$$\left[\frac{\partial v}{\partial t} \right]_{t=t_d} = \left[\frac{dv}{dt} \right]_{-} \qquad \textbf{(9.42)}$$

Two cases are distinguished now: the pressure head changes, which are induced at the (check) valve, during closure and after closure.

During valve closure The pressure head changes during valve closure directly follow from Equation (9.41). In a dimensionless form this yields:

$$\mp \frac{g\Delta H(t)}{cv_d} = \frac{v(t)}{v_d} - 1 - \left[\frac{dv}{dt}\right]_- \frac{(t - t_d)}{v_d} \qquad (t_d \leq t < t_c) \tag{9.43}$$

The pressure head changes during valve closure are determined by the reverse flow velocity v_d, the initial flow deceleration $(dv/dt)_-$ and the instantaneous fluid velocity. For check valves the character of the velocity-time function $v = f(t)$ is dependent on the type of damping.

After valve closure Assuming that the valve does not reopen after closure ($v = 0$) Equation (9.41) becomes:

$$\pm \frac{g\Delta H(t)}{cv_d} = 1 + \left[\frac{dv}{dt}\right]_- \frac{(t - t_d)}{v_d} \qquad (t \geq t_c) \tag{9.44}$$

The velocity-time history in the time interval $[t_d, t_c]$ is not relevant anymore. This implies that the pressure head changes due to the closure of damped and undamped check valves are equal, if the same fluid velocity v_d and instant t are considered. In that respect a damping device is not very useful, when the closure takes place under reflection free conditions.

Equation (9.44) may now be split up as:

$$\pm \frac{g\Delta H(t)}{cv_d} = 1 + \left[\frac{dv}{dt}\right]_- \frac{(t_c - t_d)}{v_d} + \left[\frac{dv}{dt}\right]_- \frac{(t - t_c)}{v_d} \tag{9.45}$$

With the (mean) reverse flow deceleration in the time interval $[t_d, t_c]$, already introduced in section 8.7, Equation (9.45) may be rewritten as:

$$\pm \frac{g\Delta H(t)}{cv_d} = 1 - \left[\frac{dv}{dt}\right]_- / \left[\frac{dv}{dt}\right]_+ + \left[\frac{dv}{dt}\right]_- \frac{(t - t_c)}{v_d} \tag{9.46}$$

The pressure head changes due to valve closure are proportional to the initial flow deceleration $(dv/dt)_-$ and the fluid velocity v_d and inversely proportional to the mean reverse flow deceleration $(dv/dt)_+$. The first term at the right hand side of this equation describes the pressure head changes at the instant of closure, the second term the additional changes after closure. After valve closure the pressure head changes linearly in time and proportionally to the initial flow deceleration. This phenomenon

is attributed to the inertia of the adjacent fluid columns, which continue to decelerate after valve closure. It should not be confused with the phenomenon of line packing, which is the result of friction effects.

About special cases ...

For undamped check valves follows after the instant of closure ($t_d \approx t_c$ so that $(dv/dt)_+ \rightarrow \infty$):

$$\pm\frac{g\Delta H(t)}{cv_d} = 1 + \left(\frac{dv}{dt}\right)_- \frac{(t - t_c)}{v_d} \qquad (t \geq t_c) \tag{9.47}$$

For damped check valves follows at the instant of closure:

$$\pm\frac{g\Delta H(t_c)}{cv_d} = 1 - \left(\frac{dv}{dt}\right)_- / \left(\frac{dv}{dt}\right)_+ \tag{9.48}$$

For undamped check valves follows at the instant of closure:

$$\pm\frac{g\Delta H(t_c)}{cv_d} = 1 \tag{9.49}$$

The latter equation is the equivalent of the well-known **Joukowsky equation**, after Joukowsky (1898). The Joukowsky equation describes the pressure surges due to a *gradual*, reflection free valve closure under initial, *steady flow conditions*. However, the above equation is the result of an instantaneous valve closure under initial, *unsteady flow conditions*. The Joukowsky equation directly follows from Equation (9.46) as a special case, by imposing $(dv/dt)_- = 0$. In that sense Equation (9.46) may be seen as an extension of the Joukowsky equation.

The latter two equations show that the pressure head changes at the instant of closure are smaller in the case of undamped check valves, if v_d is equal in both cases. However, in general the v_d of a damped check valve differs, since the damping becomes active before closure.

The equations illustrate that undamped valves may be considered as a special case of damped valves.

9.6 Valve closure under reflecting boundary conditions

Consider the closure of a valve in a pipeline system without pipe junctions and with upstream and downstream constant head boundaries. The initial flow deceleration is assumed to be constant. The flow deceleration at the valve starts to deviate from its initial value $(dv/dt)_-$ at the instant $t = t_d$ when $v = v_d$.

The relationship between the pressure head and fluid velocity at either side of the valve[1] is given by (Appendix B.2):

$$\mp \frac{g}{c}\Delta H(t) = v(t) - v_d - \left[\frac{dv}{dt}\right]_- (t - t_d) +$$

$$+ 2\sum_{i=1}^{\infty}(-1)^i \left[\, v(t-i2L/c) - v_d \,\right] \phi(t-t_d-i2L/c) + \qquad (9.50)$$

$$- 2\sum_{i=1}^{\infty}(-1)^i \left[\frac{dv}{dt}\right]_- \left[\, t-t_d-i2L/c \,\right] \phi(t-t_d-i2L/c)$$

where: $$\phi(y) = \begin{cases} 0 & \text{if } y \le 0 \\ 1 & \text{if } y > 0 \end{cases}$$

The first three terms at the right hand side of this equation form the solution under reflection free conditions (see Equation (9.43)). The other terms describe the effects of reflections and show that the valve closure is system dependent now.

The equation may be written in a dimensionless form as:

$$\mp \frac{g\Delta H(t)}{cv_d} = \frac{v(t)}{v_d} - 1 - \frac{2L/c}{v_d}\left[\frac{dv}{dt}\right]_- \left[\frac{t}{2L/c} - \frac{t_d}{2L/c}\right] +$$

$$+ 2\sum_{i=1}^{\infty}(-1)^i \left[\frac{v(t-i2L/c)}{v_d} - 1\right] \phi(t-t_d-i2L/c) + \qquad (9.51)$$

$$- 2\sum_{i=1}^{\infty}(-1)^i \frac{2L/c}{v_d}\left[\frac{dv}{dt}\right]_- \left[\frac{t}{2L/c} - \frac{t_d}{2L/c} - i\right] \phi(t-t_d-i2L/c)$$

Thus, the following dimensionless variables are introduced:

$$v_2 = \frac{v}{v_d} \quad ; \quad \tau_2 = \frac{t}{2L/c} \qquad (9.52)$$

[1] See sign convention in Equation (9.39).

Equation (9.51) may now be rewritten as ($\tau_d = t_d/(2L/c)$):

$$\mp \frac{g\Delta H(2L/c\tau_2)}{cv_d} = v_2(2L/c\tau_2) - 1 - \left[\frac{dv_2}{d\tau_2}\right]_- (\tau_2 - \tau_d) +$$

$$+ 2\sum_{i=1}^{\infty}(-1)^i \left[v_2(2L/c(\tau_2 - i)) - 1\right] \phi(\tau_2 - \tau_d - i) +$$

$$- 2\sum_{i=1}^{\infty}(-1)^i \left[\frac{dv_2}{d\tau_2}\right]_- [\tau_2 - \tau_d - i\,] \phi(\tau_2 - \tau_d - i) \qquad (9.53)$$

Taking into account the sign convention, this dimensionless equation is valid at either side of the valve. Therefore a distinction must be made between the upstream and downstream reflection time. After valve closure ($v = 0$) the function has a periodical character with a period $\tau_2 = 2$.

As an example the equation yields for $2 < \tau_2 - \tau_d \leq 3$:

$$\frac{g\Delta H(2L/c\tau_2)}{cv_d} = \frac{v(2L/c\tau_2)}{v_d} - \frac{2v(2L/c(\tau_2 - 1))}{v_d} + \frac{2v(2L/c(\tau_2 - 2))}{v_d} +$$

$$- 1 - \frac{2L/c}{v_d}\left(\frac{dv}{dt}\right)_- (\tau_2 - 2) \qquad (9.54)$$

and for $3 < \tau_2 - \tau_d \leq 4$:

$$\frac{g\Delta H(2L/c\tau_2)}{cv_d} = \frac{v(2L/c\tau_2)}{v_d} - \frac{2v(2L/c(\tau_2 - 1))}{v_d} + \frac{2v(2L/c(\tau_2 - 2))}{v_d} +$$

$$- \frac{2v(2L/c)(\tau_2 - 3)}{v_d} + 1 + \frac{2L/c}{v_d}\left(\frac{dv}{dt}\right)_- (\tau_2 - 4) \qquad (9.55)$$

About special cases ...

For undamped check valves at the instant $(\tau_2 - \tau_d) = 1$, at which the first reflected pressure wave arrives at the valve ($\tau_d \approx \tau_c$; $\tau \geq \tau_c$: $v = 0$):

$$\frac{g\Delta H(2L/c\tau_2)}{cv_d} = -1 - \frac{2L/c}{v_d}\left(\frac{dv}{dt}\right)_- \qquad (9.56)$$

Analogous to the initial flow deceleration, the dimensionless form of the (mean) reverse flow deceleration is:

$$\left[\frac{dv_2}{d\tau_2}\right]_+ = \frac{2L/c}{v_d}\left[\frac{dv}{dt}\right]_+ \tag{9.57}$$

The importance of the above analytical equations must be found in the fact that they show which parameters are relevant to the valve closure under reflecting boundary conditions:

$$\frac{2L/c}{v_d}\left[\frac{dv}{dt}\right]_- ; \frac{2L/c}{v_d}\left[\frac{dv}{dt}\right]_+ ; \frac{g\Delta H}{cv_d} \tag{9.58}$$

In this respect the equations are used in a dimensional analysis (chapter 11).

The question arises whether and under which conditions the above sequences can be described in the form of mathematical functions.

9.7 Pipe junctions and varying head boundaries

Thus far a pipeline system is considered without pipe junctions and with constant head boundaries. In this section the theory is extended to pipeline systems with junctions and varying head boundaries (e.g. air vessels, surge towers).

9.7.1 Pipe junctions

In case of pipe junctions the reflection times of all pipe sections at both the upstream and downstream side of the valve play a role. For M pipe sections this leads to a series of M - 1 additional dimensionless groups:

$$\frac{2L_i/c_i}{2L_j/c_j} \qquad (i,j \in \mathbb{N}) \tag{9.59}$$

Consider a pipe junction between two pipe sections. A pressure wave (H_w - H_i) and coupled flow wave (Q_w - Q_i) are approaching the junction from the downstream side. The reflected pressure and flow wave, as derived from the compatibility equations without friction term, are described by (e.g. Wylie and Streeter, 1993):

$$\frac{H_j - H_0}{H_w - H_0} = \frac{2}{1 + \dfrac{c_2/gA_2}{c_1/gA_1}} \tag{9.60}$$

and:

$$\frac{Q_j - Q_0}{Q_w - Q_0} = \frac{2}{1 + \dfrac{c_1/gA_1}{c_2/gA_2}} \tag{9.61}$$

The index 0 refers to the initial, steady flow conditions, while the indices 1 and 2 refer to the pipe sections upstream and downstream of the junction, respectively. The parameter c/gA is known as the characteristic impedance. Similar equations hold for the transmitted waves.

Note that for a flow with constant initial flow deceleration the situation is more complex, since in that case $\partial Q/\partial t$ plays a role, while $\partial H/\partial x$ differs from zero. However, under these conditions the above equations still hold. This can be seen by restricting the considerations to the vicinity of the pipe junction. This can be achieved by imposing the limit $\Delta t \rightarrow 0$ on the equations, so that the term $\partial Q/\partial t \; \Delta t$ vanishes.

The above equations show that a necessary and sufficient condition for similarly shaped reflection waves is:

$$\frac{A_i/c_i}{A_j/c_j} = C_{ij} \qquad (i,j \in \mathbb{N}) \tag{9.62}$$

where C_{ij} are constants. Note that the characteristic impedance as such is not relevant. For branched pipeline systems similar conditions hold.

9.7.2 Varying head boundaries

Thus far only constant head boundaries are considered. Neglecting pipe friction effects the pressure head H_{bnd} at the boundaries can be related to the initial, flow gradient $\partial Q/\partial t$ (section 9.4.1). For check valves these conditions are described in terms of a (constant) initial flow deceleration $(dv/dt)_-$. The above parameters are thus equivalent and either one of them can be used.

For varying head boundaries additional information is needed to characterize the boundary. It is presumed that this may be done by the following general condition:

$$\frac{H_{bnd}}{H_{bnd}(\tau_b)} = f\,(\tau_2) \tag{9.63}$$

where $H_{bnd}(\tau_b)$ is the initial pressure head at the boundary. The dimensionless time τ_2 can be based on the reflection time of any pipe section as long as Equation (9.59) is satisfied. The correctness of this group is proved in the numerical validation (section 15.1). The group allows the development of dynamic scale laws for system components like e.g. air vessels, pumps, etc. The above condition must be satisfied in order to ensure the similarity of the unsteady flow conditions.

A consequence of allowing varying head boundaries is that the flow deceleration may already vary during the first event of closure, and that reflections of pressure waves may play a role. Nevertheless, the varying head boundaries may still be represented by the initial flow deceleration, if the *mean* value of the initial flow deceleration is considered. In that case the groups are still equivalent and either of them may be used.

9.8 Rigid column theory

For the transient flow in a pipe the relationship between the fluid velocity and pressure head is described by the continuity equation and the equation of motion (section 9.1). The simplified forms of these equations are rewritten as:

$$\frac{g H_t}{c^2} + v_x = 0 \tag{9.64}$$

$$g H_x + v_t + \frac{f\, v|v|}{2D} = 0 \tag{9.65}$$

It is assumed that the fluid moves as a rigid column, so that $v_x \approx 0$ along the pipe. According to equation (9.64) this approximation is allowed if the pressure head changes in time are relatively small, so that $gH_t/c^2 \ll 1$. Note that this form of the continuity equation is only valid for prismatic tubes (section 9.1). Under these conditions Equation (9.65) can be used in an uncoupled mode.

In section 9.4.1 it is shown that the rigid column theory may also be applied to converging or diverging tubes. In that case, according to Equation (9.1), the rigid column condition $v_x \approx 0$ should be replaced by $Q_x \approx 0$.

The rigid column theory may be applied to estimate the unsteady, initial flow conditions. Consider a serial pipeline system, consisting of prismatic pipe sections and a (check) valve between constant head boundaries. The pipe flow is described by rigid column theory, and obtained from the integration of Equation (9.65). The

flow in the valve is described by the momentum equation (section 10.2.3).

This leads to:

$$H_{bnd_1} - H_{bnd_2} = \sum_{i=1}^{N} \frac{L_i}{gA_i}\frac{dQ}{dt} + \sum_{i=1}^{N} f_i \frac{L_i}{D_i}\frac{Q|Q|}{2gA_i^2} + \xi \frac{Q|Q}{2gA^2} \qquad \textbf{(9.66)}$$

The equation describes the head difference between two boundaries, due to fluid inertia and friction effects in the N pipe sections and head losses across the valve. Usually the pipe friction effects and head losses across the valve are relatively small (at least for higher velocity gradients), and may be neglected. Pump inertia effects, which may lead to a significant reduction of the flow deceleration, are not considered here. This leads to:

$$\left[\frac{dv}{dt}\right]_- = \frac{H_{bnd_1} - H_{bnd_2}}{A \sum \frac{L_i}{gA_i}} \qquad \textbf{(9.67)}$$

In this equation the initial flow conditions, expressed as a (mean) initial flow deceleration, are linked to the boundary conditions, expressed by constant head boundaries. Thus, it is shown that either of these parameters may be used. Preference is given to the initial flow deceleration, since it is physically more directly related to the check valve (constant head boundaries are located at some distance from the check valve). Note that, under the above conditions, the initial flow deceleration is a *system parameter* and not a valve parameter.

The rigid column theory may be applied to calculate the pressure head changes, induced by the check valve, if the second event of closure takes place relatively slow ($(t_c - t_d) \geqslant 2L/c$). This results in an approximate analytical solution, whereby pipe friction is ignored ($f = 0$):

$$\Delta H(t) = \mp \frac{L}{g}\left[\left[\frac{dv}{dt}\right] - \left[\frac{dv}{dt}\right]_-\right] \qquad \textbf{(9.68)}$$

where L is the distance from the check valve to the upstream/downstream boundary.

Note that the rigid column theory is inconsistent with waterhammer theory, since the pressure wave speed plays no role here. In that respect no additional scale laws, such as similarity of $(L_i/A_i)/(L_j/A_j)$ or L_i/L_j, may be derived from the above equations.

9.9 Review and conclusions

Conventional waterhammer theory is applied to the transient flow in a pipeline system with unsteady, initial flow conditions instead of the usual steady, initial flow conditions. The transient flow is assumed to be dominated by fluid inertia effects, so that non-linear effects as pipe friction may be neglected. Thus the development of scale laws for unsteady flow conditions is enabled. It is shown that under such conditions a constant, initial flow acceleration or deceleration does exist in pipeline systems with prismatic tubes and constant head boundaries. For pipeline systems with converging and diverging tubes, including system components these conditions can only be realized in approximation.

Basic differential equations are derived for the transient flow in a pipe with constant initial flow deceleration and reflection-free boundary conditions. The second order differential equations are applied to describe the closure of a damped check valve under reflection-free boundary conditions. In these analytical expressions the classical Joukowsky equation is covered and extended to unsteady flow conditions. Undamped valves may be considered as a special case of damped valves. In addition the closure of a damped check valve under reflecting (constant head) boundary conditions is described in an analytical way. In that case the valve closure is system-dependent.

The closure is accompanied with pressure surges. Under reflection-free boundary conditions these pressure surges are proportional to the initial flow deceleration, the fluid velocity at which the pressure surge is initiated (damping becomes active) and the time interval during which the damping is active. Under these conditions a damping device is not very useful. Under reflecting boundary conditions the pressure surges are also influenced by reflections of pressure waves.

The pipe equations are described in a dimensionless form, whereby the fluid velocity at which the pressure surges are initiated, and the reflection time are used to define a velocity and a time scale.

The dimensionless pipe equations show in a formal way which dimensionless (groups of) parameters are relevant to the check valve closure in pipeline systems, during the stage of active damping. In that sense they are used in the dimensional analysis.

The theory may also be used to describe the closure of control valves under unsteady, initial flow conditions.

10 Coupling of pipe and valve equations

Thus far the check valve and pipeline system are considered separately. The fluid velocity at the check valve is considered as a boundary condition in both the valve equations (chapter 8) and pipe equations (chapter 9). In this chapter the check valve and pipeline system are considered together.

For this purpose the integral form of the momentum equation is applied to the check valve as a short-length component. To describe the interaction between the check valve and pipeline system, the (dimensionless) valve and pipe equations are coupled via this integral momentum equation. This coupling results in an additional "coupling" parameter, which is used in the dimensional analysis (chapter 11) and parameterized valve models (chapter 12). The momentum equation is further used in the processing of the experimental data, to convert heads measured at some distance from the valve, to net values at the valve (chapter 13).

The check valve is considered as a short-length component in a pipeline system with a slightly compressible fluid. The valve is subjected and responds to its upstream and downstream flow conditions. A control volume is introduced, which is relatively short and fixed to the pipe (figure 10.1). The valve and adjacent pieces of pipe are assumed to be rigid bodies, so that they have no storage capacity. The valve closure is assumed to be slow, relative to the system reflection time. Thus the control volume is fixed in space.

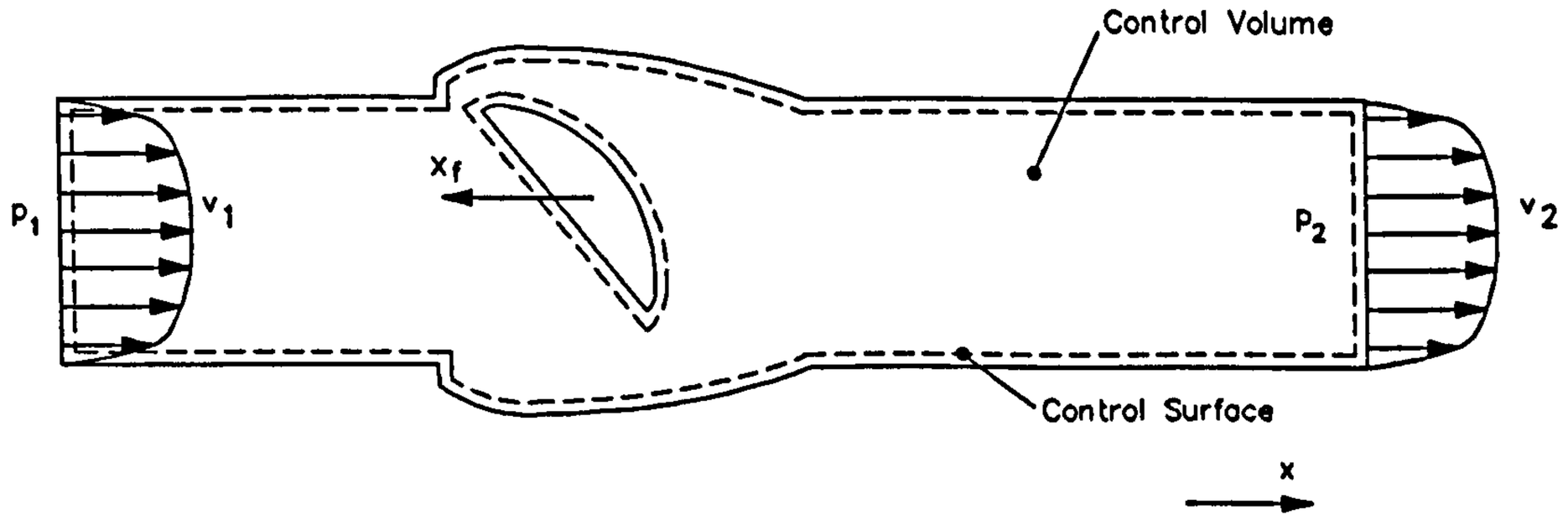

Figure 10.1 Check valve in short pipe

10.1 Conservation of mass

The integral form of the continuity equation is:

$$\frac{\partial}{\partial t} \int_{CV} \rho_f \, dV + \int_{CS} \rho_f \, \vec{v} . \vec{n} \, dA = 0 \qquad (10.1)$$

The equation describes the rate of change of mass within the control volume *CV*, due to the exchange of mass via the control surface *CS*, where *n* is the outward normal.

The only exchange of mass takes place via the inlet and outlet surfaces. It is assumed that the mass flow entering the *CV* is equal to the mass flow leaving the CV. This approximation is allowed if the *CV* is relatively short so that density variations due to transients or pressure surges may be neglected. In that case the continuity equation reduces to:

$$\frac{\partial}{\partial t} \int_{CV} \rho_f \, dV = 0 \qquad (10.2)$$

10.2 Conservation of momentum

The integral form of the momentum equation is:

$$\frac{\partial}{\partial t} \int_{CV} \rho_f \vec{v} \, dV + \int_{CS} \rho_f \vec{v} (\vec{v} . \vec{n}) \, dA = \sum \vec{F} \qquad (10.3)$$

The equation relates the rate of change of momentum of the system to the external forces acting on the system.

10.2.1 Change of momentum

The exchange of momentum takes place via the inlet and outlet surfaces only. It is assumed that the momentum entering the *CV* is equal to the momentum leaving the CV. This approximation is allowed if the *CV* is so long that the velocity profile is able to recover after the fluid has passed the valve disc. In that case the momentum equation reduces to:

$$\frac{\partial}{\partial t} \int_{CV} \rho_f \vec{v} \, dV = \sum \vec{F} \qquad (10.4)$$

About unsteady flow velocity profiles .....

It is expected that under unsteady flow conditions, the fluid velocity profiles need less length for recovery. The inertia effects, which dominate above viscous effects, tend to flatten the profiles. This phenomenon is confirmed by Van de Sande et al. (1980), who measured fluid velocity profiles in accelerating pipe flows from initial, stagnant flow conditions. The profiles were measured in time, using a Laser Doppler Anemometer. The results showed, both during the laminar and turbulent development stages, much resemblance with a plug flow.

The momentum equation in axial direction may now be written as:

$$\frac{\partial}{\partial t} \int_x \int_A \rho_f v \cos\alpha \; dA \, dx = \sum X \tag{10.5}$$

where α is the angle between the velocity vector and the axial direction.

The volume flow in axial direction is:

$$Q = \int_A v \cos\alpha \; dA \tag{10.6}$$

Neglecting the density variations over the cross section gives:

$$\frac{\partial}{\partial t} \int_x \rho_f \int_A v \cos\alpha \; dA \, dx = \frac{\partial}{\partial t} \int_x \rho_f Q \; dx = \sum X \tag{10.7}$$

If the *CV* is fixed in space the integral and differential operator may be exchanged:

$$\int_x \frac{\partial \rho_f Q}{\partial t} \; dx = \sum X \tag{10.8}$$

It is assumed that the density variations due to pressure surges may be ignored. Further it is assumed that the length L of the *CV* is so small that $Q_x \approx 0$ and thus $Q_{xt} \approx 0$ (rigid column), which leads to:

$$\boxed{\rho_f L \frac{dQ}{dt} = \sum X} \tag{10.9}$$

10.2.2 External forces

The external forces acting on the control volume arise from surface stresses (normal σ and shear τ) and distributed (body) forces B per unit volume:

$$\sum \vec{F} = \int_{CS} \sigma \, dA + \int_{CS} \tau \, dA + \int_{CV} \vec{B} \, dV \tag{10.10}$$

The surface stresses act on the inlet, wall, disc and outlet surface of the *CV*. The normal and shear stresses on the *CS* are equal to the normal and shear stresses exerted by the fluid inside the *CV*, but of opposite sign. Differences between the normal stresses and fluid pressures are ignored. Only forces in axial direction are considered.

Inlet and outlet The pressure distribution across the inlet and outlet is assumed to be uniform. The axial component of the normal stresses is now described by:

$$\int_{inlet} \sigma_x \, dA + \int_{outlet} \sigma_x \, dA = p_1 A_1 - p_2 A_2 \tag{10.11}$$

Introduce the pressure head H as:

$$p = \rho_f g (H - z) + p_{atm} \tag{10.12}$$

It is assumed that the inlet and outlet areas are equal. In that case the substitution of Equation (10.12) in Equation (10.11) yields:

$$\begin{aligned} \int_{inlet} \sigma_x \, dA + \int_{outlet} \sigma_x \, dA &= \rho_f g A (H_1 - H_2) + \rho_f g A L \frac{(z_2 - z_1)}{L} \\ &= \rho_f g A (H_1 - H_2) + \rho_f g A L \sin\gamma \end{aligned} \tag{10.13}$$

Where γ is the inclination angle of the pipe centre line with the horizontal.

The inlet and outlet surfaces are normal to the axial direction, so that the shear stresses do not contribute to the axial component of the surface forces.

Wall It is assumed that the axial component of the net pressure force on the wall is relatively small and neglectable. Thus the axial component of the normal stresses on the CV is:

$$\int_{wall} \sigma_x \, dA \approx 0 \tag{10.14}$$

This generally holds for cylindrical valve bodies. It also holds for axi-symmetrical bodies if the pressure gradient along the non-cylindrical part of the CV is relatively small. Note that the flow in the "dead chamber" around the disc is characterized by recirculation zones in which the pressure is about constant.

The shear stresses on the CV due to wall friction are approximated by:

$$\int_{wall} \tau_x \, dA \approx -\tau_o \, \pi D L \tag{10.15}$$

Where τ_o is an average wall shear stress acting on a cylinder with an equivalent wall roughness, diameter D and length L. The Darcy-Weisbach friction coefficient f is defined as (section 9.1.2):

$$\tau_o = \rho_f \frac{f \, Q|Q|}{8 A^2} \tag{10.16}$$

Substitution of Equation (10.16) in Equation (10.15) yields:

$$\int_{wall} \tau_x \, dA = -f \frac{L}{D} \frac{\rho_f Q|Q|}{2A} \tag{10.17}$$

Disc The surface forces on the *CS* are equal to the fluid (or: hydrodynamic) forces on the disc, but of opposite sign. Thus, the axial component of the surface forces may be described by:

$$\int_{disc} \sigma_x \, dA + \int_{disc} \tau_x \, dA = -X_H \tag{10.18}$$

The fluid forces may be described in the global form of the fluid equations, as introduced in chapter 7. The axial component of the hydrodynamic force on the moving valve elements is given by (section 8.8):

$$X_H = C_X \, \tfrac{1}{2} \rho_f \frac{Q^2}{A} \tag{10.19}$$

Distributed forces Distributed (body) forces generally arise due to gravitational, electrical and magnetic fields. Here only gravitation is taken into account. The axial component of the gravitational force is:

$$\int_{CV} B_x \, dV = - \int_x \int_A \rho_f g \sin\gamma \; dA \, dx \qquad \textbf{(10.20)}$$

It is assumed that the volume of the non-cylindrical part of the CV is about equal to the disc volume. In that case the fluid mass is more or less equally distributed along the x-axis. Now Equation (10.20) becomes:

$$\int_{CV} B_x \, dV = -\rho_f g \, A \, L \sin\gamma \qquad \textbf{(10.21)}$$

Sum of external forces Summation of the Equations (10.13), (10.17), (10.18) with (10.19), and (10.21) gives for the axial component of the external forces:

$$\sum X = \rho_f g A (H_1 - H_2) - f \frac{L}{D} \rho_f \frac{Q^2}{2A} - C_X \rho_f \frac{Q^2}{2A}$$

(10.22)

10.2.3 Momentum equation

Substituting Equation (10.22) in Equation (10.9) yields the momentum equation:

$$\rho_f L \frac{dQ}{dt} = \rho_f g A (H_1 - H_2) - f \frac{L}{D} \rho_f \frac{Q^2}{2A} - C_X \rho_f \frac{Q^2}{2A} \qquad \textbf{(10.23)}$$

Or:

$$H_1 - H_2 = \frac{L}{gA} \frac{dQ}{dt} + f \frac{L}{D} \frac{Q^2}{2gA^2} + C_X \frac{Q^2}{2gA^2} \qquad \textbf{(10.24)}$$

This equation describes the pressure head difference across the *CV* due to 1) fluid inertia, 2) wall friction, and 3) the fluid forces on the valve disc.

Prost (1992) investigates the behaviour of control valves under dynamic operating conditions. He measures the head loss and torque of a butterfly valve during linear opening and closure. The head loss and torque coefficients are derived from a similar equation, obtained from energy considerations.

Consider the limit case that the length of the CV becomes zero ($L \rightarrow 0$). In that case the fluid inertia and wall friction are reduced to zero. Thus follows:

$$H_1 - H_2 = C_X \frac{Q^2}{2gA^2} \tag{10.25}$$

In this equation the fluid forces on the disc are directly related to the net pressure head difference across the check valve, which is further denoted as ΔH. The global force coefficient C_X may therefore also be considered as a head loss coefficient. For valves this value is better known as the valve loss coefficient ξ. The head loss coefficient is equal to the energy loss coefficient if the inlet and outlet area are equal. The equation may now be rewritten as:

$$\boxed{\Delta H = \xi \frac{Q^2}{2gA^2}} \tag{10.26}$$

This one-dimensional momentum equation links the upstream and downstream pressure head to the flow through the valve. It thus enables the coupling of the pipe and valve equations as described in the next section.

10.3 Coupling of pipe and valve equations

The momentum equation derived in the previous section is used to couple the valve equations (chapter 8) to the pipe equations (chapter 9).

The pressure head difference across the check valve may now be described as:

$$H_u(t) - H_d(t) = \xi(t) \frac{Q_u^2(t)}{2gA^2} \tag{10.27}$$

The subscripts u and d refer to upstream and downstream, respectively.
Conservation of mass across the check valve (section 10.1) gives:

$$Q_u(t) = Q_d(t) = Q(t) \tag{10.28}$$

Introduce the upstream and downstream pressure head changes due to the closure of the check valve as ($t \geq t_d$):

$$\Delta H_u = H_u(t) - H_u(t_d)$$
$$\Delta H_d = H_d(t) - H_d(t_d) \qquad \textbf{(10.29)}$$

Substitution of the Equations (10.28) and (10.29) in Equation (10.27) gives after some manipulation:

$$\Delta H_u - \Delta H_d = \xi(t)\frac{Q^2(t)}{2gA^2} - \xi(t_d)\frac{Q^2(t_d)}{2gA^2} \qquad \textbf{(10.30)}$$

With the mean fluid velocity the equation may be rewritten as:

$$\Delta H_u - \Delta H_d = \xi\frac{v^2}{2g} - \xi_d\frac{v_d^2}{2g} \qquad \textbf{(10.31)}$$

This equation may be written in terms of dimensionless pressure head changes and fluid velocities as:

$$\boxed{\frac{g\Delta H_u}{c_u v_d}\left[\frac{c_u}{v_d}\right] - \frac{g\Delta H_d}{c_d v_d}\left[\frac{c_d}{v_d}\right] = \frac{1}{2}\xi\left[\frac{v}{v_d}\right]^2 - \frac{1}{2}\xi_d}$$

(10.32)

In this form the equation links the dimensionless pipe equations (section 9.5 and 9.6) and valve equation of motion (section 8.6) via the dimensionless fluid velocity. By coupling the equations the following (new) dimensionless parameter groups appear:

$$\left[\frac{c_u}{v_d}\right] \quad ; \quad \left[\frac{c_d}{v_d}\right] \qquad \textbf{(10.33)}$$

These groups represent the pressure wave speed and describe the interaction between the valve and pipeline system. The pressure wave speed is proportional to the pressure head changes induced by a valve closure. It thus has an indirect influence on the valve motion. As such the groups are of importance, but only during the stage of active damping, when pressure surges are induced. The flow conditions during this

stage are, to a large extent, dominated by the valve and dependent on the type of damping. For this reason the real importance of the groups is unknown. Note that the pressure wave speed is also found in the dimensionless pressure head changes.

10.4 Review and conclusions

The integral form of the momentum equation is applied to describe the check valve as short-length component in a pipeline system. The momentum equation is obtained from the following assumptions: The check valve and adjacent pieces of pipe are assumed to be rigid bodies. The valve closure is slow, relative to the system reflection time. The control volume is fixed in space. The control volume is so short that density variations due to pressure surges may be neglected. The flow rate is constant along the control volume (rigid column). The control volume is so long that the flow profile is able to recover. The pressure distribution across the inlet and outlet area is uniform. The inlet and outlet areas are equal. The axial component of the normal stresses on the valve body is relatively small. The gravitational forces are assumed to be equally distributed along the control volume.

The momentum equation describes the pressure head difference across the short-length control volume due to fluid inertia, pipe friction and the fluid forces on the valve disc. It can therefore be used to convert measured head differences at some distance from the check valve to the net head loss across the valve.

The momentum equation is applied to a control volume with infinitesimal length. It therefore directly relates the fluid forces on the valve elements to the pressure difference across the valve. The valve loss coefficient is introduced as a global, unsteady force coefficient (defined in axial direction) to describe the relationship between the net pressure difference across the valve and the flow through the valve.

The pipe and valve equations (chapter 8 and 9) are coupled via the momentum equation. This coupling results in a (new) "coupling" parameter, which has the form of a Mach number. The parameter represents the pressure wave speed and describes the interaction between check valve and pipeline system. As such it is only relevant during the stage of active damping, when the flow conditions are, to a large extent, dominated by the valve. Although the physical meaning of this group is understood, the real importance of the group is unknown.

11 Dimensional analysis

In this chapter a dimensional analysis is described. Here, the uncoupled and coupled pipe and valve equations (chapters 8, 9 and 10) serve to supply all valve, system and fluid parameters, which are relevant to the check valve dynamics in a pipeline system. The dimensional analysis becomes more complicated, since several velocity and time scales are involved. From the parameters dimensionless groups are developed, according to the Buckingham Π-theorem.

The dimensionless groups in their turn form the basis for the development of several valve characteristics and *dynamic* scale laws. Two theoretical approaches are followed. In the first approach the check valve behaviour is described in terms of (dimensionless) fluid velocity and pressure head characteristics. The second approach is based on the concept of global fluid force coefficients (chapter 7), in terms of dynamic valve loss coefficients. The valve characteristics are used in the development of valve models (chapter 12).

The check valve closure is split up into two events (figure 8.2):

1) The stage of passive damping ($t_o \leq t < t_d$), denoted as the *first event of closure*, is characterized by a (more or less) constant initial flow deceleration. Pressure surges play no role.
2) The stage of active damping ($t_d \leq t < t_c$), denoted as the *second event of closure*, is associated with pressure surges.

11.1 Variables

The variables that are relevant to the check valve behaviour are: the valve disc position (θ), the fluid velocity (v), the pressure or pressure head (p or H), time (t), and the distance along the pipe (x). The variables t and x are independent variables, while the others are dependent variables.

To ensure kinematic similarity for the valve motion the following dimensionless variables are introduced (section 8.6):

$$\boxed{\alpha_1 = \theta \quad ; \quad v_1 = \frac{v}{v_o} \quad ; \quad \tau_1 = \frac{t\, v_o}{D}} \tag{11.1}$$

Hereby the parameters v_o and D are chosen to define a velocity and a time scale. Thus follows for the dependent variables:

$$\frac{d\alpha_1}{d\tau_1} = \frac{D}{v_o}\frac{d\theta}{dt} \quad ; \quad \frac{d^2\alpha_1}{d\tau_1{}^2} = \frac{D^2}{v_o^2}\frac{d^2\theta}{dt^2} \quad ; \quad \ldots\ldots$$

$$\frac{\partial v_1}{\partial \tau_1} = \frac{D}{v_o^2}\frac{\partial v}{\partial t} \quad ; \quad \frac{\partial^2 v_1}{\partial \tau_1{}^2} = \frac{D^2}{v_o^3}\frac{\partial^2 v}{\partial t^2} \quad ; \quad \ldots\ldots \tag{11.2}$$

To ensure kinematic similarity for the pipe flow (during and after the second event of closure) the following dimensionless variables are introduced (section 9.6):

$$\boxed{\alpha_2 = \theta \quad ; \quad v_2 = \frac{v}{v_d} \quad ; \quad \tau_2 = \frac{t}{2L/c}} \tag{11.3}$$

Here the parameters v_d and $2L/c$ are chosen as velocity and time scale. Thus follows for the dependent variables:

$$\frac{d\alpha_2}{d\tau_2} = (2L/c)\,\frac{d\theta}{dt} \quad ; \quad \frac{d^2\alpha_2}{d\tau_2{}^2} = (2L/c)^2\,\frac{d^2\theta}{dt^2} \quad ; \quad \ldots$$

$$\frac{\partial v_2}{\partial \tau_2} = \frac{(2L/c)}{v_d}\frac{\partial v}{\partial t} \quad ; \quad \frac{\partial^2 v_2}{\partial \tau_2{}^2} = \frac{(2L/c)^2}{v_d}\frac{\partial^2 v}{\partial t^2} \quad ; \quad \ldots \tag{11.4}$$

Note that the distance along the pipe, which plays a role during the second event, is represented by the time via the characteristics $dx/dt = \pm c$.

The relationship between the dimensionless variables given in Equation (11.1) and those given in Equation (11.3) is:

$$\alpha_1 = \alpha_2 \quad ; \quad \upsilon_1 = \frac{\nu_d}{\nu_o}\,\upsilon_2 \quad ; \quad \tau_1 = \frac{(2L/c)\,\nu_o}{D}\,\tau_2 \tag{11.5}$$

The two time and velocity scales are linked by:

$$\boxed{\frac{\nu_d}{\nu_o} \quad ; \quad \frac{D}{(2L/c)\,\nu_o}} \tag{11.6}$$

The two sets of dimensionless variables are equivalent if they are considered together with the dimensionless groups in Equation (11.6). In that case either of the sets of dimensionless variables can be used.

About an alternative time scale .....

A typical time scale of the second event is the damping time (t_c-t_d). This would lead to:

$$\alpha_2' = \theta \quad ; \quad \upsilon_2' = \frac{\nu}{\nu_d} \quad ; \quad \tau_2' = \frac{t}{t_c - t_d} \tag{11.7}$$

In that case follows for the relationship with the dimensionless variables given in Equation (11.3):

$$\alpha_2' = \alpha_2 \quad ; \quad \upsilon_2' = \upsilon_2 \quad ; \quad \tau_2' = -\frac{2L/c}{\nu_d}\left(\frac{d\nu}{dt}\right)_* \tau_2 \tag{11.8}$$

The parameter group that links the two time scales is obtained from the Buckingham Π theorem (section 11.3.2).

11.2 Parameters

The parameters that are relevant to the *first event of closure* are obtained from: 1) the valve equation of motion without the friction and damping terms (section 8.6), 2) the initial and boundary conditions (section 8.7), and 3) the momentum equation (section 10.2). The parameters are:

D	characteristic valve diameter
ρ_f	density of pipe fluid
v_o	critical velocity
$K_{..}$	geometrical parameters of valve and damper (including θ_o, θ_{cg} and θ_{cb})
ρ_m	density of the moving valve elements
Δp_o	net pressure difference across the valve in open position
T_{So} (F_{So})	spring torque (force) on the moving element(s); valve is open
T_{Sc} (F_{Sc})	spring torque (force) on the moving element(s); valve is closed
γ	valve inclination angle
μ_f	dynamic viscosity of pipe fluid
v_i	initial, steady fluid velocity
θ_i (x_i)	initial angular (linear) valve disc position
$(dv/dt)_-$	(mean) initial flow deceleration
$p_{bnd} = \rho_f g H_{bnd}$	pressure (head) at boundary

The parameters that are relevant to the *second event of closure* are: 1) those of the first event, and the parameters obtained from: 2) the valve equation of motion including damping terms (section 8.6), 3) the pipe equations (section 9.5 and 9.6), and 4) the coupled pipe and valve equations (section 10.3). Transients in the damping device, which is relatively small, are ignored. Thermodynamic effects in both pipe and damping device are also ignored. The additional parameters are:

v_d	fluid velocity when damping becomes active
$2L/c$	reflection time or pipeline period
C_d	damping coefficient(s)
ρ_d	density of damping fluid
μ_d	dynamic viscosity of damping fluid
$(dv/dt)_+$	(mean) reverse flow deceleration
t_c - t_d	damping time
$\Delta p = \rho_f g \Delta H$	pressure (head) changes due to valve closure
c	pressure wave speed

About turbulent viscosity ...

The turbulent viscosity as parameter is not included in the above parameter list for the following reasons. The effects of turbulence are already globally described by the power law formulations for the drag coefficients (section 8.2). In the case of a laminar flow (powers of about 1) the parameter is irrelevant. In the case of a fully developed turbulent flow (powers of about 0) the fluid viscosity plays no role as parameter (section 8.6). Only in the transition zone from laminar to turbulent (powers between about 0 and 1) the turbulent viscoity is relevant. Many check valves types operate outside this transition zone, i.e. the flow in the valve is turbulent, while the damping flow is laminar. Moreover the turbulent viscosity is not easily defined and measured under unsteady flow conditions.

11.3 Dimensionless groups

If the variables or parameters involved in a physical phenomenon all can be identified, the form of the equation relating them can be globally determined by a dimensional analysis. For this purpose the following procedure may be applied. Find all the dependent and independent variables (the latter are variables which can be changed in magnitude without affecting each other) that describe the event. Denote the number of fundamental dimensions (e.g. mass, length, time) they contain as m. According to the Buckingham Π-theorem (e.g. Douglas et al., 1979) the variables can be arranged into $(n - m)$ independent dimensionless groups. From the independent variables repeating variables are chosen, which will appear in more than one group. The repeating variables should contain all the fundamental dimensions that are relevant to the problem, and be quantities which are likely to have a substantial effect on the dependent variables.

11.3.1 First event

The first event is described by $n = 14$ parameters with $m = 3$ fundamental dimensions. Choosing D, ρ_f and v_o as repeating variables $n - m = 11$ dimensionless groups can be developed[1]:

$$K_{..} \; ; \; \frac{\rho_m}{\rho_f} \; ; \; \frac{\Delta p_o}{\rho_f v_o^2} \; ; \; \frac{T_{S_o}}{\rho_f v_o^2 D^3} \; ; \; \frac{T_{S_c}}{\rho_f v_o^2 D^3} \; ; \; \gamma \qquad (1...6)$$

$$\frac{\rho_f v_o D}{\mu_f} \; ; \; \frac{v_i}{v_o} \; ; \; \theta_i \; ; \; \frac{D}{v_o^2} \left[\frac{dv}{dt}\right]_- \; ; \; \frac{\rho_f g H_{bnd}}{\rho_f v_o^2} \qquad (7...11) \qquad (11.9)$$

The first group in this list represents the valve geometry. The geometrical parameters are already dimensionless and ensure geometric similarity.

The second group represents inertia effects of the moving valve elements including the damping device. The group appears in the inertia term of the dimensionless valve equation of motion. Under steady flow conditions, when inertia does not play a role, the density of the moving valve elements is fully represented by the critical velocity.

The third group represents the hydrodynamic effects. The hydrodynamic forces on the valve disc are related to the net pressure difference across the valve by the momentum equation (section 10.2.3). In that sense this group may also be considered as a head or valve loss coefficient ξ_o. It can thus be used to represent the internal

[1] The parameters are printed in **bold** type; (1...6) refers to group numbers.

valve geometry (if it is not strongly dependent of the Reynolds number), and replaces the geometrical parameters $K_{..}$. The group may also be considered as a global force coefficient C_X, which is directly linked to the global torque coefficient C_T (section 7.2 and 8.8), so that in principle either of them can be used.

The fourth and fifth groups represent spring effects. The fourth group is fully represented by the third group if gravitational and buoyancy effects play no role (section 8.5). In that case the fourth group can be omitted. The fifth group is needed to describe the preset spring conditions.

The sixth group represents the built-in conditions in terms of an inclination angle.

The seventh group represents the viscosity effects of the pipe fluid, described by the critical Reynolds number.

The eighth and ninth groups represent the initial, steady flow conditions before closure. The groups are equivalent (section 8.7.2) and either of them may be used. The initial valve disc position, already dimensionless, is of importance when the valve is initially partly open.

The tenth group characterizes the initial, unsteady flow conditions of the first event, expressed as a (mean) initial flow deceleration.

The eleventh group represents the boundary conditions.

The latter two groups are related (section 9.8). Neglecting pipe friction and the head losses across the valve, the groups are equivalent, so that either of them can be used. Preference is given to the initial flow deceleration, since it is physically more directly related to the check valve (section 9.8).

11.3.2 Second event

The second event is described by $n = 14+9 = 23$ parameters with $m = 3$ fundamental dimensions. Choosing $2L/c$, ρ_f and v_d as repeating variables $n - m = 20$ dimensionless groups can be developed:

$$\frac{D}{(2L/c)v_d} \; ; \; \frac{v_o}{v_d} \qquad (1...2)$$

$$K_{..} \; ; \; \frac{\rho_m}{\rho_f} \; ; \; \frac{\Delta p_o}{\rho_f v_d^2} \; ; \; \frac{T_{S_o}}{\rho_f v_d^5 (2L/c)^3} \; ; \; \frac{T_{S_c}}{\rho_f v_d^5 (2L/c)^3} \; ; \; \gamma \qquad (3...8) \qquad (11.10)$$

$$\frac{\rho_f v_d^2 2L/c}{\mu_f} \; ; \; \frac{v_i}{v_d} \; ; \; \theta_i \; ; \; \frac{2L/c}{v_d}\left[\frac{dv}{dt}\right]_- \; ; \; \frac{\rho_f g H_{bnd}}{\rho_f v_d^2} \qquad (9...13)$$

$$C_d \; ; \; \frac{\rho_d}{\rho_f} \; ; \; \frac{\rho_f v_d^2 2L/c}{\mu_d} \; ; \; \frac{2L/c}{v_d}\left[\frac{dv}{dt}\right]_+ \; ; \; \frac{t_c - t_d}{2L/c} \; ; \; \frac{\rho_f g \Delta H}{\rho_f v_d^2} \; ; \; \frac{c}{v_d} \qquad (14...20)$$

The first group in this equation represents the valve size in terms of a characteristic valve diameter.

The second group represents the net effect of gravitation, buoyancy and spring(s) in terms of the critical velocity.

The first and second group are dimensionless forms of the repeating variables of the first event. They are equivalent to the groups in Equation (11.6).

The physical meaning of the third to the thirteenth group is described above. The groups are (other) dimensionless forms of the parameters of the first event.

The fourteenth group represents damping effects, in terms of an (adjustable) dimensionless damping coefficient.

The fifteenth and sixteenth group represent the properties of the damping fluid in terms of a dimensionless density and viscosity.

The seventeenth and eighteenth group characterize the flow conditions of the second event, expressed as a (mean) reverse flow deceleration and damping time, respectively. According to Equation (8.53) the groups are per definition equivalent and either of them can be used. Preference is given to $(dv/dt)_+$, since it is similar to the initial flow deceleration $(dv/dt)_-$.

The nineteenth group represent the pressure (head) changes due to valve closure.

The twentieth group represents elasticity effects of pipe and fluid, expressed by the pressure wave speed in the form of a Mach number. The parameter group appears due to the coupling of the pipe and valve equations.

11.3.3 Transformations

The dimensionless groups developed sofar are obtained from the repeating variables in a formal way. This does not necessarily mean that these forms are the most convenient ones. Other forms may be obtained by multiplying groups.

The dimensionless valve diameter (as repeating variable of the first event) may be rewritten as:

$$\frac{D}{(2L/c)v_d} \cdot \frac{v_d}{v_o} = \frac{D}{(2L/c)v_o} \tag{11.11}$$

The group may be considered as a Strouhal number (section 11.8).

The dimensionless parameter groups in Equation (11.9) are equivalent with the groups 3...13 in Equation (11.10). For example:

$$\frac{D}{v_o^2}\left[\frac{dv}{dt}\right]_- = \frac{D}{(2L/c)v_d} \cdot \left[\frac{v_d}{v_o}\right]^2 \cdot \frac{2L/c}{v_d}\left[\frac{dv}{dt}\right]_- \tag{11.12}$$

Preference is given to the forms listed in Equation (11.9).

The dimensionless spring torque in closed position may simply be written as:

$$\frac{T_{S_o}}{\rho_f v_o^2 D^3} \cdot \frac{\rho_f v_o^2 D^3}{T_{S_c}} = \frac{T_{S_o}}{T_{S_c}} \qquad \textbf{(11.13)}$$

The initial valve disc position θ_i, absolute and already dimensionless, becomes relative in the more general form:

$$\frac{\theta_i - \theta_c}{\theta_o - \theta_c} \qquad \textbf{(11.14)}$$

The subscripts *o* and *c* refer to the open and closed valve, respectively.

In a similar way the damping coefficient C_d may be replaced by a percentage of damping.

The dimensionless dynamic viscosity of the damping fluid may be rewritten as:

$$\frac{\rho_f v_d^2 (2L/c)}{\mu_d} \cdot \frac{D}{(2L/c) v_d} \cdot \frac{v_o}{v_d} \cdot \frac{\mu_f}{\rho_f v_o D} = \frac{\mu_f}{\mu_d} \qquad \textbf{(11.15)}$$

The dimensionless form of the pressure (head) changes due to valve closure may be rewritten as:

$$\frac{\rho_f g \Delta H}{\rho_f v_d^2} \cdot \frac{v_d}{c} = \frac{g \Delta H}{c v_d} \qquad \textbf{(11.16)}$$

The dimensionless pressure wave speed may be rewritten as:

$$\frac{c}{v_d} \cdot \frac{v_d}{v_o} = \frac{c}{v_o} \qquad \textbf{(11.17)}$$

In most of the above groups the reverse flow velocity v_d is eliminated now and replaced by the critical velocity v_o.

The previous operations lead to the following groups for the first event:

$$\frac{\rho_m}{\rho_f} ; \frac{\Delta p_o}{\rho_f v_o^2} ; \frac{T_{S_o}}{\rho_f v_o^2 D^3} ; \frac{T_{S_o}}{T_{S_c}} ; \gamma ; \frac{\rho_f v_o D}{\mu_f} ; \frac{\theta_i - \theta_c}{\theta_o - \theta_c} ; \frac{D}{v_o^2} \left[\frac{dv}{dt}\right]_- \qquad \textbf{(11.18)}$$

And additional groups for the second event:

$$\frac{D}{(2L/c)v_o} \; ; \; \frac{v_d}{v_o} \tag{11.19}$$

$$\%\ damping \; ; \; \frac{\rho_d}{\rho_f} \; ; \; \frac{\mu_d}{\mu_f} \; ; \; \frac{2L/c}{v_d}\left[\frac{dv}{dt}\right]_+ \; ; \; \frac{g\Delta H}{cv_d} \; ; \; \frac{c}{v_o}$$

11.3.4 Pipe junctions and varying head boundaries

Thus far only pipeline systems are considered without pipe junctions and with constant head boundaries. In the case of pipe junctions and varying head boundaries additional groups are needed.

The effects of pipe junctions are represented by the following series of dimensionless groups that describe the ratio of the reflection times and characteristic impedances of all pipe sections between the boundaries (section 9.7.1):

$$\frac{2L_i/c_i}{2L_j/c_j} \quad ; \quad \frac{A_i/c_i}{A_j/c_j} \qquad (i,j \in \mathbb{N}) \tag{11.20}$$

In the case of more than one pipe section the reflection time $2L/c$ in the dimensionless groups must be specified (e.g. $2L_i/c_i$ or $2L_u/c_u$, $2L_d/c_d$, ...).

Varying head boundaries are represented by the *mean* initial flow deceleration (section 9.7.2). In that sense no new group is needed here.

11.3.5 Check valves with translating elements

The above set of dimensionless groups applies to check valves with rotating elements. For check valves with translating elements the torques must be replaced by forces, while the angular valve disc position is replaced by a linear one:

$$\frac{F_{S_o}}{\rho_f v_o^2 D^2} \quad ; \quad \frac{F_{S_o}}{F_{S_c}} \quad ; \quad \frac{x_i - x_c}{x_o - x_c} \tag{11.21}$$

11.4 Valve and system parameters

The dimensionless parameter groups developed in the previous section may be regrouped according to:

Valve parameters, characterizing the valve materials, valve geometry, spring properties, damping and built-in conditions (e.g. horizontal, vertical):

$$\frac{\rho_m}{\rho_f} \; ; \; \frac{\Delta p_o}{\rho_f v_o^2} \; ; \; \frac{T_{S_o}}{\rho_f v_o^2 D^3} \; ; \; \frac{T_{S_o}}{T_{S_c}} \; ; \; \%\ damping \; ; \; \gamma \qquad \textbf{(11.22)}$$

System parameters, characterizing the pipeline system in terms of reflection times and characteristic impedances:

$$\frac{2L_i/c_i}{2L_j/c_j} \; ; \; \frac{A_i/c_i}{A_j/c_j} \qquad \textbf{(11.23)}$$

Valve-system parameters, characterizing the combination of check valve and pipeline system:

$$\frac{D}{(2L_i/c_i)\, v_o} \; ; \; \frac{v_o}{c_i} \qquad \textbf{(11.24)}$$

Fluid parameters, characterizing the properties of the pipe and damping fluid in terms of densities and viscosities:

$$\frac{\rho_d}{\rho_f} \; ; \; Re_o = \frac{\rho_f v_o D}{\mu_f} \; ; \; \frac{\mu_d}{\mu_f} \qquad \textbf{(11.25)}$$

(Steady and unsteady) flow parameters, characterizing the (first and second) event of closure:

$$\frac{\theta_i - \theta_c}{\theta_o - \theta_c} \; ; \; \frac{D}{v_o^2} \left[\frac{dv}{dt}\right]_- \; ; \; \frac{v_d}{v_o} \; ; \; \frac{2L_i/c_i}{v_d} \left[\frac{dv}{dt}\right]_+ \; ; \; \frac{g\Delta H_i}{c_i v_d} \qquad \textbf{(11.26)}$$

The flow parameters are listed in chronological order. The first parameter group describes the initial, steady flow conditions. The second group describes the initial, unsteady flow conditions during the first event. The third group describes the flow

conditions at the end of the first event. The fourth and fifth group describe the flow and pressure head changes during the second event. According to the basic equations for transient flow the pressure head may be derived from the fluid velocity or vice versa. In that sense the parameter groups are fully equivalent.

Complete matching of all valve and system parameters between "model" and "prototype" will be impossible. However, some of the groups are of minor importance (see further section 12.2).

11.5 Valve characteristics approach 1

11.5.1 Flow characteristics

Consider a check valve in a pipeline system. The valve and system parameters, except for the flow parameters, are constants.

From the flow parameters, formally five flow characteristics may be developed by writing one parameter as function of the others. Hereby the chronologic order of the events must be taken into account (an event is only influenced by previous events). Thus the following flow characteristics may be developed from Equation (11.26):

$$\frac{D}{v_o^2}\left(\frac{dv}{dt}\right)_- = f\left[\frac{\theta_i-\theta_c}{\theta_o-\theta_c}\right] \tag{11.27}$$

$$\frac{v_d}{v_o} = f\left[\frac{\theta_i-\theta_c}{\theta_o-\theta_c}\,,\ \frac{D}{v_o^2}\left(\frac{dv}{dt}\right)_-\right] \tag{11.28}$$

$$\frac{2L_i/c_i}{v_d}\left(\frac{dv}{dt}\right)_+ = f\left[\frac{\theta_i-\theta_c}{\theta_o-\theta_c}\,,\ \frac{D}{v_o^2}\left(\frac{dv}{dt}\right)_-\,,\ \frac{v_d}{v_o}\right] \tag{11.29}$$

$$\frac{g\Delta H_i}{c_i v_d} = f\left[\frac{\theta_i-\theta_c}{\theta_o-\theta_c}\,,\ \frac{D}{v_o^2}\left(\frac{dv}{dt}\right)_-\,,\ \frac{v_d}{v_o}\,,\ \frac{2L_i/c_i}{v_d}\left(\frac{dv}{dt}\right)_+\right] \tag{11.30}$$

The characteristic given in Equation (11.27) is rather useless, since the initial flow deceleration may be considered as a system parameter and not as a valve parameter (section 9.8), and can be omitted. According to Equation (11.28) the last group in Equation (11.29) is fully represented by the others and can be omitted here. Similar considerations hold for the last two groups in Equation (11.30).

From the flow parameters the following flow characteristics may be introduced:

The *fluid velocity characteristic for the first event*, which supplies information about the (reverse) flow velocity at which the damping becomes active:

$$\frac{v_d}{v_o} = f\left[\frac{\theta_i-\theta_c}{\theta_o-\theta_c}\,,\ \frac{D}{v_o^2}\left[\frac{dv}{dt}\right]_-\right] \qquad \textbf{(11.31)}$$

The *fluid velocity characteristic for the second event* supplies information about the damping time, boundary conditions and character of damping (section 11.5.2):

$$\frac{2L_u/c_u}{v_d}\left[\frac{dv}{dt}\right]_+ = f\left[\frac{\theta_i-\theta_c}{\theta_o-\theta_c}\,,\ \frac{D}{v_o^2}\left[\frac{dv}{dt}\right]_-\right] \qquad \textbf{(11.32)}$$

or:

$$\frac{2L_d/c_d}{v_d}\left[\frac{dv}{dt}\right]_+ = f\left[\frac{\theta_i-\theta_c}{\theta_o-\theta_c}\,,\ \frac{D}{v_o^2}\left[\frac{dv}{dt}\right]_-\right] \qquad \textbf{(11.33)}$$

The *pressure head characteristics for the second event* supply information about the upstream and downstream pressure surges induced by the check valve closure:

$$\frac{g\Delta H_u}{c_u v_d} = f\left[\frac{\theta_i-\theta_c}{\theta_o-\theta_c}\,,\ \frac{D}{v_o^2}\left[\frac{dv}{dt}\right]_-\right] \qquad \textbf{(11.34)}$$

and:

$$\frac{g\Delta H_d}{c_d v_d} = f\left[\frac{\theta_i-\theta_c}{\theta_o-\theta_c}\,,\ \frac{D}{v_o^2}\left[\frac{dv}{dt}\right]_-\right] \qquad \textbf{(11.35)}$$

Two pressure head characteristics are needed, since the pressure head changes at the upstream and downstream side are of opposite sign and in general different of magnitude. The subscripts u and d refer to upstream and downstream, respectively.

In these characteristics the mean, initial flow deceleration is defined as:

$$\left[\frac{dv}{dt}\right]_- = \frac{v_d - v_o}{t_d - t_o} \qquad \textbf{(11.36)}$$

and the mean, reverse flow deceleration as (section 8.7; figure 8.2):

$$\left[\frac{dv}{dt}\right]_{+} = \frac{-v_d}{t_c - t_d} \tag{11.37}$$

The flow characteristics are based on fluid velocities. The fluid velocity may be considered as a more basic unit than the pressure since the latter is dependent on the fluid density and pipe properties (found in the pressure wave speed).

About special cases .....

Under certain conditions the flow characteristics may be described in an analytical form.

For an ideal check valve follows:

$$\frac{v_d}{v_o} = 0 \tag{11.38}$$

With the introduction of the mean reverse flow deceleration, the boundary conditions for a reflection free valve closure (section 9.4.2) may be rewritten as:

$$\frac{2L_u/c_u}{v_d}\left(\frac{dv}{dt}\right)_{+} \leq -1 \quad \wedge \quad \frac{2L_d/c_d}{v_d}\left(\frac{dv}{dt}\right)_{+} \leq -1 \tag{11.39}$$

and the reflecting boundary conditions as:

$$-1 < \frac{2L_u/c_u}{v_d}\left(\frac{dv}{dt}\right)_{+} \leq 0 \quad \vee \quad -1 < \frac{2L_d/c_d}{v_d}\left(\frac{dv}{dt}\right)_{+} \leq 0 \tag{11.40}$$

Under reflection free boundary conditions the pressure head changes, at the instant of closure, are described by (see Equation (9.48)):

$$\pm\frac{g\Delta H(t_c)}{cv_d} = 1 - \frac{\frac{D}{v_o^2}\left(\frac{dv}{dt}\right)_{-}}{\frac{D}{(2L/c)v_o}\cdot\frac{v_d}{v_o}\cdot\frac{2L/c}{v_d}\left(\frac{dv}{dt}\right)_{+}} = 1 - \frac{\left(\frac{dv}{dt}\right)_{-}}{\left(\frac{dv}{dt}\right)_{+}} \tag{11.41}$$

For undamped check valves at the instant of closure (see Equation (9.49)):

$$\pm\frac{g\Delta H(t_c)}{cv_d} = 1 \tag{11.42}$$

For undamped check valves at the instant the first reflections reach the valve (see Equation (9.56)):

$$\frac{g\Delta H(2L/c\,\tau_2)}{c v_d} = -1 - \frac{(2L/c)v_o}{D} \cdot \frac{v_o}{v_d} \cdot \frac{D}{v_o^2}\left(\frac{dv}{dt}\right)_- = -1 - \frac{2L/c}{v_d}\left(\frac{dv}{dt}\right)_- \qquad \textbf{(11.43)}$$

Note that in the above pressure head characteristics the initial valve disc position does not appear. The effect of the initial conditions is represented by v_d. The question arises, if this parameter may generally be omitted from the pressure head characteristics given in the Equations (11.34) and (11.35).

11.5.2 Damping characteristics

The character of damping may be related to the fluid velocity characteristic for the second event. Hereto the damping is classified into three categories. In the case of *no damping* (or: no effective damping) the closure takes place under reflection free boundary conditions. In the case of *weak damping* the damping time is said to be of the same order of magnitude as the reflection time. The valve closure takes place under reflecting boundary conditions. In the case of *strong damping* the damping is (at least) one order higher than the reflection time. Reflections play a significant role. The character of the damping may now be quantified by:

no damping:

$$\frac{2L_u/c_u}{v_d}\left[\frac{dv}{dt}\right]_+ \leq -1 \quad \wedge \quad \frac{2L_d/c_d}{v_d}\left[\frac{dv}{dt}\right]_+ \leq -1 \qquad \textbf{(11.44)}$$

weak damping:

$$-1 < \frac{2L_u/c_u}{v_d}\left[\frac{dv}{dt}\right]_+ \leq -0.1 \quad \vee \quad -1 < \frac{2L_d/c_d}{v_d}\left[\frac{dv}{dt}\right]_+ \leq -0.1 \qquad \textbf{(11.45)}$$

strong damping:

$$-0.1 < \frac{2L_u/c_u}{v_d}\left[\frac{dv}{dt}\right]_+ \leq 0 \quad \vee \quad -0.1 < \frac{2L_d/c_d}{v_d}\left[\frac{dv}{dt}\right]_+ \leq 0 \qquad \textbf{(11.46)}$$

The conditions for strong damping overrule those for weak damping. Thus an overlap in the domain of the two parameters is avoided.

11.6 Valve characteristics approach 2

In the previous section the valve behaviour is described by more or less *global* flow parameters. In this section it is described in more detail. From the momentum equation (section 10.2.3) the following valve characteristic may be derived:

$$\Delta p = \xi \frac{1}{2} \rho_f v^2 \tag{11.47}$$

With the dimensionless variables (section 11.1) the following dimensionless form may be developed:

$$\frac{g \Delta H}{v_o^2} = \frac{1}{2} \xi \frac{v}{v_o} \left| \frac{v}{v_o} \right| \tag{11.48}$$

where the global force or head loss coefficient may be written as (section 8.8):

$$\xi = f \left[\frac{v}{v_o} , \frac{D}{v_o^2} \frac{dv}{dt} \right] \tag{11.49}$$

From the latter two equations directly follows:

$$\frac{g \Delta H}{v_o^2} = f \left[\frac{v}{v_o} , \frac{D}{v_o^2} \frac{dv}{dt} \right] \tag{11.50}$$

11.7 Other valve characteristics

From the parameter groups many other representations of valve characteristics can be developed. In a mathematical sense these functional relations may be perfectly valid. However, many of them will not be very useful.

Useful representations of valve characteristics may be:

$$\eta = f \left[\frac{\Delta p_o}{\rho_f v_o^2} \right] \tag{11.51}$$

where:

$$\eta = \frac{d\left[\frac{v_d}{v_o}\right]}{d\left[\frac{D}{v_o^2}\left[\frac{dv}{dt}\right]_-\right]} \tag{11.52}$$

where *d../dx* represents a derivative. The characteristic correlates the steady flow behaviour (energy losses) and the unsteady flow behaviour (valve response). Hereby the slope of the fluid characteristic for the first event (approach 1) is taken as a measure for the valve response. By considering the slope, hysteresis effects (e.g. at small initial fluid decelerations) can be excluded. In a general sense this slope will decrease with increasing valve loss coefficient. This may be illustrated by the following consideration.

Consider a swing check valve. Let the maximum opening angle be θ_o. Now a new valve design is created by reducing the maximum opening angle, so that the internal valve geometry is modified. In that case the loss coefficient ξ_o increases, while the response becomes faster, so that v_d/v_o reduces at the same initial flow deceleration. Generally the response of check valves is faster when they are initially partly open (Thorley, 1989).

Another useful representation may be:

$$\eta = f\left[\frac{\rho_m}{\rho_f}\right] \tag{11.53}$$

This characteristic shows in how far the valve response is influenced by the inertia effects of the moving elements. The characteristic may be of importance e.g. when scaling from liquids to gasses.

11.8 Common dimensionless numbers

The physical meaning of some common dimensionless numbers is studied. An overview is given of the forms in which they are introduced for check valves.

Euler number The Euler number is generally defined as:

$$Eu = \sqrt{\frac{\rho_f v^2}{\Delta p}} \tag{11.54}$$

It represents the ratio of inertia and normal (pressure) forces and is commonly used for steady flow conditions. Note that the term $\rho_f v^2$ only represents the convective acceleration of the inertia forces and not the local acceleration. For inviscid fluids similarity of the Euler number is satisfied, since the flow coefficients are only a function of the (linear and angular) position of the body.

The Euler number is equivalent with and related to the head loss or valve loss coefficient via:

$$Eu = \sqrt{\frac{2}{\xi}} \tag{11.55}$$

For check valves the following form is introduced (section 11.3):

$$Eu_o = \sqrt{\frac{\rho_f v_o^2}{\Delta p_o}} \tag{11.56}$$

Reynolds number The Reynolds number is generally defined as:

$$Re = \frac{\rho\ v\ D}{\mu} \tag{11.57}$$

It represents the ratio of inertia and shear forces and is commonly used for steady flow conditions. In literature also the time-dependent Reynolds number is found, which is based on an instantaneous fluid velocity.

Other forms are (section 5.4.1):

$$Re_1 = \frac{\rho_f (v - \dot{x})\, D}{\mu_f} \quad \wedge \quad Re_2 = \frac{\rho_f \dot{\theta}\, D^2}{\mu_f} \tag{11.58}$$

For check valves the critical Reynolds number is introduced as (section 8.5.2):

$$Re_o = \frac{\rho_f v_o D}{\mu_f} \tag{11.59}$$

Mach number The Mach number is generally defined as:

$$Ma = \frac{v}{c} \tag{11.60}$$

It represents the influence of compressibility effects and is commonly used for steady flow conditions.

For check valves the following form is introduced (section 11.3):

$$Ma_o = \frac{v_o}{c} \qquad \textbf{(11.61)}$$

Acceleration number The Acceleration number is defined as:

$$Ac^{-1} = \frac{D}{v^2}\frac{\partial v}{\partial t} \qquad \textbf{(11.62)}$$

It represents the ratio of inertia forces and forces due to changes of the local fluid velocity in time ($\partial v/\partial t$). In other words: the ratio of the forces due to convective acceleration (equivalent to the above inertia forces) and local acceleration. In the literature also the reciprocal form of the Acceleration number is found. For steady flow conditions this reciprocal form is per definition zero ($v \neq 0$).

Other forms are (section 5.4.1):

$$Ac_1^{-1} = \frac{D}{(v-\dot{x})^2}\frac{d(v-\dot{x})}{dt} \quad \wedge \quad Ac_2^{-1} = \frac{1}{\dot{\theta}^2}\frac{d\dot{\theta}}{dt} \qquad \textbf{(11.63)}$$

For check valves the following form is introduced (section 8.6):

$$Ac_o^{-1} = \frac{D}{v_o^2}\frac{dv}{dt} \qquad \textbf{(11.64)}$$

Strouhal number The Strouhal number is defined as:

$$S = \frac{f\,D}{v} \qquad \textbf{(11.65)}$$

It relates the frequency f of alternating Von Kàrmàn vortices, downstream of a body, to the fluid velocity and is commonly used for steady flow conditions.

For check valves the following form is introduced (section 11.1):

$$S_o = \frac{D}{(2L/c)\,v_o} \qquad \textbf{(11.66)}$$

11.9 Review and conclusions

A dimensional analysis is described. All variables and parameters that are relevant to the valve closure are gathered from the uncoupled and coupled, pipe and valve equations, as derived in the previous chapters.

Based on the dimensionless pipe and valve equations, the variables are written in a dimensionless form. As a result two sets of dimensionless variables ensure the kinematic similarity for the valve motion and pipe flow, respectively. These sets are linked by two dimensionless parameter groups.

The parameters that are relevant to the check valve behaviour are listed, whereby a distinction is made between the first and second event of closure. Based on the Buckingham Π-theorem dimensionless groups are developed. The repeating variables for the first and second event are consistent with the two sets of dimensionless variables.

The dimensionless parameter groups are subdivided into valve, system, valve-system, fluid and (steady and unsteady) flow parameters. From the (global) flow parameters several valve characteristics, such as fluid velocity, pressure head and damping characteristics are developed (approach 1). The damping characteristics are used to quantify the character of damping.

Alternatively, the valve behaviour is described in more detail in terms of dynamic valve loss coefficients, as derived from the momentum equation (approach 2).

From the dimensionless parameter groups additional valve characteristics are developed, which correlate the steady and unsteady flow behaviour, or correlate the inertia effects and unsteady flow behaviour. The former characteristic enables a comparison of check valve types with respect to the two essential aspects of the hydrodynamic design. The latter characteristic should enable the comparison between gas and liquid service.

Finally an overview is given of some common dimensionless numbers and the form in which they are applied to check valves.

The valve characteristics of approach 1 and 2 are used in the development of models for undamped and damped check valves in the next chapter.

12 Valve models

Semi-empirical, one-dimensional (1D) valve models are developed to simulate the dynamic behaviour of check valves in waterhammer computer codes. The models for undamped and damped check valves are based on the valve characteristics of approach 1 (section 11.5) and approach 2 (section 11.6), respectively. The models are implemented in the computer code CVWP (Check Valve Waterhammer Program).

12.1 Undamped check valve

The model for the undamped check valve is based on the valve characteristics of approach 1 (section 11.5).

Basic principle The valve closure takes place under reflection-free boundary conditions (section 9.4.2). There is no stage of active damping, so that the reverse flow velocity v_d now becomes the *maximum* reverse flow velocity, in literature often denoted as v_R. The undamped check valve closes (almost) instantaneously, after the maximum reverse flow velocity is reached (Kruisbrink, 1988). Hereby the valve may shortly interact with the system. This has, however, no consequences for the pressure head changes after closure (section 9.5). As such the system and valve-system parameters (section 11.4) play no role. The instant of closure is determined from the velocity-time history (figure 12.1.a) as the instant at which the actual fluid velocity underexceeds the maximum reverse flow velocity:

$$\text{if:} \quad v(t) \leq v_R \quad \text{then:} \quad t + \Delta t = t_c \quad \Lambda \quad v(t+\Delta t) = 0 \qquad \textbf{(12.1)}$$

The maximum reverse flow velocity is derived from the *fluid velocity characteristic for the first event* (figure 12.1.b):

$$\frac{v_R}{v_o} = f\left[\frac{\theta_i-\theta_c}{\theta_o-\theta_c} \; ; \; \frac{D}{v_o^2}\left[\frac{dv}{dt}\right]_-\right] \qquad \textbf{(12.2)}$$

The parameters θ_i and $(dv/dt)_-$ represent the initial, steady and unsteady flow conditions, respectively. The second parameter has no influence on the first one.

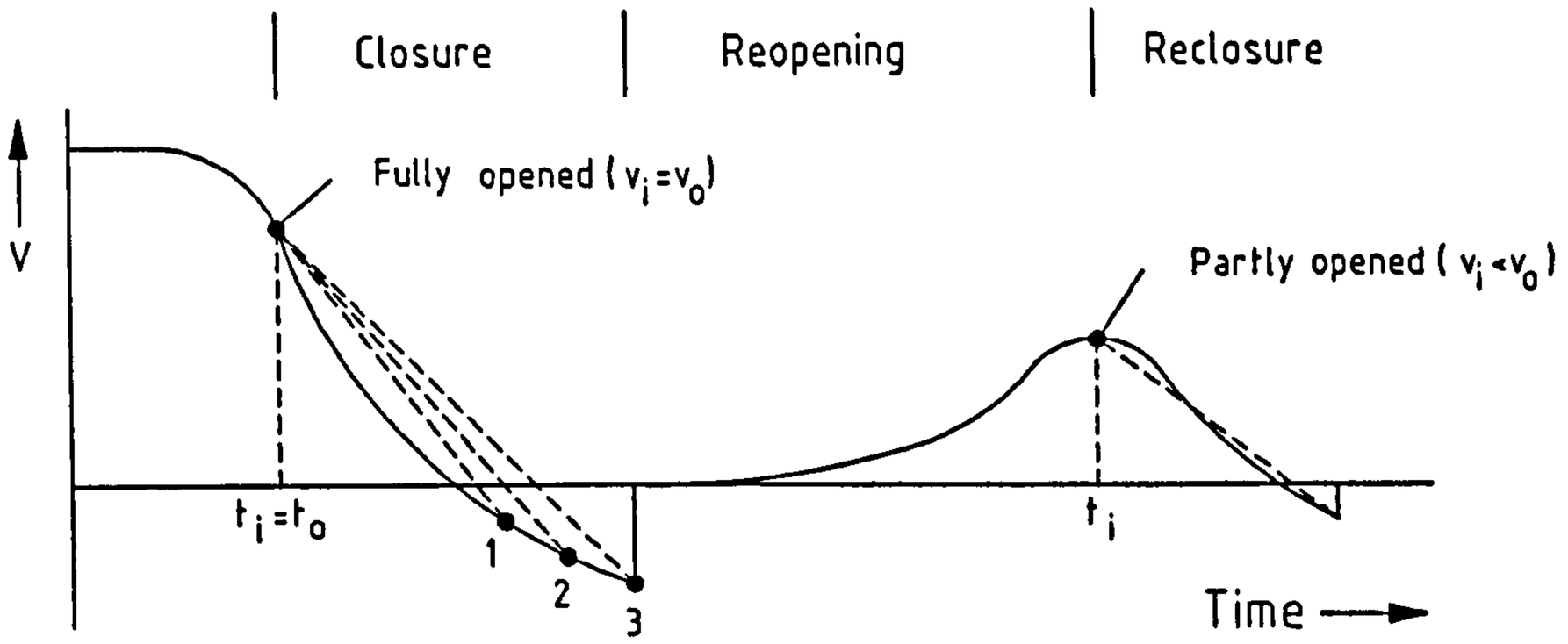

a. Velocity-time history

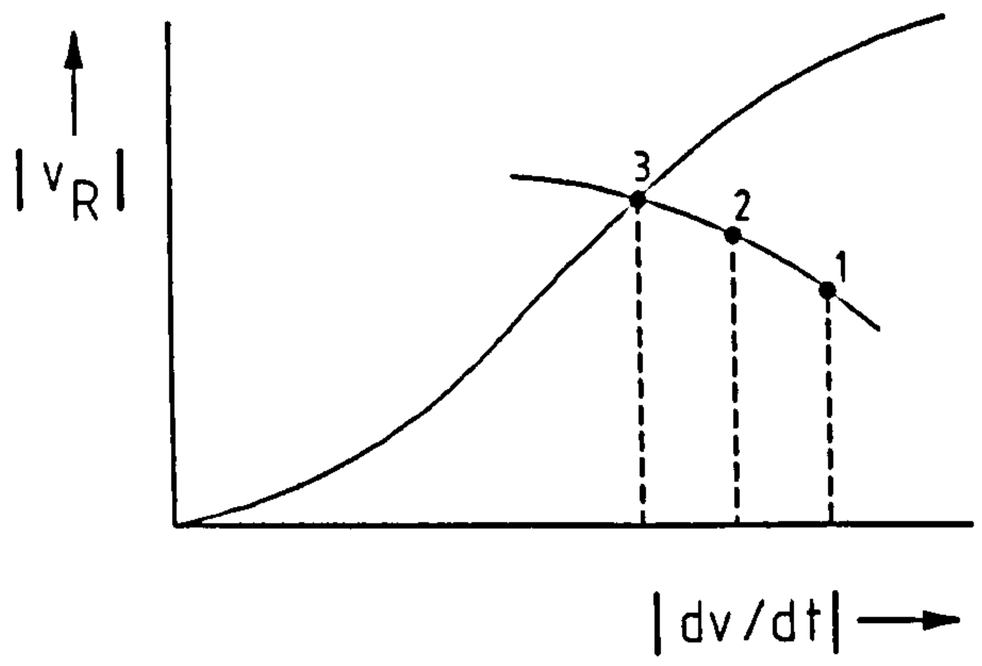

b. Fluid velocity characteristic for the first event

Figure 12.1 Valve model - undamped check valve

The first parameter may have influence on the second one, in particular for partly opened valves. In most cases, however, the influence of the check valve on the initial flow deceleration may be ignored (section 9.8). The correlation between the two parameters is assumed to be weak, so that their influence can be described by separate functions:

$$\frac{v_R}{v_o} = f_1 \left[\frac{\theta_i - \theta_c}{\theta_o - \theta_c} \right] \cdot f_2 \left[\frac{D}{v_o^2} \left[\frac{dv}{dt} \right]_- \right] \qquad (12.3)$$

Function f_1 This function accounts for the effect of an initially, partly opened valve on the valve response. It generally may be approximated by a polynomial or Taylor series as:

$$f_1\left[\frac{\theta_i-\theta_c}{\theta_o-\theta_c}\right] = a_1\left[\frac{\theta_i-\theta_c}{\theta_o-\theta_c}\right] + a_2\left[\frac{\theta_i-\theta_c}{\theta_o-\theta_c}\right]^2 + \ldots \qquad (12.4)$$

The initial valve disc position may in its turn be related to the initial fluid velocity via the steady flow characteristic. In dimensionless form this yields ($0 \leq v/v_o \leq 1$):

$$\frac{\theta-\theta_c}{\theta_o-\theta_c} = b_1\left[\frac{v}{v_o}\right] + b_2\left[\frac{v}{v_o}\right]^2 + \ldots \qquad (12.5)$$

Note that the sum of b_1, b_2, ... must be one. Experiments show that in many cases the function has the character of a linear or root function.

Substitution of Equation (12.5) in Equation (12.4) gives the form:

$$f_1\left[\frac{\theta_i-\theta_c}{\theta_o-\theta_c}\right] = c_1\left[\frac{v_i}{v_o}\right] + c_2\left[\frac{v_i}{v_o}\right]^2 + \ldots \qquad (12.6)$$

The form of this function is unknown and needs further investigation. In first instance the linear version is used in CVWP ($a_1 = b_1 = c_1 = 1$; $a_2, \ldots = 0$).

About the function f_1 in the case of a swing check valve ...

To get an idea about the character of the function, the valve response model developed in chapter 8 is applied to a swing check valve without friction and damping. The valve is subjected to a constant, initial flow deceleration, starting with steady flow conditions. The flow coefficients C_{D1} and C_{A2} are taken from literature (Thorley and Oei, 1981; Thorley 1991). The other flow coefficients are unknown, but varied during the series of calculations. These tentative results indicate that the relation between v_R and θ_i is indeed more or less linear. However, for relatively small initial flow decelerations this tendency reverses, i.e. v_R becomes inversely proportional to θ_i. The latter indicates that there exists a correlation between the parameters θ_i and $(dv/dt)_i$! The above tendencies hold for all series.

About inertia effects ...

Strictly speaking the above result may only be applied to the steady flow conditions before (the first) closure, since inertia effects are not included. In the case of reopening inertia effects, which will delay the opening, may play a role. If dynamic opening characteristics are not available, the following principle may be applied: The inertia effects during closure are the same as those during opening under similar, but reversed unsteady flow conditions. Thus, the information about inertia effects which is contained in the dynamic closure characteristics, can be used for a better estimation of the "initial" valve disc position after reopening.

Function f_2 This function represents the fluid velocity characteristic for the first event for an initially, fully opened valve (function $f_1 = 1$). The characteristic is usually obtained from experiments.

The (mean) initial flow deceleration is calculated from (figure 12.1.a):

$$\left[\frac{dv}{dt}\right]_{-} = \frac{v - v_i}{t - t_i} \tag{12.7}$$

with the boundary conditions:

$$\begin{aligned} &\text{if} \quad v_{\max} \geq v_o \quad \text{then} \quad v_i = v_o \quad \wedge \quad t_i = t_o \\ &\text{if} \quad v_{\max} < v_o \quad \text{then} \quad v_i = v_{\max} \quad \wedge \quad t_i = t_{\max} \end{aligned} \tag{12.8}$$

where v_{max} is the maximum (steady or unsteady) fluid velocity before (re)closure. Thus it is accounted for an initially, partly opened valve and its reclosure.

About additional options .....

Resistance The (partly) opened check valve may be modelled as a resistance with a specified, constant, valve loss coefficient. In that case the influence of the check valve on the initial, steady and unsteady flow conditions is taken into account. However, as stated before, in most cases this influence may be neglected (section 9.8).

Opening criteria A closed valve (re)opens when the pressure head difference across the valve exceeds a threshold value:

$$H_1 - H_2 > \Delta H_{open} \tag{12.9}$$

Check valves need some positive head difference to open, due to e.g. the preset conditions of springs or counterweights.

The above options are available in CVWP.

12.2 Damped check valve

The model for the damped check valve is based on the valve characteristics of approach 2 (section 11.6).

A valve characteristic of approach 2 may be represented by a set of points in a three-dimensional, physical space:

$$\left[\frac{v}{v_o}, \frac{D}{v_o^2}\frac{dv}{dt}, \frac{g\Delta H}{v_o^2} \right] \in \mathbb{R}^3 \qquad (12.10)$$

The characteristics are dependent on the valve and system parameters (section 11.4). Consider a set of points for which the valve and system parameters are constant. It is assumed that this set of points forms a surface in the physical space.

This surface may be represented by:

$$\Phi \left[\frac{v}{v_o}, \frac{D}{v_o^2}\frac{dv}{dt}, \frac{g\Delta H}{v_o^2} \right] = 0 \qquad (12.11)$$

The domain of the valve characteristic is divided into four quadrants, in terms of a *v-dv/dt*-plane. Consider a possible trajectory which is followed during valve closure as illustrated in figure 12.2. The valve closure is assumed to start from steady flow conditions by entering quadrant 4 ($v > 0$; $dv/dt < 0$) from the horizontal axis.

Basic principle In quadrant 4, in the adjacent part of quadrant 3, and quadrant 1, the partly opened check valve ($v/v_o < 1$) is modelled by:

$$\frac{g\Delta H}{v_o^2} = f\left(\frac{v}{v_o}, \frac{D}{v_o^2}\frac{dv}{dt}\right) \qquad (12.12)$$

The fully opened check valve ($v/v_o \geq 1$) is modelled as a resistance with valve loss coefficient ξ_o. Thus the physical domain of the valve characteristic is limited to $v/v_o \leq 1$.

In quadrant 1 ($v > 0$; $dv/dt > 0$) the opening behaviour is described. However, if no experimental data are available the opening behaviour may be modelled by the steady flow characteristics. Hereto the points (v, dv/dt) in this quadrant are projected on the horizontal axis (v, 0).

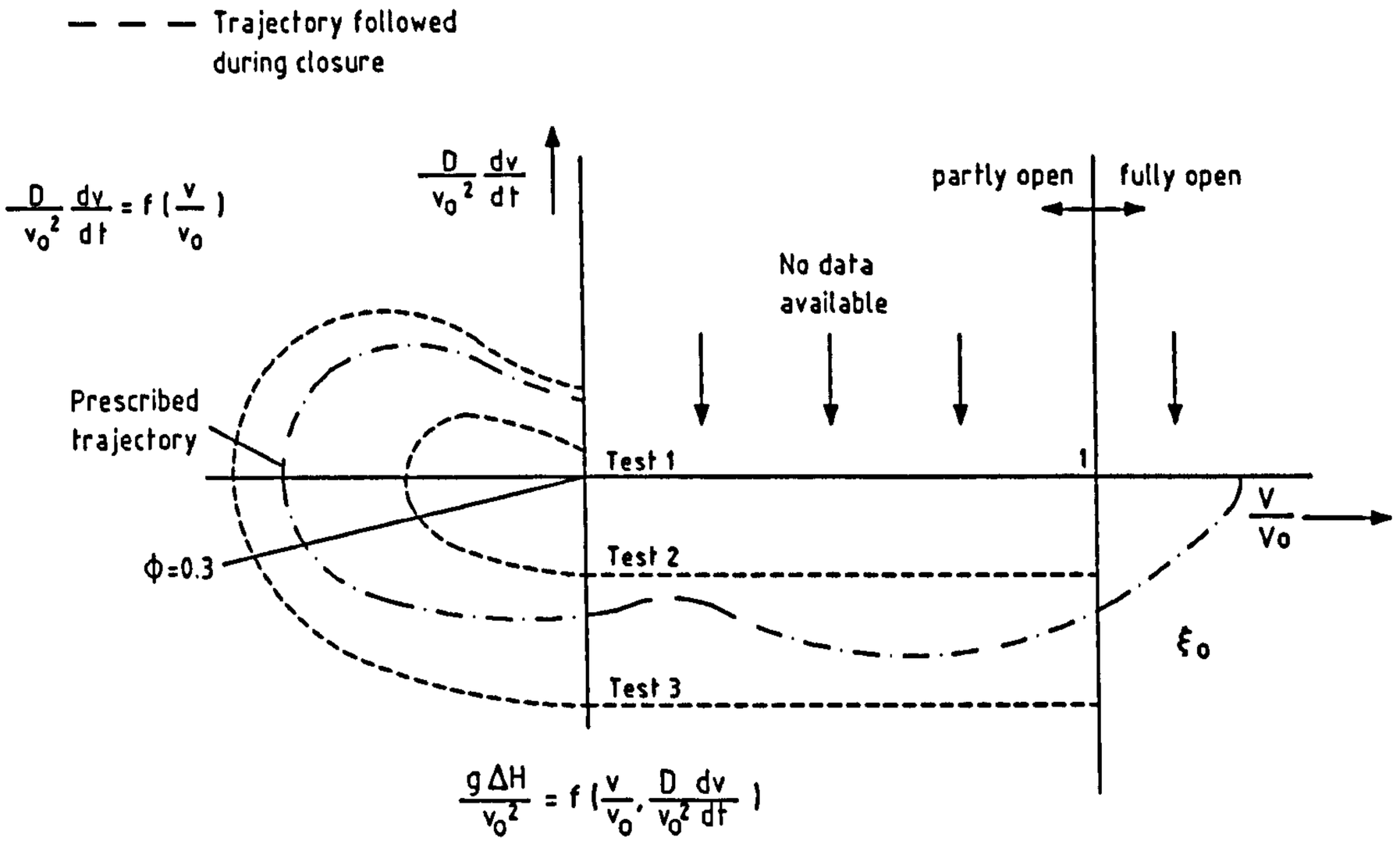

Figure 12.2 Valve model - damped check valve

In quadrant 2 and in the adjacent part of quadrant 3, the partly opened check valve is in its last stage of closure. The valve behaviour becomes physically unstable here, i.e. the valve will always tends to close under the reverse flow; no steady-state conditions exist. However, the closure is more or less controlled by the damping, which is active here. The flow conditions are assumed to be dominated by the valve and modelled by so-called prescribed trajectories (Appendix C: section C.3.5):

$$\frac{D}{v_o^2}\frac{dv}{dt} = f\left(\frac{v}{v_o}, \frac{g\Delta H}{v_o^2}\right) \qquad (12.13)$$

To enable a general application of the prescribed trajectories a relaxation is applied to the head difference ΔH. In that case a valve closure is ensured.

The valve model is formulated in table 12.1. For a detailed model description it is referred to Appendix C.

	partly open	fully open
Quadrant 1	$\frac{g\Delta H}{v_o^2}(\frac{v}{v_o}, 0)$	$\frac{g\Delta H}{v_o^2} = \frac{1}{2}\xi_o \frac{v}{v_o}\lvert\frac{v}{v_o}\rvert$ $\xi_o = 2\,\frac{g\Delta H}{v_o^2}(1, 0)$
Quadrant 2 and Quadrant 3 ($\phi \leq 0.3^*$)	$\frac{D}{v_o^2}\frac{dv}{dt}(\frac{v}{v_o}, \frac{g\Delta H}{v_o^2})$	---
Quadrant 3 ($\phi > 0.3^*$)	$\frac{g\Delta H}{v_o^2}(\frac{v}{v_o}, \frac{D}{v_o^2}\frac{dv}{dt})$	---
Quadrant 4	$\frac{g\Delta H}{v_o^2}(\frac{v}{v_o}, \frac{D}{v_o^2}\frac{dv}{dt})$	$\frac{g\Delta H}{v_o^2} = \frac{1}{2}\xi_o \frac{v}{v_o}\lvert\frac{v}{v_o}\rvert$ $\xi_o = 2\,\frac{g\Delta H}{v_o^2}(1, \frac{D}{v_o^2}\frac{dv}{dt})$

Table 12.1 Valve model - damped check valve

* The closure phase ϕ is defined as (see figure 12.2 and Appendix C: section C.3.5):

$$\phi = \left[\frac{D}{v_o^2}\frac{dv}{dt}\right] / \left[\frac{v}{v_o}\right] \qquad (12.13)$$

Valve and system parameters The dynamic valve characteristics are dependent on the valve and system parameters (section 11.4). Information about the valve parameter $\xi_o = \Delta p_o / \frac{1}{2}\rho_f v^2$ and unsteady flow parameters is implicitly included in the valve characteristics of approach 2. The other parameters must be specified:

$$\begin{aligned}
&\textit{valve:} && \frac{\rho_m}{\rho_f} \;;\; \frac{T_{S_o}}{\rho_f v_o^2 D^3} \;;\; \frac{T_{S_o}}{T_{S_c}} \;;\; \%\ \textit{damping} \;;\; \gamma \\
&\textit{system:} && \frac{2L_u/c_u}{2L_d/c_d} \;;\; \frac{A_u/c_u}{A_d/c_d} \\
&\textit{valve-system:} && \frac{D}{(2L_u/c_u)v_o} \;;\; \frac{v_o}{c_u} \;;\; \frac{v_o}{c_d} \qquad \textbf{(12.14)} \\
&\textit{fluid:} && \frac{\rho_d}{\rho_f} \;;\; Re_o = \frac{\rho_f v_o D}{\mu_f} \;;\; \frac{\mu_d}{\mu_f} \\
&\textit{flow:} && \frac{\theta_i - \theta_c}{\theta_o - \theta_c}
\end{aligned}$$

In principle the system parameters must be specified for all pipe sections of a pipeline system. Here only the upstream and downstream (subscripts *u* and *d*) pipe sections adjacent to the check valve are described, since: 1) not all pipe sections influence the check valve behaviour, 2) the valve characteristics are available for (other) simple pipeline configurations without pipe junctions and with constant head boundaries (i.e. laboratory conditions), and 3) for complex pipeline configurations it is unpractical to specify all pipe sections. This restriction implies that the valve characteristics may only applied to operational conditions which are more or less similar to the laboratory conditions, i.e. constant head boundaries (e.g. reservoirs, air vessels, headers), while the influence of the pump as resistance is small.

Within the parameters listed in Equation (12.15) a distinction can be made between parameters which are expected to be of *major imortance* (a) and those of *minor importance* (b):

$$\begin{aligned}
&\frac{T_{S_o}}{\rho_f v_o^2 D^3} \;;\; \%\ \textit{damping} \;;\; \frac{2L_u/c_u}{2L_d/c_d} \;;\; \frac{D}{(2L_u/c_u)v_o} \;;\; \frac{\theta_i - \theta_c}{\theta_o - \theta_c} && \textbf{(a)} \\
&\frac{\rho_m}{\rho_f} \;;\; \frac{T_{S_o}}{T_{S_c}} \;;\; \gamma \;;\; \frac{A_u/c_u}{A_d/c_d} \;;\; \frac{v_o}{c_u} \;;\; \frac{v_o}{c_d} \;;\; \frac{\rho_d}{\rho_f} \;;\; Re_o \;;\; \frac{\mu_d}{\mu_f} && \textbf{(b)}
\end{aligned} \qquad \textbf{(12.15)}$$

The parameter group ρ_m/ρ_f is of minor importance as long as the scaling takes place from liquid to liquid. However, the group may be of significant importance when scaling from liquids to gasses. The parameter group T_{So}/T_{Sc} is of minor importance if the preset spring force is relatively small. The parameter γ is of minor importance if gravitational and buoyancy effects are relatively small (e.g. spring-assisted valves) or independent of γ (e.g. sinking ball). The group $(A_u/c_u)/(A_d/c_d)$ is irrelevant if the diameter of check valve and adjacent pipe sections is equal. The importance of the parameter groups v_o/c_u and v_o/c_d is not quite known yet, but expected to be less than those of category *a*. The parameter groups ρ_d/ρ_f and μ_d/μ_f may be about constant for a certain valve type and its application (e.g. check valves for water service with oil as damping fluid). The parameter Re_o is not relevant if the flow in both the valve and damper is turbulent. The parameter group μ_d/μ_f is not relevant if the flow in the damper is turbulent.

More insight in the influence of the parameters may be obtained from a sensitivity analysis. In principle this can be done by means of simulations with a waterhammer computer code. Hereto enough experimental data, i.e. test series at different valve and system conditions, must be available.

Note: The parameter set applies to check valves with rotating elements. For check valves with translating elements the torques (T) should be replaced by forces (F), while the angular valve disc position (θ) should be replaced by a linear one (x).

12.3 Numerical procedures

In waterhammer computer codes like CVWP a distinction is made between pipes and components like pumps, valves, vessels, etc. The flow in the pipes is described by the transient equations and treated by the method of characteristics (section 9.2). Components are described by hydraulic equations, which are solved in a linearized form within an iteration process, together with the compatibility equations of the adjacent pipe sections. In the case that components are clustered a set of hydraulic equations must be solved simultaneously.

12.3.1 General components

In CVWP a component between two nodes (fall type) is generally described by:

$$\begin{aligned} f_1\left(H_1(t), H_2(t), Q_1(t), Q_2(t)\right) &= 0 \\ f_2\left(H_1(t), H_2(t), Q_1(t), Q_2(t)\right) &= 0 \end{aligned} \qquad \textbf{(12.16)}$$

The architecture of the scheme allows that two phenomena (e.g. energy losses and storage capacity) can be modelled at the same time.

Linearization of these equations results in:

$$f_1^{i+1}(H_1, H_2, Q_1, Q_2) = f_1^{i}(H_1, H_2, Q_1, Q_2) + \\ + \frac{\partial f_1^{i}}{\partial H_1}\Delta H_1^{i} + \frac{\partial f_1^{i}}{\partial H_2}\Delta H_2^{i} + \frac{\partial f_1^{i}}{\partial Q_1}\Delta Q_1^{i} + \frac{\partial f_1^{i}}{\partial Q_2}\Delta Q_2^{i} \qquad \textbf{(12.17)}$$

and:

$$f_2^{i+1}(H_1, H_2, Q_1, Q_2) = f_2^{i}(H_1, H_2, Q_1, Q_2) + \\ + \frac{\partial f_2^{i}}{\partial H_1}\Delta H_1^{i} + \frac{\partial f_2^{i}}{\partial H_2}\Delta H_2^{i} + \frac{\partial f_2^{i}}{\partial Q_1}\Delta Q_1^{i} + \frac{\partial f_2^{i}}{\partial Q_2}\Delta Q_2^{i} \qquad \textbf{(12.18)}$$

where:

$$\Delta H_1^{i} = H_1^{i+1} - H_1^{i} \quad ; \quad \Delta H_2^{i} = H_2^{i+1} - H_2^{i}$$
$$\Delta Q_1^{i} = Q_1^{i+1} - Q_1^{i} \quad ; \quad \Delta Q_2^{i} = Q_2^{i+1} - Q_2^{i} \qquad \textbf{(12.19)}$$

The superscripts i and $i+1$ refer to the values at the old and new instant of time.

Suppose that Equation (12.17) is satisfied at the instant $i+1$. Then the above equations adopt the form:

$$\begin{bmatrix} \frac{\partial f_1}{\partial H_1} & \frac{\partial f_1}{\partial H_2} & \frac{\partial f_1}{\partial Q_1} & \frac{\partial f_1}{\partial Q_2} \\ \frac{\partial f_2}{\partial H_1} & \frac{\partial f_2}{\partial H_2} & \frac{\partial f_2}{\partial Q_1} & \frac{\partial f_2}{\partial Q_2} \end{bmatrix}^{i} \begin{bmatrix} H_1 \\ H_2 \\ Q_1 \\ Q_2 \end{bmatrix}^{i+1} = \begin{bmatrix} CON_1 \\ CON_2 \end{bmatrix} \qquad \textbf{(12.20)}$$

where:

$$CON_1 = \frac{\partial f_1^{i}}{\partial H_1}H_1^{i} + \frac{\partial f_1^{i}}{\partial H_2}H_2^{i} + \frac{\partial f_1^{i}}{\partial Q_1}Q_1^{i} + \frac{\partial f_1^{i}}{\partial Q_2}Q_2^{i} - f_1^{i}$$
$$CON_2 = \frac{\partial f_2^{i}}{\partial H_1}H_1^{i} + \frac{\partial f_2^{i}}{\partial H_2}H_2^{i} + \frac{\partial f_2^{i}}{\partial Q_1}Q_1^{i} + \frac{\partial f_2^{i}}{\partial Q_2}Q_2^{i} - f_2^{i} \qquad \textbf{(12.21)}$$

Equation (12.21) is solved in an iteration process, together with the other component equations of that (cluster of) node(s), until a convergence criterion is satisfied.

In order to solve the equations the matrix coefficients and constants must be specified. This can be done each time step (explicit) or each iteration step (implicit). In an explicit scheme the linearized equations remain unchanged during the iteration process. In the fully implicit scheme the equations are updated every iteration step (Newton-Raphson). In the semi-implicit scheme the constants are updated, while the slope of the linearized equations is kept constant (semi-Newton-Raphson).

12.3.2 Damped check valve

For the damped check valve the hydraulic equations are:

$$f_1: \qquad H_1 - H_2 - f_1^* \left[Q_1 , \frac{dQ_1}{dt} \right] = 0 \qquad \textbf{(12.22)}$$

$$f_2: \qquad Q_1 - Q_2 = 0$$

where:

$$f_1^* \left[Q_1 , \frac{dQ_1}{dt} \right] = \frac{v_o^2}{g} \cdot \frac{g \Delta H}{v_o^2} \left[\frac{v}{v_o} , \frac{D}{v_o^2} \frac{dv}{dt} \right] \qquad \textbf{(12.23)}$$

The function f_1 is basically derived from the momentum equation (section 11.6), where f_1^* represents the valve characteristic of approach 2, given in Equation (11.50). In that sense it describes the conservation of momentum. The function f_2 describes the conservation of mass. Although the effect of rigid or non-rigid moving elements on the flow is described, it is assumed that the elements have no storage capacity. The latter assumption does not hold for the membrane type check valve tested (section 14.6). In order to describe the storage capacity the flow rate at both the upstream and downstream side of the check valve Q_1 and Q_2 must be known.

The coefficient matrix now becomes:

$$\begin{bmatrix} 1 & -1 & -\frac{\partial f_1^*}{\partial Q_1} & 0 \\ 0 & 0 & 1 & -1 \end{bmatrix} \qquad \textbf{(12.24)}$$

The derivative of f_1^* is determined numerically from the valve characteristics. This is done by an imposed increment ΔQ_1, whereby the variation of dQ_1/dt in the direction of motion (i.e the trajectory followed during closure) is taken into account.

The linearized equations are solved in a semi-explicit scheme.

As stated in section 12.2, the check valve behaviour becomes physically unstable during the last stage of closure. Consequently also the above numerical procedure becomes unstable. For this reason the valve closure is modelled here by prescribed trajectories. The hydraulic equation is basically described by:

$$\frac{dQ_1}{dt} = \frac{\pi}{4} D^2 \cdot \frac{v_o^2}{D} \cdot \frac{D}{v_o^2} \frac{dv}{dt} \left[\frac{v}{v_o} \right] \qquad (12.25)$$

The prescribed trajectory is solved iteratively by an adapted form of the θ-method. (Appendix C: section C.3.5).

Smoothing parameter The velocity gradient dv/dt is an instantaneous value, which is sensitive to the velocity fluctuations coupled with pressure surges. Therefore the sign of dv/dt may change from positive to negative. High-frequency fluctuations and sign changes may be suppressed by applying a low-pass filter to dv/dt (just like is done in the processing of experimental data; see also section 13.7.2). The velocity gradient is smoothed according to:

$$\frac{dv}{dt}(t) = \frac{\frac{1}{n_g} \sum_{n=1}^{n_g} v\left(t-(n-1)\Delta t\right) - \frac{1}{n_g} \sum_{n=1}^{n_g} v\left(t-(n+n_t-1)\Delta t\right)}{n_t \Delta t} \qquad (12.26)$$

The smoothed velocity gradient is obtained from two clusters in the velocity-time history, where n_g is the number of data per cluster, n_t is the number of time steps between the clusters and Δt is the time step.

Interpolations Within the iteration proces two interpolations are performed. One interpolation is performed within a valve characteristic of approach 2, the other within the valve and system parameters.

Suppose that m valve characteristics are available with the corresponding sets of valve and system parameters. The interpolation procedure is as follows: Within each valve characteristic the head difference ΔH_i is obtained from a linear interpolation, i.e. $\Delta H_i = f_i\,(v, dv/dt)$. This yields m head differences $\Delta H_1, \Delta H_2, .. , \Delta H_i, .. , \Delta H_m$.

The actual head difference ΔH is obtained from a (scaled) linear interpolation within the m parameter sets (laboratory conditions), based on the actual values of the parameters (application). The interpolation is described by:

$$\Delta H = a_1 \Delta H_1 + a_2 \Delta H_2 + \ldots + a_m \Delta H_m \qquad (12.27)$$

where a_1, a_2, ..., a_m are the weight factors. In most cases the number of valve characteristics is smaller than the number of valve and system parameters. Then the determination of the weight factors is based on the principle of minimum variation.

The interpolation procedure for the fluid velocity gradient dv/dt (prescribed trajectories) is essentially the same. However, in order to perform the interpolation between m prescribed trajectories it is necessary to introduce a second closure phase. The closure phase, which is defined in Equation (12.13) and is based on physical grounds, appears to give rise to inconsistent trajectories, which violate the condition $dv/d(dv/dt) = 0$ on the negative v-axis. In order to guarantee valid trajectories, which satisfy the above condition, the second closure phase is now defined as (quadrant 2):

$$\phi = 1 - \frac{v}{v_R} \qquad (12.28)$$

where v_R is the maximum reverse flow velocity of the prescribed trajectory.

The velocity gradient is then obtained from:

$$\frac{dv}{dt}(\phi) = a_1 \frac{dv}{dt_1}(\phi) + a_2 \frac{dv}{dt_2}(\phi) + \ldots + a_m \frac{dv}{dt_m}(\phi) \qquad (12.29)$$

Extrapolated prescribed trajectories (i.e. as final result of the two interpolation procedures) are allowed under the following conditions: 1) the extrapolated prescribed trajectory leaves quadrant 2 via the vertical axis, and 2) the maximum reverse flow velocity of the prescribed trajectory lies on the negative, horizontal axis. If these conditions are not satisfied the extrapolated trajectory is assumed to be too far from the available data.

For detailed descriptions of the two interpolation procedures, and other aspects like the computational domain, implicit functions, stability and flow loops, it is referred to the appendices C and D.

12.4 About neural networks ...

In the valve models the check valve is considered as a black box with input and output characteristics in terms of fluid velocities and pressures. The question arises in how far neural networks (NN) can be applied in these models.

The NN's considered here are so-called *multi-layer perceptra* (MLP), also known as *feed forward error back propagation networks*.

A MLP consists of a set of processing elements (neurons) which are ordered in an input layer, one or more hidden layers and an output layer (figure 12.3). Each neuron is connected to all the neurons of the preceding and subsequent layer. Within a neuron two operations are performed. The first operation is a weighted summation of all the inputs of the neuron. This weighted sum represents the internal state of the neuron. The second operation applies a transfer or activation function to the internal state and generates the output of the neuron. The character of this transfer function makes the NN concept non-linear.

The weight factors are determined within an iteration process, which is known as the training of the NN. Herefore a data set is required, which consists of known combinations of input and output data. The process should converge to the best fit between the input and output data. Hereby the proper choice of the architecture, i.e. the number of neurons and the number of hidden layers is essential. After the training of the NN the performance is tested with an additional data set, which should be statistically equivalent to the training set.

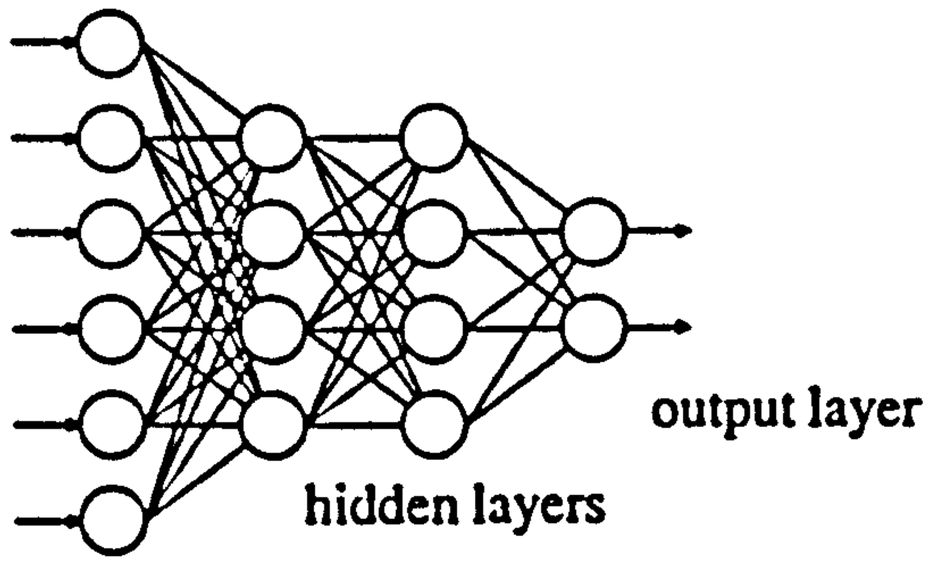

Figure 12.3 Architecture of MLP neural network

Within the model for damped check valves two interpolations are performed (section 12.3.2). In principle these interpolations can also be performed by a NN. The application of NN's to the valve characteristics of approach 2 is further explored in section 14.7.1.

12.5 Review and conclusions

Semi-empirical valve models are described to simulate the dynamic behaviour of check valves in waterhammer computer codes. The model for undamped check valves is based on the (dimensionless) valve characteristics of approach 1. The model for damped check valves is based on the valve characteristics of approach 2.

The models are implemented in the waterhammer computer code CVWP.

13 Experimental set up

In this chapter the test facility and test valves, the measuring procedures and equipment are described, which are used to measure the valve characteristics, defined in chapter 11. Measuring procedures are developed to obtain the dynamic pressures and flows at the check valve from values, measured at some distance from the valve. The data acquisition and the data processing into the valve characteristics of approach 1 and 2 are described.

13.1 Requirements

The measurements should take place under well-defined initial and boundary conditions. At the same time the range of applicability of the experimental data should be as wide as reasonably possible. In that sense the tests should simulate operating conditions. In order to measure the valve characteristics which are introduced in section 11.5 and 11.6, a test facility is required with the following features:

- The initial flow deceleration is as constant as possible and adjustable.
- The measuring section of the test facility has constant head boundaries.
- The measuring section has no pipe junctions. The diameter of the piping is equal to the diameter of the valve.
- The reflection time of the pipe sections, upstream and downstream of the check valve, is adjustable.
- The measurements take place under cavitation free conditions.

13.2 Test facility

The test rig for check valves, as available at Delft Hydraulics, is shown in figure 13.1. It consists of a pump station with eight centrifugal pumps, a head tank with overflow, an air vessel (upstream boundary), test section, high pressure tank with connected air reservoir (downstream boundary) and a control valve.

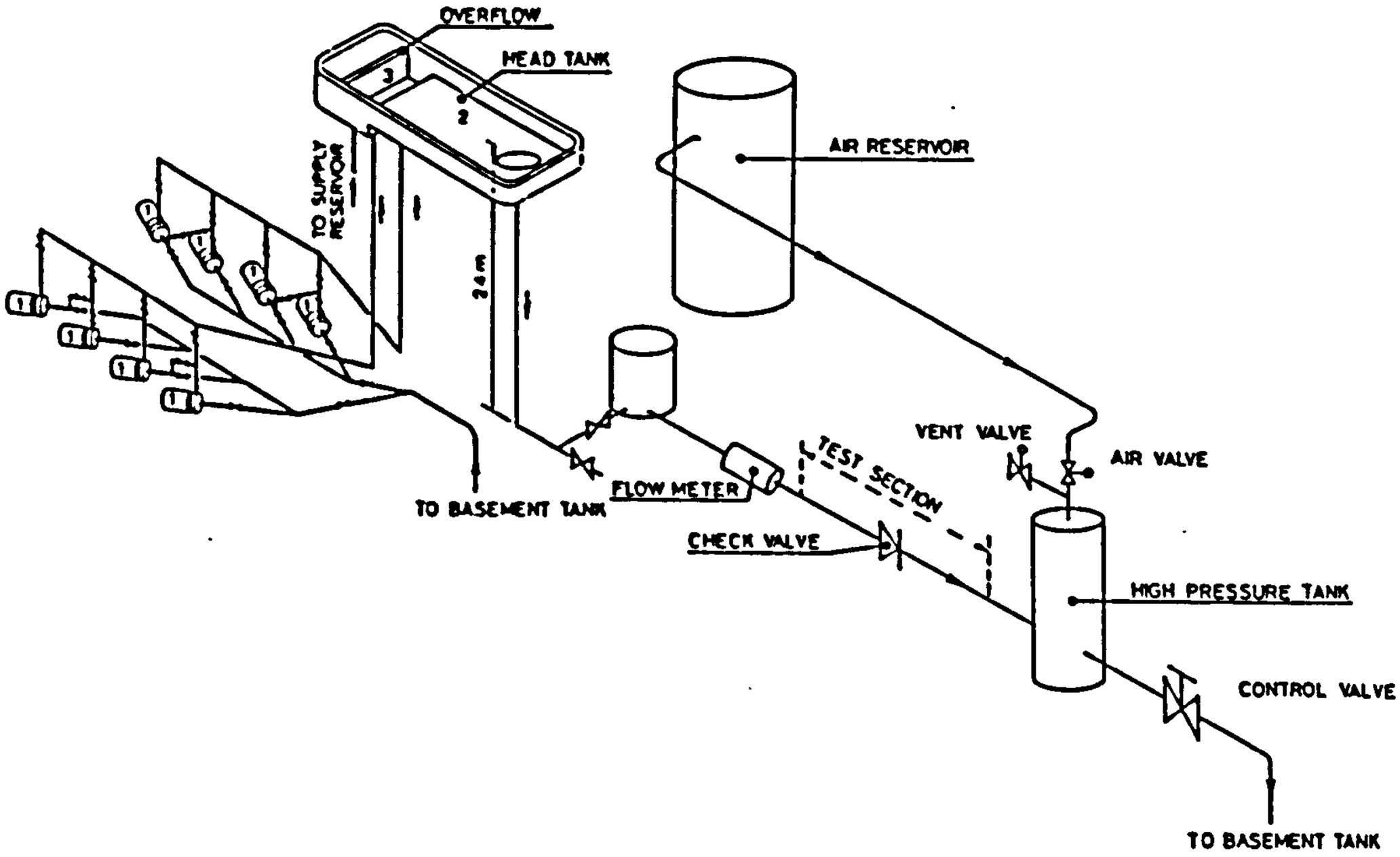

Figure 13.1 Test rig for check valves at DELFT HYDRAULICS

Principle of operation Eight centrifugal pumps supply water from the basement tank to the head tank. The water level in the head tank is fixed by means of an overflow at a height of about 25 m. Excess of water flows back through the return pipeline into the supply reservoir.

The *steady flow conditions* (in advance of a dynamic test) are controlled by a (600 mm) control valve. The water level in the upstream air vessel is adjusted. The air reservoir, which is isolated from the high pressure tank by a closed (300 mm) air valve, is pressurized to a desired level. The water level in the high pressure tank is controlled by a vent valve.

The *unsteady flow conditions* (a so-called dynamic test) are obtained by rapidly increasing the pressure head at the downstream side of the test section to a constant level. This is achieved by opening the fast-acting air valve. Due to the high air pressure the flow in the measuring section will be decelerated. The reverse flow of water is supplied by the high pressure tank.

After the closure of the check valve the air valve is shut off. Consequently the pressure in the high pressure tank will be reduced, the check valve reopens and the steady flow conditions are readjusted, so that the next test can be carried out.

About the upstream boundary .....

As upstream boundary an air vessel (volume 3 m^3) is used with a pressure relief on top of the vessel. The surge effects of the air vessel and pressure relief valve are studied by Van Hulst from the KEMA by means of simulations with the waterhammer computer code WTSL$^+$ (Van Hulst and Kruisbrink, 1993). As a result the necessity for the air vessel, in particular for the testing of larger check valves, is demonstrated. The set pressure of the pressure relief valve is adjusted to 3.50 bar (i.e. 0.10 bar higher than the stationary flow pressure in the test section).

The test section is located between the upstream air vessel and the downstream high pressure tank as shown in figure 13.2. The test section is available in 200 mm and 500 mm piping. The meterrun as unit (i.e. the shaded part with test valve and flowmeter) can be installed at different locations in such a way that the ratio of the upstream and downstream pipe lengths is adjustable to 1/3, 1 or 3. The check valve can be replaced by a dummy piece of pipe.

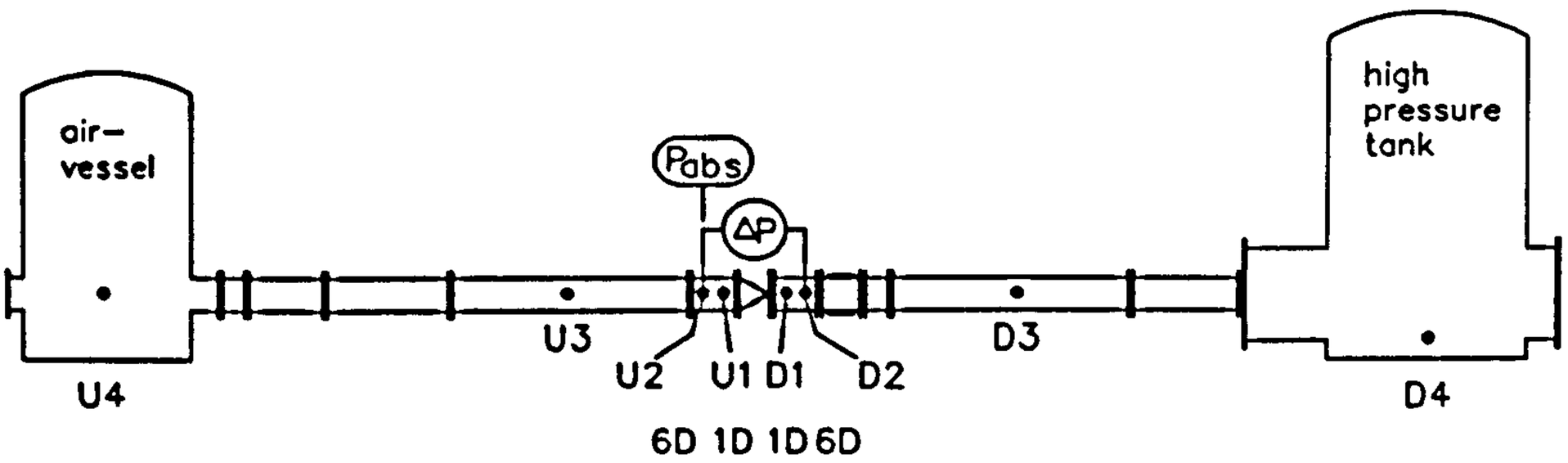

Figure 13.2 Test section with pressure tap locations

13.3 Test valves

The valves which have been tested are a 200 mm, weakly damped, membrane check valve, and 200 and 500 mm, strongly damped, butterfly check valves.

Membrane check valve The valve has a flexible membrane as closing element (figure 13.3). The membrane and its seat, which consists of a plate with holes, give a certain resistance in the normal flow direction. In the reverse flow direction the membrane moves to the plate. The elastic properties of the membrane give the valve a certain damping and storage capacity, in particular when it closes against the seat.

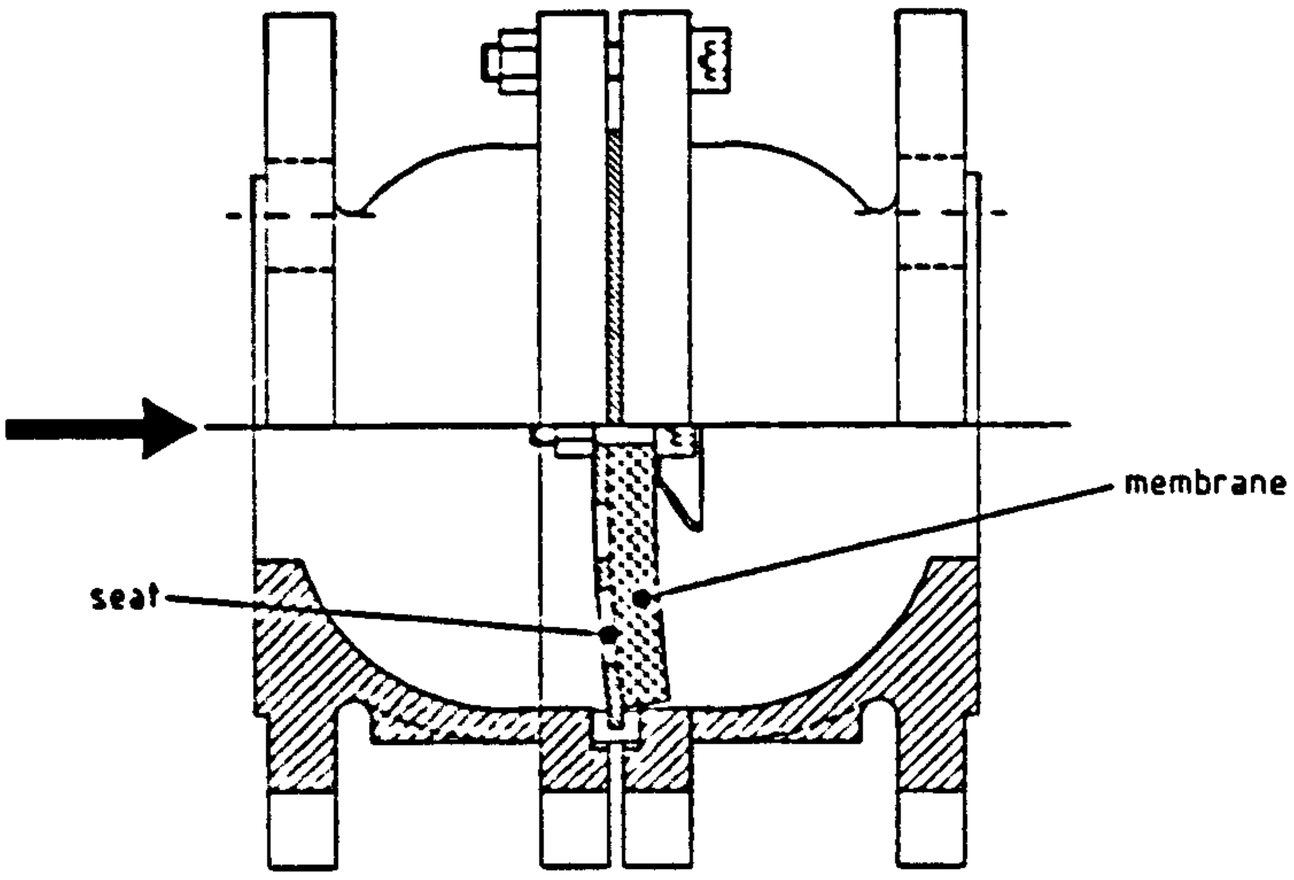

Figure 13.3 Membrane check valve

Butterfly check valve The valve has a disc as closing element. The closure is assisted by a counterweight and an external hydraulic damper (figure 13.4). The principal parts of the 200 and 500 mm valves, such as the valve disc, the centre of rotation of the disc and center of rotation of the damping device, are geometrically similar (scale 1 : 2.5). The valve is fully open at $\theta_o = 53.5°$, the damping device is activated at $\theta_d = 11.4°$ and the valve is closed at $\theta_c = 0.0°$. In the fully open position the weight arm is in a horizontal position (both valves).

The mass density of the valve disc and counterweight is $\rho_m = 7350$ kg/m^3. The mass density of the weight arm and hydraulic damper is 8000 kg/m^3.

The damper of the butterfly check valve consists of a cylinder with piston and bypass. The bypass consists of two flow loops. The first and second loop are used during the stage of passive and active damping, respectively. The throttle valve in the second loop controls the degree of damping. It is an active flow controller, designed to maintain a constant flow, independent of the pressure. This should result in a linear motion of the piston and a constant damping time. The damping time can be controlled by adjusting the amount of flow through the throttle valve. The response time of the throttle valve, as specified by the manufacturer, is of the order of milliseconds.

The principal parts of the damping devices of the 200 and 500 mm valves, such as the stroke of the piston over the first and second loop, and the diameter of the piston and cylinder, are geometrically similar (scale 1 : 2.5). The diameter of the bypass pipe is not scaled. The throttle valves of the 200 and 500 mm valves are different, although their principle of operation is similar.

The density of the damping fluid (oil) is $\rho_d = 860$ kg/m^3, and its kinematic viscosity $\nu_d = 34 \times 10^{-6}$ m^2/s at 20 °C.

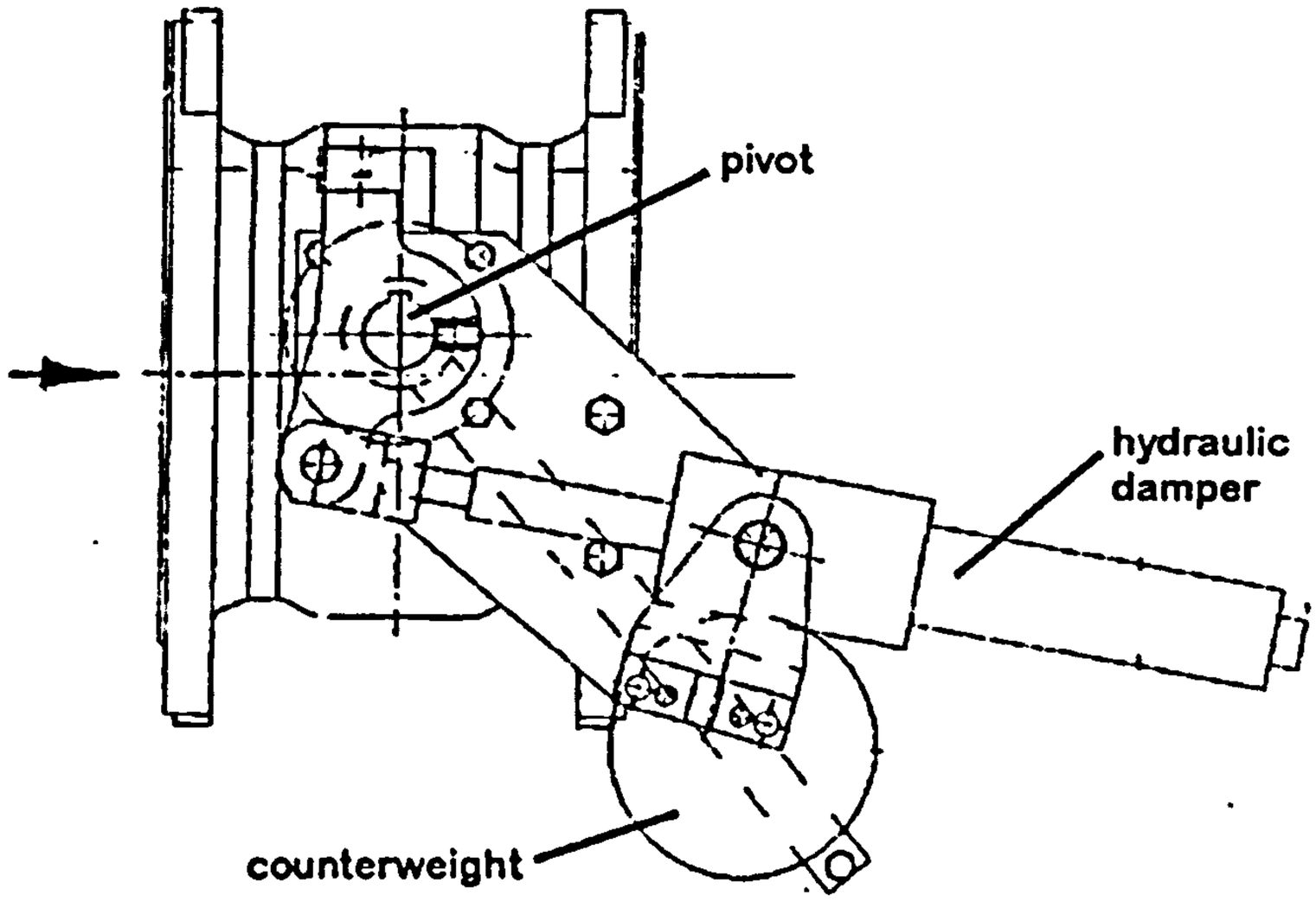

Figure 13.4 Butterfly check valve

13.4 Measuring procedures

In this section the measuring procedures are described, which are applied to obtain the pressures and flow at the check valve.

The upstream and downstream pressures cannot be measured at the check valve due to a pressure recovery effect and a non-uniform pressure distribution over the cross sections at the valve. The flow cannot be measured at the check valve due to the physical dimensions of a flowmeter and possible recirculation zones at the valve. For these reasons the pressures and flow(s) have to be measured at some distance of the check valve.

Transient flow conditions offer opportunities for alternative measuring procedures, which cannot be applied to steady flow conditions.

13.4.1 Standards

With respect to the testing of (check) valves under unsteady flow conditions no standards or instructions are available. For this reason the standards for the testing of control valves under steady flow conditions are used as a guideline.

In table 13.1 the upstream and downstream straight piping (l_1 and l_4) and the pressure tap locations (l_2 and l_3) are given, as prescribed by the British BSI and German VDI/VDE standards.

	l_1	l_2	l_3	l_4
BSI BS 5793 standard	20D	2D	6D	7D
VDI/VDE 2173 standard	20D	1D	10D	15D

Table 13.1 Standards for the testing of control valves

The length of the straight piping ensures more or less fully developed fluid velocity profiles at the pressure tap locations, which on their turn ensure a uniform pressure distribution over the cross section of the pipe. The downstream pressure tap is located at some distance from the valve, taking account of the pressure recovery effect. The location of the flowmeter is not prescribed in these standards.

	l_1	l_2	l_3	l_4
200 mm test section	56D	1D or 6D	1D or 6D	56D
500 mm test section	22D	1D or 6D	1D or 6D	22D

Table 13.2 Testing of check valves

In table 13.2 the upstream and downstream straight piping and pressure tap locations are given, which are applied here for the testing of check valves.

During a dynamic test the flow direction reverses from positive (normal flow) to negative (reverse flow), so that the pressure recovery effect may appear in both flow directions. For this reason the upstream and downstream requirements are also chosen identical with the check valve as point of symmetry.

The pressures are measured at several other locations along the test section too, as shown in figure 13.2. This offers opportunities to explore and compare measuring procedures. At the same time some redundancy is built in.

Under transient flow conditions the flow rate may differ along the pipe. In that case the location of the flowmeter becomes relevant. The flow is measured 6D downstream of the check valve; only one (fast-acting) flowmeter is available.

13.4.2 The pressures and flow close to the check valve

Taking into account fluid inertia, pipe friction and pressure recovery effects, several measuring procedures can be developed to obtain the pressures and flows close to the check valve (i.e. at a distance of 1D or 6D). The procedures are based on the equations for transient flow, but differ in number and location of the pressure and flow taps (figure 13.5).

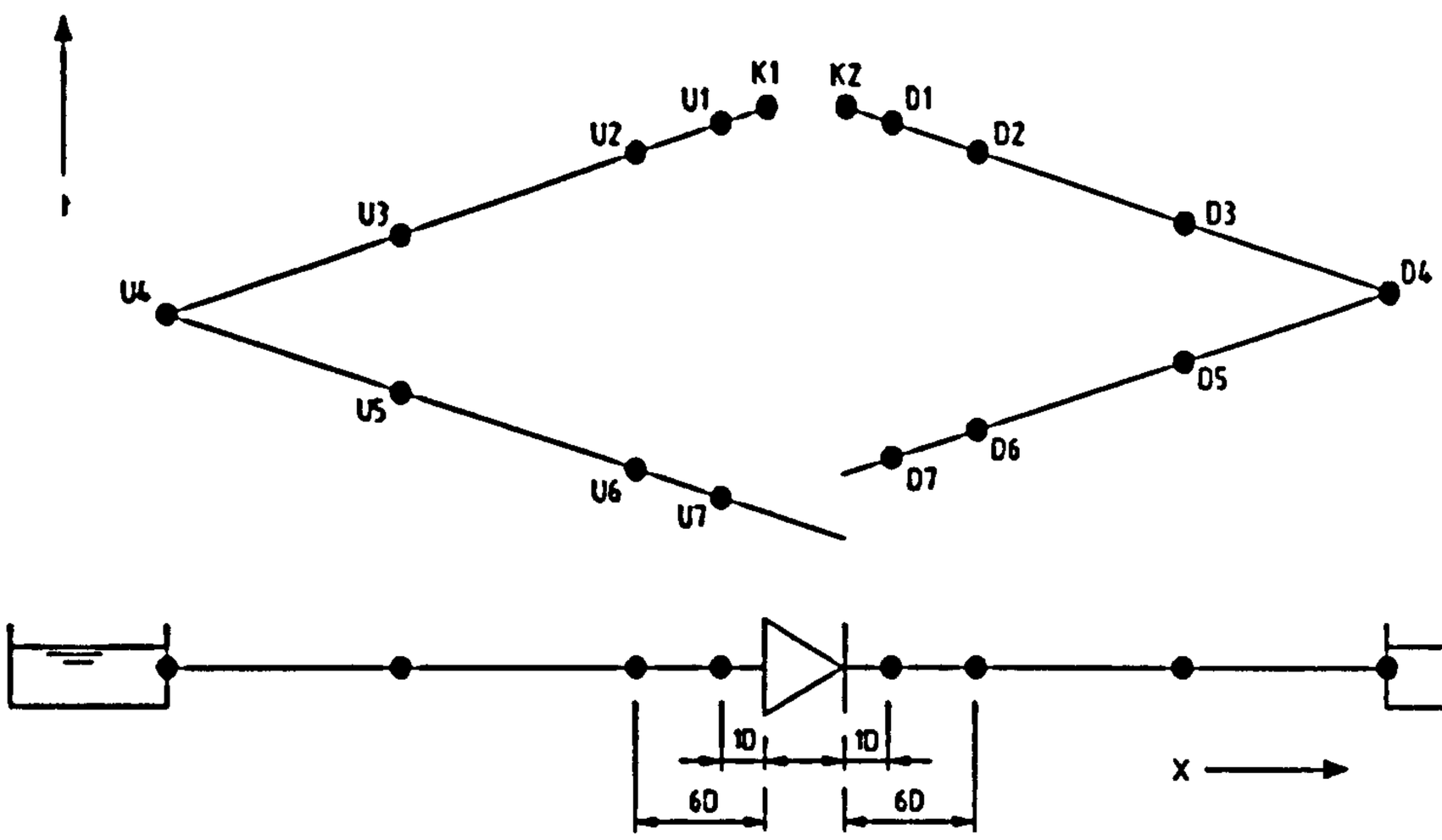

Figure 13.5 Pressure and flow measuring procedures

For details about these procedures reference is made to the CVRP report part II (Kruisbrink, 1993a). An alternative procedure for the flow measurement is described below.

About an alternative principle for flow measurement .....

The response of flowmeters, with a frequency range typically in the order of 10 to 10^2 Hz, is limited. In that sense pressure transducers, with a frequency range in the order of 10^4 Hz, have much better properties. For this reason it is interesting to investigate in how far unsteady flows can be measured from dynamic pressures only. This principle is studied here.

Consider the *x-t* diagram in figure 13.5. According to the compatibility equations (section 9.2) the relationship between pressure heads and fluid velocities along the pipe is given by:

$$\left(H + \frac{c_d}{g} v\right)_{D_6} = \left(H + \frac{c_d}{g} v\right)_{D_4} + f \frac{\Delta L_{D_4 D_6}}{D} \frac{v_{D_4}|v_{D_6}|}{2g} \tag{13.1}$$

$$\left(H - \frac{c_d}{g} v\right)_{D_2} = \left(H - \frac{c_d}{g} v\right)_{D_4} + f \frac{\Delta L_{D_2 D_4}}{D} \frac{v_{D_2}|v_{D_4}|}{2g} \tag{13.2}$$

Summation of these equations gives:

$$v_{D_2} = v_{D_6} + \frac{g}{c_d}\left(H_{D_2} - 2H_{D_4} + H_{D_6}\right) - f \frac{\Delta L_{D_2 D_4}}{D} \frac{v_{D_2}|v_{D_4}|}{2c_d} - f \frac{\Delta L_{D_4 D_6}}{D} \frac{v_{D_4}|v_{D_6}|}{2c_d} \tag{13.3}$$

In this equation the flow rate is related to the flow rate and pressure head at previous instants of time and other locations. The flow rate at the other location (D_4) may be derived from Equation (13.1).

Thus the fluid velocity may be fully derived from (measured) pressure heads, provided that the initial flow rate is known.

This alternative flow measurement has been evaluated by Mrs. L. Thorley as representative of the City University London. In first instance friction effects are assumed to be dominated by fluid inertia effects and ignored. In that case Equation (13.3) reduces to ($f = 0$):

$$v_{D_2} = v_{D_6} + \frac{g}{c_d}\left(H_{D_2} - 2H_{D_4} + H_{D_6}\right) \qquad (13.4)$$

Note that friction effects can only be dominated by fluid inertia effects under unsteady flow conditions. However, for reasons of consistency, frictions effects must also be ignored under steady flow conditions ($H_{D2} = H_{D4} = H_{D6}$), in order to prevent a drift of the steady fluid velocity.

The results of a dynamic test with the membrane check valve are used as test case. The calculated fluid velocity at location D_2, according to Equation (13.4), could thus be compared with the measured one. The calculated results show a drift of the fluid velocity, after the initial steady-state period (assuming that the flowmeter measures correctly). This drift or error accumulation is attributed to (in order of importance):

- *Friction*: The measured dynamic pressure heads are subject to friction.
- *Dynamic head*: The pressure transducer at location D_4 (in the high pressure tank) measures changes in total head, while the other transducers measure changes in static head in the pipe. The dynamic head, which has the same order of magnitude as the friction term, is usually ignored in waterhammer theory.
- *Single pressure taps*: Due to the unsteady character of the flow the pressure head may vary across the pipe cross section. However, for the plug type of flow this error is expected to be small.
- *Pressure wave speed*: The theoretical instants of time (t - L/c) do not coincide with the available instants of time (samples).

From these results it is concluded that the alternative procedure cannot be used in its present form. Friction effects must be taken into account. The friction terms in Equation (13.3) must be solved, or approximated by a friction term in which the fluid velocity at location D_4 is absent. If necessary, unsteady instead of steady pipe friction coefficients should be used.

Due to the inductive or repetitive character, the procedure is sensitive to error accumulation. Nevertheless, it is believed that the procedure offers opportunities for the flow measurement under transient conditions, at least for relatively short time scales. The frequency range of the pressure transducers is orders higher than that of flowmeters. However, the usefulness and accuracy of this alternative flow measurement needs further investigation. For further details about the evaluation it is referred to CVRP report part III: appendix D (Kruisbrink, 1993b).

The measuring procedure which is applied here is based on a direct measurement of the pressures and flow at a distance of 1D or 6D from the check valve.

13.4.3 The pressures and flow at the check valve

The measuring procedures in the previous section supply pressures and flows close to the check valve. In this section a procedure is described to convert these values to pressures and flows at the check valve (i.e the locations K_1 and K_2; figure 13.5). The virtual points K_1 and K_2 are located at the upstream and downstream, centre of the check valve, so that the virtual length of the check valve is reduced to zero. The procedure accounts for both fluid inertia and pipe friction effects.

Assume that the pressure head and the flow at the locations U_2 and D_2 are known. According to the compatibility equations the relationship between pressure heads and fluid velocities along the pipe is given by (figure 13.5):

$$\left[H + \frac{c_u}{g} v\right]_{K_1} = \left[H + \frac{c_u}{g} v\right]_{U_2} - f \frac{\Delta L_{K_1U_2}}{D} \frac{v_{K_1}|v_{U_2}|}{2g} \qquad (13.5)$$

$$\left[H - \frac{c_d}{g} v\right]_{K_2} = \left[H - \frac{c_d}{g} v\right]_{D_2} + f \frac{\Delta L_{K_2D_2}}{D} \frac{v_{K_2}|v_{D_2}|}{2g} \qquad (13.6)$$

It is assumed that at a certain instant of time $\partial Q/\partial x$ is zero along the fluid column between the points U_2 and D_2 (rigid column). The relation between the flow at the points K_1 and U_2, and the points K_2 and D_2 may be approximated by, respectively:

$$v_{K_1} = v_{U_2} + \frac{\Delta L_{K_1U_2}}{c_u} \frac{dv_{U_2}}{dt} \qquad (13.7)$$

and:

$$v_{K_2} = v_{D_2} + \frac{\Delta L_{K_2D_2}}{c_d} \frac{dv_{D_2}}{dt} \qquad (13.8)$$

Substitution of these respective equations in the above compatibility equations gives for the pressure heads at the check valve:

$$H_{K_1} = H_{U_2} - f \frac{\Delta L_{K_1U_2}}{D} \frac{v_{K_1}|v_{U_2}|}{2g} - \frac{\Delta L_{K_1U_2}}{g} \frac{dv_{U_2}}{dt} \qquad (13.9)$$

$$H_{K_2} = H_{D_2} + f \frac{\Delta L_{K_2D_2}}{D} \frac{v_{K_2}|v_{D_2}|}{2g} + \frac{\Delta L_{K_2D_2}}{g} \frac{dv_{D_2}}{dt} \qquad (13.10)$$

For the relation between the pressure heads at the points K_1 and U_1, and the points K_2 and D_1 similar expressions hold.

In a mathematical sense the Equations (13.7) and (13.8) may be replaced by:

$$Q_{K_1}(t) = Q_{U_1}(t) \approx Q_{D_2}(t) \qquad (13.11)$$

$$Q_{K_2}(t) = Q_{D_2}(t) \qquad (13.12)$$

In this formulation the velocity gradient is not present anymore, so that it is more stable in a numerical sense.

In this form the equations are used in the data processing.

About rigid column theory .....

The above procedure is based on the equations for transient flow in a pipe, whereby time and distance are coupled via the pressure wave speed. The rigid column theory (section 9.8) is applied by setting all time intervals between the pressure tap locations equal to zero. Comparing these results with results from the above procedure shows hardly any difference in the valve characteristics of approach 2. There is no significant wave activity between the measuring locations.

13.5 Measuring equipment

13.5.1 Flow

For the measurement of the flow rate, fast-acting electro-magnetic flowmeters (200 mm Foxboro and 500 mm Fischer & Porter) are used. The flow rate is measured at location D_2 (figure 13.2).

The flowmeters are calibrated under steady flow conditions (see section 14.3.1). A first attempt is made to calibrate the 200 mm flow meter under unsteady flow conditions (section 14.3.2).

About the choice of a flowmeter .....

Within flow measuring three principles may be distinguished: the point measurement (e.g. pitot tube, laser doppler anemometer), the line measurement (acoustic/ultrasone flowmeter) and the plane measurement (electro-magnetic flowmeter, turbine meter).

In principle the (integral) plane measurement is not sensitive to fluid velocity profiles. However, the flowmeters may be inaccurate if located in recirculation regions, characterized by simultaneous positive and negative fluid velocities at a cross section. The response of turbine flowmeters is affected by inertia effects, while pressure surges may cause physical damage.

Preference is given to the plane measurement, since the velocity profiles under transient flow conditions are unknown. Within the plane measurements, preference is given to the electro-magnetic flowmeter.

About the response of the flowmeters .....

The response of the flowmeters used here is mainly determined by two third order Bessel filters. The low band-pass filters are characterized by a linear phase characteristic (Johnson et al., 1982):

$$\phi(\omega) = -\tau_1 \omega \tag{13.13}$$

The time shift is given by:

$$T(\omega) = -\frac{\partial \phi(\omega)}{\partial \omega} = \tau_1 \tag{13.14}$$

where ϕ is the phase angle, $\omega = 2\pi f$ the circular frequency and τ_1 a time constant. Since the phase characteristic is linear the time shift is constant and independent of the frequency. Consequently, within the frequency range, the flow signal is measured undistorted but with a time delay.

The response of the flowmeters is improved at Delft Hydraulics by increasing the frequency of the voltage supply. The phase shift and amplitude characteristics of the filter combinations are measured at the Instrumentation Division of Delft Hydraulics. The time shift of the 200 and 500 mm flowmeters appears to be 4.3 and 14.2 ms, the frequency range (-3 dB point) is 100 and 30 Hz, respectively. For the time shift a correction is made (see also section 13.7.1).

The increase of the frequency range causes, however, a decrease of the stability. The flowmeters appear to be sensitive to mechanical shocks, causing a zero offset. For this offset a correction is made (see also section 13.7.1).

13.5.2 Pressures

The absolute pressure is measured with a pressure transducer (Statham, series 2000) with a pressure range of 0-10 bar and an accuracy better than $\pm$ 1% of the measured value. The absolute pressure is measured at location U_2 (see figure 13.2), only during the initial, steady flow conditions.

The pressure difference across the valve is measured with diffused silicon ΔP/I transducers (Honeywell, model 411) with an overall accuracy better than $\pm$ 0.5 % of the measured value. The pressure difference is measured between the pressure tap locations U_2 and D_2 (see figure 13.2), only during the initial, steady flow conditions.

The above pressure transducers are sensitive to mechanical shocks. For protectional reasons they are disconnected from the test rig after the initiation of a dynamic test. Due to the low-frequency range the transducers are unable to measure dynamic pressures.

The dynamic pressures are measured with piezo-electric pressure transducers (Kistler, type 410B), with a pressure range of 100 bar, frequency range of 40 kHz and an overall accuracy within ± 1%. The dynamic pressures are measured at the pressure tap locations U_1 to U_4, and D_1 to D_4 (see figure 13.2). The transducers registrate pressure changes (and no absolute pressures). To start with zero values they must be reset in advance of each dynamic test. For the remaining (small) zero offset a correction is made (see also section 13.7.1).

13.5.3 Other instruments

The valve disc position is measured by a potentiometer fixed to the hinge pin (not applicable to the membrane check valve).

The axial valve motion is measured by means of a displacement transducer (HBM type W20) with a displacement range of 20 mm, frequency range 0 - 1 kHz and an overall accuracy of ± 1% of the measured value ± 0.01 mm.

For the measurement of other signals like the sound pressure level (SPL) and anchoring forces it is referred to CVRP report part III: section 2.4 (Kruisbrink, 1993b).

13.6 Data acquisition

The measurement signals are recorded on two 8 channel data acquisition cards, with a storage capacity of 6000 samples (1000 pretrigger and 5000 posttrigger samples) and a sample frequency of 500 or 1000 Hz. The flow rate is used as trigger signal (trigger level: 85% of the initial flow rate). The experimental data are stored on two parallel 486 PC's, where also the graphical representation of the physical data is carried out.

13.7 Data processing

In this section the conversion from measured pressures to pressure heads and from flow rates to fluid velocities is described. The application of numerical filters is described. Further it is described how the valve characteristics are obtained from the (processed) measuring signals.

The data processing is executed on a HP 9000/8F30 computer (server) under the UNIX operating system. Hereto the voltage output of the instruments is converted to physical data, which are stored in data files (extension .PHD). The physical data are converted to pressure heads and fluid velocities and processed according to the measuring procedures in section 13.4. Herefore a FORTRAN computer code is written.

13.7.1 Pressure heads and fluid velocities

The absolute pressure is measured at location U_2 and during the steady flow period only (section 13.5.2). To obtain the values at the other locations pipe friction effects and the pressure difference Δp across the valve (measured between the locations U_2 and D_2; figure 13.2) are taken into account. As an example, this yields for the downstream location D_3:

$$p_{abs_{D_3}} = p_{abs_{U_2}} - \Delta p - f \frac{L_{D_2D_3}}{D} \frac{1}{2} \rho_f v^2 \qquad (13.15)$$

The piezo-electric pressures transducers, used for the measurement of the dynamic pressures, registrate pressure changes (and no absolute pressures) with initial values of about zero (see section 13.5.2). For the small zero offset, which is calculated as the average value over the first 500 pretrigger samples, a correction is made. The corrected dynamic pressures are added to the steady flow absolute pressures. The pressure heads are obtained from:

$$H = \frac{p_{abs} + p_{transducer}}{\rho_f g} \qquad (13.16)$$

The flowmeters reveal a significant zero offset after mechanical shocks induced by check valve closure (see section 13.5.1). For this reason, only the flow rate of the first dynamic test of a series is measured correctly up to the instant of valve closure. After this instant the flow rate may be shifted in magnitude. Consequently the flow rates of subsequent dynamic tests may be shifted too. For the zero offset a correction is made by assuming that the initial flow rate of a dynamic test is equal to the initial flow rate of the *first* dynamic test of that series (during a series of dynamic tests the controlled pump speed and disc position of the 600 mm control valve in the test section remain unchanged). The initial flow rate of a dynamic test is calculated as the average value over the first 500 pretrigger samples.

The fluid velocity at location D_2 is calculated from the measured flow rate, and based on the pipe diameter. Hereby a correction is made for the time shift of the flowmeter (section 13.5.1). The fluid velocities at the check valve are based on the inlet diameter of the check valve.

13.7.2 Numerical filters

dv/dt-filters The pressure heads at the check valve (locations K_1 and K_2) are calculated according to the Equations (13.9) and (13.10). The fluid velocity gradient in these equations is, in first instance, calculated from its definition:

$$\frac{dv(t)}{dt} = \frac{v(t+\Delta t) - v(t)}{\Delta t} \qquad (13.17)$$

As expected the velocity gradient reveals strong fluctuations, varying from positive to negative values and vice versa. To suppress these fluctuations a *dv/dt*-filter is introduced:

$$\frac{dv(t)}{dt} = \frac{v(t+n\Delta t) - v(t-n\Delta t)}{2n\Delta t} \qquad (13.18)$$

where n is denoted as the order of the filter.

Examples of unfiltered and filtered pressure head signals are given in figure 13.6. The pressure heads at the locations K_1 and K_2 are derived from and compared with the pressure heads measured at the locations U_2 and D_2, respectively.
The unfiltered signals show strong fluctuations with frequencies in the order of 100 Hz, which are considered to be physically unrealistic, since they cannot be found in the measured ones. The fluctuations in the calculated pressure heads vanish when *dv/dt*-filters are used. The differences between the filters are relatively small. The correlation between the measured and the filtered pressure head histories is good, when 8th- or 12th-order *dv/dt*-filters are used. For the data processing an 8th-order *dv/dt*-filter is used.

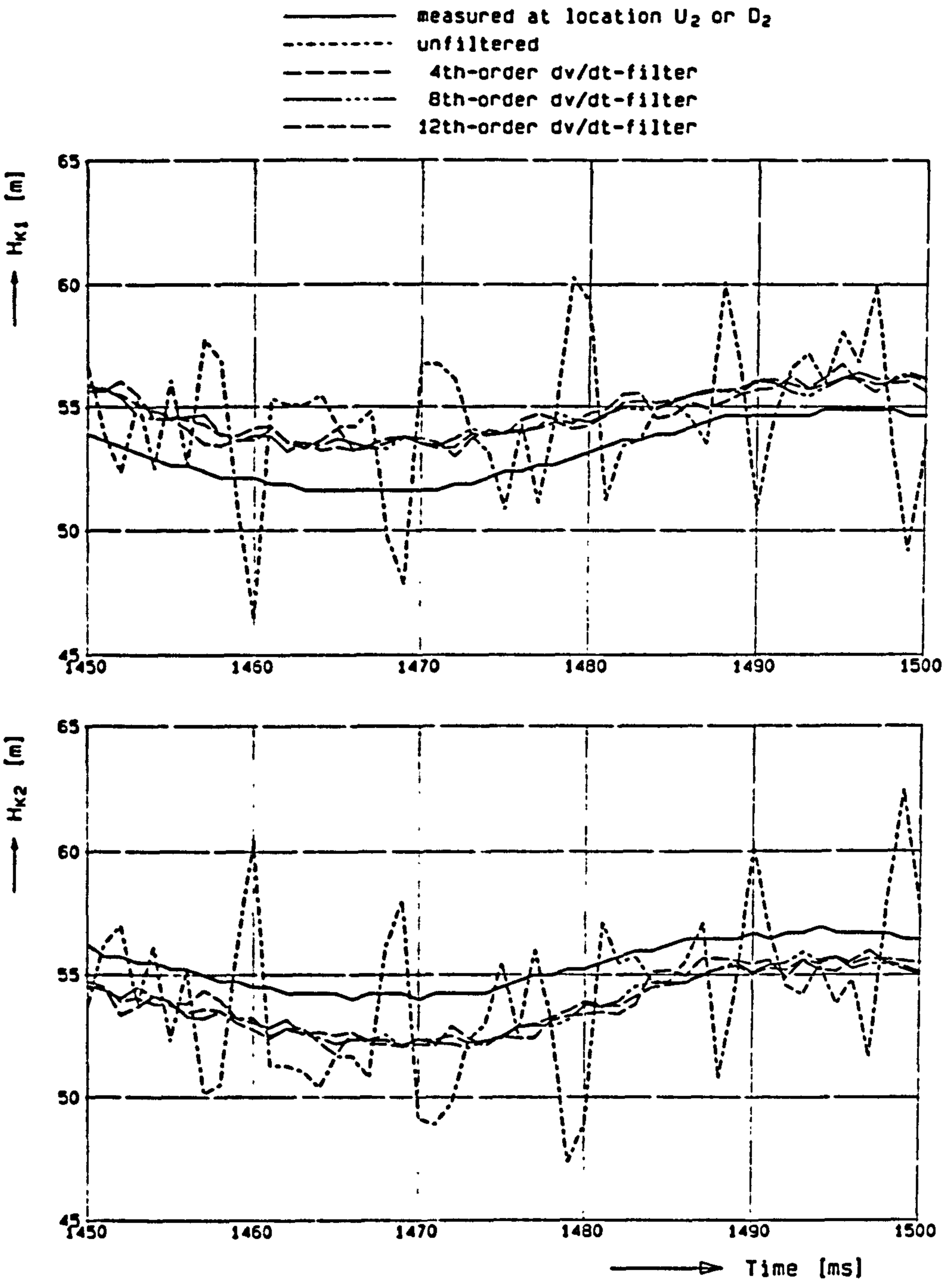

Figure 13.6 Unfiltered and filtered, calculated pressure heads at the valve

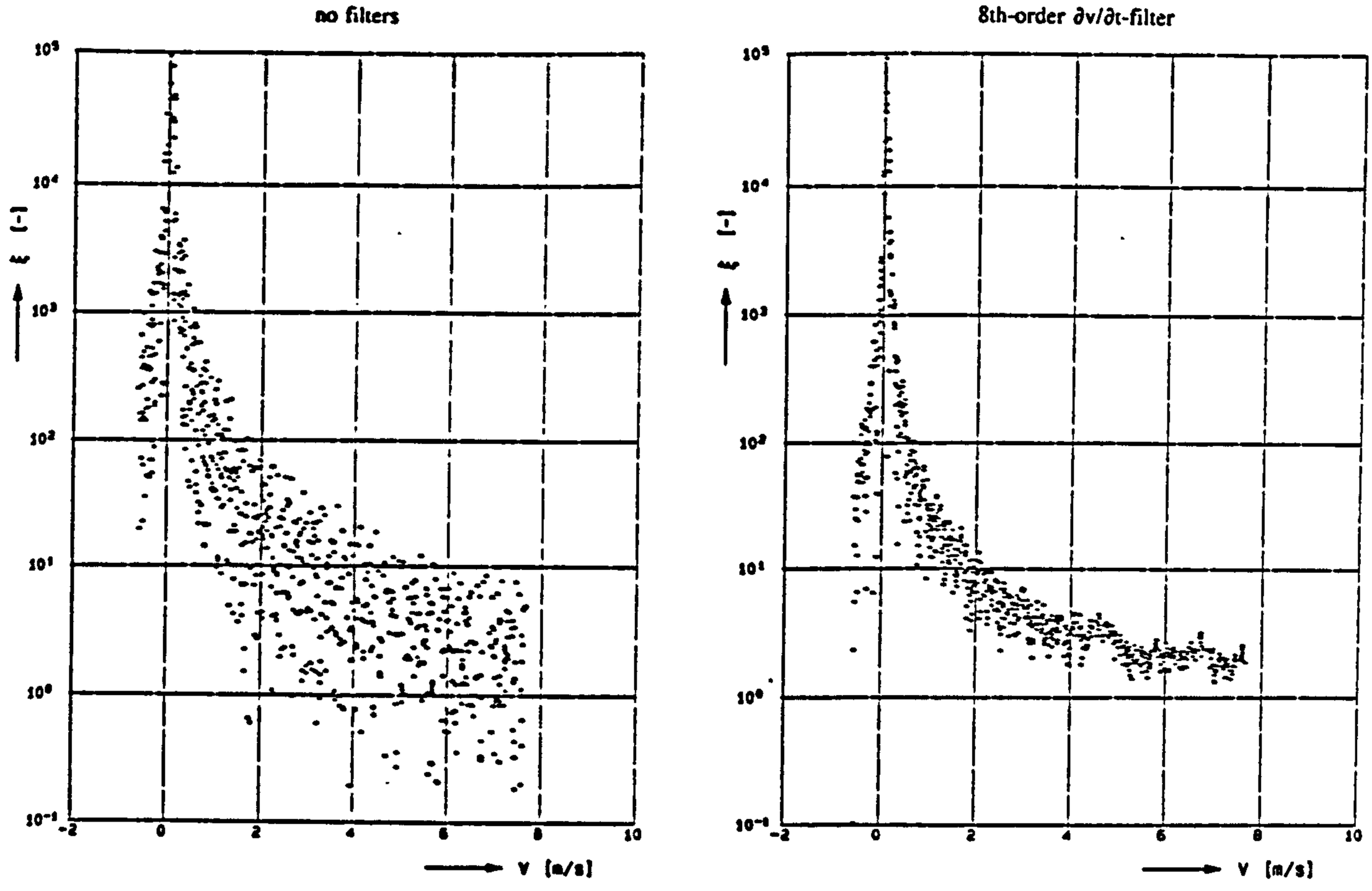

Figure 13.7 Unfiltered and filtered ξ-values

Shumann-filters are generally defined as:

$$x(t) = \frac{1}{4}x(t-1) + \frac{2}{4}x(t) + \frac{1}{4}x(t+1) \quad \text{(1st order)}$$

$$x(t) = \frac{1}{9}x(t-2) + \frac{2}{9}x(t-1) + \frac{3}{9}x(t) + \frac{2}{9}x(t+1) + \frac{1}{9}x(t+2) \quad \text{(2nd order)}$$

$$x(t) = \ldots\ldots\ldots + \frac{3}{16}x(t-1) + \frac{4}{16}x(t) + \frac{3}{16}x(t+1) + \ldots\ldots\ldots \quad \text{(3rd order)}$$

$$\ldots\ldots \qquad \textbf{(13.19)}$$

Shumann filters are applied to the fluid velocity, pressure head, and the processed ξ-values. The order of the v-filter and H-filter is chosen the same, since the pressure head and flow are coupled. This coupled filter is further denoted as v/H-filter.

Several combinations of second-, fourth- and eighth-order, v/H- and ξ-filters are explored. Comparing the results with "no filters" shows that the v/H-filter as well as the ξ-filter reduces the scatter in the ξ-values. Thus the pattern which is followed during valve closure becomes better visible (figure 13.7). The second- and fourth-order v/H-filters do not affect, while the ξ-filters do affect the peak values, in particular the extreme ξ-values at negative fluid velocities. There is hardly any difference between the second- and fourth-order v/H-filter. Based on these results it is decided to apply the second order v/H-filter in the data processing.

For details about the investigation into numerical filters it is referred to CVRP report part III: appendix E (Kruisbrink, 1993b).

About pressure recovery effects ...

In first instance the pressures close to the check valve are taken from the locations U_2 and D_2. Alternatively the pressures may be taken from the locations U_1 and D_1. At these locations pressure recovery effects may play a role.

The pressure recovery effect is the conversion of kinetic energy per unit volume $\frac{1}{2}\rho v^2$ into pressure, which takes place downstream of the vena contracta. In practice the pressure recovery is moved in a downstream direction due to flow separation.

In figure 13.7.b and c, dynamic valve loss coefficients are presented, which are derived from the locations at 6D and 1D from the check valve, respectively. The latter results show (apart from a reduction of scatter) that the ξ-values are generally lower and even in better agreement with the steady flow values (see figure 14.14). The pressure recovery effect tends to increase the ξ-values in the normal as well as in the reverse flow direction. For this reason it is concluded that the pressures at the locations U_1 and D_1 are not visibly influenced by pressure recovery effects.

It is believed that under unsteady flow conditions the pressure recovery effect becomes less dominant. The wake is per definition caused by flow separation and characterized by recirculation zones with capricious velocity profiles. As such it is the typical result of viscous effects. In an accelerating flow the development of the wake may be suppressed by inertia effects, which dominate the viscous effects and tend to flatten the velocity profiles.

Van de Sande et al. (1980) measure fluid velocity profiles in accelerating pipe flows from stationary flow conditions. The profiles are measured in time, using a Laser Doppler Anemometer. The results show, during both the laminar and turbulent development stages, much resemblance with a plug flow.

Apart from the above *spatial* pressure recovery another pressure recovery effect exists. This effect is revealed by the valve characteristics of approach 2. The experimental results in the next chapter (figures 14.14 to 14.17) show that, after the transition from normal to reverse flow, the initially positive pressure head difference across the valve is maintained for a while. This unsteady flow effect may be considered as a *time* pressure recovery, not to be confused with the above described *spatial* pressure recovery. However, the two are related, since during the time pressure recovery the transition of the spatial pressure recovery from the initial downstream side to the upstream side takes place. A typical example of the time pressure recovery is that the net pressure difference at zero flow has a positive value instead of zero.

13.7.3 Valve characteristics

The valve characteristics of approach 1 (section 11.5) are obtained from the pressures measured at 1D from the check valve (locations U_1 and D_1), and the flow rate measured at 6D from the valve (location D_2). The values are not converted to values at the valve. The error thus introduced is estimated by comparing the pressure head changes ΔH_{D1} and ΔH_{D2} at 1D and 6D from the valve. The differences between these pressure head changes are within 5%.

To obtain the valve characteristics of approach 1 several fluid velocities, pressure heads and instants of time need to be determined from the (processed) measurement signals (figure 8.2).

The critical velocity v_o is determined from steady flow tests as the fluid velocity at which the check valve is just fully open. If necessary a correction is made for hysteresis effects (section 8.5).

The instant t_o is determined from the fluid velocity signal as the instant at which the critical velocity v_o is reached.

The instant t_d (damping becomes active or effective) is determined from the pressure head signal as the instant at which the downstream pressure head, induced by valve closure, visibly starts rising. Note that this instant is not derived from the valve disc position at which the damping device is activated.

If the pressure head rise is taken from a measured pressure head (close to the check valve), the instant t_d is corrected to the value at the check valve (weakly damped check valve only).

The reverse flow velocity v_d is defined as the fluid velocity at the instant t_d. Up to this instant the initial flow deceleration and fluid velocity are about constant along the test section ($v_x = 0$, $v_{xt} = 0$; rigid column theory).

The instant t_c (valve is just closed) is determined from the valve disc position signal. Time shift effects of the valve disc position indicator are assumed to be neglectable.

If the valve disc position is not measured, this instant is taken from the fluid velocity as the instant at which the reverse flow becomes zero. Hereby it is assumed that the fluid velocity at the check valve and flowmeter are equal (rigid column theory). In that case a maximum error of $\Delta L/c \approx 1$ ms is made.

The pressure head changes ΔH_u and ΔH_d are defined as the difference between the first extreme value of the pressure head after the instant t_d and the pressure head at the instant t_d.

The valve characteristics of approach 2 (section 11.6) are obtained from the pressures measured at 1D or 6D from the check valve (locations U_1, D_1 or U_2, D_2), and the flow rate measured at 6D from the valve (location D_2). These values, measured close to the check valve, are converted to the values at the valve according to the procedures described in section 13.5.3. Thus the pressure head difference across the valve is a net value which is corrected for fluid inertia and pipe friction effects.

The fluid velocities at the check valve, such as v_o and v_d are based on the inlet diameter of the check valve.

13.8 Review and conclusions

The requirements for the measurement of the valve characteristics are defined. The test facility and test valves are described, which are used to measure the valve characteristics of approach 1 and 2, and other valve characteristics.

For the dynamic testing of (check) valves no standard procedures are available. Measuring procedures are described, which are used to measure the pressures and flow close to the check valve. Hereby the standards for the testing of control valves are used as guideline. The values close to the valve (i.e. at a distance of 1D or 6D) are converted to the pressures and flow at the check valve. This conversion is based

on the compatibility equations, accounts for pipe friction and fluid inertia effects and shows much resemblance with the rigid column theory.

For the dynamic testing of (check) valves no standard equipment is available. For this purpose special pressure transducers and flowmeters are used. The response of the flowmeters is characterized by a time shift and a zero offset (the latter due to mechanical shocks). For these effects corrections are made.

Fluctuations in the calculated fluid velocity gradient lead to physically unrealistic fluctuations in the calculated pressure heads at the check valve, and a scatter in the calculated dynamic valve loss coefficients. To suppress these fluctuations a numerical filter is applied. In addition Shumann-filters are applied to the fluid velocity, pressure head and the calculated ξ-values. The effects of these filters are explored. As a result an 8th-order dv/dt-filter in combination with second-order v/H-filters are used in the processing of the experimental data.

The pressures measured at a distance 1D from the check valve are not visibly influenced by "spatial" pressure recovery effects. For this reason the pressures at these locations may be used in the data processing. Applying these pressures instead of the pressures at a distance 6D from the check valve reduces the fluid inertia and friction correction terms, and even reduces the scatter in the dynamic valve loss coefficients.

The measuring procedures are applied to the experimental results, which are presented in the next chapter.

14 Experimental results

In this chapter the experimental results are described. Steady-state tests are performed to determine the pipe friction coefficients. Dynamic tests are performed to determine the pressure wave speeds in pipes, with and without flexible hoses. The flowmeters are calibrated under steady and unsteady flow conditions. Steady-state and dynamic tests are performed on weakly and strongly damped check valves. From the experiments the previously defined, valve characteristics are derived.

14.1 Pipe friction coefficient

The pipe friction coefficient of the test section is obtained from pressure loss measurements, which are performed under steady flow conditions without check valve. Hereto the effective pipe friction coefficient f_{eff} is introduced as:

$$\Delta p = f_{eff} \frac{L}{D} \frac{1}{2} \rho_f v^2 \tag{14.1}$$

The pressure loss across the test section is the result of pipe friction and losses across the flanges. Equation (14.1) may therefore be written as:

$$\Delta p = \left[f_{pipe} \frac{L}{D} + n \, \xi_{flange} \right] \frac{1}{2} \rho_f v^2 \tag{14.2}$$

Thus follows:

$$f_{eff} = f_{pipe} + \frac{D}{L} n \, \xi_{flange} \tag{14.3}$$

Two series of pressure loss measurements are performed with a different number of flanges, but at the same Reynolds numbers. Thus the pipe friction and flange loss coefficients can be derived from Equation (14.3). The results of the 200 mm test section are given in table 14.1 (columns 1 through 3).

Re [*10^5]	f_{pipe} [-]	ξ_{flange} [-]	f_{eff} [-]
2.957	0.0103	0.0943	0.0197
4.480	0.0083	0.1099	0.0192
6.834	0.0063	0.1297	0.0192
9.076	0.0056	0.1310	0.0186
11.463	0.0047	0.1418	0.0188

Table 14.1 Pipe friction and flange loss coefficients

The pipe friction coefficients in this table have unrealistic low values at higher Reynolds numbers; they are even smaller than those for hydraulically smooth pipes. This is attributed to the fact that the energy losses over the pipe and flanges are mixed. A flange may cause a local flow separation with a downstream recirculation zone. This zone shortens the effective pipe length along which pipe friction plays a role and should not be taken into account in the calculation of the pipe friction coefficient. Since the size of these recirculation zones is unknown, the pipe friction coefficient is calculated from the full pipe length, which leads to the low values presented above.

The effective pipe friction coefficient of the *entire* test section (L = 22.80 m, D = 0.206 m, n = 11 flanges) is calculated from Equation (14.3). Hereby it is assumed that the friction coefficient of the flowmeter and expansion joint are equal to the pipe friction coefficient. The results are given in table 14.1 (column 4). In good approximation the effective pipe friction coefficient is f_{eff} = 0.019. This constant value is used in the data processing.

14.2 Pressure wave speed

The pressure wave speed in circular pipes can be derived to be (e.g. Wylie and Streeter, 1993):

$$\frac{1}{c^2} = \rho_f \left[\frac{1}{K} + \frac{D}{E\,e}\, c_1 \right] \qquad (14.4)$$

where c_1 is a constant which accounts for the support conditions of the pipe:

$c_1 = 1 - \nu/2$ if the pipe is anchored at its upstream end only,

$c_1 = 1 - \nu^2$ if the pipe is anchored throughout against axial movement,
$c_1 = 1$ if the pipe is anchored with expansion joints throughout.

Remenieras (1952) developed the following expression for the pressure wave speed in a circular pipe with an air filled flexible hose in it:

$$\frac{1}{c^2} = \rho_f \left[\frac{1}{K} + \frac{A_p}{A_p - A_h} \frac{D}{E e} + \frac{A_h}{A_p - A_h} \frac{1}{p_{hose}} \right] \qquad (14.5)$$

where A_p and A_h are the cross sectional areas of the pipe and flexible hose, while p_{hose} is the initial pressure of the compressed air in the hose. The three terms in this equation describe the storage capacity of the pipe fluid, pipe wall and compressed air, respectively. The storage capacity of the wall of the flexible hose is neglected by assuming that the wall is thin and that the wall stresses are much smaller than the pressures. Note that the constant c_1 is assumed to be 1 here.

The *overall* pressure wave speed may be determined from the pipeline period. Hereto the propagation of a pressure wave through a pipeline system with constant head boundaries is considered. At a certain location the pressure-time history is a harmonic function with a period equal to the pipeline period or reflection time $2L/c$. The pressure wave speed may now be determined from:

$$\Delta T = n \frac{2L}{c} \qquad (14.6)$$

Where ΔT is the overall time, $2L/c$ is the reflection time or pipeline period and n is the number of periods.

About the *local* pressure wave speed .....

The pressure wave speed may be also determined from the time shift between two pressure signals, measured at different locations. This is only allowed under reflection free conditions and if friction effects may be neglected. In that case the pressure waves propagate without significant deformation, which may be written as (Appendix B.1.2):

$$H_{P_2}(t) = H_{P_1}(t - L/c) + \left(\frac{\partial H}{\partial x} \right)_{t=0} L \qquad (14.7)$$

where L is the distance between the pressure tap locations P_1 and P_2. The method gives information about the local pressure wave speed. For test results see CVRP report part III (Kruisbrink, 1993b).

14.2.1 Standard pipe

The pipe data of the 200 and 500 mm test section are given in table 14.2. The fluid is water with a density $\rho_f = 998.23$ kg/m^3 and a bulk modulus of elasticity $K = 2.19 \times 10^9$ ($T = 20$ °C).

material	D [m]	e [m]	E [N/m^2]	υ [-]
steel	0.206	0.0059	2.1×10^{11}	0.3
steel	0.489	0.0095	2.1×10^{11}	0.3

Table 14.2 Pipe data

The theoretical pressure wave speed, according to Equation (14.4), is given in table 14.3 for different support conditions. Since the exact support conditions are unknown, the theoretical pressure wave speed is taken as the average value, which results in $c = 1282$ m/s (200 mm test section) and 1212 m/s (500 mm test section).

support conditions	200 mm test section	500 mm test section
$c_1 = 0.85$	1294	1227
$c_1 = 0.91$	1284	1214
$c_1 = 1.00$	1268	1195

Table 14.3 Theoretical pressure wave speed

The pressure wave speed in the 200 mm test section is obtained from dynamic tests without check valve. Pressure surges are generated in the high pressure tank from initial, stagnant flow conditions. A typical example of such a test is given in figure 14.1 (for pressure tap locations see figure 13.2). The (overall) pressure wave speed is obtained from the periodical pressure signals, according to Equation (14.6), and varies between 1222 and 1285 m/s with an average value $c = 1241$ m/s. This value is about 3% lower than the theoretical value. It is further used in the data processing.

For the 500 mm test section the theoretical value $c = 1212$ m/s is used in the data processing, since no experimental data are available.

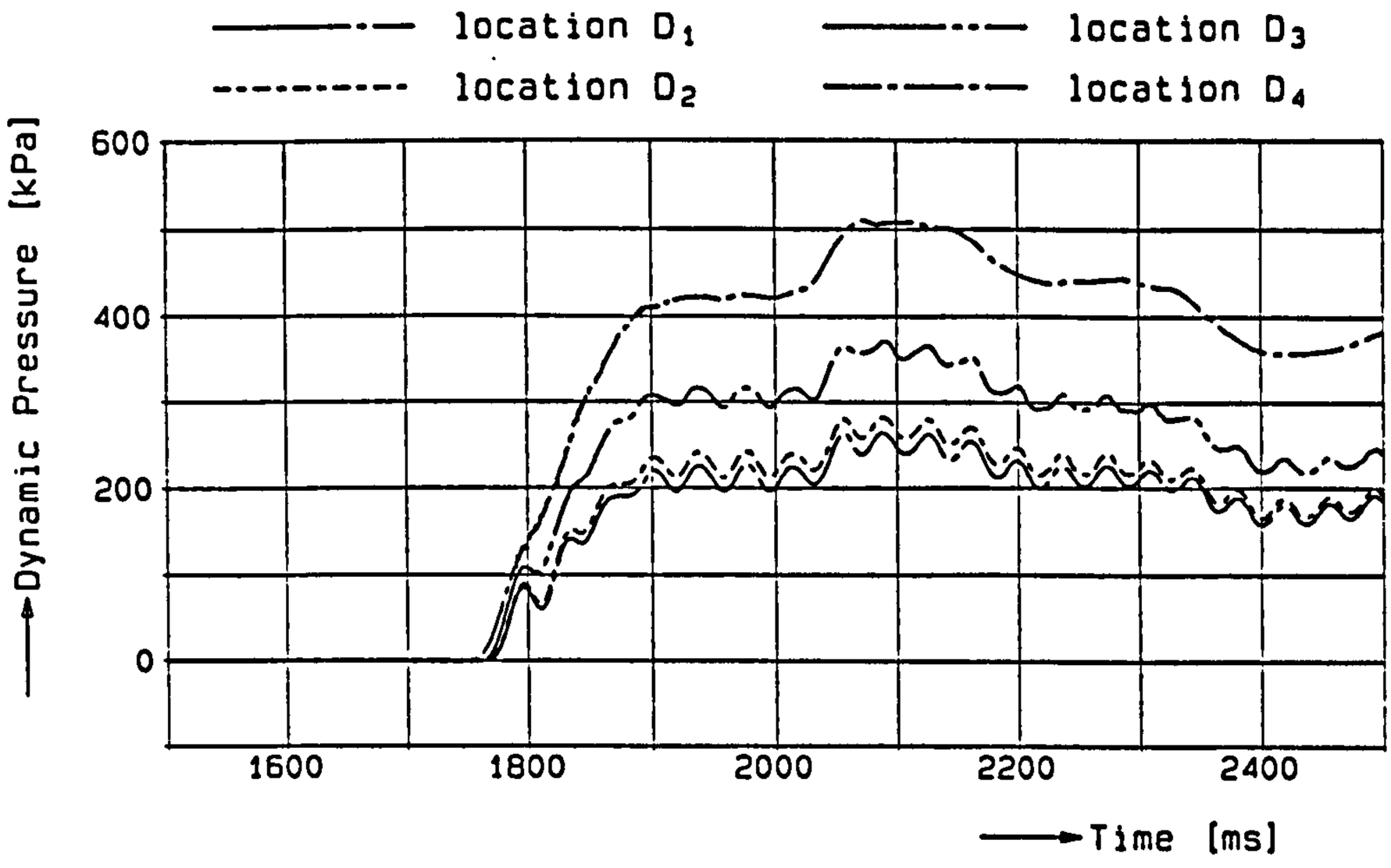

Figure 14.1 Measurement of pressure wave speed (200 mm test section)

14.2.2 Pipe with flexible hose

To reduce the pressure wave speed in steel pipes flexible hoses may be used. The effect of such a wave speed reduction is that liquid pulsations (pressure surges) and pipe vibrations are reduced. For this purpose also plastic pipes, non-circular pipes or gas dampers are applied. An additional effect of a wave speed reduction is that the reflection time of the pipe section is enlarged. In the latter sense the flexible hoses are applied here. The idea is to give the test section the properties of a longer section, without changing its physical dimensions. In this way a smaller and larger check valve can be tested, under such conditions that one of the dynamic scale laws, i.e. similarity of the dimensionless group $D/(2L/c)/v_o$, is satisfied. More about this in section 14.5.

To reduce the pressure wave speed in the steel pipes of the test section a flexible hose is used. The air filled, floating hose is mounted in the pipes along the entire test section (see figure 14.2). To enable the installation of a check valve in the test section the hose is divided into an upstream and a downstream piece. The two hose ends are connected to a small air vessel outside the test section, which is used to control the initial air pressure in the hose. The pressure wave speed is controlled by adjusting the initial air pressure.

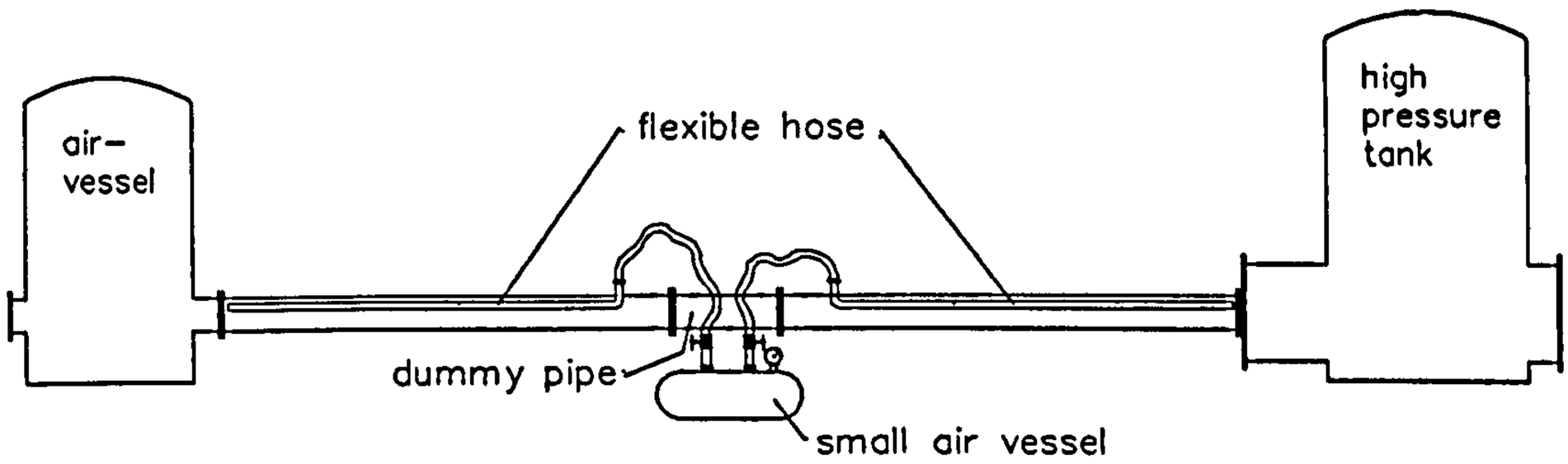

Figure 14.2 Test section with flexible hose

Two types of flexible hoses are used: Type I is a non-toxic, reinforced, PVC hose (Polyflex) with an operational pressure of 14 bar and a burst pressure of 30 bar, which has resistance against collapsing due to underpressures. Type II is an industrial rubber (water) hose (Inducord type 10) with an operational pressure of 10 bar, which has hardly any resistance against collapsing due to underpressures. The flexible hose data are given in table 14.4. The modulus of elasticity of these hoses is unknown.

material	D [m]	e [m]
flexible PVC	0.019	0.004
rubber	0.022	0.004

Table 14.4 Flexible hose data

The theoretical pressure wave speed, according to Equation (14.5), varies from c = 108 to 279 m/s (hose type I), and from c = 93 to 245 m/s (hose type II), for air pressures p_{hose} from 1 to 7 bar.

The pressure wave speed in the 200 mm test section is obtained from dynamic tests without check valve, from initial, stagnant flow conditions with a water pressure of 3.35 bar. During the test series the initial air pressure in the hose is varied from 1 to 7 bar. The amplitude of the pressure wave is varied by controlling the level of the downstream pressure rise (Δp = 2, 3 or 4 bar). Some tests are performed with the small air vessel disconnected, so that the air inside the hose cannot escape into this vessel. Remenieras (1952) uses hoses with compartments of 10 m long, separated by diaphragms, to suppress the transmission of pressure surges in the hose.

The (overall) pressure wave speed is obtained from periodical pressure head signals, measured at the locations U_1 and U_3, according to Equation (14.6). Hereby the following remarks are made: The periodical character of the pressure signal is

clearly visible, if the hose has already collapsed in advance of a test (at low initial air pressures). Damping effects are relatively small. The periodical character of the pressure signal is hardly or not visible, if the hose collapses during a test (at medium, initial air pressures). The collapsing of the hose is coupled with strong damping (storage) effects. The periodical character of the pressure signal improves with increasing air pressure, if the hose does not collapse at all (at higher initial air pressures). The amplitude of the signal increases. Damping effects are still strong, but become smaller.

The test results are presented in figure 14.3, where the pressure wave speed is represented against the initial air pressure in the hose.

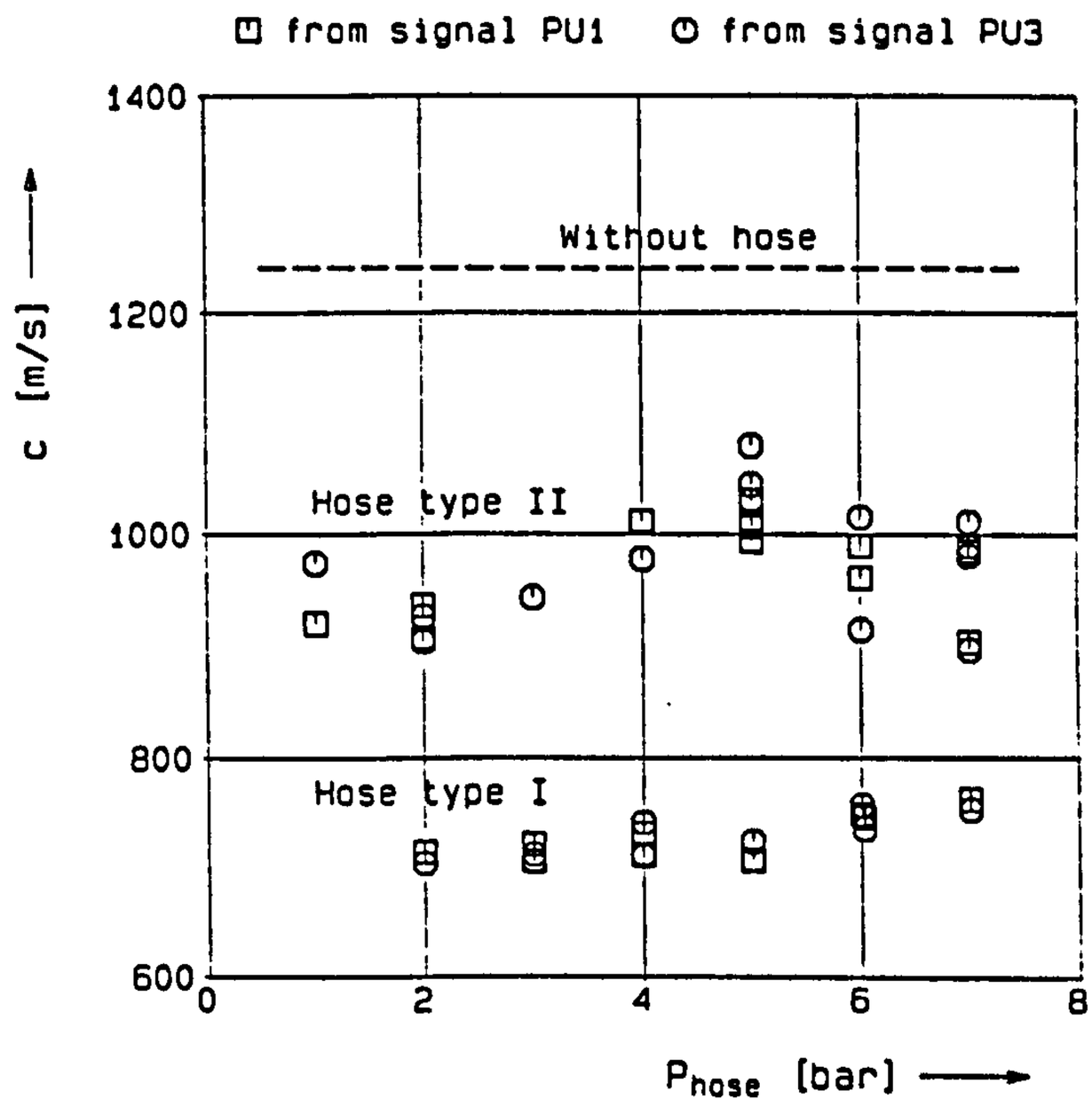

Figure 14.3 Measured pressure wave speeds (200 mm test section)

From these results the following conclusions may be drawn:

- The pressure wave speeds, as derived from the pressure head signals at location U_1 and U_3, show no remarkable differences (as expected).
- The amplitude of the pressure wave has no significant, direct influence on the pressure wave speed, but is indirectly found in the phenomenon of collapsing.
- The pressure wave speeds, measured with and without air vessel, are the same. Apparently, the influence of the (connected or disconnected) small air vessel on the storage capacity of the entire hose system is small.
- Hose type I shows a slight increase of the wave speed (from 700 to 760 m/s) with increasing air pressure. This may be attributed to an increasing rigidity of the hose, which is proportional to the air pressure in the hose. However, this effect was expected to be much larger.

- Hose type II behaves like the more rigid, since it gives higher pressure wave speeds. This was not expected since this non-reinforced hose is more sensitive to collapsing.
- The measured pressure wave speeds are much higher than the theoretical ones. Apparently, the influence of the rigidity of the hose, which is not taken into account in Remenieras' Equation (14.5), cannot be neglected.

The tendency of increasing pressure wave speed with increasing air pressure is not strong enough to control the pressure wave speed over a wider range. This is attributed to a relatively high wall thickness of the hose and a relatively small range of air pressures from 1 to 7 bar. The latter is confirmed by the results of Remieneras, who considers air pressures up to 100 bar.

It is recommended to use the flexible hose type I as pressure wave speed reducer. This hose gives a stronger reduction of the pressure wave speed, allows some degree of controlling the pressure wave speed, and is less sensitive to collapsing. The hose should be pressurized in such a way that it is either always collapsed or does not collapse at all. Under these conditions the pressure wave speed is the best defined.

14.3 Calibrations

The electro-magnetic flowmeters are calibrated under steady flow conditions. A first attempt has been made to perform a calibration under unsteady flow conditions.

14.3.1 Steady flow

The 200 mm and 500 mm electro-magnetic flowmeters are calibrated under steady flow conditions in the calibration rig for flowmeters at Delft Hydraulics. The calibration is based on the principle of weighing tanks. The flowmeters are calibrated in normal and reverse flow direction.

The flow range of the 200 mm flowmeter can be adjusted to 60, 150 or 300 l/s. The relative error is smaller than 2% of the measured value in the 20-100 % flow ranges. Within the 0-20 % ranges the relative error increases rapidly towards zero flow. The absolute error in the 0-100 % ranges is within 1 l/s, except for the flow range of 150 l/s, in which case an absolute error within 2 l/s is found.

The flow range of the 500 mm flowmeter is 2000 l/s. The relative error is smaller than 4% of the measured value in the 20-100 % flow ranges. Within the 0-20 % range the relative error increases rapidly towards zero flow. The absolute error in the 0-100 % range is within 12 l/s in the normal flow direction and within 60 l/s in the reverse flow direction.

14.3.2 Unsteady flow

The purpose of the unsteady flow calibration is to determine the reponse of the flowmeter to transient flow conditions. The calibration is based on the principle that changes in the fluid velocity and pressures are related to each other. The response of pressure transducers (frequency range in the order of 10 kHz) is much higher than the response of flowmeters (frequency range in the order of 10-100 Hz), so that the pressures can be used as reference.

The relationship between the fluid velocity and pressure head is described by the basic equations for transient flow (section 9.1). Assuming that storage effects are small (rigid column theory), the relationship is described by the pipe equation of motion (section 9.1.2):

$$gH_x + v_t + \frac{f\, v|v|}{2D} = 0 \qquad \textbf{(14.8)}$$

This equation may be applied to flow conditions, where v_t is approximately constant along the fluid column of consideration. In that case also H_x is about constant and can be calculated from the pressure head difference across the fluid column, after correction for pipe friction effects.

The experimental data which are used for the unsteady flow calibration are taken from the dynamic tests with the check valves, which are characterized by a more or less, constant initial flow deceleration. An example of such a calibration is presented in figure 14.4, where the fluid velocity at location D_2, the pressure heads at the locations D_2 and D_3, the calculated pressure and velocity gradients, and the difference between these gradients are plotted against time. The initial flow deceleration is about -15 m/s^2 here.

The fluid velocity gradient v_t is derived from the flow signal by using an 8th-order *dv/dt*-filter (section 13.7.2). The pressure head gradient H_x is calculated from the pressure head difference between the locations D_2 and D_3, after correction for pipe friction effects, and the distance between these locations (4.38 m $\approx$ 22*D*).

Comparing the fluid velocity and pressure head gradients show that the response of the flowmeter, measured in terms of $-1/g\ dv/dt$, is about equal to dH/dx and even tends to exceed it. The latter means that the flowmeter is able to measure the fluid velocity gradients considered.

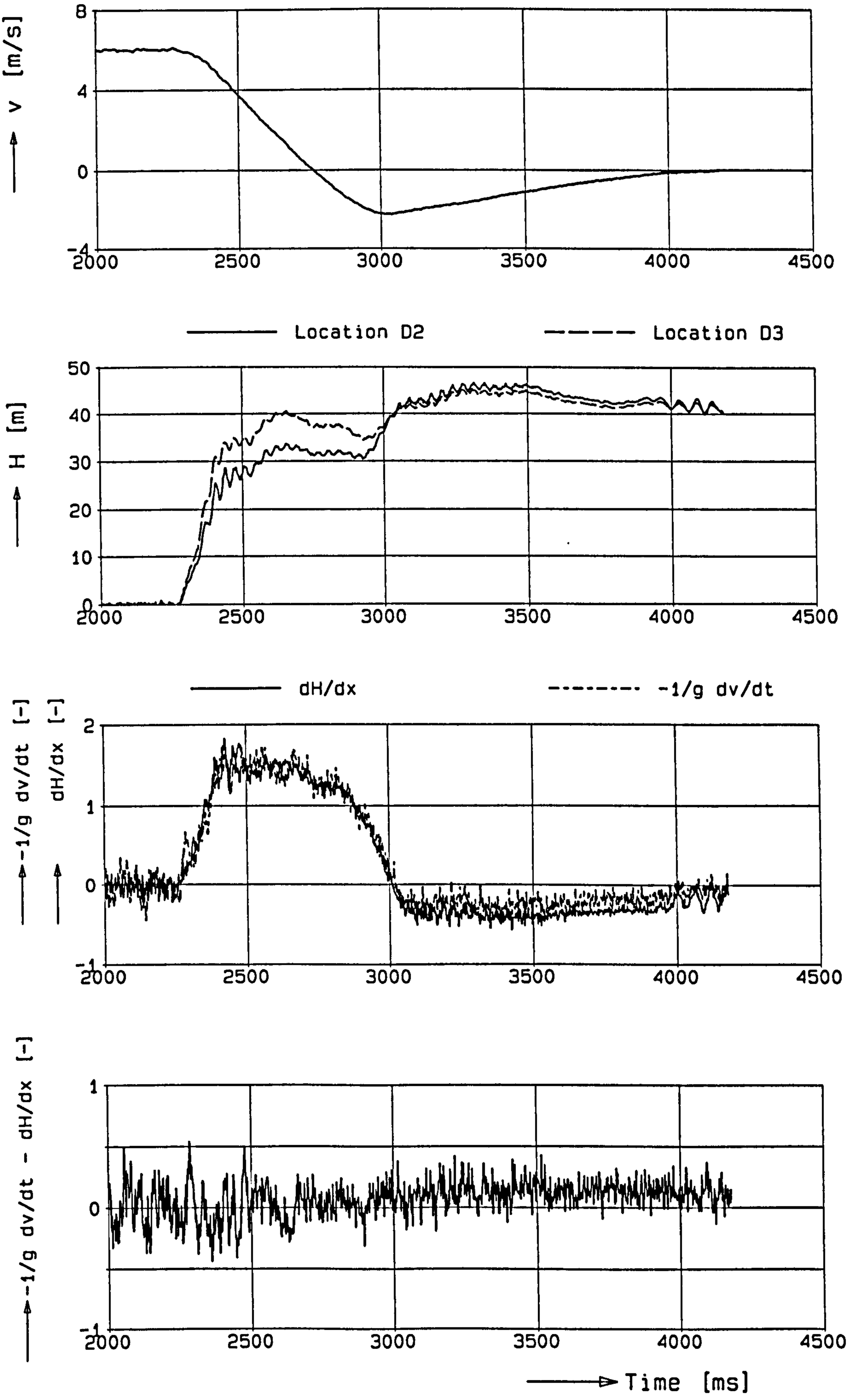

Figure 14.4 Unsteady flow calibration; 200 mm flowmeter

14.4 Steady-state characteristics

Membrane check valve The steady-state characteristics of the 200 mm valve are given in figure 14.5, where the pressure loss across the valve and the valve loss coefficient are plotted against the fluid velocity. The values are corrected for pipe friction effects. The graphs show data measured during a (stepwise) increasing and (stepwise) decreasing, steady flow.

From these results it is concluded that there is no hysteresis at all, so that the hysteresis factor $Y(\theta) = 0$. The critical velocity v_o is 7.60 m/s.

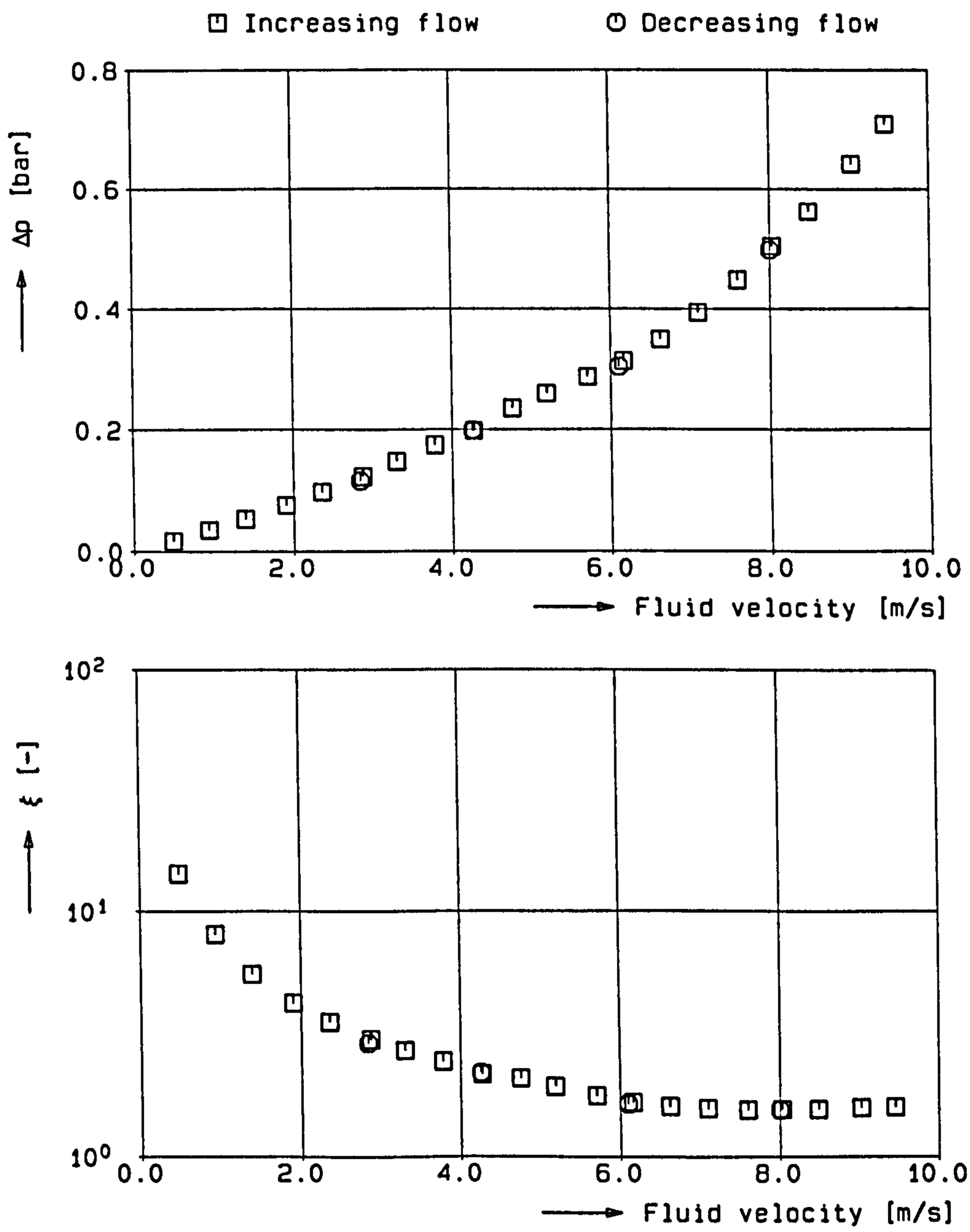

Figure 14.5 Steady-state characteristics; membrane valve

Butterfly check valve The steady-state characteristics of the 200 mm valve (counterweight 9.6 kg) are presented in figure 14.6.

The differences between the characteristics, as measured during increasing and decreasing flow, are attributed to hysteresis effects, mainly caused by strong friction effects in the hydraulic damper. From these results it is concluded that the critical velocity in an increasing flow $v_o\uparrow = 5.21$ and in a decreasing flow $v_o\downarrow = 2.97$ m/s. The average critical velocity, calculated from Equation (8.32), is $v_o = 4.24$ m/s. Hereby the critical flow is assumed to be turbulent ($k = 0$).

In figure 14.7 the hysteresis factor $Y(\theta)$, as derived from the steady flow characteristics according to Equation (8.29), is presented as function of the valve disc position. The factor decreases with increasing valve disc position. Apparently, the importance of hysteresis decreases, relative to the net effect of gravitation and buoyancy (or: hydrodynamic effects). The results of the 500 mm valve illustrate that the hysteresis decreases with increasing valve size.

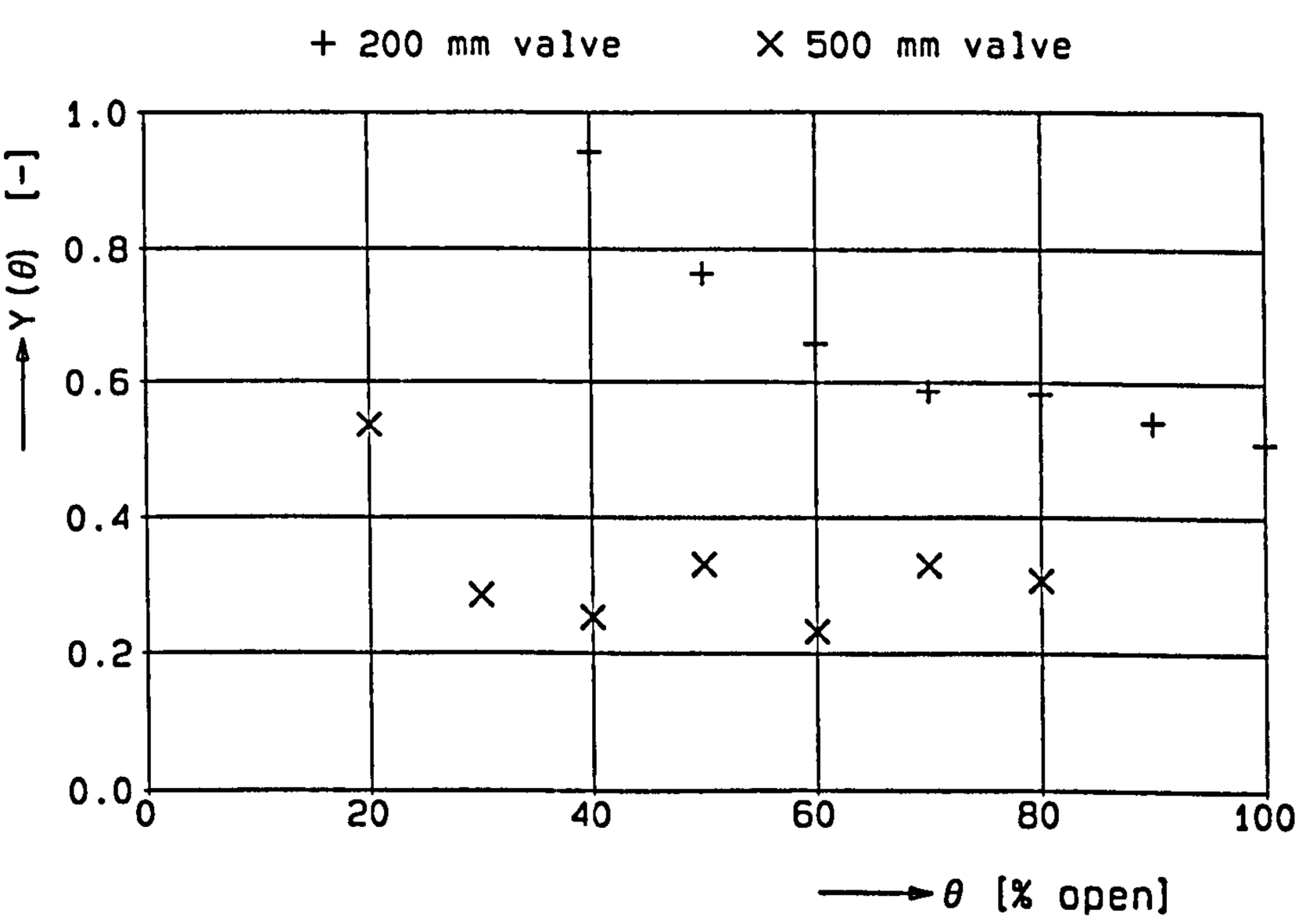

Figure 14.7 Hysteresis factor; butterfly valve

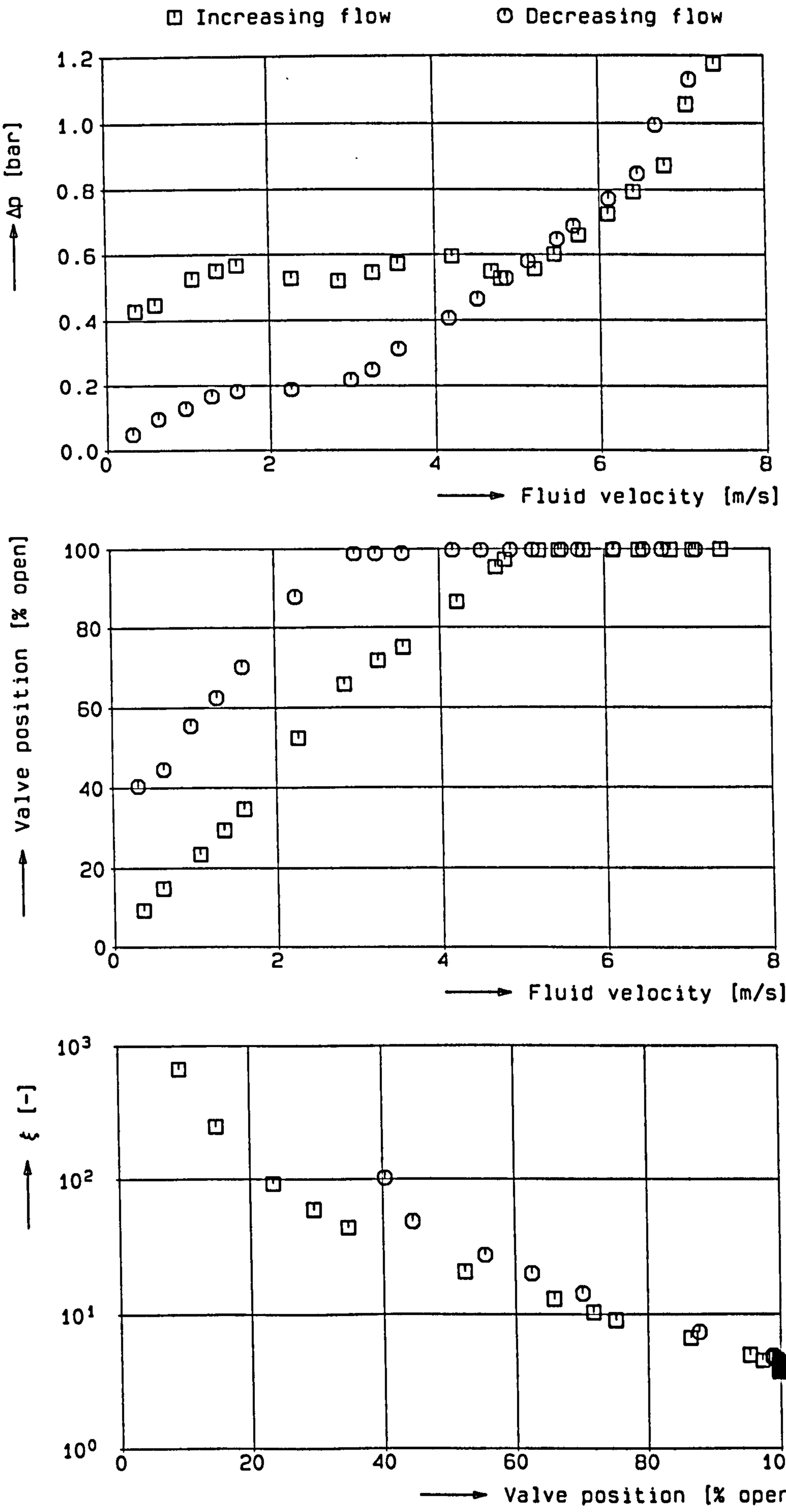

Figure 14.6 Steady-state characteristics; 200 mm butterfly valve

14.5 Dynamic tests

Membrane check valve The dynamic tests with the membrane check valve are performed under the conditions listed in table 14.5. During the test series 1 and 2 the 200 mm valve (D = 0.201 m) is installed in the middle of the test section, so that $(2L_u/c_u)/(2L_d/c_d) = 1$ and upstream in the test section, where $(2L_u/c_u)/(2L_d/c_d) = 1/3$.

In principle the initial fluid velocity is chosen about 15% above the critical velocity, to ensure that initiation effects are more or less damped out before the check valve starts closing. However, at this fluid velocity cavitation was observed in the check valve. Therefore the initial fluid velocity is chosen about 4% higher than the critical velocity, so that the valve is still initially fully opened $((\theta_i-\theta_c)/(\theta_o-\theta_c) = 1)$.

A typical recording of a dynamic test is presented in figure 14.8, where the flow rate at location D_2, the pressures at the locations D_4, D_2, U_2 and U_4, and the axial displacement of the valve are plotted against time (see figure 13.2 for the pressure tap locations).

The results show that the initial flow deceleration is approximately constant. The maximum reverse flow velocity is quickly reduced to zero (valve closed), so that the stage of active damping is short. The damping effect of the membrane is relatively low.

After closure the upstream and downstream pressure heads become in phase. From this phenomenon it is concluded that the valve reopens.

Butterfly check valve The dynamic tests with the butterfly valve are performed under the conditions listed in table 14.6. The test series 1 and 2 are performed on the 200 mm valve (D = 0.198 m) with a counterweight of 9.6 kg (v_o = 4.24 m/s) and a counterweight of 5.0 kg (v_o = 3.18 m/s). The series 3 and 4 are performed on the 500 mm valve (D = 0.500 m) with strong damping (75%) and medium damping (50%), in both cases with a counterweight of 47.8 kg.

During the test series 1 and 2 the initial fluid velocity is chosen about 15% above the critical velocity $v_o\uparrow$ = 5.21 m/s (counterweight 9.6 kg). Consequently the valve is initially fully opened, so that $(\theta_i-\theta_c)/(\theta_o-\theta_c) = 1$.

During the test series 3 and 4 the initial fluid velocity is chosen about 22% lower than the estimated critical velocity (v_o = 4.77 m/s), to ensure that the tests are cavitation free and that air entrainment from the upstream air vessel into the test section is avoided. The capacity of the test rig is not sufficient to open the 500 mm valve fully, so that $(\theta_i-\theta_c)/(\theta_o-\theta_c) = 0.83$. The critical velocity of the 500 mm valve is an estimated value, which is obtained by means of scaling from the steady-state characteristics of the 200 mm valve.

During all the test series the check valve was installed in the middle of the test section, so that $(2L_u/c_u)/(2L_d/c_d) \approx 1$.

The Reynolds numbers Re_o and Re_d show that the (initial) flow in the valve is turbulent while the flow in the hydraulic damper is laminar.

About the Reynolds number in the hydraulic damper .....

The Reynolds number Re_d of the flow in the damper is based on the diameter of the bypass pipe, the average fluid velocity in the bypass pipe during the stage of active damping, and the kinematic viscosity of the damping fluid.

The average fluid velocity in the bypass pipe is calculated from the displaced piston volume, divided by the damping time. Here the damping time is about constant within a test series.

About scale laws .....

In first instance it was tried to satisfy the scale laws, so that all relevant valve and system parameters are similar for the two test series with the 200 and 500 mm valve. For this purpose the pressure wave speeds of steel pipes with flexible hoses is measured (section 14.2.2).

Consider the parameter group $D/(2L_u/c_u)/v_o$. The valve diameter (200 mm valve) is increased by a factor 2.5 (500 mm valve). Geometric scaling of the 5.0 kg counterweight (200 mm valve) gives a value of $5.0 \times 2.5^3 = 78.1$ kg (500 mm valve). For this a 83.5 kg counterweight was available. Scaling of the critical velocity $v_o = 3.18$ m/s (200 mm valve) gives $v_o = 3.18 \times \sqrt{2.5} = 5.03$ m/s (500 mm valve). Consequently, also the reflection time should be enlarged by a factor $\sqrt{2.5}$. This can be achieved by reducing the pressure wave speed from 1241 m/s (200 mm standard piping) to $1241 / \sqrt{2.5} = 784$ m/s (500 mm piping). This is a typical value, which is obtained with flexible hose type I in the 200 mm piping (section 14.2.2).

If the reflection time is increased by a factor $\sqrt{2.5}$, then also the damping time should be enlarged by a factor $\sqrt{2.5}$. Scaling of the damping time of about 1.2 sec (96% damping; 200 mm valve) gives a damping time $1.2 \times \sqrt{2.5}$ sec $= 1.9$ sec (96% damping; 500 mm valve). Note that in principle the degree of damping does not need to be altered for this purpose.

However, the above scale laws could not be satisfied for two reasons. Scaling the counterweight would lead to a further reduction of the initial valve disc position. The flow capacity of the test rig is not sufficient to open the valve fully. Scaling the damping time could not be realized. The capacity of the high pressure tank is not sufficient to deliver a reverse flow until valve closure, if the damping time exceeds about 1.7 sec (strong damping).

A typical recording of a dynamic test is presented in figure 14.9. The maximum reverse flow velocity is gradually reduced to zero (valve closed), so that the stage of active damping is long here. The damping effect of the hydraulic damper is relatively high. The disc position signal shows that the valve closes linearly in time during the stage of active damping. In that respect the hydraulic damper operates as expected.

parameters	series 1	series 2
D [m]	0.201	0.201
v_o [m/s]	7.60	7.60
ρ_m/ρ_f	***	***
ξ_o	1.55	1.55
$T_{So}/(\rho_f v_o^2 D^3)$	***	***
T_{So}/T_{Sc}	***	***
damping	***	***
γ	0	0
$(\theta_i-\theta_c)/(\theta_o-\theta_c)$	1.00	1.00
$(2L_u/c_u)/(2L_d/c_d)$	1	1/3
$(A_u/c_u)/(A_d/c_d)$	1	1
$D/(2L_u/c_u)/v_o$	1.44	2.88
v_o/c_u	0.0612	0.0612
v_o/c_d	0.0612	0.0612
ρ_d/ρ_f	***	***
Re_o	$1.53\ 10^6$	$1.53\ 10^6$
μ_d/μ_f	***	***
Re_d	***	***

Table 14.5 Valve and system parameters; membrane check valve

parameters	series 1	series 2	series 3	series 4
D [m]	0.198	0.198	0.500	0.500
v_o [m/s]	4.24	3.18	4.77	4.77
ρ_m/ρ_f	7.35	7.35	7.35	7.35
ξ_o	4.10	4.10	3.90	3.90
$T_{So}/(\rho_f v_o^2 D^3)$	***	***	***	***
T_{So}/T_{Sc}	***	***	***	***
damping	96%	96%	75%	50%
γ	0	0	0	0
$(\theta_i-\theta_c)/(\theta_o-\theta_c)$	1.00	1.00	0.83	0.83
$(2L_u/c_u)/(2L_d/c_d)$	1.00	1.00	1.07	1.07
$(A_u/c_u)/(A_d/c_d)$	1.00	1.00	1.00	1.00
$D/(2L_u/c_u)/v_o$	2.54	3.39	5.40	5.40
v_o/c_u	0.0034	0.0026	0.0039	0.0039
v_o/c_d	0.0034	0.0026	0.0039	0.0039
ρ_d/ρ_f	0.86	0.86	0.86	0.86
Re_o	$8.38\ 10^5$	$6.29\ 10^5$	$2.38\ 10^6$	$2.38\ 10^6$
μ_d/μ_f	29.24	29.24	29.24	29.24
Re_d	37	42	287	441

Table 14.6 Valve and system parameters; butterfly check valve

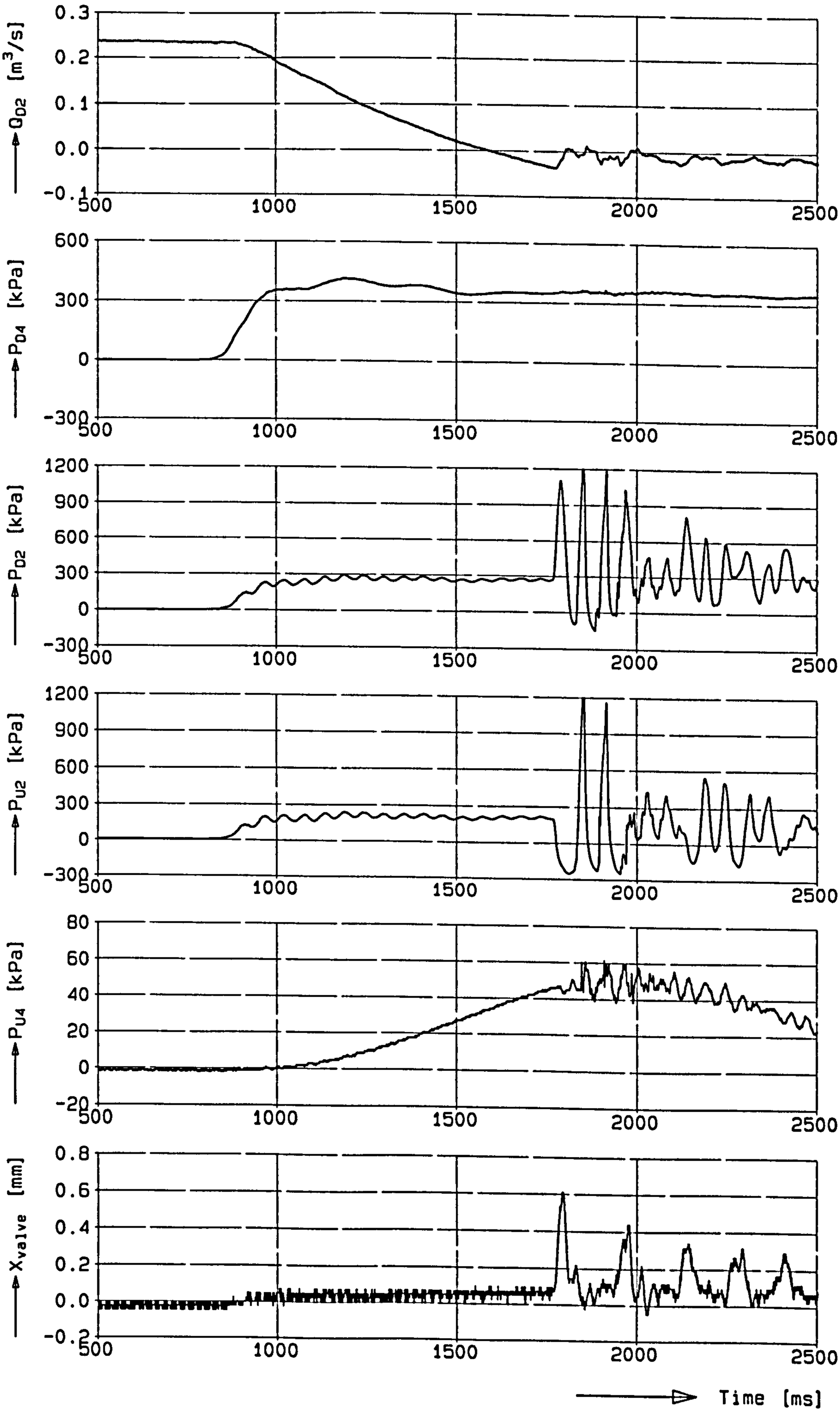

Figure 14.8 Recording of dynamic test; membrane valve

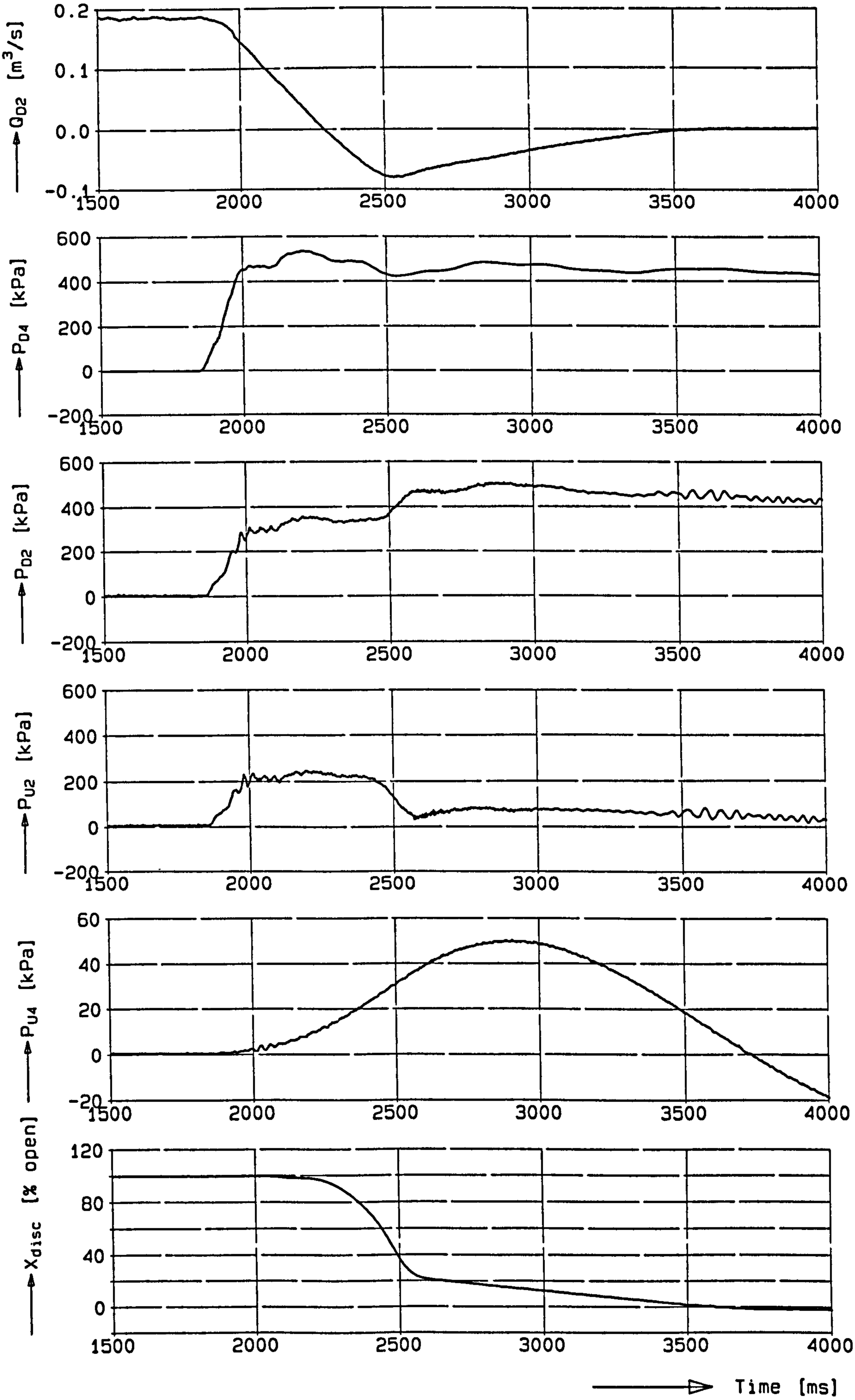

Figure 14.9 Recording of dynamic test; 200 mm butterfly check valve

14.6 Valve characteristics approach 1

The valve characteristics of approach 1 are defined in section 11.5.

Membrane check valve The results of the two series of dynamic tests with the 200 mm membrane check valve are presented in figure 14.10, in which the fluid velocity characteristics for the first and second event and the pressure head characteristics for the second event are given.

The fluid velocity characteristics for the first event are similar for the two test series, and independent of the location of the valve in the test section, as expected.

The downstream pressure head changes of series 2 exceed those of series 1. This is expected since the the influence of the downstream boundary is smaller, if the valve is located upstream in the test section. For opposite reasons the (absolute values of the) upstream pressure head changes of series 2 are smaller. Although the pressure head changes ΔH_d and ΔH_u differ for the two test series, the difference (ΔH_d - ΔH_u) is about the same at corresponding initial flow decelerations!

Note that not all tests are cavitation free. Cavitation is observed during test series 1 only, when the initial flow deceleration exceeds about 10 m/s^2 (dv/dt < -10 m/s^2).

The magnitude of the pressure head changes at the upstream and downstream side differ significantly. This is not expected, since the pressure head changes in theory are reversely symmetrical, if the check valve is located in the middle of the test section. The differences are not attributed to: 1) *cavitation*, since they are also found for cavitation free tests, 2) *pressure recovery effects*, since they are also observed at other pressure tap locations, 3) the fact that the *constant head boundaries* are not ideal, since the time scale of the head changes at the boundaries (order 1 sec) is much larger than that of the head changes induced by the check valve (order 0.01 sec), while the magnitude of the head changes is much smaller (figure 14.8). Finally, the phenomenon is attributed to the *check valve* itself. Apparently, The effects of the damping or storage capacity of the flexible membrane differ at the upstream and downstream side. This is attributed to the presence of the valve seat (figure 13.3).

In figure 14.11 the valve characteristics are presented in a dimensionless form. The fluid velocity characteristic for the second event shows dimensionless reverse flow decelerations between -1.0 and -0.1, which means that the damping time is of the same order as the reflection time and that the valve may be categorized as a weakly damped check valve (section 11.5.2).

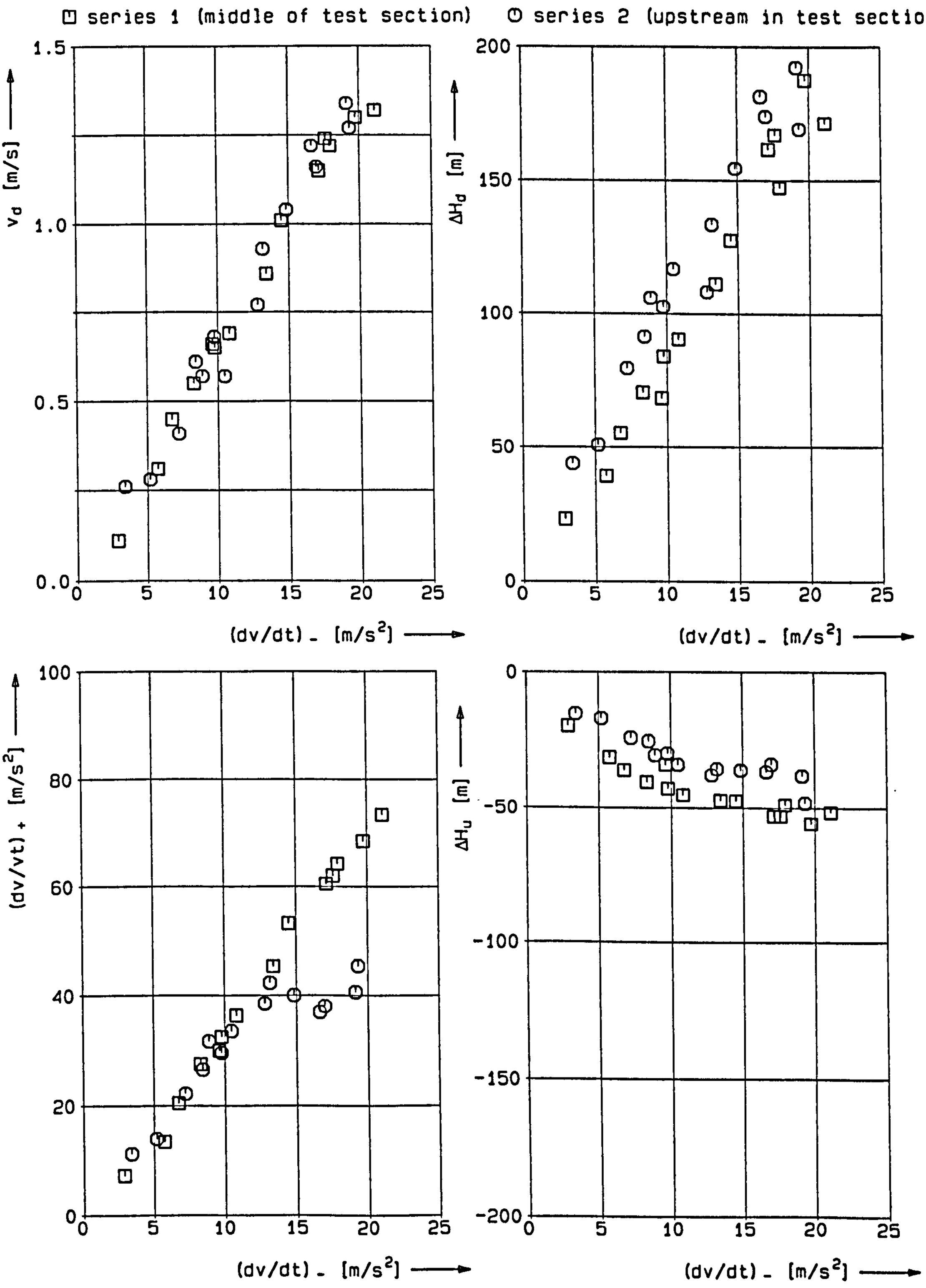

Figure 14.10 Valve characteristics approach 1; membrane check valve

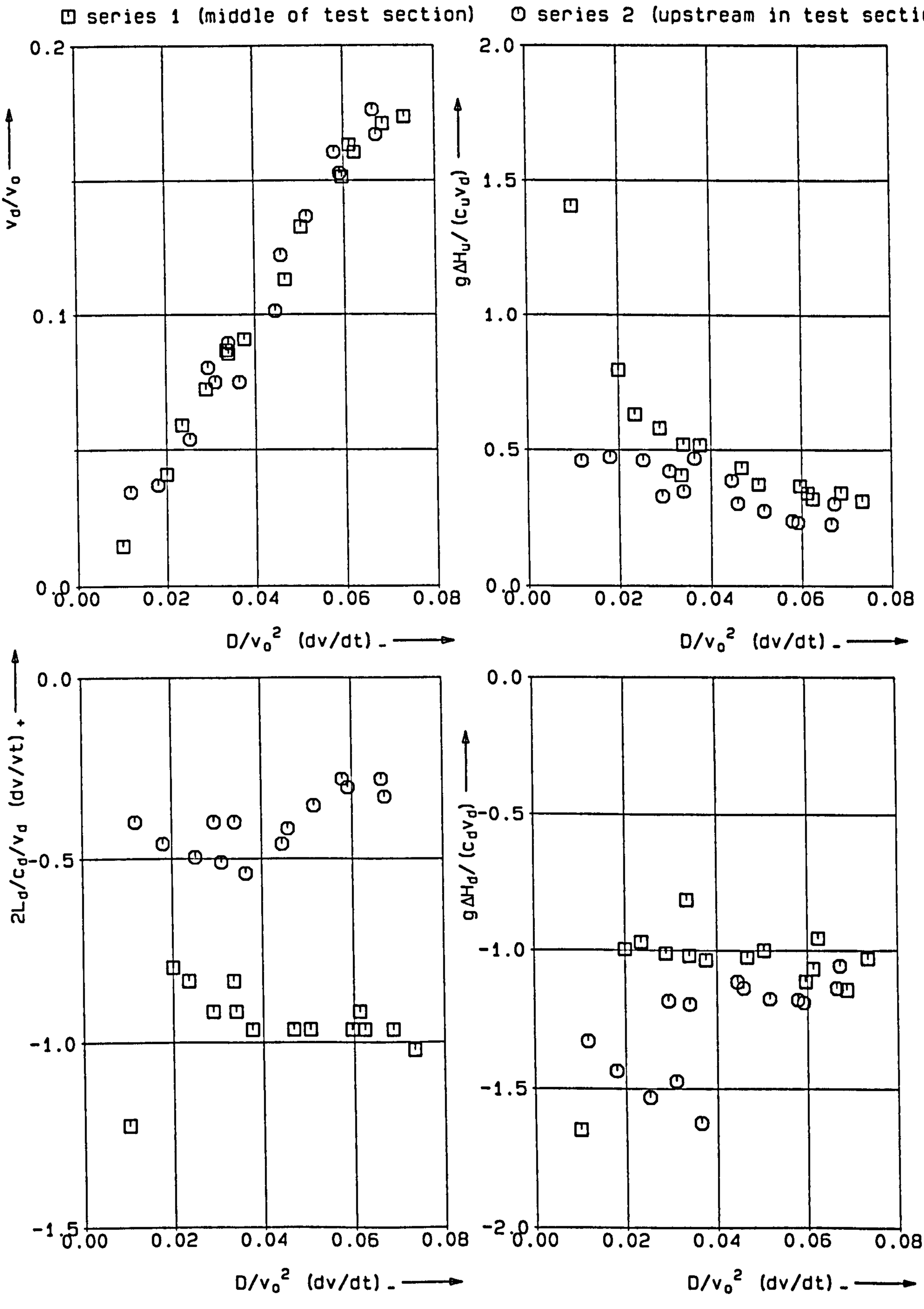

Figure 14.11 Dimensionless valve characteristics approach 1; membrane check valve

For one test both $(2L_d/c_d)/v_d\,(dv/dt)_+ \leq -1$ and $(2L_u/c_u)/v_d\,(dv/dt)_+ \leq -1$, which are the boundary conditions for a reflection free closure (section 11.5.2). In this particular case the dimensionless pressure head changes exceed $\pm$ 1 (the equivalent of the dimensionless Joukowsky pressure head change for undamped check valves), which is in agreement with the theory.

Butterfly check valve The results of the two series of dynamic tests with the 200 mm butterfly check valve are presented in figure 14.12.

The fluid velocity characteristic for the first event shows smaller reverse flow velocities for series 1 (9.6 kg counterweight). The valve response improves with increasing critical velocity, as expected. The reverse flow velocities for series 1 are relatively high at small initial flow decelerations, which is attributed to friction effects. The relative influence of friction effects, which tend to delay the valve closure, vanishes with higher initial flow decelerations. Note that the net effect of inertia, gravitational, buoyancy and hydrodynamic effects is unknown.

The fluid velocity characteristic for the second event shows a similar tendency, due to the fact that the damping time in $(dv/dt)_+ = -v_d/(t_c - t_d)$ is about constant. The dimensionless reverse flow decelerations lie between -0.1 and 0, which means that the valve may be categorized as a strongly damped check valve (section 11.5.2).

The pressure head characteristics show that the upstream and downstream pressure head changes, as induced by the check valve closure, are more or less reversely symmetrical, as expected. The pressure head changes of test series 2 (5.0 kg counterweight) exceed those of series 1 (9.6 kg counterweight), which is a direct consequence of the fact that the reverse flow velocities are higher, while the damping time is about the same (see below).

In figure 14.13 the valve characteristics are presented in a dimensionless form. The figure shows that, despite geometrical differences and strong friction effects, the dimensionless fluid velocity characteristics for the first event more or less coincide.

The fluid velocity characteristic for the second event shows that for all tests, both $-1 < (2L_d/c_d)/v_d\,(dv/dt)_+ < 0$ and $-1 < (2L_u/c_u)/v_d\,(dv/dt)_+ < 0$, which are the reflecting boundary conditions. The damping time is much larger than the reflection time, about constant for test series 1 ($t_c - t_d \approx 1.2$ s) and slightly decreasing for series 2. The hydraulic damper, designed to maintain a constant damping time, operates as expected. At the highest flow decelerations the damping time tends to decrease. Here the hydraulic damper is overloaded, which is confirmed by a strong increase of the pressure head changes and the fact that valve hammer was observed.

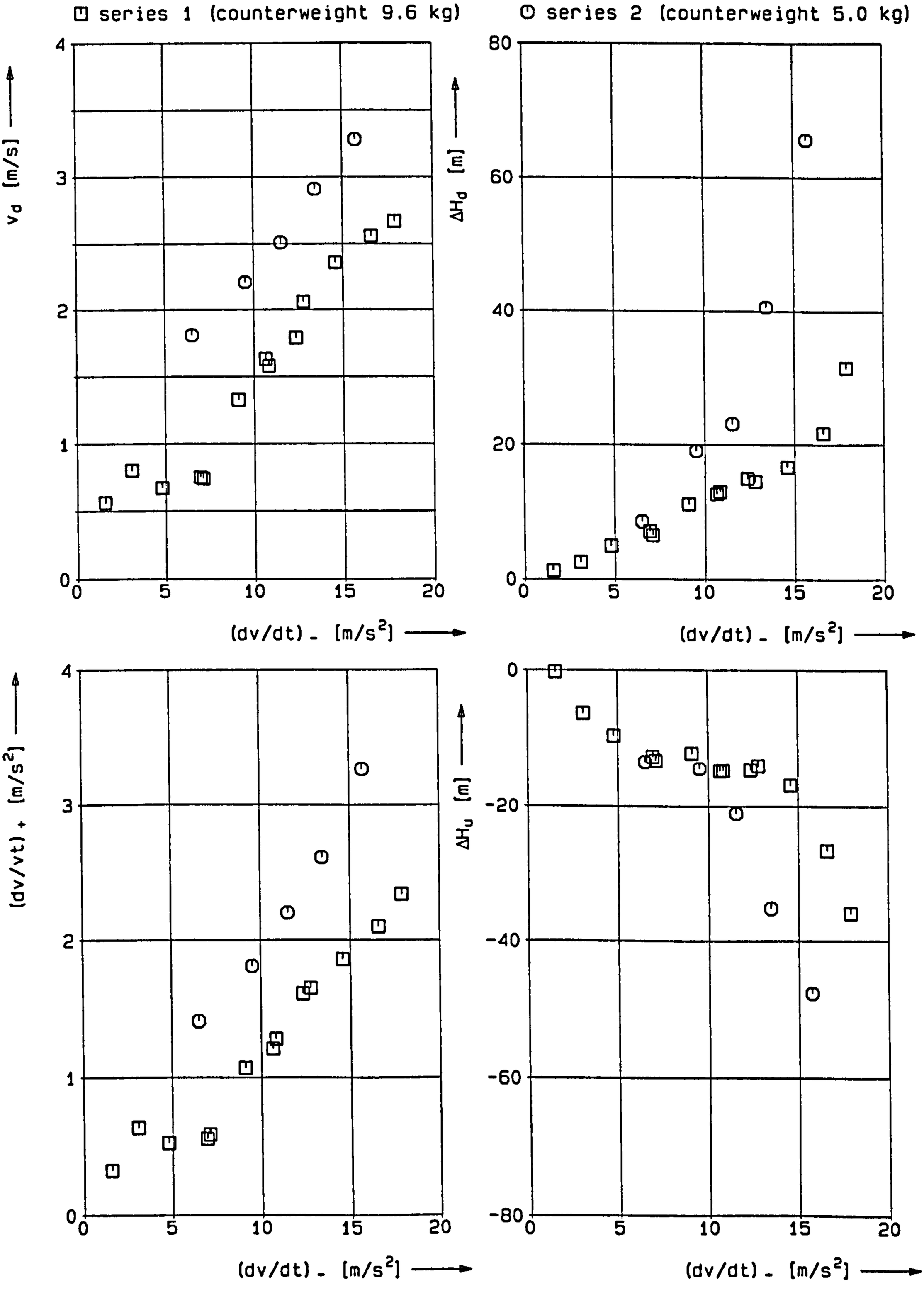

Figure 14.12 Valve characteristics approach 1; 200 mm butterfly check valve

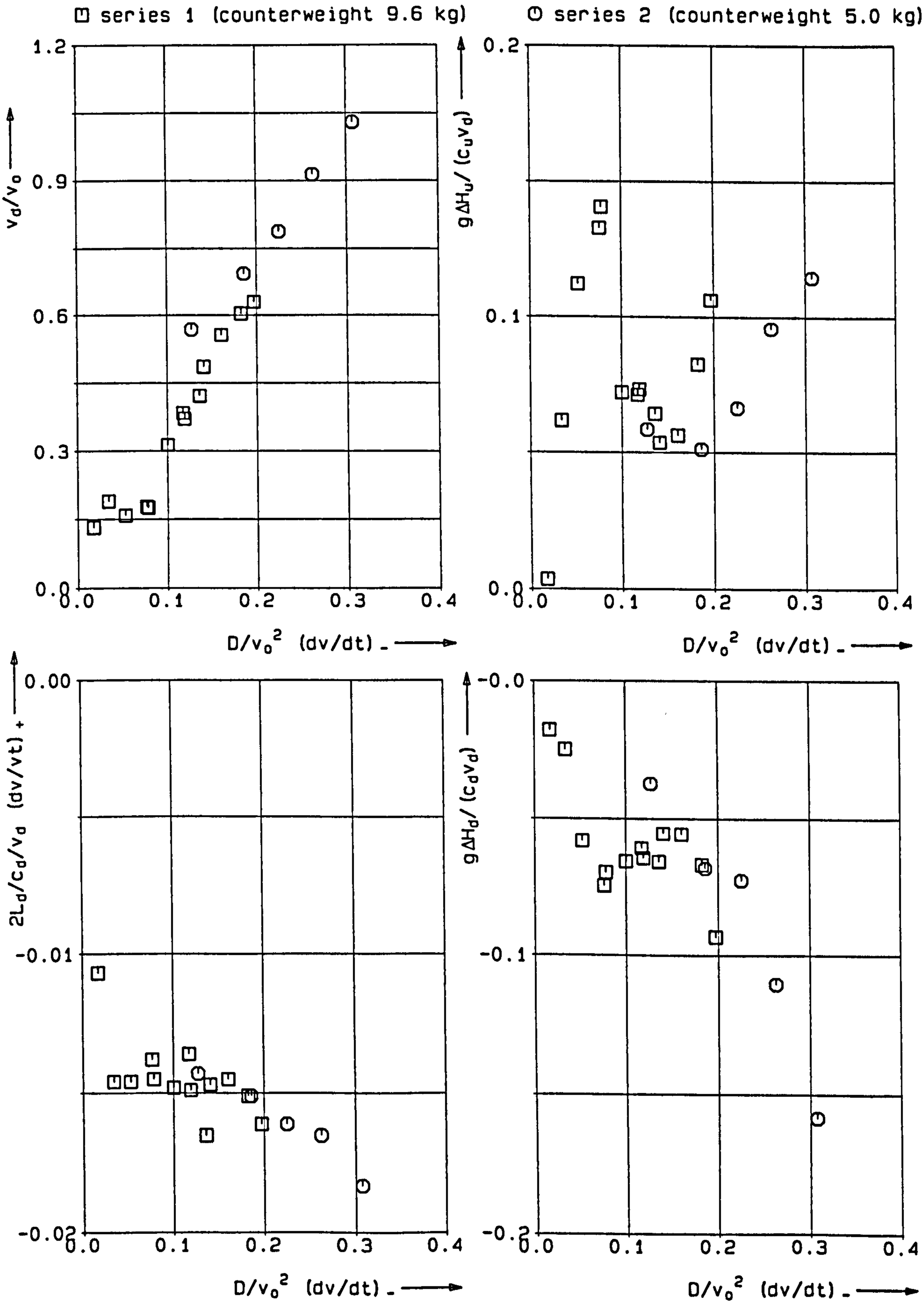

Figure 14.13 Dimensionless valve characteristics approach 1; 200 mm butterfly check valve

The pressure head characteristics show that the absolute values of the dimensionless upstream and downstream pressure head changes are much smaller than 1 (the equivalent of the dimensionless Joukowsy pressure head change for undamped check valves). The damping strongly reduces the pressure head changes.

14.7 Valve characteristics approach 2

The valve characteristics of approach 2 are defined in section 11.6.

Membrane check valve The results of one single dynamic test are presented in figure 14.14, where the dynamic valve coefficient, dimensionless pressure head difference across the valve, and the dimensionless fluid velocity gradient are plotted against the dimensionless fluid velocity.

About the representation of the dynamic valve loss coefficients .....
The dynamic valve loss coefficients are usually represented on a logarithmic scale, which only allows positive values. Here the coefficients ξ are represented by a root function $\xi^{0.2}$, since the root function allows negative values if the root power is an odd number, while coefficients of the order 1 or 10 (which are relevant during the main part of closure) remain their order.

The valve characteristics show four datasets: Data (samples) measured during the first event in the time interval $[t_o, t_d]$, data measured during the second event in the time interval $[t_d, t_c]$, and steady flow values, measured during a (stepwise) increasing and (stepwise) decreasing flow ($dv/dt = 0$). The dynamic characteristics reveal the pattern which is followed during valve closure.

Starting at a high fluid velocity ($v/v_o > 1$) the dynamic valve loss coefficients coincide with the steady flow ones. With decreasing flow the unsteady flow values slightly exceed the steady flow ones (this effect is stronger for series 2). At the asymptote a limit case is reached with infinite positive values ($v/v_o \downarrow 0$) and infinite negative values ($v/v_o \uparrow 0$). After the maximum reverse flow is reached the loss coefficient increases to infinite positive values again (valve closed).

The characteristics show negative ξ-values after flow reversal. Apparently, the pressure head is still positive after flow reversal. This effect is better visible for the butterfly valve (see below).

In figure 14.15 the results of four dynamic tests, at different initial flow decelerations, are presented.

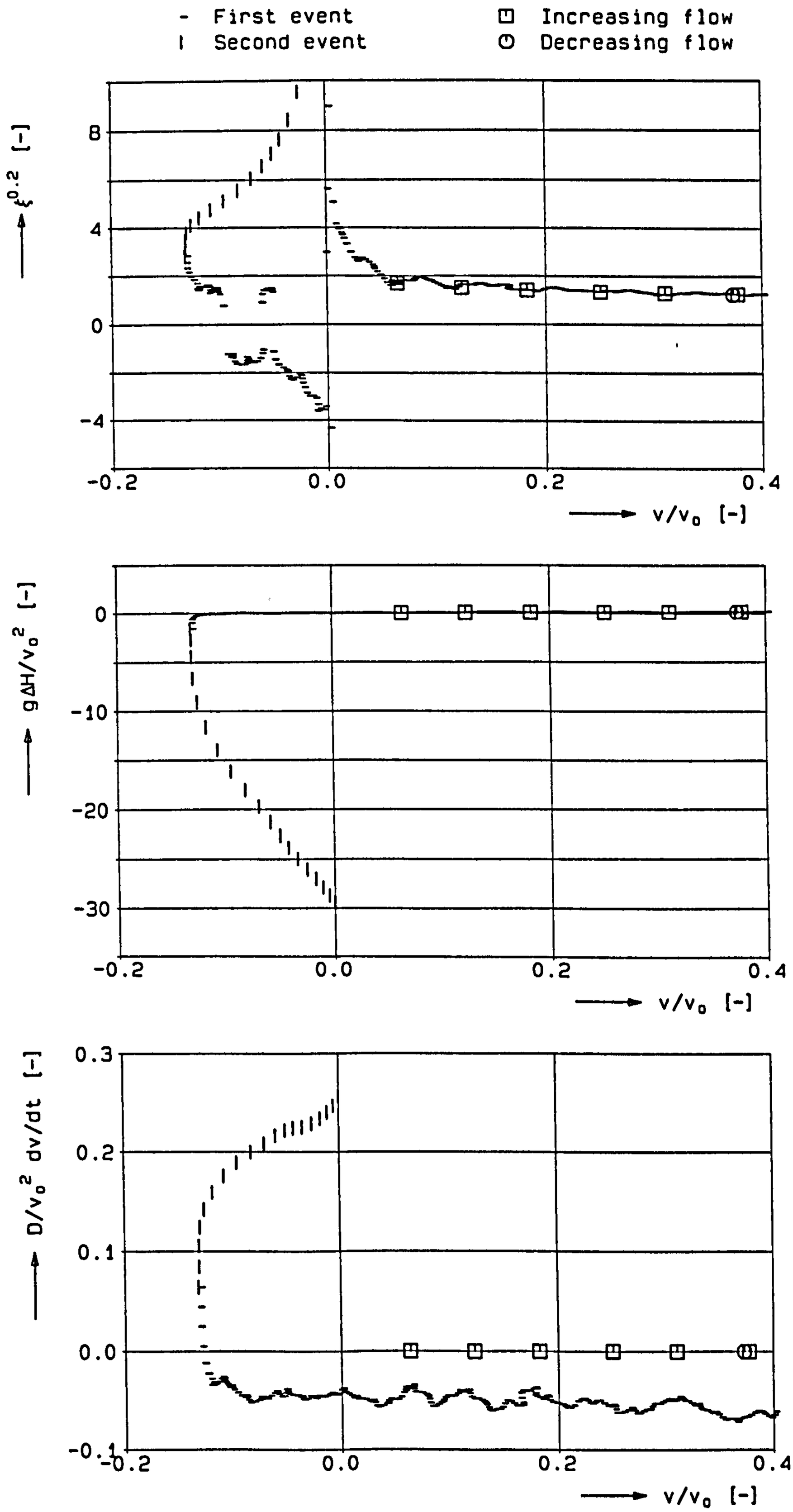

Figure 14.14 Valve characteristics approach 2; membrane check valve (series 1)

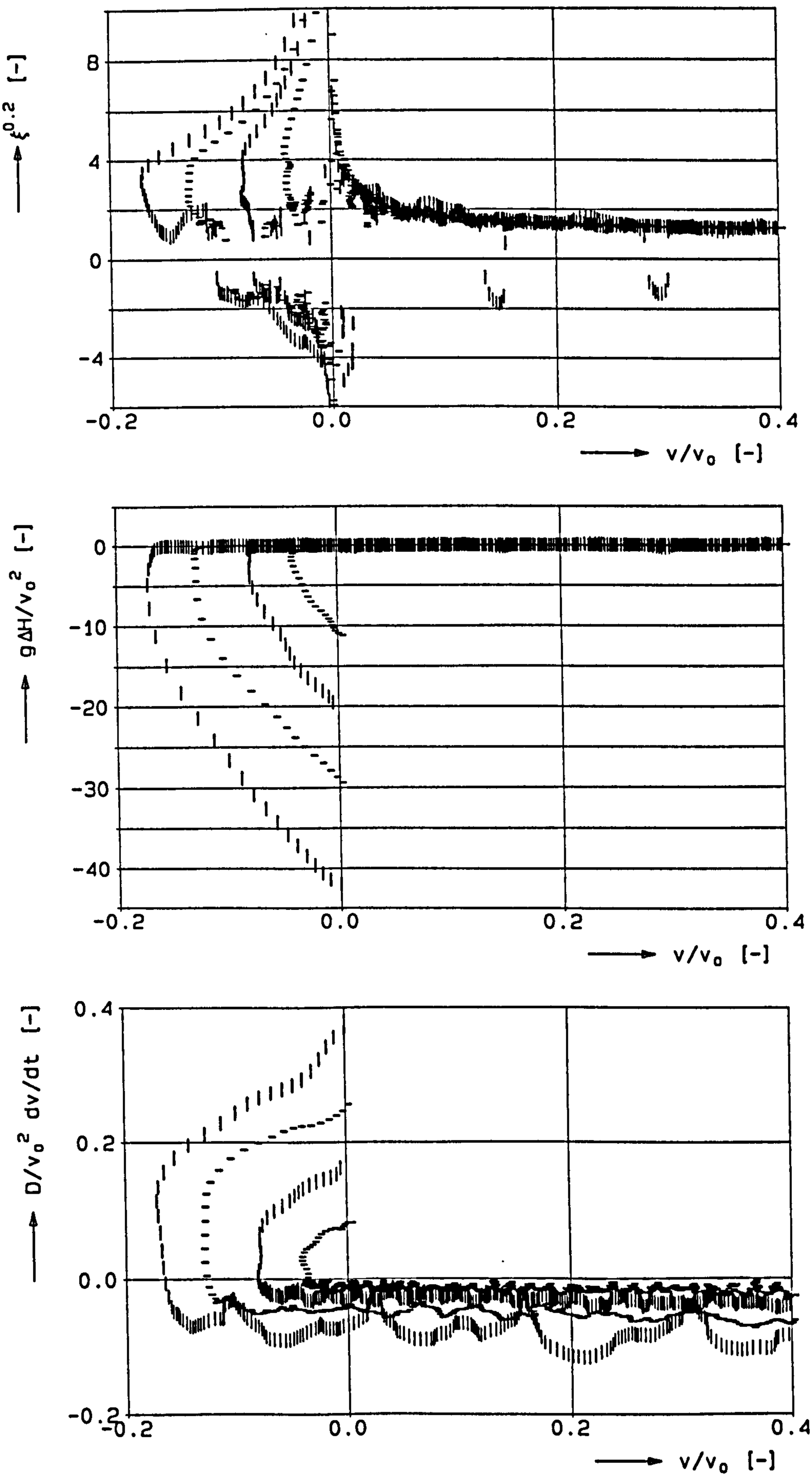

Figure 14.15 Valve characteristics approach 2; membrane check valve (series 1)

The valve loss coefficient is defined as:

$$\xi = \frac{\Delta H \, 2g}{v|v|} \tag{14.9}$$

This definition finds its origin in the fact that under steady-state conditions always positive ξ-values are guaranteed, i.e. under normal and reverse flow conditions. However, for check valves no steady-state conditions exist under reverse flow conditions.

Butterfly check valve The results of one single dynamic test with the 200 mm butterfly check valve (series 1) are presented in figure 14.16.

Also here, the dynamic valve loss coefficient and pressure head difference coincide with the corresponding steady flow ones. It is interesting to see that the values measured during valve closure, tend to exceed the steady flow ones, measured during a (stepwise) decreasing flow.

In figure 14.17 the results of four dynamic tests are presented. The scatter just before closure ($v \uparrow 0$) is the result of valve hammer, observed during the test with the highest initial flow deceleration.

The characteristics show negative ξ-values after flow reversal, due to the fact that the pressure head difference remains positive for a while. Apparently the pressure head difference needs some time to change sign. This effect may be seen as a "time" pressure recovery effect, not to be confused with the "spatial" pressure recovery effect (see further the notes in section 13.7.2).

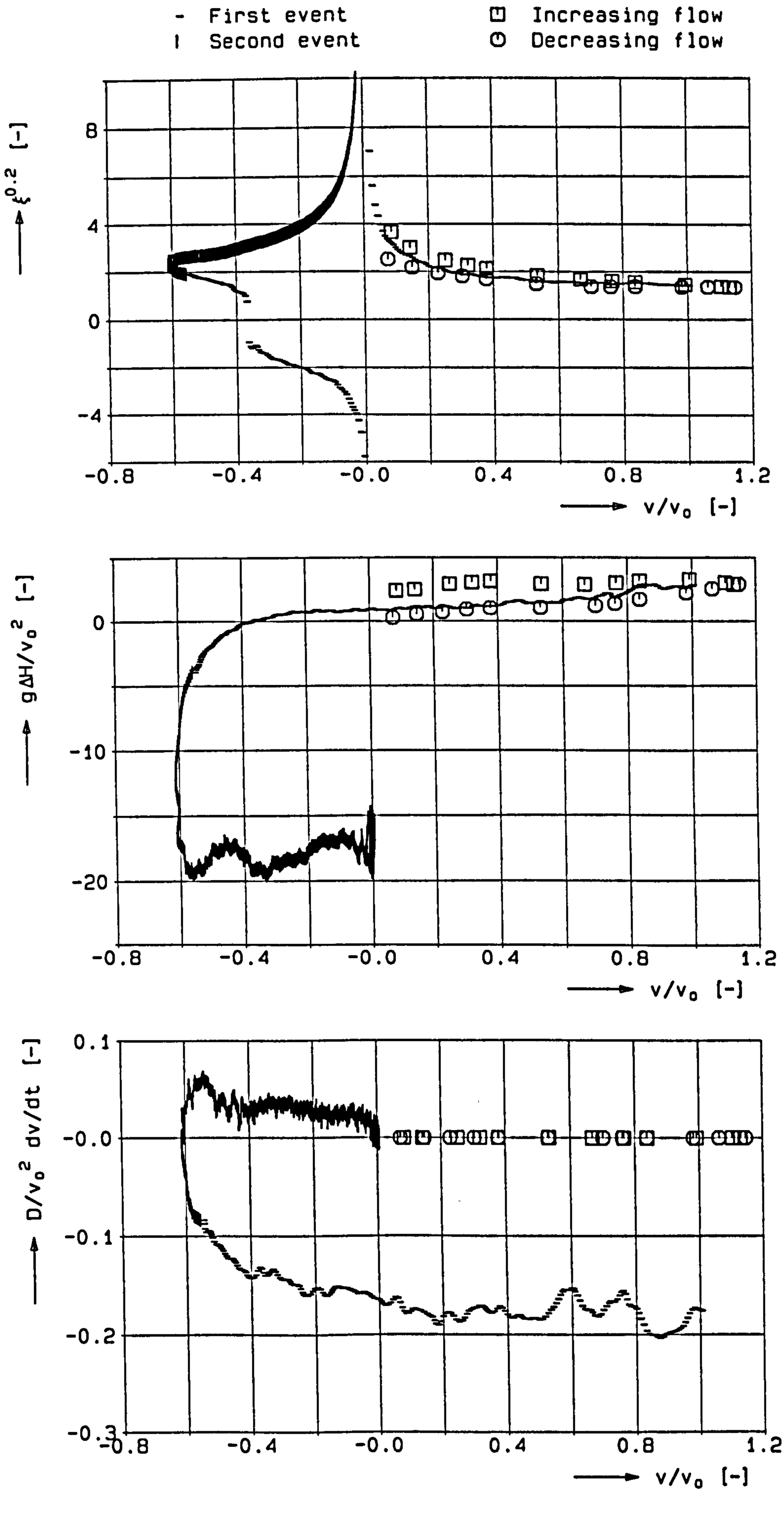

Figure 14.16 Valve characteristics approach 2; 200 mm butterfly check valve

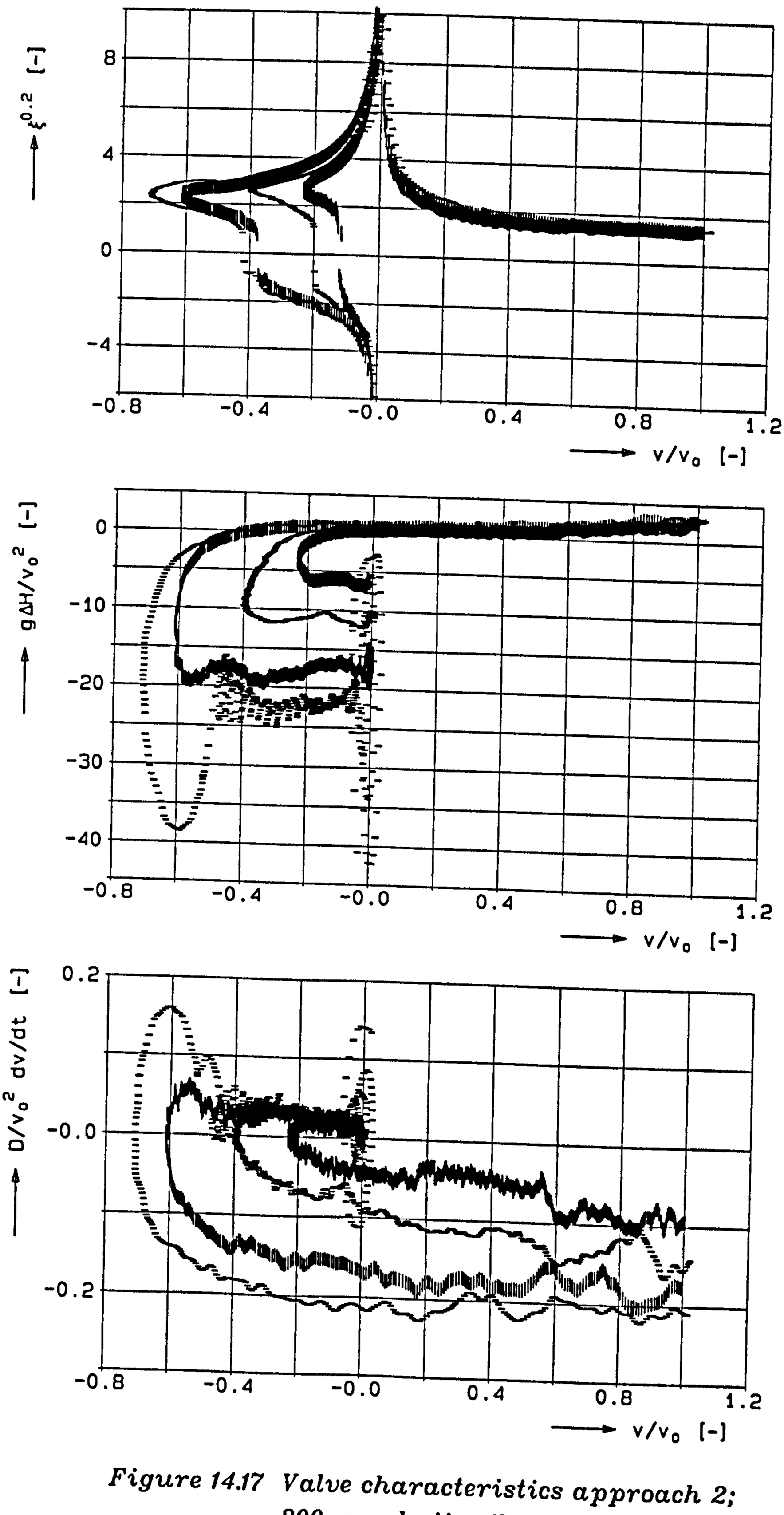

Figure 14.17 Valve characteristics approach 2; 200 mm butterfly check valve

14.7.1 Neural networks

In this section the application of neural networks to the valve characteristics of approach 2 is explored.

The neural network (NN) used here is a *multi-layer perceptron* (section 12.4) with the following architecture: an input layer with two neurons, one hidden layer with 6, 9 or 12 neurons, and an output layer with two neurons. Based on the number of neurons in the hidden layer, the three options are denoted as NN_6, NN_9 and NN_{12}. The inputs of the NN are the dimensionless forms of the fluid velocity v and velocity gradient dv/dt. The outputs of the NN are a scaled form of the absolute value of the dynamic valve loss coeffient $|\xi|$ and the sign of ξ.

About scaling the loss coefficient .....

Just like in the graphical representation of the valve characteristics, the loss coefficients are scaled according to $\xi \rightarrow \xi^{0.2}$. The range of ξ-values $[-10^5, 10^5]$ is reduced to [-10, 10]. It thus could be avoided that the training is too much concentrated on the accurate reproduction of large ξ-values only.

About the number of output neurons .....

In first instance the NN was trained with one output neuron $\xi^{1/5}$. In that case the performance of the NN was reasonably well, both for the train and test set. However, the accuracy near the asymptote $v = 0$ was less satisfactory. This transition region is characterized by $\xi \uparrow \infty$ for $v \downarrow 0$ and $\xi \downarrow -\infty$ for $v \uparrow 0$. Furthermore, the sign of the predicted ξ-values did not always correspond with the sign of the ξ-values of the targets in the train and test set. Obviously, this sign performance depends on the architecture of the NN. In the case of NN_{12} at least 10 incorrect signs are found. The performance of the NN could significantly be improved by separating the magnitude and sign of the loss coefficients. Hereto the absolute value of $\xi^{1/5}$ is considered, while the sign of ξ is added as second output neuron. Thus the steep slope in the transition region from $\xi \uparrow \infty$ to $\xi \downarrow -\infty$ is not "seen" by the NN.

As data set four dynamic tests are selected from series 1 of the 200 mm butterfly valve (table 14.6), whereby only samples are used in the time interval $[t_o, t_c]$. This results in a set of about 3000 samples, from which 2000 samples are used as train set and the rest as test set.

The performance of the NN is presented in table 14.7, where the differences between the output of the NN and the targets (i.e. training set or test set) are given in the form of RMS-values. The performance of the NN on the training set and test set is very similar, since the sets are statistically equivalent (i.e. the samples of the two sets are taken random from the same data set). The performance of the NN improves with increasing number of neurons in the hidden layer, as long as the NN is not "overtrained".

	NN_6	NN_9	NN_{12}
training set	0.42	0.25	0.22
test set	0.43	0.27	0.23

Table 14.7 Performance of neural network

More detailed information about the performance is given in scatter plots, where the output of the NN is presented against its target. An example of such a plot is given in figure 14.18 (the + and × sign refer to training and test set, respectively).

A three-dimensional graphical representation of the valve characteristics of approach 2 is given in figure 14.19. The loss coefficients are generated with NN_9 on a grid in the *v-dv/dt*-plane. In the graph also the original data, i.e. the trajectories of the four selected dynamic tests, are plotted. Note that quadrant 1, which is reserved for opening characteristics, is extrapolated from closure characteristics.

About the quality of the data set .....

The quality of the original data set plays a role in the choice of a NN architecture. It makes no sense to strive for a high reproducibility if the quality of the data set is poor.

The quality of the dynamic tests is determined by the quality of the test facility and measuring equipment. The fluid velocity and velocity gradient are subject to fluctuations, which are partly attributed to initiation effects, non-ideal boundary conditions and possibly, the response of the flowmeter. Due to these fluctuations the trajectories, which are followed during valve closure, have a more or less capricious character (figure 14.19). The question arises in how far these fluctuations must be incorporated in the valve characteristics.

About the number of neurons in the hidden layer .....

The above-mentioned "capricious character" of the original data set is reproduced better if the number of neurons in the hidden layer increases (i.e. more degrees of freedom). This tendency is found inside the domain of the original data set (interpolation area), but also outside it (extrapolation area). In the latter case the fluctuations may even be amplified, in particular at remote extrapolation areas, which leads to oscillations. Although the performance improves with an increasing number of neurons, it is doubtful if these oscillations have a physical meaning.

As long as the NN is only used for interpolation, NN_{12} gives the best performance. However, if it is also used for extrapolation, physical aspects must be taken into consideration (during training and interpretation of the results). An example of such a physical aspect might be that the output values show minimal variation in extrapolation areas. These additional, physical or mathematical conditions, which must be satisfied during training (optimisation or calibration) are known as *regularizations*. This is not further considered here.

As compomise between reproducibility and physical reality NN_9 is qualified as the best.

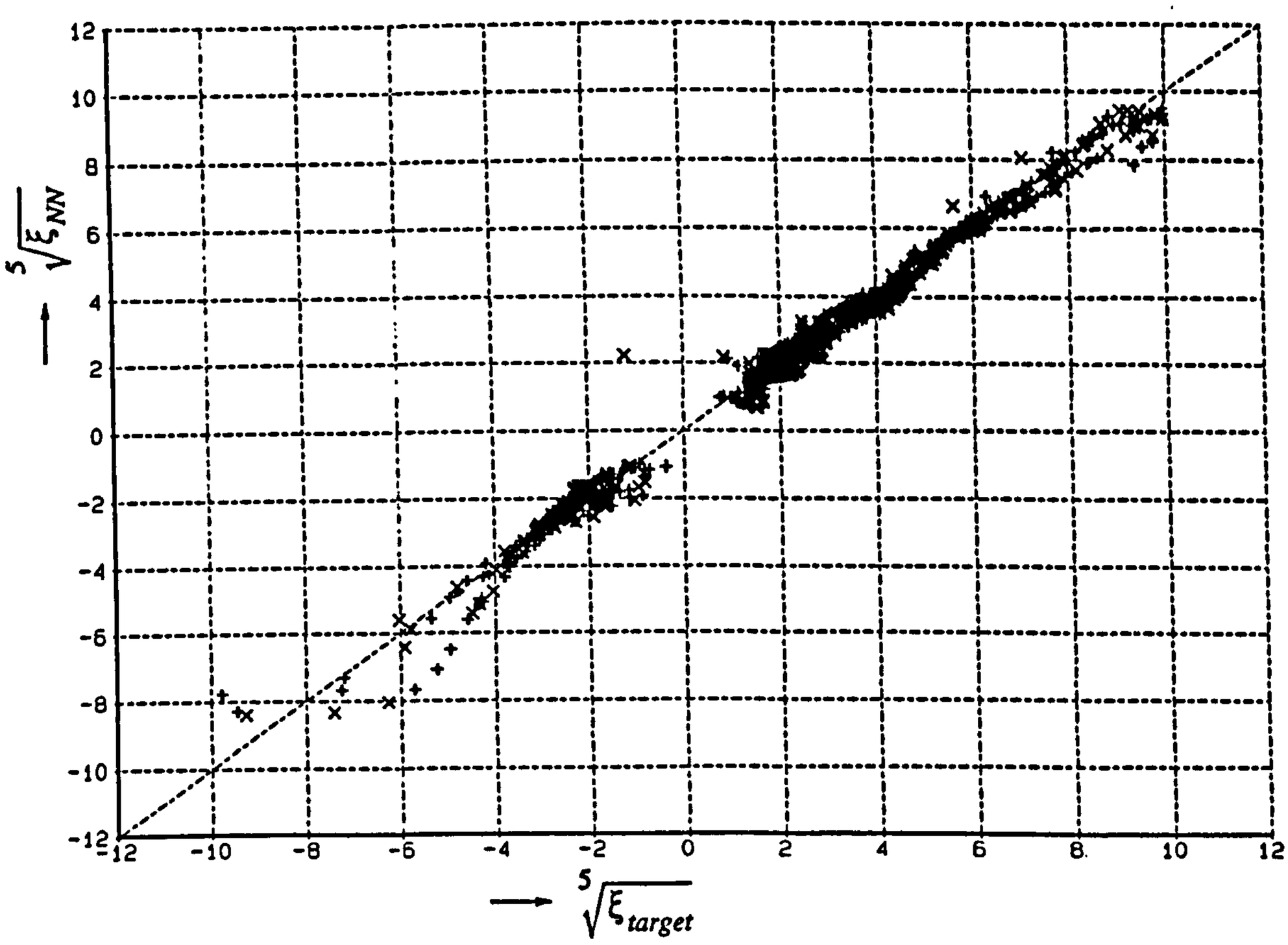

Figure 14.18 Performance of NN in scatter plot (NN_9)

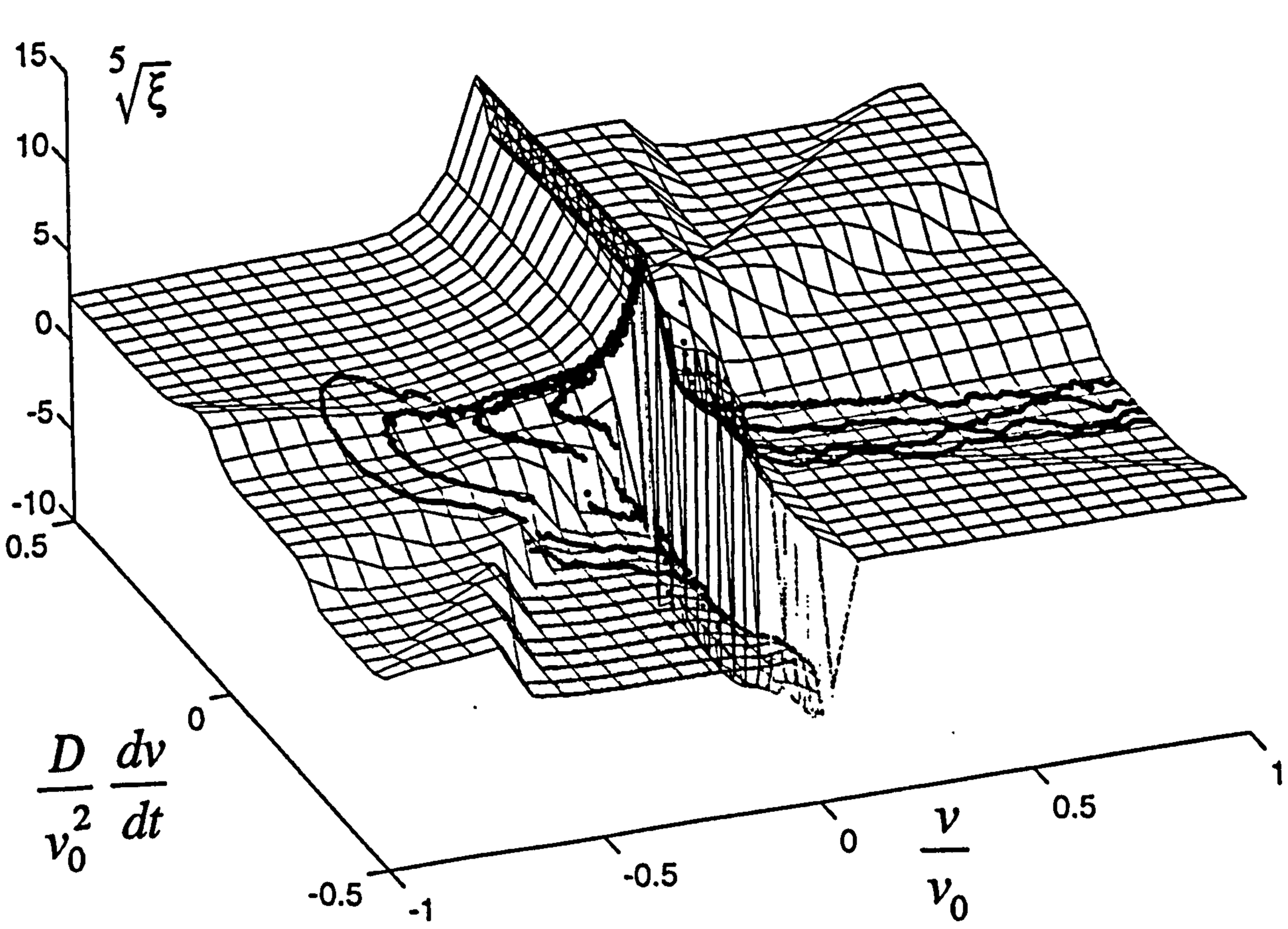

Figure 14.19 Valve characteristic of approach 2 (NN_9)

The benefits of NN's may be:

- The interpolation within the valve characteristics of approach 2 is non-linear. In principle, the accuracy of the interpolation is improved, in particular in regions with strong gradients and in extrapolation areas.
- A better insight into and a more complete overview of the surface is obtained, which is formed by a series of dynamic tests in the three-dimensional physical space of the valve characteristics of approach 2.
- The application the NN's may be extended to the interpolation within the valve and system parameters and possibly to the phenomenon of flow loops.

14.8 Other valve characteristics

In figure 14.20 the axial valve displacement of the 200 mm membrane and the butterfly check valves is presented as function of the initial flow deceleration. The graph represents the changes induced by the check valve closure (during the second event). The axial valve displacement increases more or less linear with the initial flow deceleration and is limited to about 1 mm.

The axial valve motion gives information about the importance of fluid-structure interaction effects, which are ignored in the theory. From the valve displacement signal it is concluded that the axial valve velocity is of the order 0.001/0.02 = 0.05 m/s (membrane check valve) and 0.0005/0.1 = 0.005 m/s (butterfly valve). Tijsseling and Lavooij (1989) and Tijsseling (1993) have performed an extensive study on the effects of fluid-structure action. In small-scale test facilities with elbows, etc. axial pipe wall velocities are measured, typically in the order of 1 m/s. Comparing the results it is concluded that fluid-structure effects play no role of significance here.

In figure 14.21 the steady-state and dynamic behaviour of the check valves are correlated. The steady-state behaviour is represented by the valve loss coefficient ξ_b, i.e. the initial value in advance of a dynamic test (the valve may be partly opened). The dynamic behaviour is represented by the slope η in the dimensionless fluid velocity characteristic for the first event (see section 11.7). By considering the slope at relatively high, initial fluid decelerations, friction effects are excluded. Obviously the characteristic of the ideal valve would coincide with the origin.

The results of the butterfly valves show that the valve response improves with increasing initial valve loss coefficient. Note that the 500 mm valve is initially partly opened (table 14.6).

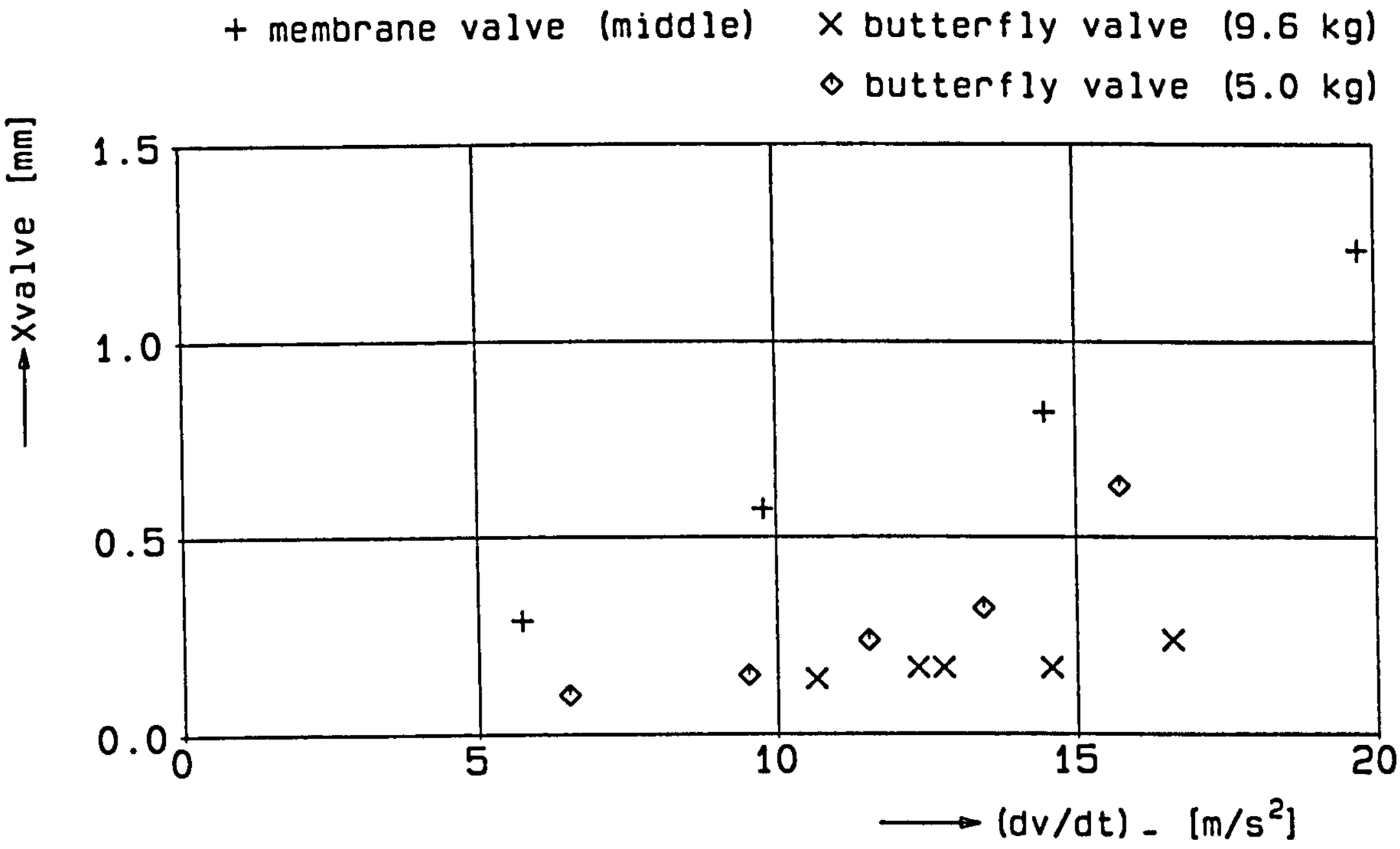

Figure 14.20 Axial valve displacement

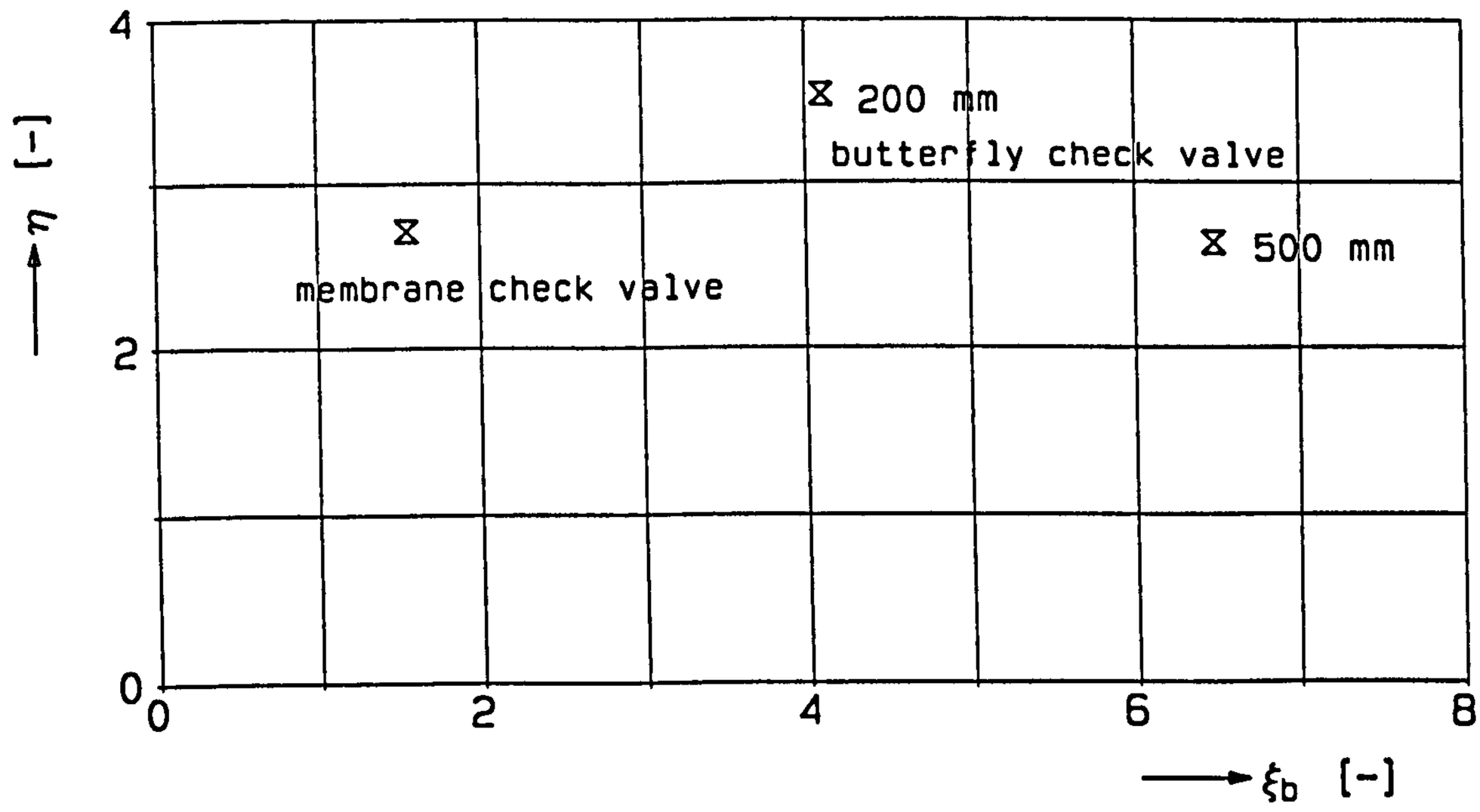

Figure 14.21 Correlation between steady and dynamic behaviour

14.9 Review and conclusions

The (effective) pipe friction coefficient of the pipes in the test section is measured, taking into account pipe friction and losses across the flanges. The values are used in the data processing.

The pressure wave speed of the water filled pipes in the test section is measured, without and with an air filled, flexible hose. The flexible hoses reduce the pressure wave speed from about 1240 m/s (200 mm standard pipe) to 730 m/s (hose type I) and 980 m/s (hose type II). The influence of the air pressure on the pressure wave speed is not strong enough to control the pressure wave speed within the test range of 1 -7 bar. The hoses are sensitive to collapsing. The collapsing is coupled with strong damping effects.

The measured pressure wave speeds of the standard pipe are used in the data processing. The results of the flexible hoses are not used. However, in principle the hoses can be used as pressure wave reducer in order to satisfy the dynamic scale laws. For the scaling of the rotating type of check valve from 200 to 500 mm, in theory the pressure wave speed must be reduced by a factor $\sqrt{2.5}$, at equal pipe lengths. For this purpose hose type I seems to be suited if its dimensions are scaled up to the 500 mm piping, in such a way that the pressure wave speed remains unchanged.

The theoretical pressure wave speeds of Remenieras are much smaller than the measured ones. The influence of the rigidity of the hose cannot be neglected in his equation.

The flowmeter is calibrated under unsteady flow conditions. Hereby the pressure head gradient along the pipe is used as a reference. It is demonstrated that the response of the flowmeter can be measured by comparing the instantaneous fluid velocity gradient with the instantaneous pressure head gradient along the pipe. As a result the flowmeter tested is able to respond to the flow decelerations imposed.

Steady-state characteristics are measured. The characteristics supply information about hysteresis and the critical velocities in an increasing and decreasing flow. From these values the average critical velocity and critical Reynolds number are calculated.

Several series of dynamic tests are performed on weakly and strongly damped check valves under different laboratory conditions, whereby the location of the valve in the test section, the critical velocity and the degree of damping are varied.

From the series of dynamic tests the valve characteristics of approach 1 and 2 and other valve characteristics are derived.

From the fluid velocity characteristic for the second event (approach 1) the character of damping is determined. The membrane and butterfly check valves are categorized as weakly and strongly damped check valves, respectively. From the pressure head characteristics of the strongly damped check valve it is concluded that the damping strongly reduces the pressure head changes, relative to those induced by an undamped version.

The pressure head difference across the valve and dynamic valve loss coefficients (approach 2) reveal a *time* pressure recovery effect. From the axial valve displacement it is concluded that fluid-structure interaction plays no role of significance.

The overall behaviour of the valves is described in a valve characteristic, which correlates the steady and dynamic behaviour. Thus a better comparison of valve types can be made.

The application of neural networks to the valve characteristics of approach 2 is explored. In principle the accuracy of the interpolation and the extrapolation within a valve characteristic is improved by the NN. It gives a better insight into and a more complete overview of the surface, which is formed by a series of dynamic tests in the three-dimensional physical space of the valve characteristics of approach 2.

In principle the NN concept can also be applied to the interpolation within the valve and system parameters and possibly to describe the phenomenon of flow loops. This needs further investigation.

15 Numerical and experimental validation

In this chapter the dynamic scale laws, as derived in the dimensional analysis (chapter 11), are validated by means of numerical simulations. Further the model for damped check valves (chapter 12) is validated against experiments.

15.1 Numerical validation of scale laws

To verify the scale laws, which are applied to the valve characteristics of approach 1 (section 11.5), simulations are made of a serial pipeline system with pipe junctions and constant head boundaries. The system consists of four pipe sections and a check valve between the second and third section (figure 15.1). The simulations are made with a special version of the waterhammer computer code WTSL$^+$, which enables to start from unsteady, initial flow conditions instead of from the usual steady, initial flow conditions. The (check) valve is modelled as a component with prescribed velocity-time history.

During the first event the fluid velocity at the (check) valve is prescribed by a constant, initial flow deceleration (figure 8.2). During the second event it is prescribed by a third-order polynomial, described by:

$$v = a_1 + a_2 (t-t_d) + a_3 (t-t_d)^2 + a_4 (t-t_d)^3 \qquad \textbf{(15.1)}$$

With the boundary conditions:

$$\begin{aligned} t = t_d: \quad & v = v_d \quad \Lambda \quad \frac{dv}{dt} = \left[\frac{dv}{dt}\right]_- \\ t = t_c: \quad & v = 0 \quad \Lambda \quad \frac{dv}{dt} = \beta \left[\frac{dv}{dt}\right]_- \end{aligned} \qquad \textbf{(15.2)}$$

The parameter β is introduced to vary the character of the velocity-time function.

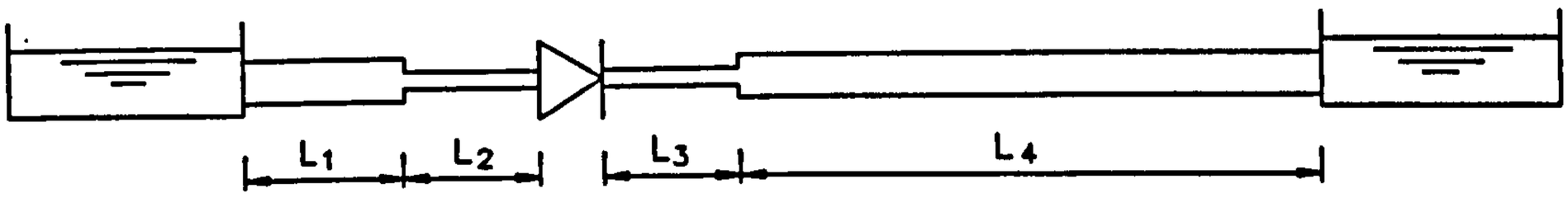

Figure 15.1 Check valve in serial pipeline system

Sim[1]	D [m]	v_d [m/s]	v_o [m/s]	$(dv/dt)_-$ [m/s^2]	$(dv/dt)_+$ [m/s^2]
C_1	0.5	-1	1	-20	2
C_2	1	-1	1	-10	1
C_3	2	-2	2	-20	2

$$\frac{D}{(2L_2/c_2)v_0} = 12.5 \; ; \; \frac{D}{v_o^2}\left(\frac{dv}{dt}\right)_- = -10 \; ; \; \frac{v_d}{v_o} = -1 \; ; \; \frac{2L_2/c_2}{v_d}\left(\frac{dv}{dt}\right)_+ = -0.08$$

a. valve, valve-system and flow parameters

Sim[1]	L_1 [m]	L_2 [m]	L_3 [m]	L_4 [m]	D_1 [m]	D_2 [m]	D_3 [m]	D_4 [m]	c_1 [m/s]	c_2 [m/s]	c_3 [m/s]	c_4 [m/s]
C_1	10	20	30	40	1	0.5	0.5	1	500	1000	1000	500
C_2	40	20	30	160	4	1	1	4	1000	500	500	1000
C_3	10	40	60	40	$\sqrt{8}$	2	2	$\sqrt{8}$	250	1000	1000	250

$$\frac{2L_1/c_1}{2L_2/c_2} = 1 \; ; \; \frac{2L_1/c_1}{2L_3/c_3} = \frac{2}{3} \; ; \; \frac{2L_1/c_1}{2L_4/c_4} = \frac{1}{4} \; ; \; \frac{A_1/c_1}{A_2/c_2} = 8 \; ; \; \frac{A_1/c_1}{A_3/c_3} = 8 \; ; \; \frac{A_1/c_1}{A_4/c_4} = 1$$

b. system parameters

Table 15.1 Numerical validation of scale laws

[1] Sim = simulation

The valve and system parameters, which are used in the simulations are listed in table 15.1.a and b. The parameters are chosen in such a way that the numerical value of the dimensionless groups is equal in the simulations. The character of the velocity-time function is chosen to be represented by $\beta = 0$ here. The simulation time is chosen as $t = 25\ (2L_2/c_2)$ seconds, while the time step $\Delta t = (2L_2/c_2)/16$ seconds.

The results of the simulations are presented in figure 15.2, where the fluid velocity and the pressure head at the check valve, at the upstream side of the pipe junction and at the downstream boundary are given as function of time (downstream piping only).

In figure 15.3 the same results are presented in a dimensionless form, where the gravitational acceleration is chosen equal to 10 m/s^2.

Note that the dimensionless fluid velocities and pressure heads are based on *local* values of c and v_d. However, the dimensionless pressure head may also be based on *remote* values, since the terms $(c.v_d)_i$ and $(c.v_d)_j$ are related via the ratio of the characteristic impedances of the pipe sections i and j. The dimensionless fluid velocity cannot be based on remote values. Here, flow rates instead of fluid velocities may be considered as an alternative.

The results of different flow conditions and pipeline configurations are reduced to one single curve as long as the numerical values of the dimensionless groups and the character of the velocity-time function remain the same. Thus it is demonstrated that the (dimensionless) unsteady flow parameters (section 11.4) are well defined, and that the dimensionless fluid velocity and pressure head changes, as induced by the (check) valve closure, may be described by dimensionless flow characteristics in the form of the Equations (11.31) through (11.35).

The scale laws hold for any point along the pipe. If these points are considered as varying head boundaries, the results demonstrate that the general condition, as formulated in Equation (9.63), is correct.

Note that this validation refers to the pipe equations only and not to the valve equations, since the fluid velocity at the valve is prescribed as boundary condition. In that respect similarity of the valve-system parameter c/v_o is not satisfied. However, similarity of the groups $D/(2L/c)/v_o$ and v_d/v_o is a necessary condition, since the dimensionless initial flow deceleration is described in terms of D and v_o.

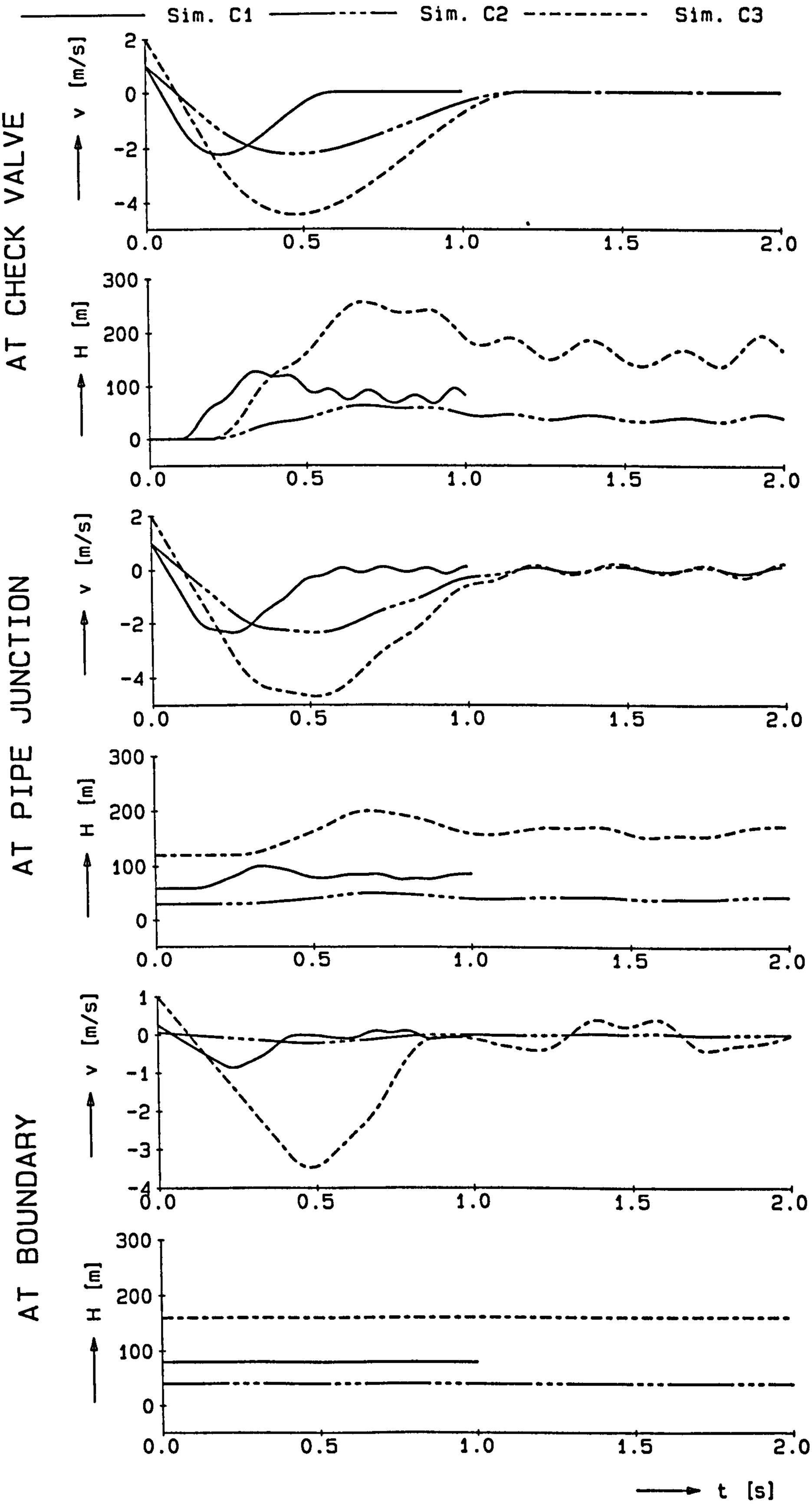

Figure 15.2 Numerical validation of scale laws; v–t and H–t histories at downstream piping

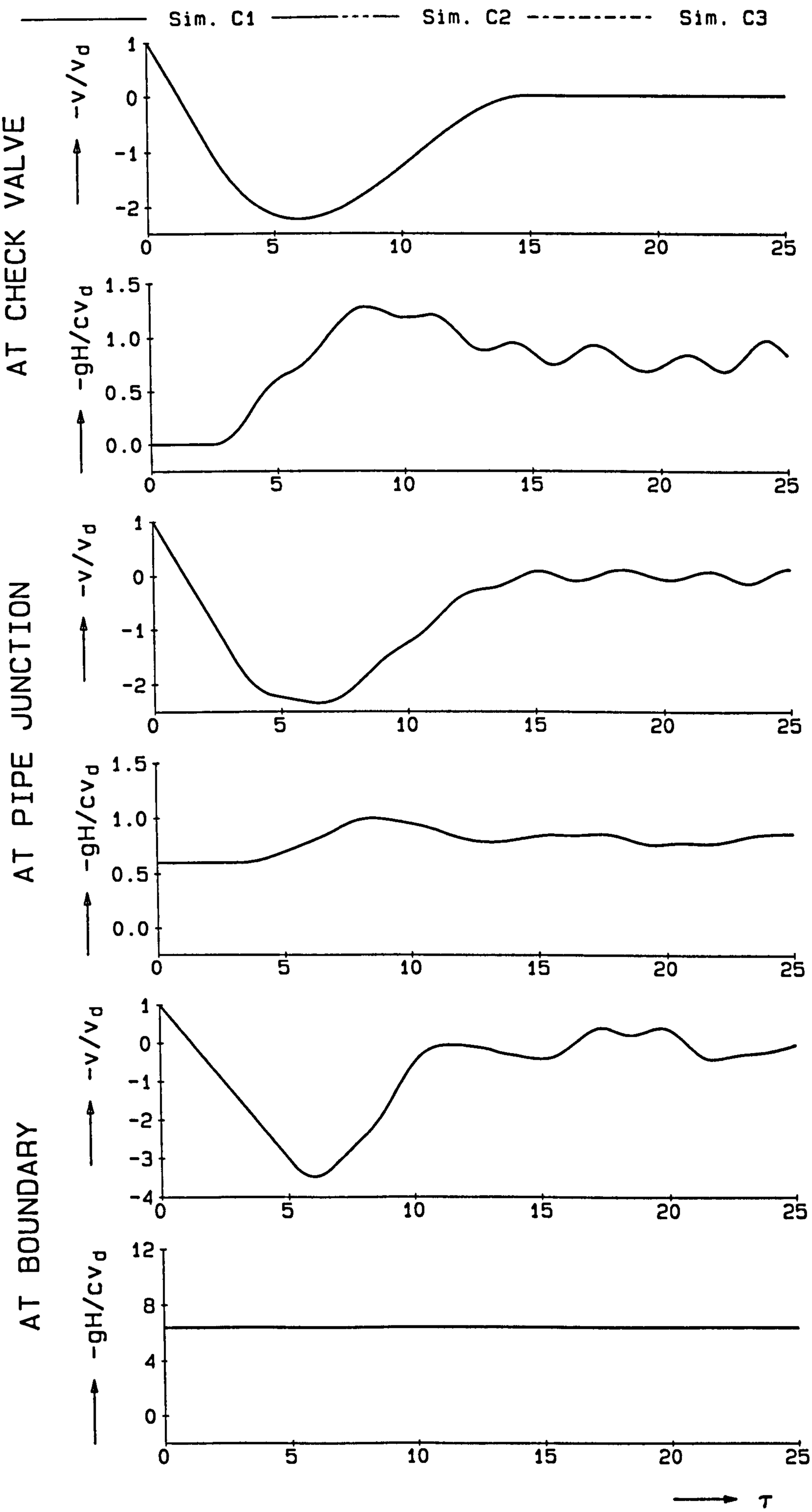

Figure 15.3 Numerical validation of scale laws; Dimensionless time-histories at downstream piping

15.2 Experimental validation of valve models

The model for damped check valves (section 12.2), which is implemented in the waterhammer computer code CVWP, is validated by the simulation of dynamic tests with the membrane and butterfly check valves (chapter 14).

15.2.1 Model

The test facility (figure 13.1) is modelled by an upstream high reservoir (B_1), vertical pipe section (P_1), two horizontal pipe sections with a resistance (P_2, P_3, R_1), an air vessel (A_1), test section with check valve (P_4, C_1, P_5), and a downstream reservoir (B_2). A hydraulic scheme of the test facility is given in figure 15.4.

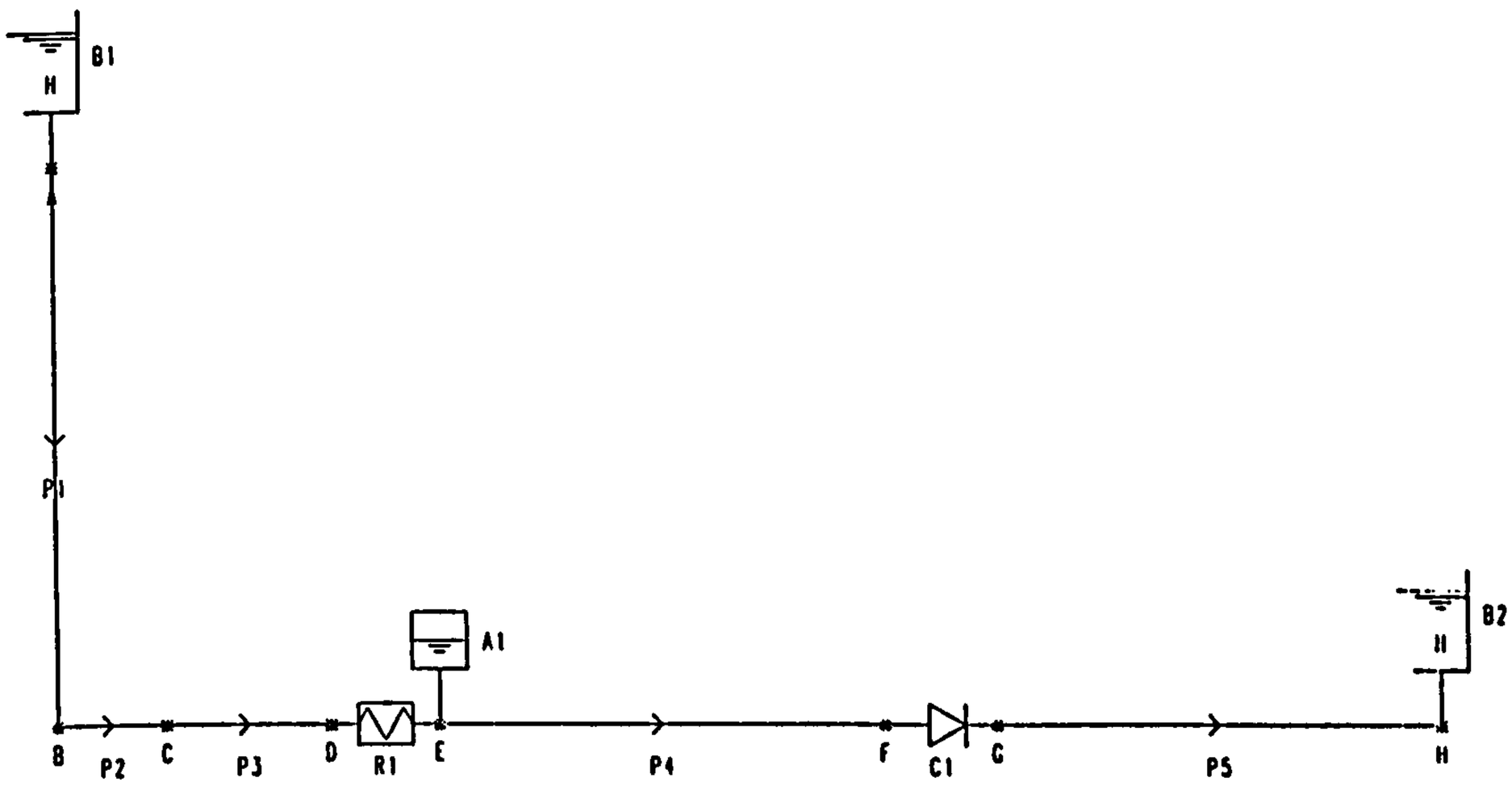

Figure 15.4 Hydraulic scheme of the test facility

The pipes are modelled by the transient equations and treated by the method of characteristics (section 9.2). The pipe data are given in table 15.2.

Pipe	L [m]	D [mm]	f [-]	e [mm]	E [N/m^2]
P1	22.6	1000	0.017	10.0	$2.1\ 10^{11}$
P2	3.28	1000	0.017	10.0	$2.1\ 10^{11}$
P3	8.85	390	0.015	7.9	$2.1\ 10^{11}$
P4	11.39	206/489	0.019	5.9/9.5	$2.1\ 10^{11}$
P5	11.39	206/489	0.019	5.9/9.5	$2.1\ 10^{11}$

Table 15.2 Pipe data

The air vessel is modelled as a vertical, non-vented, air vessel (AIRVvn) with a volume of 3 m^3, a chamber area of 1 m^2, an initial fluid level of about 2 m and a Laplace coefficient 1 (isothermal expansion).

The pressure relief valve on top of the air vessel was not active during the dynamic tests with the 200 mm valves. For this reason it is not modelled here.

The upstream and downstream reservoir are modelled as constant head boundaries. In order to simulate a dynamic test with decelerating flow, the downstream pressure head is increased to a constant level by prescribing the pressure head in time.

The resistance accounts for the air vessel inflow losses (with loss coefficient 1.0) and bend losses (90° bends with loss coefficients of 0.2 each).

The check valve is modelled as a damped check valve (section 12.2). For the membrane and butterfly valves the valve characteristics of approach 2 are available in the check valve database in CVWP.

15.2.2 Simulations and results

Several simulations are made, whereby the numerical time step, *dv/dt*-smoothing parameter (section 12.3.2) and closure phase angle ϕ (section 12.2) are varied.

Some of these results are given in the figures 15.5 to 15.7, where the measured and calculated flow rate at location D_2, and the pressures at the locations D_4, D_1, U_1 or U_2, and U_4 are plotted against time (see figure 13.2 for pressure tap locations).

Figure 15.5 shows a simulation of a dynamic test with the membrane check valve. The maximum pressures are predicted rather well, while the minimum pressures are underestimated. The latter is attributed to the fact that cavitation is not modelled (CVWP has no cavitation model).

Figure 15.6 shows a simulation of a dynamic test with the butterfly check valve. The agreement between simulation and experiment is rather good, except for the pressure head oscillations, which are quickly damped in the experiment.

Figure 15.7 shows a simulation of a dynamic test with valve hammer due to an overloaded damper. The flow rate and pressures are predicted reasonably well up to the minimum flow rate. Hereafter the measured pressures at the check valve show violent oscillations. The effects of valve hammer are not seen in the simulation, since the flow loops associated with reopening and reclosure are not represented in these characteristics.

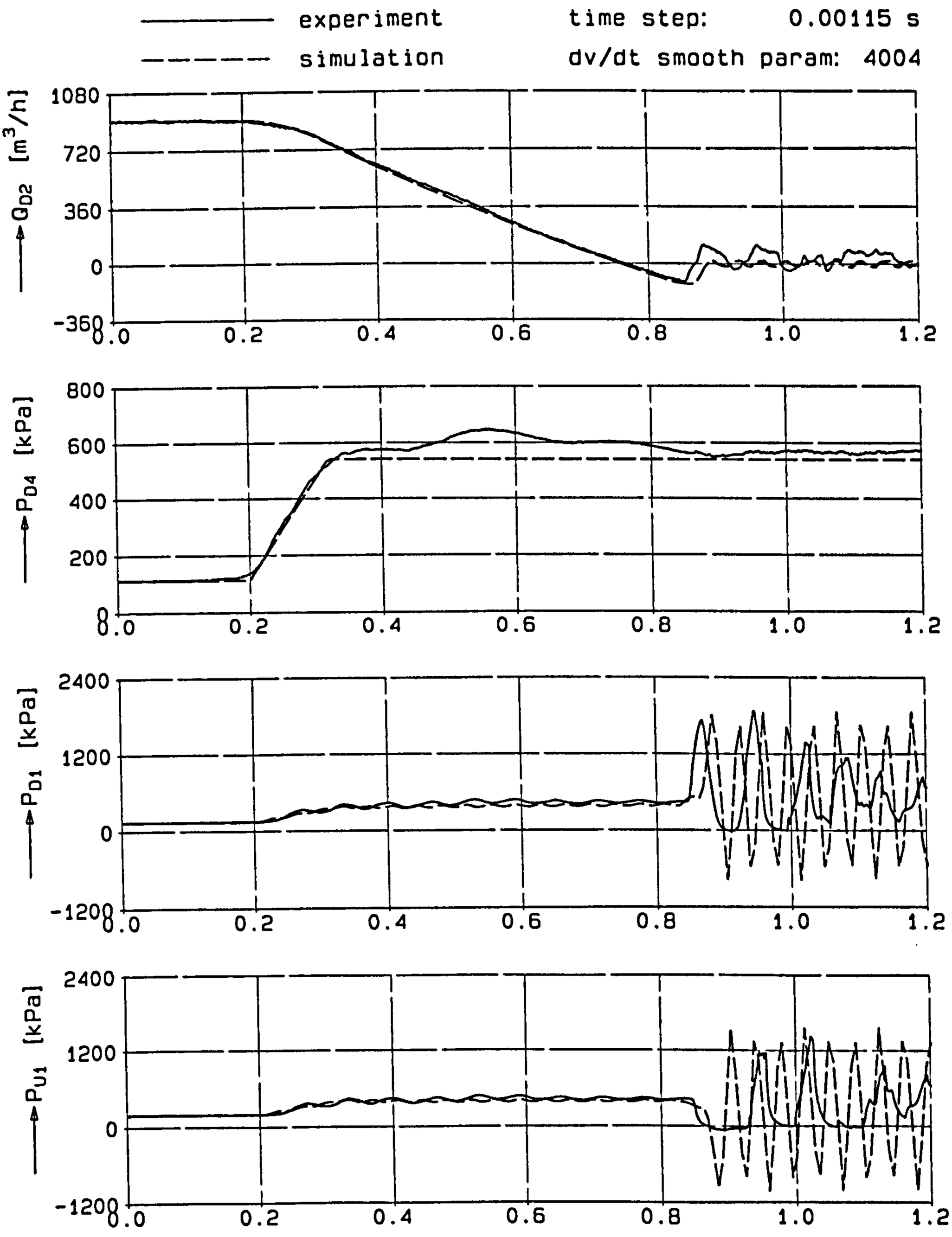

Figure 15.5 Simulation of dynamic test; membrane check valve

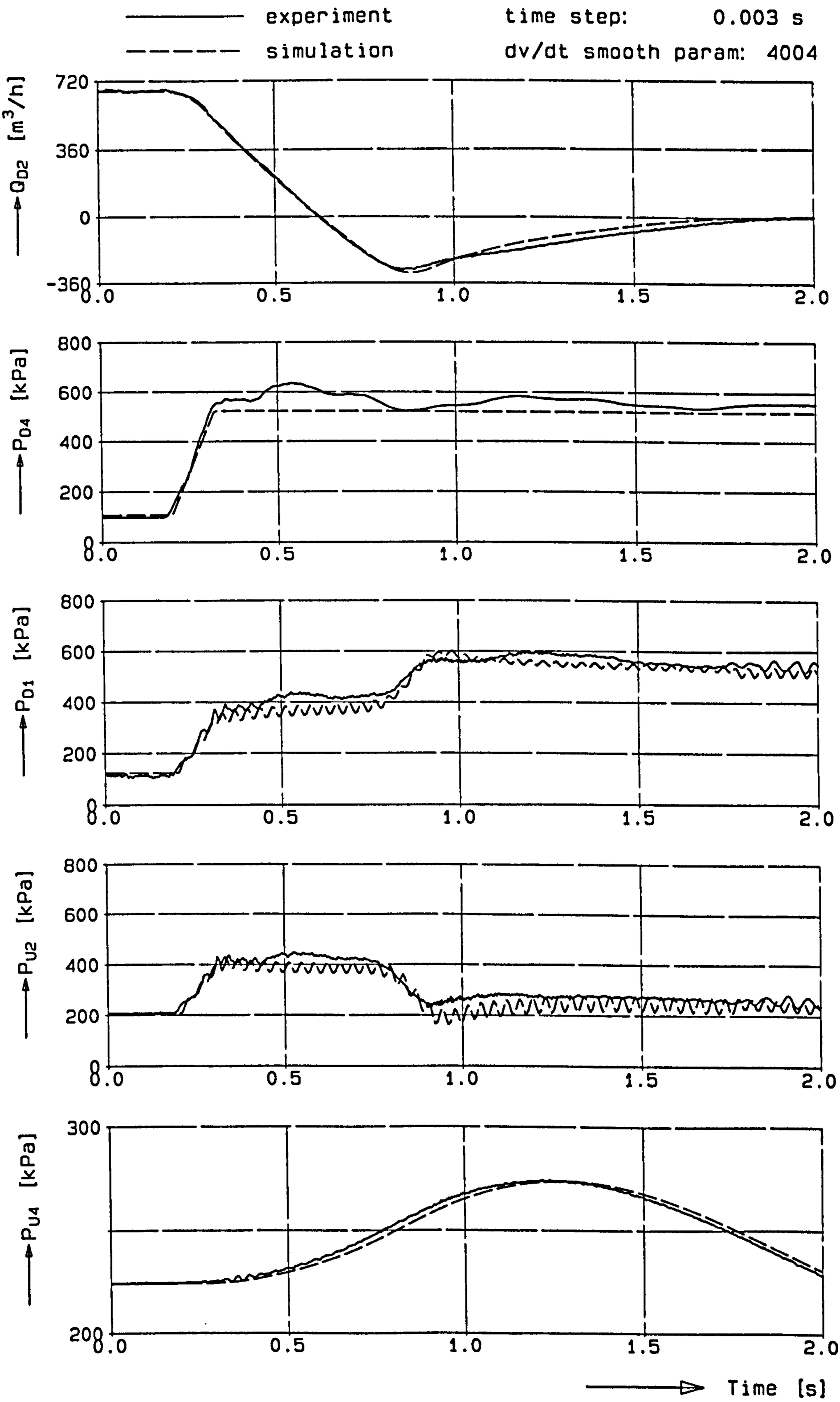

Figure 15.6 Simulation of dynamic test; 200 mm butterfly check valve

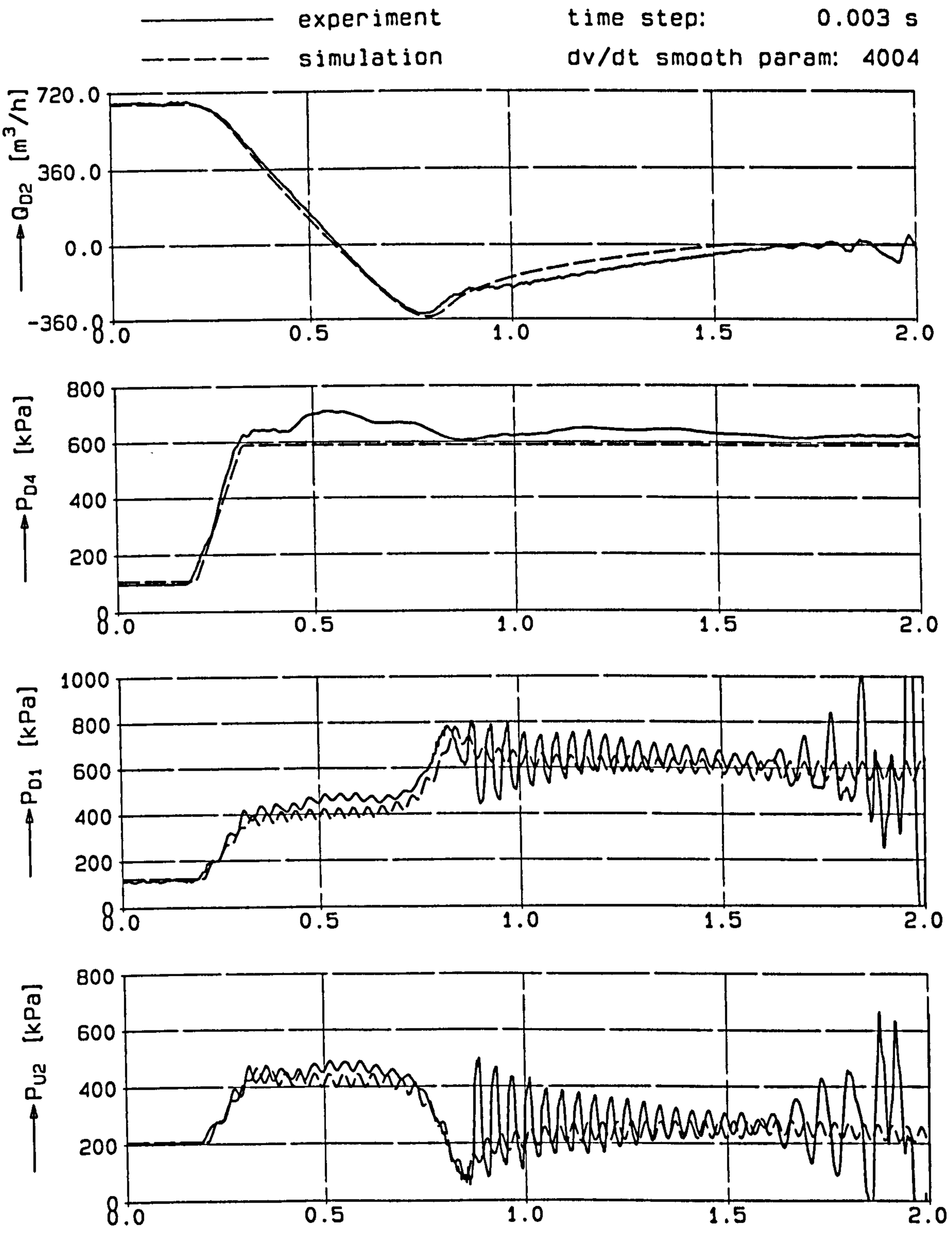

Figure 15.7 Simulation of dynamic test; 200 mm butterfly check valve

For the complete data set and further details about the simulations it is referred to CVRP report part V (Kruisbrink, 1996).

General remarks with respect to the simulations are:

- The locations in the simulations (i.e. grid points) are time step dependent. Therefore these locations do not exactly coincide with the pressure tap locations of the experiments.
- The pressure at the high pressure tank is too low in the simulations, while the initial flow deceleration is correctly simulated. This is attributed to inertia effects in the high pressure tank and in the short adjacent 800 mm pipe, which are not taken into account (the short pipe with a length of 1.50 m is not modelled). Including these inertia effects would require a higher pressure at the pressure tank.

Based on all simulations the following general conclusions can be made (note that not all conclusions can be drawn from the results presented here):

- The resemblance between simulation and experiment increases slightly with decreasing time step, as expected, although the sensitivity for the time step is rather small.
- The resemblance between simulation and experiment slightly decreases with increasing filtering, as expected, although the differences are rather small.
- The influence of the closure phase angle ϕ is small here.
- The effects of cavitation are not simulated (CVWP has no cavitation model).
- The effects of valve hammer are not simulated.
- The overall accuracy in terms of fluid velocities and pressure head changes at the check valve is within 15%, with the exception of cavitation and valve hammer effects.

15.3 Review and conclusions

The dynamic scale laws are validated by means of numerical simulations with a special version of the waterhammer computer code WTSL$^+$, which enables to start from initial, unsteady flow conditions. It is concluded that the dimensionless, unsteady flow parameters and the dimensionless valve characteristics of approach 1 are well defined and consistent with conventional waterhammer theory.

The model for damped check valves is validated against experiments. The simulations of dynamic tests show an acceptable reproducibility (overall accuracy within 15%), with the exception of cavitation and valve hammer effects, which are not described by the valve characteristics of approach 2.

16 Conclusions and recommendations

16.1 Final conclusions

A semi-empirical method is developed to describe the dynamic behaviour of check valves in pipeline systems. The method is based on "*parameterized*" valve models, which describe the overall behaviour of the check valve in the form of dimensionless valve characteristics. The characteristics are determined from experiments, whereby the check valve is considered as a *black box*, and described in terms of dimensionless flow variables, valve and system parameters. The method can be applied to all types of check valves. Undamped check valves may be considered as a special case of damped check valves.

An extensive survey of literature reveals that within the research into the dynamic behaviour of check valves mainly a *direct* approach is followed. For many different valve types, valve reponse models are developed, whereby the description of the hydrodynamic effects is subject to some speculation. The valve response models are used in uncoupled or coupled mode with waterhammer computer programs. The research is restricted to case studies. No attempts are made to generalize, non-dimensionalize or standardize the application of these tools.

More general studies in the field of aerodynamics and hydrodynamics are mainly restricted to translating bodies. Not much is known about the unconfined or confined flow problem of rotating bodies in unsteady fluid flows.

Although many different check valve types exist, the internal geometry of the valves including the moving elements, is characterized by at least one plane of symmetry. In most cases the moving elements are translating or rotating bodies. These geometrical conditions are used to derive general equations of motion for check valves, and descriptions for the hydrodynamic (fluid) forces on the moving elements.

Much attention is paid to the description of the hydrodynamic (fluid) forces on translating or rotating bodies with one plane of symmetry, in inviscid or viscous, unconfined or confined, unsteady fluid flows.

The equations of motion for a body in an unconfined, inviscid fluid are based on the dynamical theory of Kirchhoff, extended to an unsteady fluid flow. Based on an analogy between an eccentricity and viscosity the step from inviscid to viscous fluids

is made. The equations of motion for a body in a confined, inviscid fluid are based on Lagrange's method of generalized coordinates.

In the Lagrangian approach of the dynamical theory of Kirchhoff the coefficients in the kinetic energy equations are constants, determined by the geometry of the body. This enables the development of analytical expressions for the fluid force terms and coefficients. It thus gives insight into the basic properties of these quantities.
In the Eulerian approach of Lagrange's method of generalized coordinates the coefficients in the kinetic energy equations are not longer constants. Analytical expressions generally become very complex, but do exist for a few academical cases. The equations are used in a qualitative sense only.

In both approaches the fluid forces and torques are described by drag, added mass, history and pressure terms, used in a somewhat extended sense. The drag coefficients are assumed to be dominated by viscous effects, while the added mass coefficients are assumed to be dominated by unsteady flow effects. The coefficients are approximated and described by power law formulations.

The fluid equations are described in a global form, analogous to the conventional drag term, whereby several options for the dynamic pressure are explored. Based on the properties of the fluid force coefficients it is concluded that some of these options are more suited to unconfined fluids, and others to confined fluids. The global form of the fluid equations for confined fluids is applied to check valves.

A general valve equation of motion is derived for most of the existing check valve types. The equation is described in a dimensionless form, whereby the critical velocity and the valve diameter are used to define a velocity and a time scale.

Conventional waterhammer theory is applied to describe the transient flow in a pipeline system due to a valve closure under unsteady, initial flow conditions and reflection free or reflecting boundary conditions. Hereto basic differential equations are derived for a flow with constant initial flow deceleration. The classical Joukowsky equation is extended to unsteady flow conditions.

The integral form of the momentum equation is used to describe the check valve as short length component. The fluid forces on the valve elements, described in the form of a global force coefficient (i.e. the dynamic valve loss coefficient), are related to the pressure difference across the valve. The valve and pipe equations are coupled via this momentum equation. This leads to a dimensionless group in the form of a Mach number, of which the importance is unknown here.

The uncoupled and coupled, (dimensionless) pipe and valve equations show formally which (dimensionless) variables and valve, system and fluid parameters are relevant during the stages of passive and active damping. In that sense they are used in a dimensional analysis to develop valve characteristics and dynamic scale laws.

Two approaches are followed. In the first approach the check valve behaviour is described in terms of global, (dimensionless) fluid velocity, pressure head and damping characteristics. In the second approach the behaviour is described more detailed in terms of dynamic valve loss coefficients.

Additional dimensionless valve characteristics are introduced. A characteristic which correlates the steady and unsteady flow behaviour, enables a more general comparison of check valve types. A characteristic which correlates the inertia effects to the unsteady flow behaviour should enable the scaling from or comparison between liquid and gas service.

Semi-empirical models are developed to simulate the dynamic behaviour of check valves in waterhammer computer codes. The models for undamped and damped check valves are based on the valve characteristics of approach 1 and 2, respectively. The behaviour of undamped check valves is system-independent, which enables to define a valve model, that is generally applicable. The behaviour of damped check valves is system-dependent. Therefore the application of the valve characteristics is restricted to applications, which are about similar to the laboratory conditions.

The application of neural networks (NN) is explored for the non-linear interpolation and extrapolation in the valve characteristics of approach 2. The NN gives a better insight into the surface which is formed by a series of dynamic tests in the three-dimensional physical space.

The valve models are implemented in the waterhammer computer code CVWP.

A method is described to calibrate flowmeters under unsteady flow conditions. The method is based on rigid column theory, whereby the pressure head gradient along the pipe is used as a reference. It is demonstrated that the method can be applied in practice.

Several series of steady and dynamic tests on weakly and strongly damped check valves are performed in the test rig for check valves at Delft Hydraulics. From the experimental data the valve characteristics of approach 1 and 2 and other valve characteristics are derived.

The dynamic scale laws laws are validated by means of numerical simulations and found to be consistent with the conventional waterhammer theory. The valve models are validated against the experimental data by simulating the dynamic tests in the laboratory with the waterhammer computer code CVWP. The results show an acceptable reproducibility (accuracy within 15 %). Hereby the effects of cavitation and valve hammer, which are not modelled, are excluded.

The results of the study provide a method for valve comparison and classification, and an engineering tool in pipeline and valve design, valve selection, adjustment of damping devices and pressure surge analyses.

16.2 Recommendations for further research

In the model for undamped check valves (approach 1) a function is introduced, which accounts for the effect of an initially, partly opened valve on the valve response. This function is in first instance chosen as a linear form of the steady flow characteristic, whereby inertia effects are ignored. Further research is needed into the character of this function. In principle the information about inertia effects, which is contained in the dynamic closure characteristics, can be used for a better estimation of the "initial" valve disc position after reopening.

During the last stage of closure the check valve behaviour is physically unstable. This is revealed by numerical instabilities in the model for damped check valves (approach 2). To overcome these instabilities prescribed trajectories are introduced. The question arises, if the prescribed trajectories in the present model can be replaced by another numerical procedure which ensures stability. In this respect it should be mentioned that the valve disc position is not used here, since it cannot always be measured. However it possibly may be used as auxiliary variable to ensure a stable closure (e.g. linear motion during the stage of active damping).

The storage capacity of check valves with non-rigid, moving elements, like the membrane check valve, is neither described in the model for damped check valves, nor measured. In order to describe this effect, the upstream *and* downstream flow rate must be known (In the present study only one flowmeter is used). Since the differences between these flow rates are generally very small, measurement equipment is needed with an extreme high accuracy, far beyond that of the flowmeters used.

The relative importance of all valve and system parameters is not yet known, (e.g. the ratio of fluid density and density of the moving valve elements, the ratio of critical velocity and pressure wave speed). For this purpose a sensitivity analysis must be performed. In principle this can be performed by means of simulations with a computer code like CVWP, after enough experimental data have become available.

The application of neural networks is thus far restricted to the flow variables within the valve characteristics of approach 2. However, in principle it may be extended to the valve and system parameters as well. In that case the valve and system parameters must be added to the NN as input parameters. As a next step the

phenomenon of flow loops may also be described by the NN. Here some counter may be added to the input parameters for the registration of the flow loop number.

The present study is limited to the measurement of closure characteristics. In addition also opening characteristics can be measured, although their practical relevance is less. Thus the (re)opening model for undamped check valves can be improved, and the gap in the characteristics for damped check valves (quadrant 1) can be filled in.

Although it was strived after, an experimental validation of the scale laws could not be realized, due to practical problems with the valves as well as with the test facility. In this respect it is encouraging that the follow up of the Check Valve Research Project is ensured within the Large Installations Program (LIP part III) of the EC. Within this program a project proposal about the validation of dynamic scale laws, by means of series of dynamic tests under different laboratory conditions has been accepted.

As a next step the validation of the valve models against practical applications can be mentioned.

The present study is restricted to slightly compressible fluids. An important step is that from liquid to gas service. It is believed that, in a qualitative sense, the present results are also applicable to compressible fluids, if the Mach number is relatively low (smaller than about 0.15).

In this respect it should be mentioned that Novacor and NOVA Gas Transmission (Canada) work on compressible flow applications. Botros et al. (1996) describe a large scale, air test loop for the dynamic testing of check valves. Botros and Roorda (1996) apply the dimensional analysis of the present study to compressible flow applications. Although pressure surges are less relevant in gases, the check valve becomes more sensitive to valve chatter.

The results of the present study may directly be applied to *control valves*. The major difference is that the disc position of control valves is prescribed in time. In that sense control valves may be considered as a special case of check valves.

The dynamic scale laws, as developed for check valves in pipeline systems, allow the development of equivalent scale laws for other system components like air vessels, pumps, etc. The theory may be extended to *fluid-structure interaction*. In that case additional velocity and time scales arise, due to the structural motion and wave speed. It is concluded with the remark that, as such, the study forms a basis for a further generalization of the methodology (by means of dimensional analysis or otherwise) for pipeline systems and its components.

References

Alonso, M. and Finn, E.J., 1976: *Fundamentele Natuurkunde; Deel 1 mechanica* (derde, herziene druk), Elsevier, Amsterdam-Brussel.

Basset, A.B., 1888: *A Treatise on Hydrodynamics*, Volume 2, Deighton Bell and Co., Cambridge, England.

Billington, M.J., Harrison, D. and Vivian, B.E., 1985: *The identification and evaluation of valve problems*, Proceedings of the International Conference on Developments in Valves and Actuators for Fluid Control, BHRA, Oxford, England, pp. 305-318.

Blasius, H., 1913: *Das Ähnlichkeitsgesetz bei Reibungsvorgängen in Flüssigkeiten*, Forschg. Arb. Ing.-Wes. No.134, Berlin.

Botros, K.K., Jones, B.J. and Roorda, O., 1996: *Flow characteristics and dynamics of swing check valves in compressible flow applications (Part I)*, Paper presented at the ASME Pressure Vessels and Piping Conf., Montreal, Canada, July 21-26.

Botros, K.K. and Roorda, O., 1996: *Flow characteristics and dynamics of swing check valves in compressible flow applications (Part II)*, Paper presented at the ASME Pressure Vessels and Piping Conference, Montreal, Canada, July 21-26.

Boussinesq, J., 1885: *Sur la résistance qu'oppose un liquide ... au mouvement varié d'une sphere solide ... et produits soient negligeables*, Comptes Rendues Acad. Science Paris 100, pp. 935-937.

Campbell, W.F., 1982: *The added mass of some rectangular and circular flat plates and diaphragms*, Nat. Res. Council Canada, Report LTR-LA-223.

Charbonneau, A.G., 1988: *Innovations in non-intrusive testing and trending of motor operated valves and check valves*, Proceedings of the 2nd Int. Conference on Developments in Valves and Actuators for Fluid Control, BHRA, Manchester, England, pp. 301-310.

Cho, S.M. and Kane, R.S., 1980: *Techniques for the thermal/hydraulic analysis of LMFBR check valves*, ASME Journal of Engineering for Power, Vol. 102, pp. 660-665.

Cleijne, H. and Smulders, P., 1987: *Valve motion in piston pumps*, World Pumps, March 1987, pp. 64-70.

Colebrook, C.F., 1939: *Turbulent flow in pipes with particular reference to the transition region between the smooth and rough pipe laws*, J. Institution Civil Engineers, 1939; see also: Engineering hydraulics (H. Rouse, ed.), Chapter VI: Steady flow in pipes and conduits, by V.L. Streeter, New York, 1950.

Collier, S.L., 1980: *Understanding design and operation of self-actuating check valves*, Plant Engineering, August 7, 1980.

Collier, S.L., 1983: *Knocking from valve hammer in triplex pumps*, ASME Paper no. 83-PET-29.

Collier, S.L. and Hoerner, C.C., 1981: *Development of affinity relations for modeling characteristics of check valves*, ASME Journal of Energy Resources Technology, Vol. 103, pp. 196-200.

Collier, S.L. and Hoerner, C.C., 1982: *A facility and approach to performance test of check valves*, Proc. of the ASME Energy Sources Technology Conference & Exhibition, New Orleans, USA, March 1982, Paper No. 82-Pet-16; ASME Journal of Energy Resources Technology, Vol. 105, March 1983, pp. 62-67.

Collier, S.L., Hoerner, C.C. and Davila, C.E., 1983: *Behavior and wear of check valves*, ASME Journal of Energy Resources Technology, Vol. 105, March 1983, pp. 58-61.

Combes, G., 1982: *Battement des clapets anti-retour*, T.S.M.-l'Eau, February 1982, pp. 111-113.

Deich, A. and Jörgl, H.P., 1981: *Ein dynamisches Modell für Exzenter-Rückschlag-klappen*, Regelungstechnik, 29. Jahrgang, Heft 2, pp. 47-52.

Dooley, W.T. and Mosby, W.R., 1983: *Comparison of NUPIPE-II and SAP IV predicted and experimentally determined dynamic structural responses for German standard problem 4A*, Presented at the ASME 4th National Congress on Pressure Vessel & Piping Technology, Portland, U.S.A., June 19-24; Advances in Fluid Structure Interaction Dynamics, PVP-Vol. 75, pp. 95-119, Moody and Shin (editors), New York, 1984.

Douglas, J.F., Gasiorek, J.M. and Swaffield, J.A., 1979: *Fluid Mechanics*, Pitman Publishing Limited, London.

Douglas, J.M., 1969: *The Glenfield 'Recoil' check valve*, The Glenfield Gazette, No. 230, pp. 23-25.

Ellis, J., 1980: *Study of pipe-liquid interaction following pump trip and check-valve closure in a pumping station*, Proceedings of the 3rd International Conference on Pressure Surges, BHRA, Canterbury, England, pp. 203-220.

Ellis, J. and Mualla, W., 1983: *Wave induced transients in a pumping station storm overflow*, Proceedings of the 4th International Conference on Pressure Surges, BHRA, Bath, England, pp. 243-262.

Ellis, J. and Mualla, W., 1986: *Numerical modeling of reflux valve closure*, ASME Journal of Pressure Vessel Technology, Vol. 108, No.1, pp 92-97.

Erdödy, I. and Bökemeier, V., 1981: *The closure behaviour of undamped swing check valves*, Proceedings of the 5th Int. Symposium on Water Column Separation, IAHR, Obernach.

Esleeck, S.H. and Rosser, R.M., 1959: *Check valve water hammer characteristics*, Paper presented at the American Nuclear Society Meeting, November 1959.

Föllmer, B., 1987: *Production and development of check valves with a good dynamic behaviour*, Paper presented at the one-day conference on check valves at Delft Hydraulics, Delft, The Netherlands, March 20.

Fox, R.E., 1980: *Dungeness 'B' Power Station condensate system surge tests*, APC Report No. 1, March 1980 and Report No. 3, April 1981.

Goldstein, H., 1980: *Classical mechanics*, Addison-Wesley Publishing Company, Reading Massachusetts.

Gronau, M. and Zwink, E., 1984: *Untersuchungen eines dynamischen Modells für Exzenter Rückschlagklappen am Analog- und Digitalrechner*, Regelungstechnik, 32. Jahrgang, Heft 3, pp. 90-96.

Gwinn, J.M., 1974: *Swing-check valves under trip loads*, ASME, Paper 74-PVP-51.

Halliday, D. and Resnick, R., 1966: *Physics*, John Wiley and Sons, New York · London ·Sydney.

Haynes, H.D., 1991: *Check valves: Oak Ridge's new diagnostics*, Mechanical Engineering, May 1991, pp. 64-69.

Henry, J.M., Huet, J.L. and Ziegler, B., 1989: *Damped check valves for nuclear pressure vessel isolation*, Proceedings of the 6th International Conference on Pressure Surges, BHRA, Cambridge, United Kingdom, pp. 281-294.

Hinze, J.O., 1975: *Turbulence*, McGraw-Hill, New York.

Horsten, J.B.A.M., 1990: *On the analysis of moving heart valves*, Ph.D. Thesis, Eindhoven Univ. of Technology, Wibro, Helmond, The Netherlands.

Houghton, G., 1963: *The behaviour of particles in a sinusoidal velocity field*, Proc. R. Society, 272A, pp. 33-43.

Hsu, S.T. and Ramey, M.P., 1988: *Transients induced by large check valves*, ASME Paper 88-WA/FE-11, presented at the Winter Annual Meeting, Chicago, Illinois, U.S.A., November 27-December 2.

Huet, J.L., Garcia, J.L, Coppolani, P. and Ziegler, B., 1987: *Experimental and analytical studies on water hammer generated by the closing of check valves*, Trans. of SMiRT IX, Lausanne, Switzerland, Paper F3.

Hughes, R.R. and Gilliland, E.R., 1952: *Chemical Eng. Progr.*, 48, pp. 497.

Hulst van, L.P.D.M. and Kruisbrink, A.C.H., 1993: *Check Valve Research Project, WTSL$^+$ simulations*, KEMA Report 33119-FPP-938010.

Jeanmougin, N.M., 1986: *NRC valve performance test program - check valve testing*, Paper presented at the Water Reactor Safety Meeting, Washington, December.

Johnson, D.E., Johnson, J.R. and Moore, H.P., 1982: *Handboek actieve filters*, Maarten Kluwer's Internationale Uitgeversonderneming.

Joukowsky, N., 1898: *Über den hydraulischen Stoss in Wasserleitungsröhren*, Mémoires de l'Académie Impérial des Sciences de St.-Pétersbourg, 1900, Series 8, Vol. 9, No. 5.

Kim, H.T., 1989: *A feedwater system waterhammer analysis*, ASME Paper PVP V 156, Pressure Vessels and Piping Division, pp. 11-15.

Kirchhoff, 1869: *Über die Bewegung eines Rotationskörpers in einer Flüssigkeit*, Crelle, lxxi. 237, Ges. Abh. pp. 376; Mechanik, Leipzig, c. xix.

Kirik, M.J. and Gradle, R.J., 1980: *A model for check valve/feedwater system waterhammer analysis*, ASME Paper 80-C2/PVP-27, presented at the Century 2 Pressure Vessels & Piping Conference, San Francisco, U.S.A.

Koch, B., 1981: *Computer simulation of waterhammer applied to check valves and valve stroking in pipe networks*, Paper presented at the Conference on Computer Simulation, Harrogate, May 13-15.

Koetzier, H., Kruisbrink, A.C.H. and Lavooij, C.S.W., 1986: *Dynamic behaviour of large non-return valves*, Proceedings of the 5th International Conference on Pressure Surges, BHRA, Hannover, F.R. Germany, pp. 237-244.

Kruisbrink, A.C.H., 1988: *Check valve closure behaviour; experimental investigation and simulation in waterhammer computer programs*, Proceedings of the 2nd International Conference on Developments in Valves and Actuators for Fluid Control, BHRA, Manchester, England, pp. 281-300.

Kruisbrink, A.C.H., 1990: *Modelling of safety and relief valves in waterhammer computer codes*, Proceedings of the 3rd Int. Conference on Developments in Valves and Actuators for Fluid Control, BHRA, Bournemouth, United Kingdom, 27-29 March, pp. 137-150.

Kruisbrink, A.C.H., 1992*: *Check Valve Research Project, Part I: Theory*, Report J0666, Delft Hydraulics, Delft, September 1992.

Kruisbrink, A.C.H., 1993a*: *Check Valve Research Project, Part II: Theory and set up experiments*, Report J0667, Delft Hydraulics, Delft, April 1993.

Kruisbrink, A.C.H., 1993b*: *Check Valve Research Project, Part III: Experiments*, Report J0667, Delft Hydraulics, Delft, November 1993.

Kruisbrink, A.C.H., 1994*: *Check Valve Research Project, Part IV: Experiments (continued)*, Report J0667, Delft Hydraulics, Delft, September 1994.

Kruisbrink, A.C.H., 1996*: *Check Valve Research Project, Part V: Reference book*, Report J0668, Delft Hydraulics, Delft, June 1996.

Kruisbrink, A.C.H., and Thorley, A.R.D., 1994: *Dynamic characteristics for damped check valves*, Proceedings of the 2nd International Conference on Water Pipeline Systems, Edingburgh, Scotland, United Kingdom, 24-26 May, pp. 459-476.

Kubie, J., 1982: *Performance and design of plug-type check valves*, Proc. Instn. Mechanical Engineers, Vol. 196, pp. 47-56.

Lamb, H., 1932: *Hydrodynamics* (reprinted 6th edition in 1963), University Press, Cambridge.

Landau, L.D. and Lifshitz, E.M., 1987: *Fluid mechanics*, Course on theoretical physics, Volume 6 (2nd edition), Pergamon Press, Oxford, pp. 83-85.

* Confidential, not published.

Lewinsky-Kesslitz, H.P., 1965: *Über die Dynamik der Rückschlagklappe*, Österreichische Ingenieur-Zeitschrift, 8. Jahrgang, Heft 6, pp. 185-191.

Livingston, A.C., 1954: *Reflux and allied self closing valves*, Proceedings of the 3rd Conference on Hydromechanics, BHRA, Paper SP 490.

Massey, B.S., 1971: *Units, Dimensional analysis and physical similarity*, Van Nostrand Reinhold Company, London.

Maxey, M.R., and Riley, J.J., 1982: *Equations of motion for a small rigid sphere in a non-uniform flow*, Phys. Fluids, 26(4), pp. 863-889.

Mei, R., Adrian, R.J. and Hanratty, T.J., 1991: *Particle dispersion in isotropic turbulence under Stokes drag and Basset force with gravitational settling*, Journal of Fluid Mechanics, Vol. 225, pp. 481-495.

Merk, H.J., 1982: *Fysische stromingsleer*, Lecture notes, Delft Univ. of Technology, Laboratory for Aero and Hydrodynamics, The Netherlands.

Müller, W.C., 1987: *Piping analysis of large scale experiments with ADINA and DAPSY*, Computers & Structures, Vol. 26, No. 1/2, pp. 111-121.

Obering, Von, Eschment and Zedlitz, 1966: *Rückschlagorgane in Rohrleitungen*, Bohrtechnik Brunnenbau Rohrleitungsbau, 17. Jahrgang, May 1966.

Odar, F., and Hamilton, R.H., 1964: *Forces on a sphere accelerating in a viscous fluid*, Journal of Fluid Mechanics, 18, pp. 302.

O'Keefe, W., 1976: *Check Valves*, Power, Vol. 120, No. 8, pp. 25-36.

Oseen, C.W., 1927: *Hydrodynamik*, Akademische Verlagsgesellschaft, Leipzig.

Pake, M.C., 1983: *Non-return valve testing, description of a rig and preliminary results for a double-disc valve*, Proceedings of the 6th International Symposium on Hydraulic Transients in Power Stations, IAHR, Gloucester, England.

Panet, M. and Martin, R., 1988: *Tests of check valves at EDF: development of a damped check valve*, Proc. of the 2nd Int. Conf. on Developments in Valves and Actuators For Fluid Control, BHRA, Manchester, England, pp. 257-280.

Pool, E.B., Porwit, A.J. and Carlton, J.L., 1962: *Prediction of surge pressure from check valves for nuclear loops*, ASME Paper No. 62-WA-219, presented at the Winter Annual Meeting, New York, November 25-30.

Prost, J., 1992: *Versuche an Drosselklappen unter dynamischen Betriebsbedingungen*, 3R International, 31 (1992), Heft 1/2, pp. 22-28.

Provoost, G.A., 1980: *The dynamic behaviour of non-return valves*, Proceedings of the 3rd Int. Conf. on Pressure Surges, BHRA, Canterbury, England, pp. 415-428.

Provoost, G.A., 1982: *The dynamic characteristic of non-return valves*, Paper presented at the 11th Symposium of the Section of Hydraulic Machinery, Equipment and Cavitation: "Operating problems of pump stations and power plants", IAHR, Amsterdam, the Netherlands, September 13-17.

Provoost, G.A., 1983a: *Theoretical approach to a check valve response in the cooling water circuit of a power plant*, Paper presented at the 6th Int. Symposium on Hydraulic Transients in Power Stations, Gloucester, England, September 19-20.

Provoost, G.A., 1983b: *A critical analysis to determine dynamic characteristics of non-return valves*, Proceedings of the 4th Int. Conference on Pressure Surges, BHRA, Bath, England, pp. 275-286.

Remenieras, G., 1952: *Dispositif simple pour réduire la célérité des ondes élastiques dans les conduites en charge*, La Houille Blanche, No Spécial A/1952.

Rommel, J.C., Traiforos, S.A. and Bell, J.H., 1984: *A methodology for calculating a check valve closure following a postulated line break*, ASME Paper PVP Vol. 91, Two-phase flow and waterhammer loads in vessels, piping and structural systems, New York, June 1984.

Rop, K., 1987: *Selection of check valves; safety and reliability in industrial plants*, Paper presented at the one-day conference on check valves at Delft Hydraulics, Delft, The Netherlands, March 20.

Sande, E. van de, Belde, A.P. and Hamer, B.J.G., 1980: *Velocity profiles in accelerating pipe flows started from rest*, Proceedings of the third Int. Conference on Pressure Surges, BHRA, Canterbury, England, pp. 1-14.

Sauren, A.A.H.J., Steenhoven ,A.A. van, Renterghem, R.J., Rousseau, E.P.M., 1981: *Onderzoek aan aortaklep voor ontwerp vliesklepprothese*, De Ingenieur, Nummer 1/2, pp. 17-21.

Schlichting, H., 1979: *Boundary-layer theory*, McGraw-Hill, New York.

Schneider, D., 1985: *Dynamisches Verhalten von Doppelrückschlagklappen*, 3R International, 24. Jahrgang, Heft 4.

Schultz-Grunow, F., 1935: *Reibungswiderstand rotierender Scheiben in Gehäusen*, ZAMM 15, pp. 191-204. See also: H. Föttinger, 1937, ZAMM 17, pp.356-358 and K. Pantell, 1950, Forschg. Ing.-Wes. 16, pp. 97-108.

Schöneborn, P.R., 1974: *The interaction between a single particle and an oscillating fluid*, Int. Journal Multiphase Flow, Vol. 2, pp. 307-317.

Sellgren, A., 1983: *Unsteady motion of particles in water*, W.R.E.L., Series A, no. 119, Lulea University, Sweden.

Siikonen, T., 1983: *Computational method for the analysis of valve transients*, ASME Journal of Pressure Vessel Technology, Vol. 105, pp. 227-233.

Slegers and Wölk (year unknown): *Fluid und Ventildynamik* (Bericht KWU).

Standard, 1959: *Keerkleppen voor water in nominale maten tot en met 50 mm*, KIWA, Keuringseisen nr. 25; "Water", The Netherlands, 16 April 1959.

Standard, 1975a: *Keerkleppen voor water in nominale maten tot en met 50 mm*, KIWA, Kwaliteitseisen nr. 25 (1e herziening), The Netherlands, 16 January 1975.

Standard, 1975b: *Bau und Prüfung von Rückflussverhinderern bis NW 50*, DVGW, Wasserversorgung Verbrauchsanlagen, Arbeitsblatt W376, Germany, November 1975.

Standard, 1977: *Wafer-type check valves*, API Standard 594 (second edition), U.S.A., December 1977.

Standard, 1990: *Keerkleppen voor water in nominale maten tot en met 1200 mm, klasse B*, KIWA, Kwaliteitseisen nr. 87, The Netherlands, 8 November 1990.

Steenhoven, A.A. van, and Dongen, M.E.H. van, 1979: *Model studies of the closing behaviour of the aortic valve*, Journal of Fluid Mechanics, Vol. 90, Part 1, pp. 21-32.

Steetzel, H.J., 1984: *Beweging van vaste deeltjes in een niet-stationaire waterbeweging*, M.Sc. Thesis, Vakgroep Vloeistofmechanica, Technische Hogeschool Delft, November.

Stokes, G.G., 1851: *On the effect of internal friction of fluids on the motion of pendulums*, Trans. Cambridge Phil. Society 9, Part II, pp. 8-106 or College Papers III, 55.

Suzuki, K., Taketomi, T. and Sato, S., 1991: *Interaction between oil hammer and poppet valve*, Japan Hydraulics and Pneumatics Soc., Journal 22(6), pp. 673-679 (in: Japanese).

Talman, J.A., 1994: *On the unsteady drag coefficients of single spherical particles in two-dimensional motion*, M.Sc. Thesis, Faculty of Applied Physics, Delft University of Technology, June 1994, Delft.

Tchen, C.M., 1947: *Mean value and correlation problems connected with the motion of small particles suspended in a turbulent fluid*, Ph.D. thesis, Delft University of Technology.

Thorley, A.R.D. and Oei, J.H., 1981: *Dynamic behavior of a swing check valve*, Proceedings of the 5th International Symposium on Water Column Separation, IAHR, Obernach, September 26-28.

Thorley, A.R.D., 1982: *A comparative review of check valve performance*, Confidential Report No. TF/1282/1, The City University, London.

Thorley, A.R.D., 1983: *Dynamic response of check valves*, Proceedings of the 4th International Conference on Pressure Surges, BHRA, Bath, England, pp. 231-242.

Thorley, A.R.D., 1985: *Can we develop a safe check valve?*, Proceedings of the International Conference on Developments in Valves and Actuators for Fluid Control, BHRA, Oxford, England, pp. 293-304.

Thorley, A.R.D., 1989: *Check valve behavior under transient flow conditions, a state-of-the-art review*, ASME Journal of Fluids Eng., Vol. 111, June 1989, pp. 178-183.

Thorley, A.R.D., 1991: *Fluid transients in pipeline systems*, D. & L. George Ltd, Hadley Wood, Barnet, England, 1991.

Tijsseling, A.S. and Lavooij, C.S.W., 1989: *Fluid structure interaction and column separation in a straight elastic pipe*, Proceedings of the 6th Int. Conference on Pressure Surges, BHRA, Cambridge, United Kingdom, pp. 27-41.

Tijsseling, A.S., 1993: *Fluid-structure interaction in case of waterhammer with cavitation*, Ph.D. Thesis, Delft University of Technology, Dept. of Civil Eng.; also published in the series "Communications on Hydraulic and Geotechnical Engineering", Dept. of Civil Engineering, Report No. 93-6.

Torobin, L.B. and Gauvin, W.H., 1959: *Fundamental aspects of solids-gas flow, Part III: Accelerated motion of a particle in a fluid*, Canadian Journal of Chemical Engineering, 37, no. 6, pp. 224-236.

Torobin, L.B. and Gauvin, W.H., 1961: *The drag coefficients of single spheres moving in a steady and accelerated motion in a turbulent motion*, American Institute of Chemical Engineering, Journal 7, no. 4, pp. 615-619.

Travis, J.R. and Torrey, M.D., 1985: *Thermal hydraulics of a feed-water pipe breakage with a back-pressure check valve*, ASME Fluids Engineering Division, Paper FED, Vol. 29, presented at the Winter Annual Meeting, Miami Beach, U.S.A., February 17-22.

Valibouse, B.S. and Verry, Ph.H., 1983: *Modelling check valve slamming*, Proc. of the 4th Int. Conference on Pressure Surges, BHRA, Bath, England, pp. 263-273.

Vennard, J.K. and Street, R.L., 1982: *Elementary fluid mechanics*, John Wiley and Sons, New York.

Weisshaupl, H., Schauki, N. and Braddy, R., 1989: *Analysis, testing and optimization of check valves*, Proceedings of the Pressure Vessels and Piping Conference, ASME, Honolulu, Hawaii, July 23-27.

Whiteman, K.J. and Pearsall, I.S., 1959: *Reflux valve and surge tests at Kingston pumping station*, BHRA-NEL Joint Report No. 1.

Worster, R.C., 1959: *The closing of reflux valves*, Paper presented at the 6th Conf. on Hydromechanics, BHRA, Troon, Scotland, May 5-10.

Worster, R.C., 1960: *The use of linearised equations in calculating the motion of reflux valves*, Report RR 676, British Hydromechanics Research Association, Cranfield, England.

Wylie, E.B., 1983: *Advances in the use of MOC in unsteady pipeline flow*, Proc. of the 4th Int. Conference on Pressure Surges, BHRA, Bath, England, pp. 27-37.

Wylie, E.B. and Streeter, V.L., 1993: *Fluid transients*, McGraw-Hill, New York.

Yamada, Y. and Imao, S., 1987: *Prevention of waterhammer by a check valve*, Paper presented at the 2nd Japan-China Joint Conference on Fluid Machinery, Sian, China, October 12-15.

Appendix A Valve equations

In this appendix general friction and damping models are described, which may be applied to most of the check valves types.

A.1 Friction model

Friction has a non-linear character which is not easily described. Several researchers like e.g. Worster (1960), Pool et al (1962), Piwinger (1971), Deich and Jörgl (1981), Thorley and Oei (1981), Gronau and Zwink (1984) have made attempts to describe the friction torque of check valves.

Worster (1960) describes the friction torque of a swing type check valve by:

$$T_F = \mu \, (F_G + F_B) \, r_f \qquad \textbf{(A.1)}$$

Where μ is a friction coefficient, $(F_G + F_B)$ represents the weight of the moving parts in water (all parts are submerged) and r_f is the radius of the sliding surface of the pivot pin.

Pool et al (1962) describe the bearing friction torque of a swing type check valve by:

$$T_F = \mu \, (\vec{F}_G + \vec{F}_H + \vec{F}_I) \, r_f \approx \mu \, \vec{F}_G \, r_f \qquad \textbf{(A.2)}$$

Where μ is the bearing friction coefficient, $F_{..}$ represent the forces due to gravitation, hydrodynamics and inertia, and r_f is the radius of the pivot pin bearing. Since the vector sum of the bearing forces is difficult to deterjmine, in first approximation only the disc weight is used as bearing load.

Piwinger (1971) describes the friction torque of a check valve with eccentrical disc and counterweight. He distincts packing friction:

$$T_F = \mu_p \, \frac{d_f^2}{2} \, (sign \; \dot{\theta}) \qquad \textbf{(A.3)}$$

And bearing friction:

$$T_F = \mu_b \, (\vec{F}_G + \vec{F}_H) \, \frac{d_f}{2} \, (sign \; \dot{\theta}) \qquad \textbf{(A.4)}$$

Where d_f is the diameter of the packing. The friction coefficient μ_p is taken as a constant. The bearing force is the vector sum of the gravitational and hydrodynamic forces, and thus a function of the angular valve disc position. Piwinger distincts static friction and sliding friction, both represented by the friction coefficient μ.

Deich and Jörgl (1981) follow the ideas of Piwinger.

Gronau and Zwink (1984) describe packing friction by:

$$\begin{aligned} &\dot{\theta} \neq 0 : && T_F = \mu_p \, d^2 \, sign(\dot{\theta}) \\ &\dot{\theta} = 0 \;\wedge\; T_G - T_H \leq T_{F_{max}} : && T_F = (T_G - T_H) \end{aligned} \qquad \textbf{(A.5)}$$

The sliding friction torque T_F ($\dot{\theta} \neq 0$) is taken as a constant, similar to Piwinger's value for packing friction. The static friction torque T_F ($\dot{\theta} = 0$) is taken as the net gravitational and hydrodynamic torque, as long as a threshold value (i.e. maximum static friction torque) is not exceeded.

Thorley and Oei (1981) describe the friction torque of a swing check valve in the form:

$$T_F = K_{f_1} + K_{f_2} \, \dot{\theta}^n \qquad \textbf{(A.6)}$$

Where K_{f1} and K_{f2} are constants and n is an arbitrary, and perhaps constant, power. However, they conclude from experiments that this approach is not very succesfull.

By combining the above-mentioned ideas the following friction model is applied without loss of generality:

$$\boxed{T_F = \sum K_f \, r_f \, F_n \, sign \dot{\theta}} \qquad \textbf{(A.7)}$$

Where K_f is a friction coefficient, r_f the moment arm of the friction force (e.g. radius of spindle, shaft, pin), and F_n the normal force on the friction surface(s). The friction torque is the sum of all friction effects in both valve and damper.

A.2

The friction coefficient K_f represents both static and sliding friction. In the case of static friction ($\dot{\theta} = 0$) the sign of $\dot{\theta}$ is determined by the sum of the other torques ($\dot{\theta} = 0^+$ or $\dot{\theta} = 0^-$). When the static friction torque exceeds a threshold value, the valve starts moving and sliding friction becomes relevant. In the common practice the static friction coefficient exceeds the sliding friction coefficient. The friction coefficient may be considered as a geometrical parameter since it is determined by surface roughness.

In the above friction model the friction force is proportional to the normal components of the (other) forces on the valve disc and damper. Thus it is suggested that the friction force is scalable, if the (other) forces are scalable. However, in practice the friction torque is hardly scalable due to:

- the relative surface roughness of larger valves is generally speaking smaller, so that friction coefficients tend to decrease with increasing valve size.
- clearance fits and tolerances are per definition unscalable.
- the magnitude of the static as well as the sliding friction coefficient is rather unpredictable due to wear (erosion and corrosion).

A.2 Damping model

The damper is modelled as a piston moving in a cylinder with bypass and throttle valve (figure A.1).

The damping torque on the valve shaft is described by:

$$T_D = (p_1 - p_2) A_{pn} e_d \qquad \textbf{(A.8)}$$

Where A_{pn} is the cross sectional area of the piston and e_d is the eccentricity of the piston from the centre of rotation of the valve disc.

It is assumed that the pressure difference across the piston is about equal to the pressure difference across the bypass:

$$p_1 - p_2 \approx \Delta p_{bp} \qquad \textbf{(A.9)}$$

The momentum equation for the fluid in the bypass is (section 10.2.3):

$$\rho_d L_{bp} A_{bp} \frac{dv_{bp}}{dt} = \rho_d g A_{bp} \Delta H_{bp} - f \frac{L_{bp}}{D_{bp}} \frac{1}{2} \rho_d v_{bp}^2 A_{bp} - X_f \qquad \textbf{(A.10)}$$

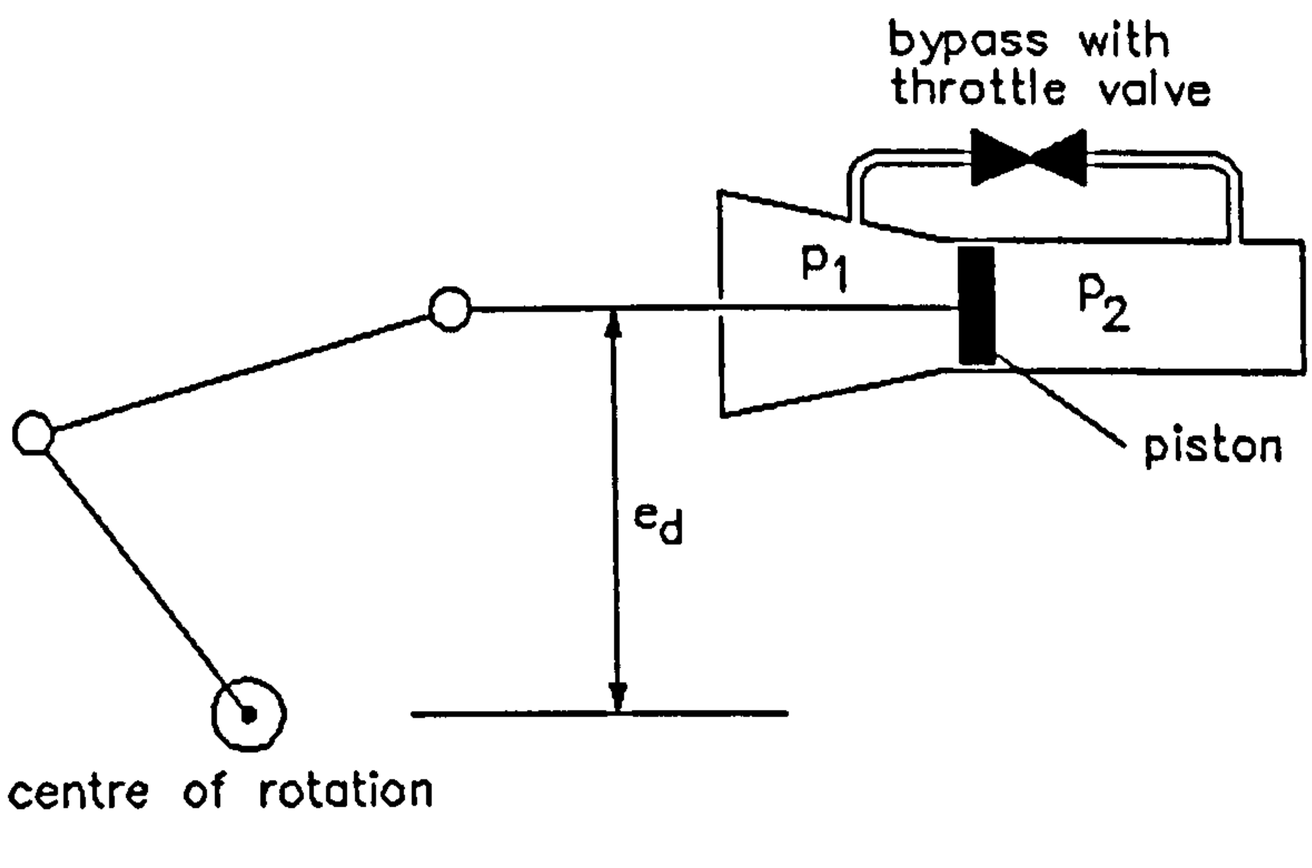

Figure A.1 Damping model

Where ΔH_{bp} is the pressure head difference across the bypass, f is the friction coefficient and L_{bp} is the length of the bypass pipe, and X_f is the fluid force on the throttle valve.

Although active or self-controlling throttle valves do exist (e.g. tested butterfly check valve), it is assumed that the throttle valve does not move ($\dot{x} = 0$). The fluid force on the throttle valve (*th*) may now be described by (section 6.5.1):

$$X_f = C_{D_{th}} \frac{1}{2} \rho_d v_{bp}^2 A_{bp} + \left(C_{A_{th}} + 1\right) \rho_d V_{th} \frac{dv_{bp}}{dt} \qquad \textbf{(A.11)}$$

Substitution of Equation (A.11) in Equation (A.10) gives:

$$\Delta p_{bp} = \left[C_{D_{th}} + f \frac{L_{bp}}{D_{bp}} \right] \frac{1}{2} \rho_d v_{bp}^2 + \left(\left(C_{A_{th}} + 1\right) V_{th} + L_{bp} A_{bp} \right) \frac{\rho_d}{A_{bp}} \frac{dv_{bp}}{dt} \qquad \textbf{(A.12)}$$

The first term in this equation may be considered as the drag of the bypass, while the second term may be considered as the sum of the added mass and pressure term of the bypass.

Substitution of the Equations (A.12) and (A.9) in Equation (A.8) gives for the damping torque:

$$T_D = \left[C_{D_{th}} + f \frac{L_{bp}}{D_{bp}} \right] \frac{1}{2} \rho_d v_{bp}^2 A_{pn} e_d + \left[\left(C_{A_{th}} + 1\right) \frac{V_{th}}{A_{bp}} + L_{bp} \right] \rho_d \frac{dv_{bp}}{dt} A_{pn} e_d \qquad \textbf{(A.13)}$$

Where (section 6.8):

$$C_{D_{th}} = \frac{C_t}{Re_d^p} \quad \Lambda \quad C_{A_{th}} = \frac{C_{tt}}{Ac_d^q} \tag{A.14}$$

And:

$$Re_d = \frac{\rho_d v_{bp} d_{bp}}{\mu_d} \quad \Lambda \quad Ac_d^{-1} = \frac{d_{bp}}{v_{bp}^2} \frac{dv_{bp}}{dt} \tag{A.15}$$

The damping torque is now described in terms of damping parameters. As a next step the above parameters are converted to valve parameters.

The Reynolds number of the flow in the damping device may be based on the average fluid velocity in the bypass pipe, during the stage of active damping. This is described by:

$$\bar{v}_{bp} = \frac{1}{t_c - t_d} \int_{t_d}^{t_c} v_{bp}\, dt \tag{A.16}$$

With the substitution of Equation (A.18):

$$\bar{v}_{bp} = \frac{1}{A_{bp}(t_c - t_d)} \int_{t_d}^{t_c} A_{pn} v_{pn}\, dt = \frac{V_{pn}}{A_{bp}(t_c - t_d)} \tag{A.17}$$

Where V_{pn} is the displaced piston volume and $(t_c - t_d)$ the damping time.

The dimensions of the damping are assumed to be small, relative to those of the pipeline system, so that pressure surges in the damping device may be ignored. In that case the fluid velocity v_{bp} in the bypass is proportional to the piston velocity v_{pn} (continuity; no leakage):

$$A_{bp} v_{bp} = A_{pn} v_{pn} \tag{A.18}$$

The piston velocity on its turn may be related to the angular disc position by:

$$v_{pn} = K_{v_{pn}} \dot{\theta} D \tag{A.19}$$

In general K_{vpn} is a function of the angular valve disc position.

All the dimensions of the damping device may now be related to the valve diameter via geometrical parameters $K_{..} = f(\theta)$. For instance:

$$e_d = K_{e_d} D \quad ; \quad A_{pn} = K_{A_{pn}} D^2 \quad ; \quad \ldots\ldots \qquad \textbf{(A.20)}$$

After some manipulation the Equations (A.13) to (A.15) may now be written in the form:

$$\boxed{T_D = C_{D_3} \frac{1}{2} \rho_d \dot{\theta}^2 D^5 + C_{A_3} \rho_d \frac{d\dot{\theta}}{dt} D^5}$$

(A.21)

Where:

$$C_{D_3} = \frac{C_3}{Re_3^p} \quad \Lambda \quad C_{A_3} = \frac{C_{33}}{Ac_3^q} \qquad \textbf{(A.22)}$$

And:

$$Re_3 = \frac{\rho_d \dot{\theta} D^2}{\mu_d} \quad \Lambda \quad Ac_3^{-1} = \frac{1}{\dot{\theta}^2} \frac{d\dot{\theta}}{dt} \qquad \textbf{(A.23)}$$

Note that the free motion of the piston in the cylinder, during the stage of passive damping, is not described here. For this purpose the present form of the momentum equation may not be used.

Appendix B Pipe equations

In this appendix basic differential equations are derived for a flow with constant initial flow deceleration, under reflection free and reflecting boundary conditions. The relations between pressure head and fluid velocity are derived from the compatibility equations (section 9.2). Pipe friction effects are ignored.

Consider the closure of a (check) valve in a pipeline system. Until the instant t_d the initial flow deceleration is assumed to be constant. After this instant the flow is influenced by the valve (e.g. damping). The velocity-time history $v = f(t)$ at the valve is assumed to be known.

B.1 Valve closure under reflection free boundary conditions

B.1.1 Relationship between pressure head and fluid velocity

Consider the x,t-plane as shown in figure B.1. The horizontal axis represents the distance along the pipe with the valve as boundary condition, while the vertical axis represents the time. The point pairs {A1, P1} and {A2, P2} are connected by characteristic lines $dx/dt = +c$, and the pairs {B1, Q1} and {B2, Q2} are connected by characteristic lines $dx/dt = -c$.

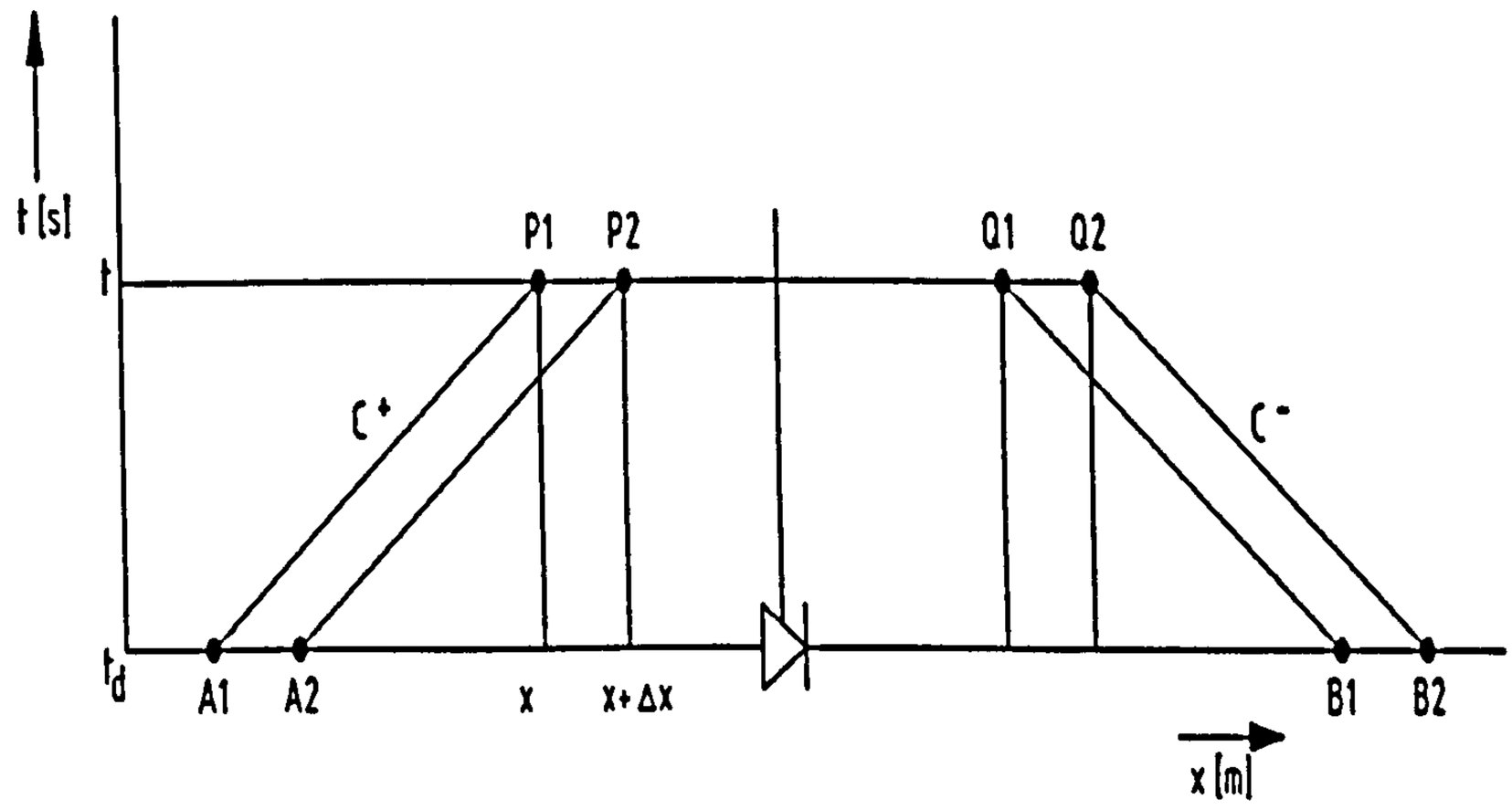

Figure B.1 Relationship between pressure head and fluid velocity

According to the compatibility Equation (9.16) the relationship of the point pairs at the initial upstream side is given by:

$$\left[H + \frac{c}{g} v\right]_{P_1} = \left[H + \frac{c}{g} v\right]_{A_1} \tag{B.1}$$

$$\left[H + \frac{c}{g} v\right]_{P_2} = \left[H + \frac{c}{g} v\right]_{A_2} \tag{B.2}$$

The limit case in which point P_2 approaches point P_1 is given by:

$$\lim_{\Delta x \to 0} \frac{\left[H + \frac{c}{g} v\right]_{P_2} - \left[H + \frac{c}{g} v\right]_{P_1}}{\Delta x} = \lim_{\Delta x \to 0} \frac{\left[H + \frac{c}{g} v\right]_{A_2} - \left[H + \frac{c}{g} v\right]_{A_1}}{\Delta x} \tag{B.3}$$

Or:

$$\frac{\partial}{\partial x}\left[H + \frac{c}{g} v\right]_{P_1} = \frac{\partial}{\partial x}\left[H + \frac{c}{g} v\right]_{A_1} \tag{B.4}$$

The initial flow conditions are (section 9.4.1):

$$\left[\frac{\partial v}{\partial t}\right]_{A_1} = \text{constant} \; ; \; \left[\frac{\partial H}{\partial x}\right]_{A_1} = -\frac{1}{g}\left[\frac{\partial v}{\partial t}\right]_{A_1} \; ; \; \left[\frac{\partial H}{\partial t}\right]_{A_1} = 0 \; ; \; \left[\frac{\partial v}{\partial x}\right]_{A_1} = 0 \tag{B.5}$$

Substitution of Equation (B.5) in Equation (B.4) yields:

$$\frac{\partial}{\partial x}\left[H + \frac{c}{g} v\right]_{P_1} = \left[\frac{\partial H}{\partial x}\right]_{A_1} = \text{constant} \tag{B.6}$$

Differentiation of Equation (B.6) in time yields:

$$H_{xt} + \frac{c}{g} v_{xt} = 0 \tag{B.7}$$

Differentiation of the simplified Equations (9.10) and (9.13) in time yields ($f = 0$):

$$H_{tt} + \frac{c^2}{g} v_{xt} = 0 \tag{B.8}$$

$$g H_{xt} + v_{tt} = 0 \tag{B.9}$$

Finally, after some manipulation with the Equations (B.7), (B.8) and (B.9) follows:

$$\boxed{H_{tt} + \frac{c}{g} v_{tt} = 0} \tag{B.10}$$

This relation is valid in any point along the prismatic tube at the upstream side of the valve.

In a similar way it can be derived that at the initial downstream side of the valve the relationship between the pressure head and fluid velocity is given by:

$$\boxed{H_{tt} - \frac{c}{g} v_{tt} = 0} \tag{B.11}$$

B.1.2 Relationship between pressure heads along the pipe

Consider the x,t-plane in figure B.2. The point pairs {A1, P1}, {A2, P2} and {K, Q2, Q1} are connected by characteristic lines $dx/dt = -c$, and the pairs {B1, Q1}, {B2, Q2} and {K, P1, P2} are connected by characteristic lines $dx/dt = +c$.

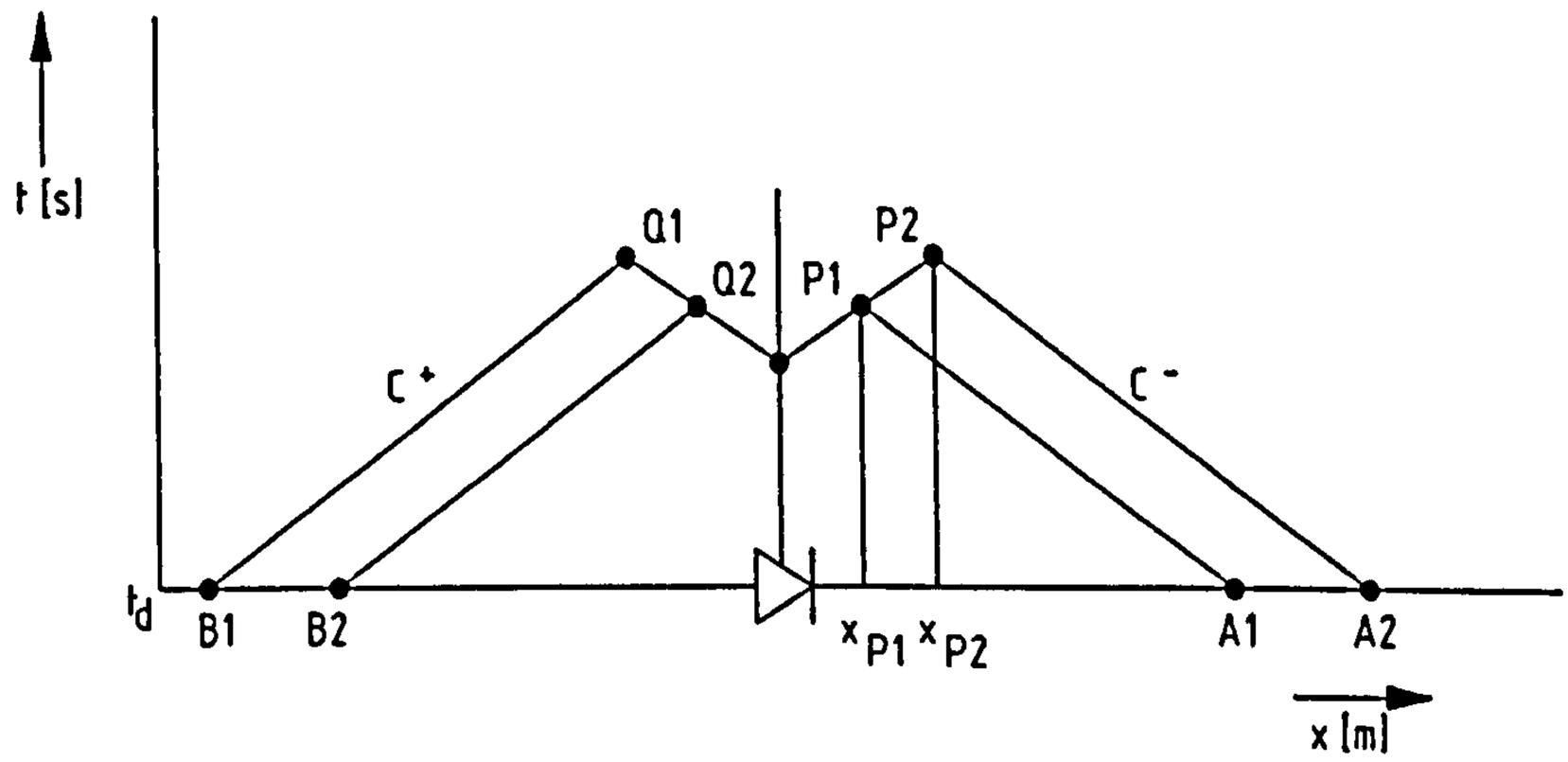

Figure B.2 Relationship between the pressure heads along the pipe

The relationship between the points along the characteristic lines is given by the Equations (9.16) and (9.17):

C^+ -equations:

$$\left[H + \frac{c}{g} v\right]_{P_1} = \left[H + \frac{c}{g} v\right]_K \qquad \textbf{(B.12)}$$

$$\left[H + \frac{c}{g} v\right]_{P_2} = \left[H + \frac{c}{g} v\right]_K \qquad \textbf{(B.13)}$$

C^- -equations:

$$\left[-H + \frac{c}{g} v\right]_{P_1} = \left[-H + \frac{c}{g} v\right]_{A_1} \qquad \textbf{(B.14)}$$

$$\left[-H + \frac{c}{g} v\right]_{P_2} = \left[-H + \frac{c}{g} v\right]_{A_2} \qquad \textbf{(B.15)}$$

From the Equations (B.12) and (B.13) follows at the initial downstream side of the valve:

$$H_{P_2} - H_{P_1} = -\frac{c}{g}\left(v_{P_2} - v_{P_1}\right) \qquad \textbf{(B.16)}$$

From the Equations (B.14) and (B.15) follows:

$$H_{P_2} - H_{P_1} = +\frac{c}{g}\left(v_{P_2} - v_{P_1}\right) + H_{A_2} - H_{A_1} - \frac{c}{g}\left(v_{A_2} - v_{A_1}\right) \qquad \textbf{(B.17)}$$

Summation of the Equations (B.16) and (B.17) gives:

$$2\left(H_{P_2} - H_{P_1}\right) = H_{A_2} - H_{A_1} - \frac{c}{g}\left(v_{A_2} - v_{A_1}\right) \qquad \textbf{(B.18)}$$

According to the initial conditions given in Equation (B.5):

$$v_{A_1} = v_{A_2} \quad \Lambda \quad H_{A_2} - H_{A_1} = \left[\frac{\partial H}{\partial x}\right]_{t=t_d}\left(x_{A_2} - x_{A_1}\right) \qquad \textbf{(B.19)}$$

Further:

$$x_{A_2} - x_{A_1} = 2\left(x_{P_2} - x_{P_1}\right) \qquad \textbf{(B.20)}$$

Substitution of the Equations (B.19) and (B.20) in Equation (B.18) results in:

$$H_{P_2} - H_{P_1} = \left[\frac{\partial H}{\partial x}\right]_{t=t_d}\left(x_{P_2} - x_{P_1}\right) \qquad \textbf{(B.21)}$$

Equation (B.21) is valid along the characteristic line $dx/dt = +c$ and may be rewritten as:

$$H_{P_2}(t) = H_{P_1}(t - (x_{P_2} - x_{P_1})/c) + \left[\frac{\partial H}{\partial x}\right]_{t=t_d}\left(x_{P_2} - x_{P_1}\right) \qquad \textbf{(B.22)}$$

In words: the pressure head in point *P2* is, except from a constant, i.e. the initial pressure head difference over the points *P1* and *P2*, equal to the pressure in point *P1* with a time delay of $(x_{P2} - x_{P1})/c$ seconds.

In a similar way it can be derived that at the initial upstream side of the valve the relationship between the pressures in two points is given by (figure B.2):

$$H_{Q_2}(t) = H_{Q_1}(t + (x_{Q_2} - x_{Q_1})/c) + \left[\frac{\partial H}{\partial x}\right]_{t=t_d}\left(x_{Q_2} - x_{Q_1}\right) \qquad \textbf{(B.23)}$$

These results are of particular interest for experiments since they relate measured pressures (at some distance of the valve) to the pressures at the valve.

B.1.3 Relationship between fluid velocities along the pipe

Substitution of Equation (B.21) in Equation (B.16) results in:

$$v_{P_2} - v_{P_1} = -\frac{g}{c}\left[\frac{\partial H}{\partial x}\right]_{t=t_d}\left(x_{P_2} - x_{P_1}\right) \qquad \textbf{(B.24)}$$

Substitution of Equation (B.5) in (B.24) results in:

$$v_{P_2} - v_{P_1} = \left[\frac{\partial v}{\partial t}\right]_{t=t_d}\frac{\left(x_{P_2} - x_{P_1}\right)}{c} \qquad \textbf{(B.25)}$$

This equation may be rewritten as:

$$v_{P_2}(t) = v_{P_1}(t - (x_{P_2} - x_{P_1})/c) + \left[\frac{\partial v}{\partial t}\right]_{t=t_d}\frac{\left(x_{P_2} - x_{P_1}\right)}{c} \qquad \textbf{(B.26)}$$

In words: the fluid velocity in point *P2* is, except from a constant, equal to the fluid velocity in point *P1* with a time delay of $(x_{P2} - x_{P1})/c$ seconds.

In a similar way it can be derived that at the initial upstream side of the valve the relationship between the fluid velocities in two points is given by (figure B.2):

$$v_{Q_2}(t) = v_{Q_1}(t + (x_{Q_2} - x_{Q_1})/c) - \left[\frac{\partial v}{\partial t}\right]_{t=t_d}\frac{\left(x_{Q_2} - x_{Q_1}\right)}{c} \qquad \textbf{(B.27)}$$

Also these results may be of interest for experiments since they relate measured fluid velocities (at some distance of the valve) to the fluid velocities at the valve.

B.2 Valve closure under reflecting boundary conditions

Consider the closure of a (check) valve in a pipeline system with upstream and downstream constant head boundaries, as shown in the x-t-diagram in figure B.3.

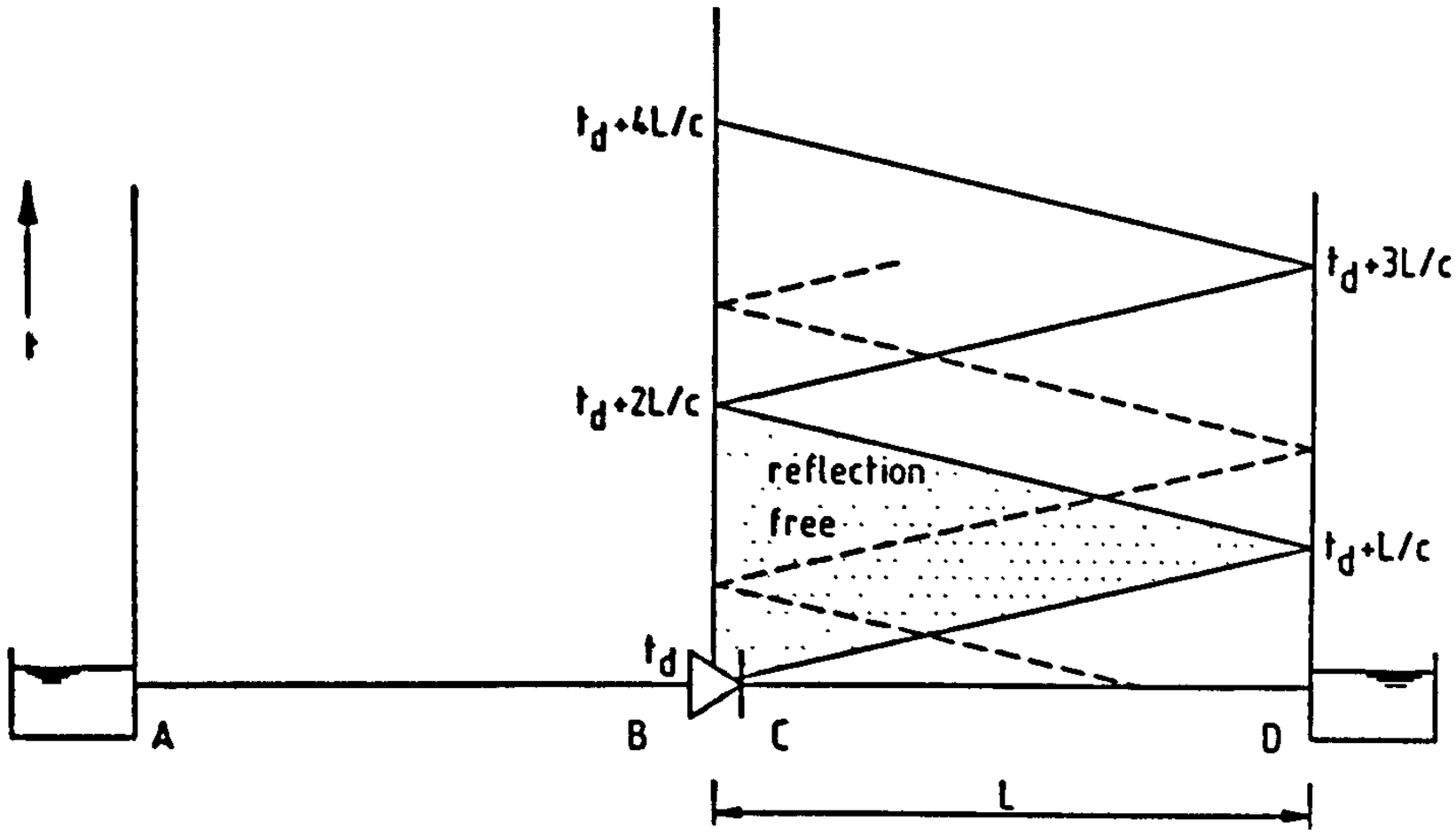

Figure B.3 The relationship between pressure head and fluid velocity

$\underline{t = t_d}$ (initial conditions)

The initial flow conditions are (section B.1.1):

$$\frac{\partial v}{\partial t} = \text{constant} \; ; \; \frac{\partial H}{\partial x} = -\frac{1}{g}\frac{\partial v}{\partial t} \; ; \; \frac{\partial H}{\partial t} = 0 \; ; \; \frac{\partial v}{\partial x} = 0 \qquad \textbf{(B.28)}$$

Integration of the second initial condition in Equation (B.28) along x yields:

$$\int_0^x \left[\frac{\partial H}{\partial x}\right]_{t=t_d} dx = \int_0^x -\frac{1}{g}\left[\frac{\partial v}{\partial t}\right]_{t=t_d} dx \qquad \textbf{(B.29)}$$

With:

$$\left[\frac{\partial v}{\partial t}\right]_{t=t_d} = \left[\frac{dv}{dt}\right]_- \qquad \textbf{(B.30)}$$

follows that:

$$H_P(t_d) - H_C(t_d) = -\frac{x}{g}\left[\frac{dv}{dt}\right]_- \qquad \textbf{(B.31)}$$

The pressure head at the downstream boundary is described by ($x = L$; H_D = constant):

$$H_D - H_C(t_d) = -\frac{L}{g}\left[\frac{dv}{dt}\right]_- \qquad \text{(B.32)}$$

Integration of the fourth initial condition in Equation (B.28) along x yields:

$$v_P(t_d) = v_C(t_d) \qquad \text{(B.33)}$$

$\underline{t_d \leq t \leq t_d + 2L/c}$ (reflectionfree conditions)

Applying the compatibility equations along the characteristic lines (i.e. the dashed path in figure B.3) yields:

$$H_C(t) - \frac{c}{g}v_C(t) = H_P(t_d) - \frac{c}{g}v_P(t_d) \qquad \text{(B.34)}$$

Substitution of the Equations (B.31) and (B.33) in Equation (B.34) gives:

$$H_C(t) - \frac{c}{g}v_C(t) = H_C(t_d) - \frac{x}{g}\left[\frac{dv}{dt}\right]_- - \frac{c}{g}v_C(t_d) \qquad \text{(B.35)}$$

With $dx/dt = c$ or $x = c\,(t - t_d)$ this may be rewritten as:

$$H_C(t) - \frac{c}{g}v_C(t) = H_C(t_d) - \frac{c}{g}\left[\frac{dv}{dt}\right]_-(t - t_d) - \frac{c}{g}v_C(t_d) \qquad \text{(B.36)}$$

Substitution of Equation (B.32) yields:

$$H_C(t) = \frac{c}{g}\left[v_C(t) - v_C(t_d)\right] - \frac{c}{g}\left[\frac{dv}{dt}\right]_-\left[t - t_d - \frac{L}{c}\right] + H_D \qquad \text{(B.37)}$$

$\underline{t_d+L/c < t \leq t_d+3L/c}$

Applying the compatibility equations along the dashed path in figure B.3 yields:

$$\frac{g}{c}H_D + v_D(t) = \frac{g}{c}H_C(t-L/c) + v_C(t-L/c) \qquad \text{(B.38)}$$

$H_C(t - L/c)$ is described by Equation (B.37) which is valid L/c seconds before. Replacing t by $(t - L/c)$ and substitution in Equation (B.38) yields:

$$v_D(t) = 2v_C(t-L/c) - v_C(t_d) - \left[\frac{dv}{dt}\right]_- \left[t - t_d - \frac{2L}{c}\right] \qquad \text{(B.39)}$$

$\underline{t_d+2L/c < t \leq t_d+4L/c}$

Applying the compatibility equations along the dashed path in figure B.3 yields:

$$H_C(t) - \frac{c}{g}v_C(t) = H_D - \frac{c}{g}v_D(t-L/c) \qquad \text{(B.40)}$$

$v_D(t - L/c)$ is described by Equation (B.39) which is valid L/c seconds before. Replacing t by (t - L/c) and substitution in Equation (B.40) yields:

$$\begin{aligned} H_C(t) = {} & \frac{c}{g}\left[v_C(t) - 2v_C(t-2L/c) + v_C(t_d)\right] \\ & + \frac{c}{g}\left[\frac{dv}{dt}\right]_- \left[t - t_d - \frac{3L}{c}\right] + H_D \end{aligned} \qquad \text{(B.41)}$$

Continuing this procedure along the dashed path in figure B.3 yields:

$\underline{t_d+3L/c < t \leq t_d+5L/c}$

$$\begin{aligned} v_D(t) = {} & 2v_C(t-L/c) - 2v_C(t-3L/c) + v_C(t_d) \\ & + \left[\frac{dv}{dt}\right]_- \left[t - t_d - \frac{4L}{c}\right] \end{aligned} \qquad \text{(B.42)}$$

$\underline{t_d+4L/c < t \leq t_d+6L/c}$

$$H_C(t) = \frac{c}{g}\left[v_C(t) - 2v_C(t-2L/c) + 2v_C(t-4L/c) - v_C(t_d)\right] - \frac{c}{g}\left[\frac{dv}{dt}\right]_- \left[t - t_d - \frac{5L}{c}\right] + H_D \quad \textbf{(B.43)}$$

$\underline{t_d+5L/c < t \leq t_d+7L/c}$

$$v_D(t) = 2v_C(t-L/c) - 2v_C(t-3L/c) + 2v_C(t-5L/c) - v_C(t_d) - \left[\frac{dv}{dt}\right]_- \left[t - t_d - \frac{6L}{c}\right] \quad \textbf{(B.44)}$$

$\underline{t_d+6L/c < t \leq t_d+8L/c}$

$$H_C(t) = \frac{c}{g}\left[v_C(t) - 2v_C(t-2L/c) + 2v_C(t-4L/c) - 2v_C(t-6L/c) + v_C(t_d)\right] \quad \textbf{(B.45)}$$

$$+ \frac{c}{g}\left[\frac{dv}{dt}\right]_- \left[t - t_d - \frac{7L}{c}\right] + H_D$$

..... etc .....

The previous results may be summarized in the following sequence:

$$\frac{g}{c}H_C(t) = v_C(t) - v_C(t_d) - \left[\frac{dv}{dt}\right]_- \left[t - t_d - \frac{L}{c}\right] + \frac{g}{c}H_D + 2\sum_{i=1}^{\infty}(-1)^i\left[v_C(t-i2L/c) - v_C(t_d)\right]\phi(t-t_d-i2L/c) \quad \textbf{(B.46)}$$

$$- 2\sum_{i=1}^{\infty}(-1)^i\left[\frac{dv}{dt}\right]_-\left[t-t_d-i2L/c\right]\phi(t-t_d-i2L/c)$$

Where:

$$\phi(y) = \begin{cases} 0 & \text{if } y \leq 0 \\ 1 & \text{if } y > 0 \end{cases}$$

With the introduction of $\Delta H_C = H_C(t) - H_C(t_d)$ and substitution of Equation (B.32) this may be rewritten as:

$$\frac{g}{c}\Delta H_C(t) = v_C(t) - v_C(t_d) - \left[\frac{dv}{dt}\right]_- (t - t_d)$$

$$+ 2\sum_{i=1}^{\infty}(-1)^i \left[\, v_C(t-i2L/c) - v_C(t_d) \,\right] \phi(t-t_d-i2L/c) \quad \textbf{(B.47)}$$

$$- 2\sum_{i=1}^{\infty}(-1)^i \left[\frac{dv}{dt}\right]_- \left[\, t-t_d-i2L/c \,\right] \phi(t-t_d-i2L/c)$$

In this equation the pressure head changes at the valve are related to the fluid velocity at the valve. The first three terms in the right hand side of this equation form the solution for a valve closure under reflectionfree conditions (see Equation (9.41)). The other terms describe the influence of reflections and show that the valve closure is system dependent. The equation is valid at the initial downstream side of the valve.

In a similar way follows for the pressure head changes at the initial upstream side of the valve:

$$\frac{g}{c}\Delta H_B(t) = - v_B(t) + v_B(t_d) + \left[\frac{dv}{dt}\right]_- (t - t_d)$$

$$- 2\sum_{i=1}^{\infty}(-1)^i \left[\, v_B(t-i2L/c) - v_B(t_d) \,\right] \phi(t-t_d-i2L/c) \quad \textbf{(B.48)}$$

$$+ 2\sum_{i=1}^{\infty}(-1)^i \left[\frac{dv}{dt}\right]_- \left[\, t-t_d-i2L/c \,\right] \phi(t-t_d-i2L/c)$$

Whereby $2L/c$ is now the upstream reflection time.

Appendix C

Interpolation in valve characteristics

In this appendix the interpolation procedure is described, which is performed within one single valve characteristic of approach 2.

C.1 Representation of valve characteristics

C.1.1 Physical domain

The valve characteristics of approach 2 (section 11.6) may be represented by a set of points in a three-dimensional, physical space:

$$\left\{ \left[\frac{v}{v_o} , \frac{D}{v_o^2} \frac{dv}{dt} , \frac{g\Delta H}{v_o^2} \right] \in \mathbb{R}^3 \right\} \tag{C.1}$$

In general the valve characteristics are dependent of the valve and system parameters (section 11.4). Consider a set of points for which the valve and system parameters, except from the unsteady flow parameters, are constants. It is assumed that this set of points forms a surface in the three-dimensional physical space. Replacing the coordinates in the above equation by x, y and z, respectively, this surface S may be represented by:

$$S: = \left\{ (x,y,z) \in \mathbb{R}^3 \mid \Phi(x,y,z) = 0 \right\} \tag{C.2}$$

C.1.2 Computational domain

The surface S is represented by a finite number of grid points. These grid points are mapped from the physical domain (x, y, z) to the computational domain (i, j):

$$S: = \left\{ (x_{i,j},y_{i,j},z_{i,j}) \in \mathbb{R}^3 \mid \Phi(x_{i,j},y_{i,j},z_{i,j}) = 0 \right\} \tag{C.3}$$

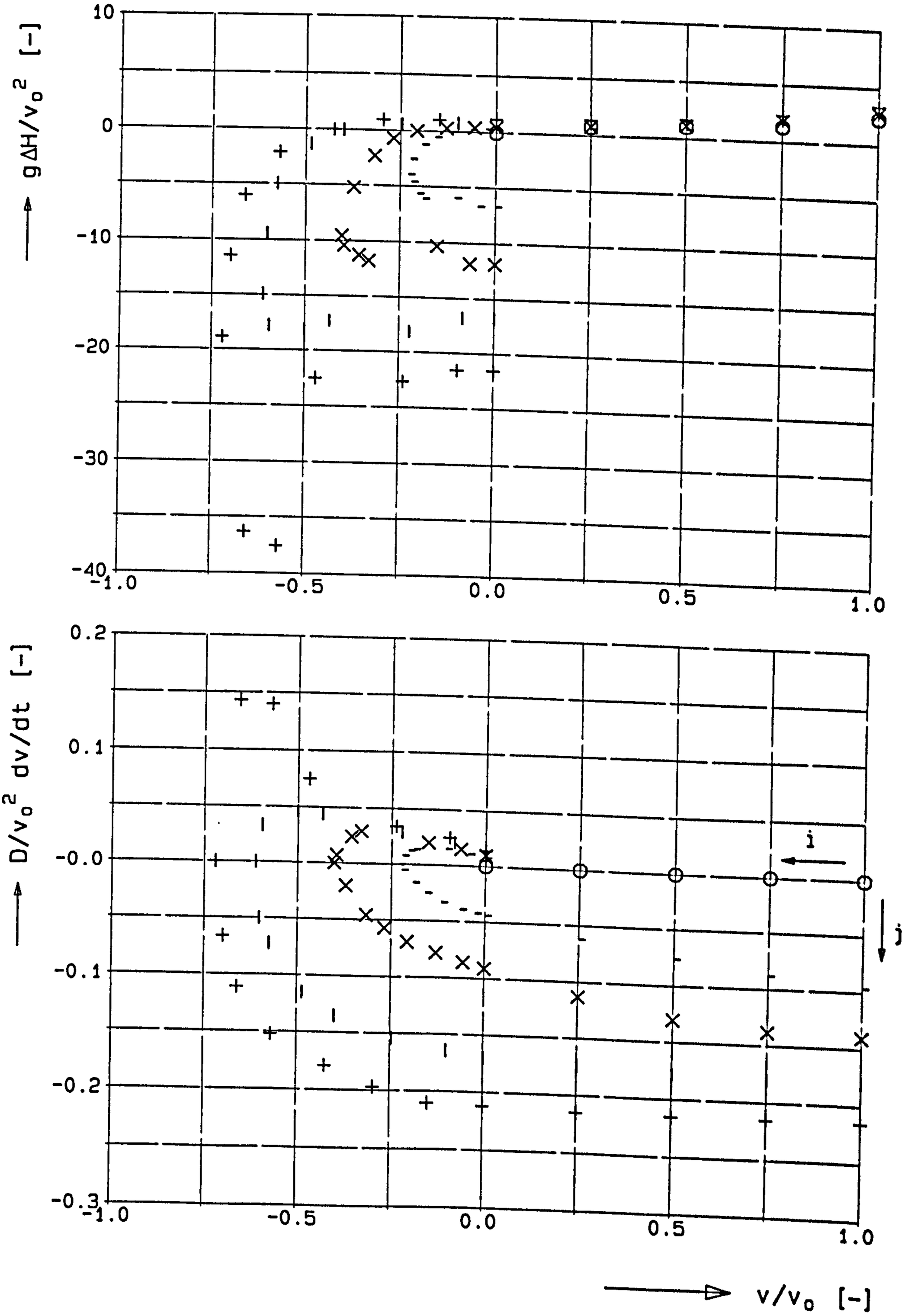

Figure C.1 Representation of valve characteristics

The grid points form a rectangular grid in the computational domain. The discrete coordinate i (1, 2, ..., M) represents a point along a trajectory or path which is followed during closure (read: the path followed during a dynamic test). It represents a certain stage of the valve closure. The initial stage $i = 1$ represents the fully opened valve ($v/v_o = 1$), while the final stage $i = M$ represents the closed valve ($v/v_o \uparrow 0$).

The discrete coordinate j (1, 2, ..., N) is the trajectory or path number (read: test number). The trajectory $j = 1$ represents steady flow values ($dv/dt = 0$). The trajectories $j = 2, 3, \ldots$ represent successive tests with increasing initial flow deceleration. An example of a discrete valve characteristic is given in figure C.1.

C.2 Interpolation

The surface S is reconstructed from the grid points by means of interpolation. Hereto, from the grid points a grid cell is formed. The interpolation is based on the local formation of grid cells, so that no grid generation or storage is needed.

C.2.1 Interpolation surface

The surface S between four adjacent grid points is approximated by (figure C.2):

$$\begin{bmatrix} x_A \\ y_A \\ z_A \end{bmatrix} = \begin{bmatrix} x_{i,j} \\ y_{i,j} \\ z_{i,j} \end{bmatrix} + \alpha \begin{bmatrix} x_{i+1,j} - x_{i,j} \\ y_{i+1,j} - y_{i,j} \\ z_{i+1,j} - z_{i,j} \end{bmatrix} \tag{C.4}$$

$$\begin{bmatrix} x_B \\ y_B \\ z_B \end{bmatrix} = \begin{bmatrix} x_{i,j+1} \\ y_{i,j+1} \\ z_{i,j+1} \end{bmatrix} + \alpha \begin{bmatrix} x_{i+1,j+1} - x_{i,j+1} \\ y_{i+1,j+1} - y_{i,j+1} \\ z_{i+1,j+1} - z_{i,j+1} \end{bmatrix} \tag{C.5}$$

$$\begin{bmatrix} x^* \\ y^* \\ z^* \end{bmatrix} = \begin{bmatrix} x_A \\ y_A \\ z_A \end{bmatrix} + \beta \begin{bmatrix} x_B - x_A \\ y_B - y_A \\ z_B - z_A \end{bmatrix} \tag{C.6}$$

Where α and β are interpolation coefficients.

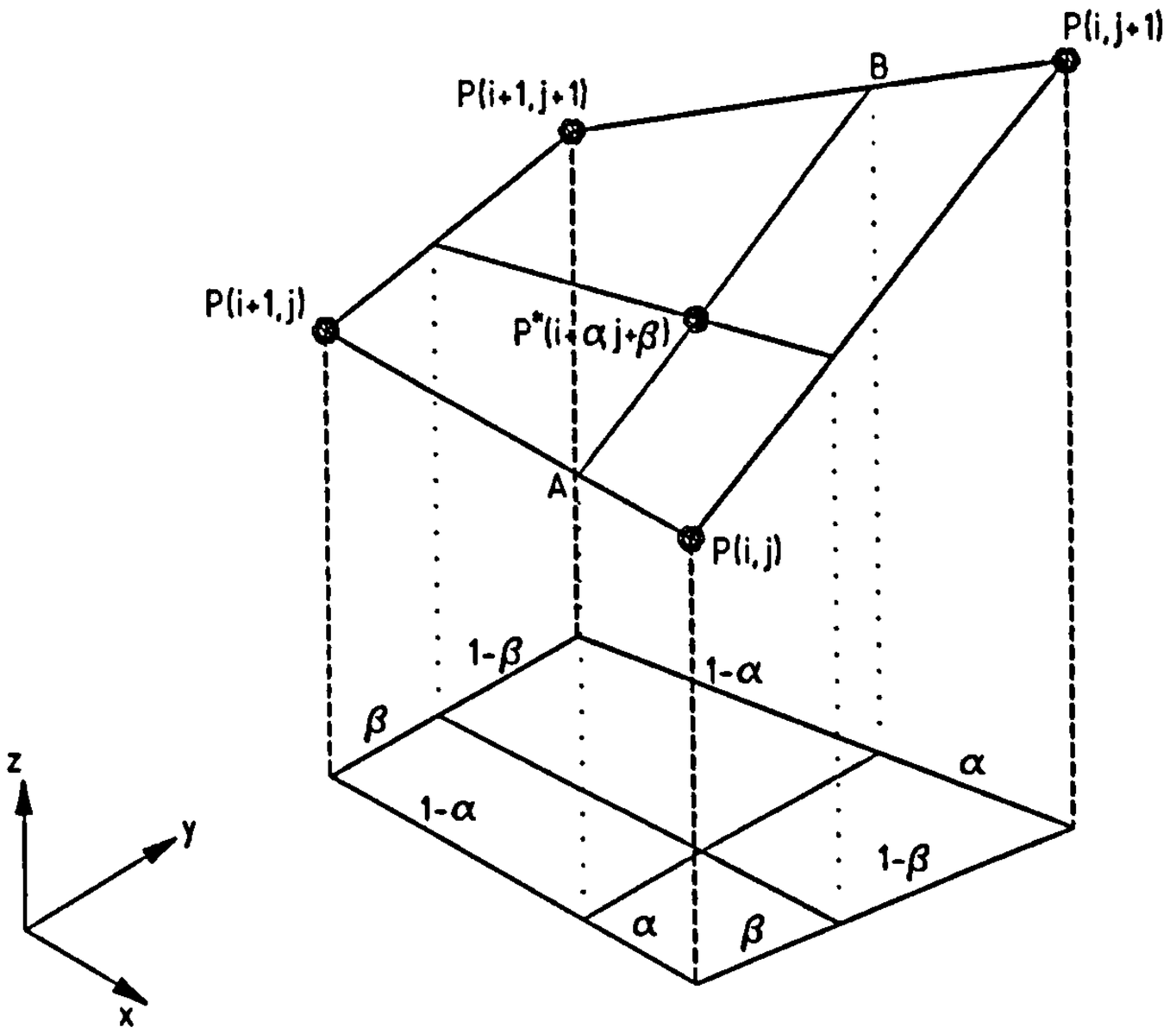

Figure C.2 Interpolation in valve characteristics

Substitution of the auxiliary Equations (C.4) and (C.5) in Equation (C.6) yields a four-points interpolation, described by:

$$\begin{bmatrix} x^* \\ y^* \\ z^* \end{bmatrix} = (1-\alpha)(1-\beta) \begin{bmatrix} x_{i,j} \\ y_{i,j} \\ z_{i,j} \end{bmatrix} + \alpha(1-\beta) \begin{bmatrix} x_{i+1,j} \\ y_{i+1,j} \\ z_{i+1,j} \end{bmatrix} + \tag{C.7}$$

$$+ \beta(1-\alpha) \begin{bmatrix} x_{i,j+1} \\ y_{i,j+1} \\ z_{i,j+1} \end{bmatrix} + \alpha\beta \begin{bmatrix} x_{i+1,j+1} \\ y_{i+1,j+1} \\ z_{i+1,j+1} \end{bmatrix}$$

The interpolated surface S^* may now, in short notation, be represented as:

$$S^* := \{ (i,j) \in \mathbb{N}^2 \; ; \; (\alpha,\beta) \in \mathbb{R}^2 \mid \Phi^* (i+\alpha, j+\beta) = 0 \} \tag{C.8}$$

Two special classes of functions are:

$$S^* := \{ (i,j) \in \mathbb{N}^2 \; ; \; (\alpha,\beta) \in \mathbb{R}^3 \mid \Phi^* (i_o+\alpha_o, j+\beta) = 0 \} \tag{C.9}$$

And:

$$S^* := \left\{ (i,j) \in \mathbb{N}^2 \; ; \; (\alpha,\beta) \in \mathbb{R}^3 \mid \Phi^* (i+\alpha, j_o+\beta_o) = 0 \right\} \qquad \textbf{(C.10)}$$

Where i_o, j_o are integer constants and α_o, β_o are real constants. Each class yield a set of straight lines which form a curved surface S^* (figure C.2). The class of functions in Equation (C.10) is used to describe so-called "prescribed" trajectories in the valve model (section C.3.5).

C.2.2 Interpolation coefficients

Equation (C.7) forms a set of three equations with five unknowns, i.e. x^*, y^*, z^*, α, and β. In order to interpolate two of the five must be known. It is assumed that two of the variables x^*, y^*, z^* are known.

Suppose that x and y are known, so that $x^* = x$ and $y^* = y$. In that case the interpolation coefficients can be solved implicitly from Equation (C.7), or explicitly from the auxiliary Equations (C.4) to (C.6). This may be written as $\alpha, \beta = f(x, y)$. A graphical representation is obtained by considering the projections of the points on the x-y-plane (figure C.2). When α and β are known, z is approximated from the remaining equation, which may be written as: $z^* = f(\alpha, \beta)$. Combining the latter two functions yields an implicit function of the form $z^*(x, y)$.

The other variables x^* and y^* may be treated in a similar way, so that formally three implicit functions exist:

$$x^*(y,z) \quad \Lambda \quad y^*(x,z) \quad \Lambda \quad z^*(x,y) \qquad \textbf{(C.11)}$$

In the computational domain the implicit functions may be written as:

$$x^*(i+\alpha,j+\beta) \quad \Lambda \quad y^*(i+\alpha,j+\beta) \quad \Lambda \quad z^*(i+\alpha,j+\beta) \qquad \textbf{(C.12)}$$

The implicit functions can be used for interpolation ($0 \leq \alpha \leq 1$ and $0 \leq \beta \leq 1$) as well as extrapolation ($\alpha < 0$ or $\alpha > 1$ and $\beta < 0$ or $\beta > 1$). For extrapolation extra rules are necessary in the case that the (inner or outer) boundaries are concave curves. The allocation of extrapolation areas to cells is given in figure C.3. In the case of concave curves the extrapolation areas become triangular.

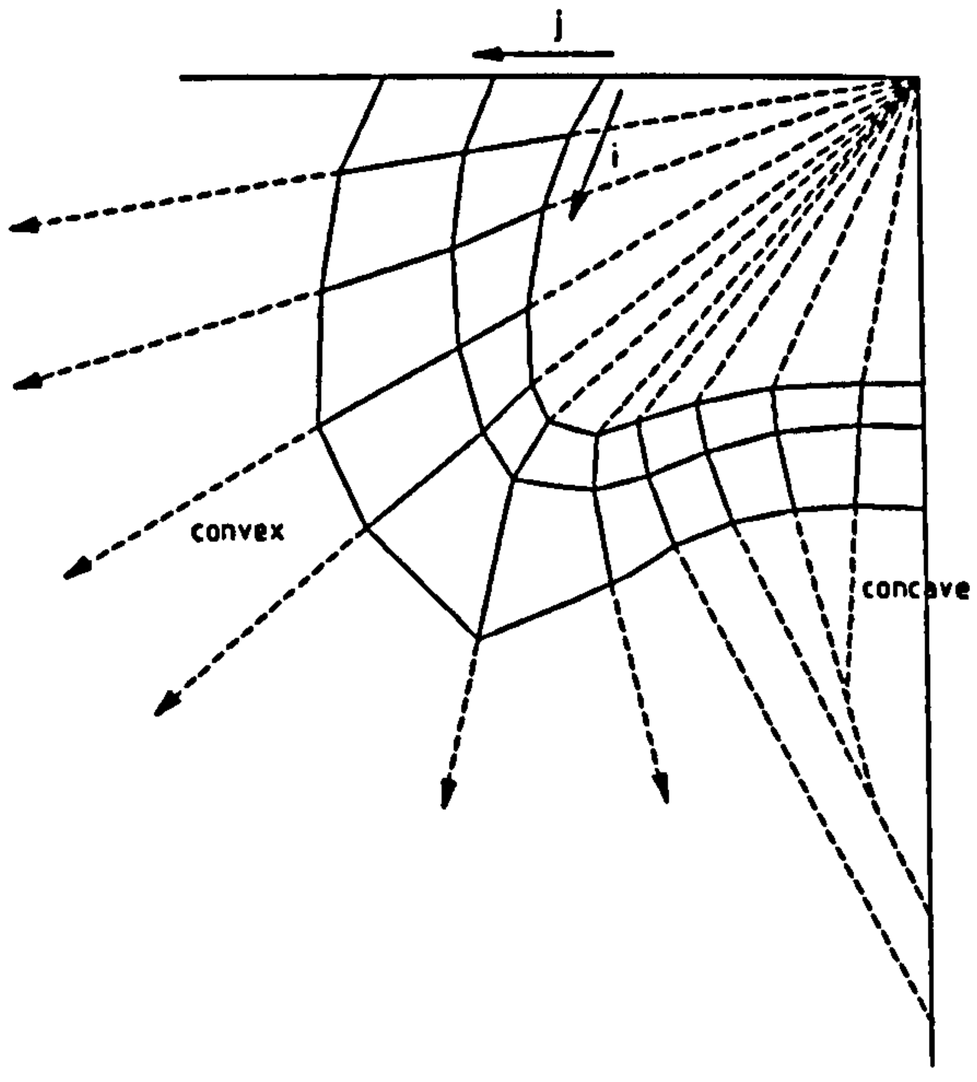

Figure C.3 Extrapolation in valve characteristics

In principle either of the three implicit functions may be used, although they will not give exactly the same interpolation coefficients. However, some of them are more suited to interpolation than others. The properties of the implicit functions are studied in the next section.

C.3 Implicit functions

C.3.1 Implicit function theorem

The implicit functions which may formally be derived from $\Phi(x,y,z) = 0$ are:

$$x(y,z) \quad \Lambda \quad y(x,z) \quad \Lambda \quad z(x,y) \tag{C.13}$$

The above implicit functions exist locally if, respectively:

$$\frac{\partial\Phi(x_o,y_o,z_o)}{\partial x} \neq 0 \;;\; \frac{\partial\Phi(x_o,y_o,z_o)}{\partial y} \neq 0 \;;\; \frac{\partial\Phi(x_o,y_o,z_o)}{\partial z} \neq 0 \tag{C.14}$$

This condition is known as the implicit function theorem.

The implicit functions are used for an interpolation, which takes place within an iteration process. The interpolation is the most accurate and the iteration process is

the most stable for the implicit function, which derivative in Equation (C.14) is relatively high. Then the implicit function is a "weak varying" function and well conditioned. Consequently the other implicit functions are relatively poor conditioned. For example: If $\partial\Phi/\partial z$ is high, then $z(x, y)$ is a "weak varying" function, while the others $x(y, z)$ and $y(x, z)$ are "strong varying" functions.

C.3.2 Properties of implicit functions

In this section the properties of the implicit functions are studied. The functions, for convenience represented by physical variables, are numbered as the *first*, *second* and *third* implicit function, respectively:

$$\frac{v}{v_o}\left[\frac{D}{v_o^2}\frac{dv}{dt}\,,\,\frac{g\Delta H}{v_o^2}\right] \quad ; \quad \frac{D}{v_o^2}\frac{dv}{dt}\left[\frac{v}{v_o}\,,\,\frac{g\Delta H}{v_o^2}\right] \quad ; \quad \frac{g\Delta H}{v_o^2}\left[\frac{v}{v_o}\,,\,\frac{D}{v_o^2}\frac{dv}{dt}\right] \tag{C.15}$$

Further the three-dimensional physical domain is divided into sections. Hereto the *v-dv/dt*-plane is divided into four quadrants, which are numbered in the usual way (e.g. in the second quadrant $v < 0$ and $dv/dt > 0$).

The properties of the functions are studied by means of the measured valve characteristics in figure C.1. For this purpose also the virtual tests in figure C.4 and the experimental results in section 14.7 may be used.

Quadrant 4 During the first stage of closure the pressure head difference is characterized by small values, which are about equal to the steady flow values, and small variations. It has an almost linear character for $v/v_o < 1$, and a parabolic character for $v/v_o > 1$. The third implicit function is a "weak varying" function, which is well conditioned and suited to interpolation. Consequently the other implicit functions are poor conditioned here.

Quadrant 3 This stage of closure is characterized by a decrease of the pressure head difference to relatively large, negative values, coupled with an increase of the fluid velocity gradient from negative values to zero. The quadrant forms the bridge between quadrant 2 and 4. The implicit functions have the properties of those in the adjacent quadrants.

Quadrant 2 The last stage of closure is characterized by high negative values and strong variations of the pressure head difference.

For weakly damped check valves these variations are more or less proportional to the fluid velocity gradient (figure 14.15). In that sense they do not violate the conditions of the third implicit function.

For strongly damped check valves, the fluid velocity gradient is characterized by

small values, which are gradually reduced to zero (valve closed). These values are hardly dependent of the previous flow conditions (figure 14.17). In those cases the second implicit function is a weak varying function. Consequently, the other implicit functions are poor conditioned, and not suited to interpolation here.

Quadrant 1 In this quadrant the properties of the implicit functions are unknown since no opening characteristics are available.

The properties of the three implicit functions are summarized in table C.1.

Quadrant	x (y,z)	y (x,z)	z (x,y)
4	--	--	++
3	-	-	+
2	--	++	--
1	?	?	?

++ well conditioned -- poor conditioned

Table C.1 Properties of implicit functions

It is concluded that the properties of the implicit functions may vary strongly from quadrant to quadrant. In particular for strongly damped check valves not all the functions are suited to interpolation, so that a good choice is strictly necessary.

C.3.3 Trajectories in the *v-dvdt*-plane

In this section the properties of the trajectories in the *v-dv/dt*-plane are studied. The trajectories have some special features due to the fact that the fluid velocity and velocity gradient are coupled.

The velocity time history may generally be described by a polynomial as:

$$v = a_0 + a_1 t + a_2 t^2 + \ldots\ldots + a_N t^N \qquad \textbf{(C.16)}$$

So that:

$$\frac{dv}{dt} = a_1 + 2 a_2 t + \ldots\ldots + N a_N t^{N-1} \qquad \textbf{(C.17)}$$

Consider the trajectories described by Equation (C.10) and suppose that the projection of these trajectories on the *v-dv/dt*-plane may also be described in the form of a series as:

$$v = A_0 + A_1 \frac{dv}{dt} + A_2 \left[\frac{dv}{dt}\right]^2 + \ldots\ldots + A_M \left[\frac{dv}{dt}\right]^M \qquad \textbf{(C.18)}$$

It is evident that the order of the Equations (C.16) and (C.18) must be the same. After the substitution of Equation (C.17) in Equation (C.18) follows:

$$N = (N-1)\, M \qquad \textbf{(C.19)}$$

The only solution is $N = 2$ and $M = 2$, which means that both the velocity time history as well as the projected trajectory must be approximated by second order polynomials (parabolic functions). In that case the second derivative of the fluid velocity in time is constant.

From the above result the following can be concluded. If the projections of the measured trajectories ($\beta_o = 0$) on the *v-dv/dt*-plane are approximated by polynomials, the interpolation must be of *second order* or lower order, for reasons of consistency.

About parabolic functions ...

If the velocity time history is of second order ($N = 2$) then Equation (C.16) reduces to:

$$v = a_0 + a_1 t + a_2 t^2 \qquad \textbf{(C.20)}$$

So that:

$$\frac{dv}{dt} = a_1 + 2 a_2 t \qquad \textbf{(C.21)}$$

Elimination of t from the above equations gives:

$$v = a_0 - \frac{a_1^2}{4a_2} + \frac{1}{4a_2}\left(\frac{dv}{dt}\right)^2 \qquad \textbf{(C.22)}$$

So that the coefficients in Equation (C.18) become:

$$A_0 = a_0 - \frac{a_1^2}{4a_2} \quad ; \quad A_1 = 0 \quad ; \quad A_2 = \frac{1}{4a_2} \quad ; \quad A_3 = 0 \quad ; \quad \ldots \qquad \textbf{(C.23)}$$

Thus follows with Equation (C.18):

$$\frac{dv}{d(dv/dt)} = 2A_2\left(\frac{dv}{dt}\right) \qquad \textbf{(C.24)}$$

With on the horizontal axis ($dv/dt = 0$):

$$\frac{dv}{d(dv/dt)} = 0 \qquad \textbf{(C.25)}$$

The latter condition must also hold for other functions than the above polynomials, since the velocity time history is characterized by a local extreme value here.

Now reconsider the functions in Equation (C.9) and (C.10) and the measured valve characteristics in figure C.1. The condition in Equation (C.25) demonstrates that the two classes of functions form an orthogonal grid around the horizontal axis of the v-dv/dt-plane. It is presumed that the orthogonality also holds for the rest of the plane. However, this needs to be proven.

C.3.4 Stability

In order to study the stability of the check valve behaviour the term *stability* must be defined. The check valve behaviour is said to be stable if the (steady or unsteady) flow conditions can be reproduced after a small disturbance, without intermediate valve closure. The check valve is primarily controlled by the flow, which means that also the valve disc position must be reproducable. Let the flow conditions be described in terms of v, dv/dt and ΔH. In a mathematical sense the definition for stability may be formulated as: The valve behaviour in the point (v, dv/dt, ΔH) is said to be stable if there exists a flow loop around this point. In that case the process is reversible.

Suppose that the valve is subjected to a flow disturbance:

$$v = v_b + A \sin \omega t \qquad \textbf{(C.26)}$$

So that:

$$\frac{dv}{dt} = A\omega \cos \omega t \qquad \text{(C.27)}$$

Thus a flow loop is created around the point (v_b, 0) in the *v-dv/dt*-plane, with basis $2A$ and altitude $A\omega$. The stability of the valve can be studied by substituting the above flow disturbance in the valve equation of motion. Here the stability analysis is restricted to more qualitative considerations.

Consider the check valve under initial, steady state conditions, described by the points (v_b, 0, ΔH) where $v_b > 0$. It is obvious that a flow loop exists around this point if the flow disturbance is small and low frequent. Let the flow disturbance be small but finite ($A \approx 0$) and high frequent. In the limit case $\omega \rightarrow \infty$, the valve disc has no time to change of position ($\dot{\theta} \rightarrow 0$), due to inertia. Now a flow loop is created around the point (v_b, 0) in the *v-dv/dt*-plane, with basis $2A$ and altitude $A\omega \rightarrow \infty$. All the points within such a flow loop are stable. Thus it is illustrated in a qualitative sense that the check valve behaviour in the quadrants 1 and 4 is stable.

Consider the check valve under initial conditions, described by (v_b, 0, ΔH), while $v_b < 0$. In this case no steady state conditions exist. In the quadrants 2 and 3 the valve disc is closing under the reverse flow, so that $\dot{\theta} < 0$ here. Consequently no flow loop exists that results in the same disc position. The valve behaviour is an unstable, irreversible process that ends in a closure.

About the physical and numerical aspects of the unstable valve behaviour the following. The fluid velocity gradient changes from negative, more or less constant values in quadrant 2, to positive values in quadrant 3. According to the principles of waterhammer this increment of *dv/dt* is coupled with a downstream pressure rise and upstream pressure drop (chapter 9), resulting in a decrement of ΔH. A small increment of *dv/dt* leads to a relatively large decrement of ΔH, which on its turn leads to a further increment of *dv/dt*, etc.

In a qualitative sense this unstable behaviour is physically correct. The combination of decreasing upstream pressure and increasing downstream pressure tends to accelerate the motion of the valve disc into its seat.

In a quantitative sense this behaviour may give rise to numerical instabilities within the solver of the coupled pipe and valve equations (section 12.3). This is revealed by an uncontrolled, accelerated closure (like undamped check valves).

C.3.5 Prescribed trajectories

In the previous section it is illustrated that the valve closure is, physically as well as numerically, unstable in the last stage of closure. To overcome the numerical problems associated with these instabilities "prescribed" trajectories are introduced.

Reconsider the trajectories given in Equation (C.10) together with the physical domain:

$$\Phi\left[\frac{v}{v_o}\,,\,\frac{D}{v_o^2}\frac{dv}{dt}\,,\,\frac{g\Delta H}{v_o^2}\right] = 0 \quad \wedge \quad \Phi(i+\alpha, j_o+\beta_o) = 0 \qquad \textbf{(C.28)}$$

Prescribing a trajectory implies that the relationship between v, dv/dt and ΔH is prefixed. This relationship is obtained from tests and therefore consistent with laboratory conditions. If the characteristics are applied to other conditions the consistency of the variables is no longer guaranteed. To enable a general application of prescribed trajectories a relaxation must be applied to one of the variables. In that case formally six functions implicit functions arise:

$$\begin{gathered}\frac{v}{v_o}\left[\frac{D}{v_o^2}\frac{dv}{dt}\right] \;;\; \frac{v}{v_o}\left[\frac{g\Delta H}{v_o^2}\right] \;;\; \frac{D}{v_o^2}\frac{dv}{dt}\left[\frac{v}{v_o}\right] \\ \frac{D}{v_o^2}\frac{dv}{dt}\left[\frac{g\Delta H}{v_o^2}\right] \;;\; \frac{g\Delta H}{v_o^2}\left[\frac{v}{v_o}\right] \;;\; \frac{g\Delta H}{v_o^2}\left[\frac{D}{v_o^2}\frac{dv}{dt}\right]\end{gathered} \qquad \textbf{(C.29)}$$

The main features of these functions are:

- The fifth and sixth implicit function do not guarantee a valve closure. The fluid velocity gradient must be increased from negative values to positive values. Hereto a certain critical (negative) pressure head difference is needed, which in general is system-dependent. When this critical value is not exceeded, the flow continues to decelerate. The (absolute value of the) prescribed pressure head difference may be too small to create such a positive fluid velocity gradient, which is necessary to reduce the reverse flow to zero and close the valve.
- The second and fourth implicit function may be ambigious within a quadrant, i.e. ΔH gives more than one solution for v and dv/dt (figure C.1 and C.4.c).
- Similar considerations hold for the first implicit function.
- The third implicit function is unambigious, stable and always guarantees a valve closure.

Based on the above arguments the relaxation is applied to ΔH.

The prescribed trajectories may now be described by:

$$\Phi\left[\frac{v}{v_o}\ ,\ \frac{D}{v_o^2}\frac{dv}{dt}\right] = 0 \quad \Lambda \quad \Phi\left(i+\alpha, j_o+\beta_o\right) = 0 \tag{C.30}$$

About the θ-method ...

The prescribed trajectory may numerically be solved by the well known θ-method. For this purpose Equation (C.30) is discretized as:

$$\Phi^*\left(\theta\, v^{n+1}+(1-\theta)\, v^n\ ,\ \frac{v^{n+1}-v^n}{\Delta t}\right) = 0 \tag{C.31}$$

Where n represents the discrete time. The equation is solved iteratively by (k is iteration step):

$$\frac{\tilde{v}^{n+1,k}-v^n}{\Delta t} = \phi^*\left(\theta\, v^{n+1,k-1}+(1-\theta)\, v^n\right) \tag{C.32}$$

And a relaxation:

$$v^{n+1,k} = \omega\, \tilde{v}^{n+1,k}+(1-\omega)\, v^{n+1,k-1} \tag{C.33}$$

With as initial value $v^{n+1,0} = v^n$. The θ-method is stable in quadrant 2 for $\theta = 0$ (explicit), and in quadrant 3 for $\theta = 1$ (fully implicit).

In CVWP the prescribed trajectories are treated by an adapted form of the above-mentioned standard θ-method. Hereto Equation (C.32) is replaced by:

$$\frac{\tilde{v}^{n+1,k}-v^n}{\Delta t} = \theta\ \phi^*\left(v^{n+1,k-1}\right) + \left(1-\theta\right)\ \phi^*\left(v^n\right) \tag{C.34}$$

Where $\theta = ½$, while no relaxation is applied ($\omega = 1$). The standard θ-method and adapted version give the same solution for linear functions ϕ^*. However, the adapted version gives an exact solution for parabolic functions.

In section C.3.3 it is demonstrated that the trajectories in the *v-dv/dt*-plane may only be described by second order or lower order polynomials. Here, linear forms of the function ϕ^* are used, except for grid points around the horizotal axis, where parabolic functions are used (see below).

About points on the *v*-axis ...

The prescribed trajectories are basically used to reconstruct the velocity-time history. For this purpose linear functions can be used, except for points around the *v*-axis. Once a point on this axis is arrived at, it will never be left, since the velocity does not change in time anymore ($dv/dt = 0$). This is physically incorrect, at least for negative velocities. To pass the *v*-axis higher order information is needed, which is found in e.g. the second derivative of the velocity-time history. In order to include such information, non-linear functions must be used. The presribed trajectory around the negative *v*-axis is in CVWP described by (see also section C.3.3):

$$v = A_0 + A_2 \left(\frac{dv}{dt}\right)^2 \qquad \text{(C.35)}$$

This formulation allows changes of the fluid velocity gradient. The parabolic functions are constructed from two (measured) grid points of the same trajectory, one on and one close to (below or above) the horizontal axis, and the condition in Equation (C.25).

Note that in the case of parabolic functions the interpolation becomes of second order. This has consequences for the determination of the interpolation coefficients α_0 and β_0, although α_0 in good approximation may be obtained from linear interpolation here.

The question arises in howfar the prescribed trajectories may be used. The flow conditions in a pipeline system are generally influenced by the system as well as the check valve. However, certain flow conditions are dominated by the system, others by the check valve. The prescribed trajectories may only be used in the region where the flow conditions are dominated by the check valve. This region may be defined by means of the valve characteristics of approach 1.

The fluid velocity characteristic for the first event (approach 1) gives information about the reverse flow velocity at which the damping becomes active (section 11.5). It thus gives direct information about the end of the first event and the beginning of the second event. Experiments show that the characteristic in many cases has a linear character. Based on this linear relationship the *closure phase angle*, that divides the *v-dv/dt*-plane into the first and second event may now be introduced as:

$$\phi_d = \left[\frac{D}{v_o^2}\left[\frac{dv}{dt}\right]_-\right] / \left[\frac{v_d}{v_o}\right] \qquad \text{(C.36)}$$

The first event is dominated by the system, while the second event is dominated by the check valve. The latter event is characterized by pressure surges induced by the check valve.

Although ϕ_d varies from valve type to valve type, in CVWP in first instance a fixed value is used. The prescribed trajectories are used in the region $\phi \leq 0.3$, which is illustrated in figure 12.2.

With the prescribed trajectories a compromise is found between robustness (numerical stability) and accuracy. The valve behaviour is stable and a valve closure is guaranteed.

C.4 Flow loops

In this section the phenomenon of flow loops is studied. This is done by means of virtual valve characteristics.

Consider the virtual tests in figure C.4. The time histories for the fluid velocity, pressure head difference and valve disc position in figure C.4.a are composed of third-order polynomials. The valve loss coefficient in this figure is derived from the other variables. The same data are plotted in figure C.4.b and C.4.c against the fluid velocity and pressure head difference, respectively. The virtual valve characteristics thus obtained are representative for the measured valve characteristics of approach 2 (section 14.7).

Now consider the simulation in figure C.4. The velocity-time history is assumed to be known. The other variables are obtained from linear interpolation within the virtual tests. Hereby the interpolation coefficients α and β are obtained from the trajectories in the *v-dv/dt*-plane.

Flow loops arise through the combination of a local minimum and local maximum in the velocity-time history (figure C.4.a). They are imposed by the system, not by the valve, and temporarily interrupt the valve opening or closure. Flow loops are formed across the horizontal axis of the *v-dv/dt*-plane (figure C.4.b), so that always more quadrants are involved. In theory a loop can be formed over four quadrants. In that case the vertical axis ($v = 0$) is passed without valve closure. However, this case is not considered further. Here only loops across two quadrants are considered. The loop across the quadrants 1 and 4 is introduced as *normal flow loop* ($v > 0$) and the loop across the quadrants 2 and 3 is introduced as *reverse flow loop* ($v < 0$).

In the following models for the normal and reverse flow loop are described.

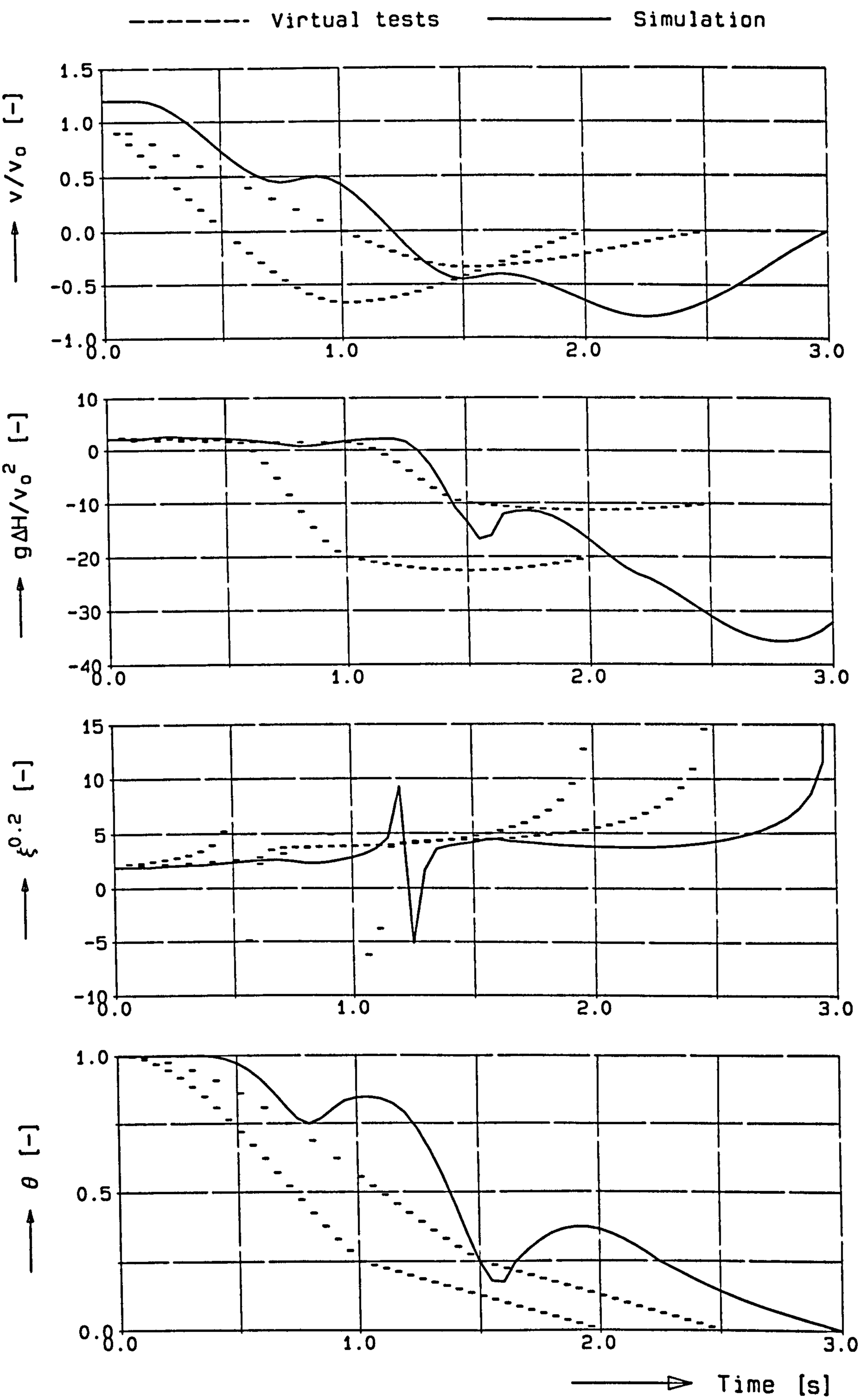

Figure C.4.a Interpolation in valve characteristics

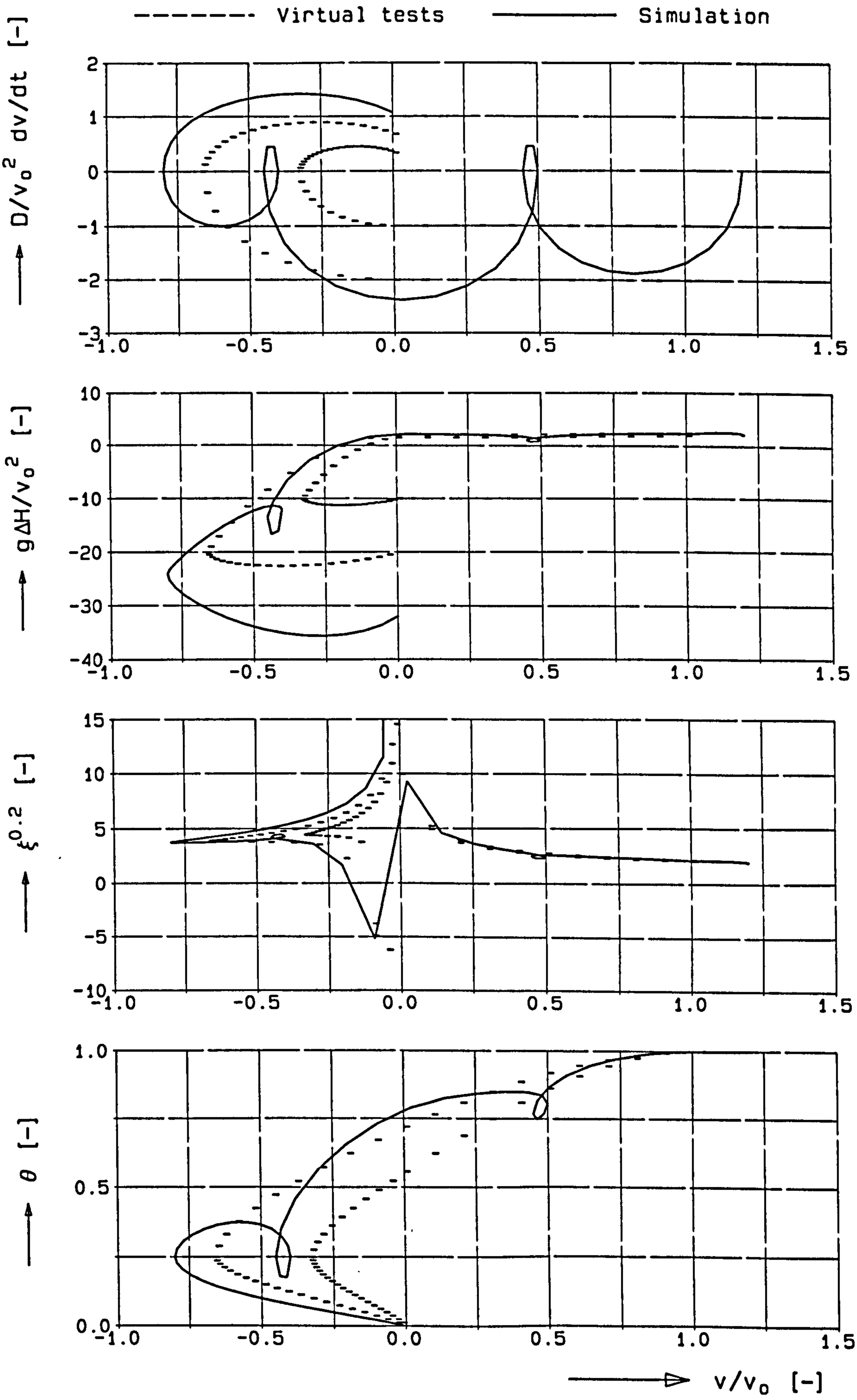

Figure C.4.b Interpolation in valve characteristics

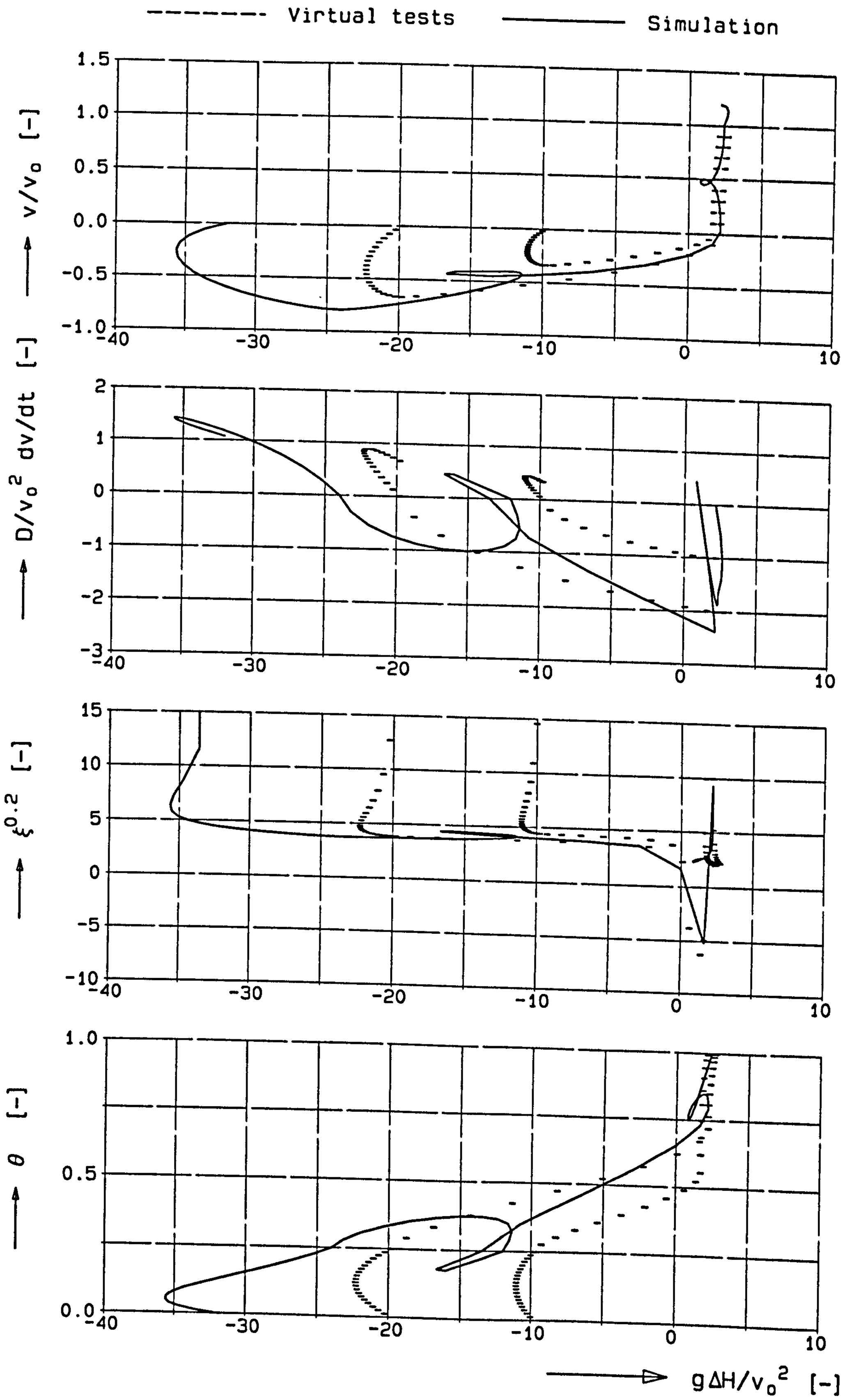

Figure C.4.c Interpolation in valve characteristics

C.4.1 Normal flow loop ($v > 0$)

If quadrant 1 is entered from quadrant 4, or vice versa, the valve opening or closure is interrupted by a normal flow loop (figure C.4.b).

In principle the valve closure may be modelled by the third implicit function, which is well conditioned in quadrant 4 and expected to be well conditioned in quadrant 1. However, if no opening characteristics are available in quadrant 1, another approach must be followed.

Experiments show that in quadrant 4 the pressure head difference is about equal to the steady flow values (even for higher flow decelerations). It is expected that this tendency also holds for quadrant 1, at least close to the v-axis. For this reason a substitute for the valve characteristics in quadrant 1 is the steady flow characteristic. This leads to the implicit function:

$$\frac{g\Delta H}{v_o^2}\left[\frac{v}{v_o}\,,\,\frac{D}{v_o^2}\frac{\partial v}{\partial t}=0\right] \quad \vee \quad \frac{g\Delta H}{v_o^2}(i+\alpha\,,j=1) \qquad \textbf{(C.37)}$$

The path number $j = 1$ represents steady flow values. In that sense it may be considered as a prescribed trajectory. The model error is expected to be small, since the pressure head difference in (the lower part of) quadrant 1 is relatively small.

C.4.2 Reverse flow loop ($v < 0$)

If quadrant 3 is entered from quadrant 2, or if quadrant 2 is *re*-entered from quadrant 3, the valve closure is interrupted by a reverse flow loop (figure C.4.b).

Consider the case that quadrant 3 is entered from quadrant 2. The standard interpolation in the valve characteristics gives a valve loss coefficient that temporarily decreases and a valve disc position that temporarily increases in time (figure C.4.a). This is physically incorrect since the increasing reverse flow velocity tends to close the valve and increase the (dynamic) valve loss coefficient.

The above inconsistency arises from the fact that it is assumed that the valve characteristic forms one single surface in the 3D physical space (section C.1.1). Thus it is suggested that this surface can be crossed in all directions, which is only true if the process is a reversible process. The latter no longer holds here. Consequently, the reverse flow loop cannot be described by this valve characteristic in the present form, unless additional information is added.

The valve closure may be modelled as:

$$\frac{g\Delta H}{v_o^2} = \frac{1}{2}\xi\frac{v}{v_o}\left|\frac{v}{v_o}\right| \qquad \text{(C.38)}$$

Where:

$$\xi = \xi_{Q2\rightarrow Q3} + \left[\frac{\partial\xi}{\partial t}\right]_{Q2\rightarrow Q3}\left(t - t_{Q2\rightarrow Q3}\right) \qquad \text{(C.39)}$$

The subscript Q2→Q3 refers to the instant that quadrant 3 is entered from quadrant 2. The procedure is based on the principle of *increasing valve loss coefficient*. This is physically correct since the increasing reverse flow velocity tends to accelerate the closure. The increase of the valve loss coefficient may even be stronger than above described. In that case higher order information is needed.

Consider the case that quadrant 2 is *re*-entered from quadrant 3. The valve is now further closed then if quadrant 2 is entered for the first time. The valve may be modelled by the principle of increasing valve loss coefficient, as described above. However in the last stage of closure the order of the valve coefficient changes rapidly. A better approach is:

$$\frac{g\Delta H}{v_o^2} = \frac{g\Delta H}{v_o^2}(i+\alpha, j+\beta) + C_{Q3\rightarrow Q2} \qquad \text{(C.40)}$$

The pressure head difference is no longer determined from the valve characteristics only. The effects of the reverse flow loop are taken into account by a constant. In order to guarantee a continuous transition from quadrant 3 to quadrant 2, the constant may be determined as:

$$C_{Q3\rightarrow Q2} = \frac{g\Delta H_{Q3\rightarrow Q2}}{v_o^2} - \frac{g\Delta H}{v_o^2}\left((i+\alpha)_{Q3\rightarrow Q2}, (j+\beta)_{Q3\rightarrow Q2}\right) \qquad \text{(C.41)}$$

Where $Q3 \rightarrow Q2$ represents the entrance values of quadrant 2. The first term may now e.g. be obtained from Equation (C.38). Note that the entrance values of the coordinates $i_o+\alpha_o$ and $j_o+\beta_o$ are no longer the same in the x-y-plane and x-z-plane. The interpolation in the x-y-plane appears to give a smooth transition, while the interpolation in the x-z-plane gives a kink in the pressure head-velocity relation.

C.5 Valve model

The final valve model is based on the valve characteristics of approach 2, as given in Equation (C.1). For the interpolation the valve characteristics are mapped from the physical to the computational domain, and described by discrete coordinates i (path along trajectory) and j (number of measured trajectory). The initial stage $i = 1$ represents per definition the fully opened valve ($v/v_o = 1$), while $i = M$ represents the closed valve ($v/v_o \uparrow 0$). The discrete coordinate $j = 1$ represents per definition the steady flow values ($dv/dt = 0$).

The characteristics are applied in the form of implicit functions. The properties of these functions vary strongly per quadrant. Therefore only functions can be used which are well conditioned. A scheme of these functions is given in table C.2.

Quadrant 4 The valve is in its initial stage of closure. The pressure head difference is described as function of the fluid velocity and velocity gradient.

Quadrant 3 See quadrant 4 and 2.

Quadrant 2 The valve is in its last stage of closure. The velocity gradient is described as function of the fluid velocity by means of prescribed trajectories. Hereby the coordinates j_o and β_o are constants, that are prefixed at the values at which the closure phase $\phi = 0.3$ is crossed.

Note: The prescribed trajectories may be used for interpolation and extrapolation. In the case of interpolation positive values are guaranteed (if the tests are consistent). However, extrapolation may lead to negative fluid velocity gradients (in the region of small velocities and velocity gradients), which interrupt the valve closure. Such an extrapolation is only allowed under certain conditions (see further section 12.3.2).

Quadrant 1 The opening behaviour is modelled by steady flow characteristics, since no opening characteristics are available, so that $j = 1$ here.

Note: The *normal flow loop* is included in the valve model in modified version, since no opening characteristics are available. The *reverse flow loop* is not included in the valve model, but suppressed by using prescribed trajectories.

	partly opened	fully opened
Quadrant 1	$\frac{g\Delta H}{v_o^2}(i+\alpha, j=1)$	$\frac{g\Delta H}{v_o^2} = \frac{1}{2}\xi_o \frac{v}{v_o}\left\lvert\frac{v}{v_o}\right\rvert$ $\xi_o = 2\,\frac{g\Delta H}{v_o^2}(i=1, j=1)$
Quadrant 2 and Quadrant 3 ($\phi \leq 0.3^*$)	$\frac{D}{v_o^2}\frac{dv}{dt}(i+\alpha, j_o+\beta_o)$	---
Quadrant 3 ($\phi > 0.3^*$)	$\frac{g\Delta H}{v_o^2}(i+\alpha, j+\beta)$	---
Quadrant 4	$\frac{g\Delta H}{v_o^2}(i+\alpha, j+\beta)$	$\frac{g\Delta H}{v_o^2} = \frac{1}{2}\xi_o \frac{v}{v_o}\left\lvert\frac{v}{v_o}\right\rvert$ $\xi_o = 2\,\frac{g\Delta H}{v_o^2}(i=1, j+\beta)$

Table C.2 Model for damped check valves in computational domain

* The closure phase is defined as:

$$\phi = \left[\frac{D}{v_o^2}\frac{dv}{dt}\right] / \left[\frac{v}{v_o}\right] \qquad \textbf{(C.50)}$$

Appendix D

Interpolation in valve and system parameters

In this appendix the interpolation procedure is described, which is performed within the valve and system parameters.

List of notations

- N is the total number of valve characteristics
- M is the number of parameters in a valve characteristic
- The vector $\left(x_1^n, x_2^n, \cdots, x_M^n\right)^T$ represents the M parameters of the n-th valve characteristic
- $\vec{r}^n$ is a compact notation for the vector $\left(x_1^n, x_2^n, \cdots, x_M^n\right)^T$
- ξ^n represents the loss coefficient for the n-th valve characteristic
- $f(\cdot)$ is a function $\mathbb{R}^M \rightarrow \mathbb{R}$ that describes the dependency of the loss coefficient on the parameters of the valve characteristic
- *superscripts* are used for the number n ($1 \leq n \leq N$) of a valve characteristic
- *subscripts* are used for the valve parameters
- $(\vec{\nabla} f)^n$ is the gradient of $f(\cdot)$ at $\vec{r}^n$, i.e.

$$(\vec{\nabla} f)^n = \left(\left.\frac{\partial f}{\partial x_1}\right|_{\vec{r}=\vec{r}^n}, \left.\frac{\partial f}{\partial x_2}\right|_{\vec{r}=\vec{r}^n}, \cdots, \left.\frac{\partial f}{\partial x_M}\right|_{\vec{r}=\vec{r}^n} \right)^T \qquad \text{(D.1)}$$

- $\| \vec{s} \|$ denotes the norm of vector $\vec{s}$
- ϵ^n is a random noise denoting the uncertainty in the loss coefficient ξ^n
- q^n is the standard deviation of the noise ϵ^n
- $E[\epsilon]$ is the expected value of ϵ based on a probability density function
- I is the unit diagonal matrix = diag [1, 1, ..., 1]

D.1 Introduction

In general terms the interpolation problem can be formulated as follows. Given are N valve characteristics. For each characteristic a valve loss coefficient or pressure head difference is available (hereafter the pressure head differences are omitted). The valve and system parameters and loss coefficients of these valve characteristics can be represented by a set:

$$\left\{ \left(x_1^n, x_2^n, \cdots, x_M^n; \xi^n\right) \,\middle|\, 1 \le n \le N \,,\; \xi^n = f(x_1^n, x_2^n, \cdots, x_M^n) \right\} \qquad \text{(D.2)}$$

Given a 'new' combination $\vec{r} := (x_1, x_2, \cdots, x_M)^T$ of the valve parameters, the available parameters and loss coefficients $(\vec{r}^n; \xi^n)$ $(1 \le n \le N)$ are used to estimate the loss coefficient $\xi = f(\vec{r})$.

With respect to the available number of valve characteristics three cases may be distinguished:

Case A. The number of valve characteristics is greater than the number of valve and system parameters, inclusive ξ, so that $N > M+1$.

Case B. The number of valve characteristics is equal to the number of valve and system parameters, including ξ, so that $N = M+1$.

Case C. The number of valve characteristics is smaller than the number of valve and system parameters, including ξ, so that $N < M+1$.

These three case will be considered below. The proposed interpolation technique is outlined in the following three paragraphs. Finally a summary of the procedure is given.

D.2 Normalisation of valve and system parameters

The parameters, represented by the components of the vector $\vec{r}$ have different orders of magnitude (e.g. the Reynolds number may vary from from 0 to 10^7, whereas the Mach number varies from 0 to 1). Therefore an appropriate scaling is applied to the x_m-coordinates before the interpolation is applied.

This scaling is as follows. Let the coordinate x_m $(1 \le m \le M)$ assume values between its extremes $-w_m$ and w_m. x_m is then scaled to x_m' according to:

$$x_m' = \frac{x_m}{w_m} \qquad \text{(D.3)}$$

In the following the primes in the coordinates x_m' will be omitted although it is worked with the scaled coordinates.

D.3 Interpolation

Hereafter the valve characteristic n will be represented as a point with coordinates $\left(x_1^n, x_2^n, \cdots, x_M^n, \xi^n\right)$ in a (M+1)-dimensional space.

Case A (N > M+1)

The number of points N is greater that the dimensions of the space M+1. The system is overdetermined and no unique solution exists for ξ. In principle enough information is available to apply a higher-order interpolation method. Another approach is to reduce the number of available valve characteristics to N= M+1 and apply a first order (linear) interpolation method (case B). The reduction of the valve characteristics may be based on the distance between $\vec{r}$ and $\vec{r}^n$.

Case B (N = M+1)

The number of points N is equal to the dimension of the space M+1. In that case a "plane" N-1 dimensional surface can be constructed through the N points $\left(\vec{r}^n; \xi^n\right)$. With $\vec{r}^n$ as 'origin', such a plane can be described by the linear function $f: \mathbb{R}^M \to \mathbb{R}$ defined by:

$$\xi = f(x_1, x_2, \cdots, x_M) = \xi^n + \sum_{m=1}^{M} s_m \cdot \left(x_m - x_m^n\right) \qquad \textbf{(D.4a)}$$

In short notation this may be written as:

$$f(\vec{r}) = \xi^n + \vec{s} \cdot (\vec{r} - \vec{r}^n) \qquad \textbf{(D.4b)}$$

Vector $\vec{s} := \left(s_1, s_2, s_3, \cdots, s_M\right)^T$ is a normal vector of the plane through the N points $\left(\vec{r}^n; \xi^n\right)$. In the next, expressions will be derived for $\vec{s}$. With this vector the loss coefficient ξ is then estimated by the right hand side of Eq.(D.4).

Obviously Eq.(D.4) gives $f(\vec{r}^n) = \xi^n$, but for any j ($1 \leq j \leq N$, $j \neq n$) it must hold that:

$$\xi^j = f(\vec{r}^j) = \xi^n + \vec{s} \cdot (\vec{r}^j - \vec{r}^n) \qquad \textbf{(D.5)}$$

This leads to the following linear equation for $\vec{s}$:

$$\xi^j - \xi^n = \sum_{m=1}^{M} \left(x_m^j - x_m^n \right) s_m \tag{D.6}$$

This approach can be followed for all data sets j with $j \neq n$ leading to a set of N-1 linear equations:

$$\begin{pmatrix} \xi^1 - \xi^n \\ \xi^2 - \xi^n \\ \vdots \\ \xi^{n-1} - \xi^n \\ \xi^{n+1} - \xi^n \\ \vdots \\ \xi^N - \xi^n \end{pmatrix} = \begin{pmatrix} x_1^1 - x_1^n & x_2^1 - x_2^n & x_3^1 - x_3^n & \cdots & x_M^1 - x_M^n \\ x_1^2 - x_1^n & x_2^2 - x_2^n & x_3^2 - x_3^n & \cdots & x_M^2 - x_M^n \\ \vdots & \vdots & \vdots & \cdots & \vdots \\ x_1^{n-1} - x_1^n & x_2^{n-1} - x_2^n & x_3^{n-1} - x_3^n & \cdots & x_M^{n-1} - x_M^n \\ x_1^{n+1} - x_1^n & x_2^{n+1} - x_2^n & x_3^{n+1} - x_3^n & \cdots & x_M^{n+1} - x_M^n \\ \vdots & \vdots & \vdots & \cdots & \vdots \\ x_1^N - x_1^n & x_2^N - x_2^n & x_3^N - x_3^n & \cdots & x_M^N - x_M^n \end{pmatrix} \begin{pmatrix} s_1 \\ s_2 \\ s_3 \\ s_4 \\ \vdots \\ \vdots \\ \vdots \\ s_{M-3} \\ s_{M-2} \\ s_{M-1} \\ s_M \end{pmatrix} \tag{D.7}$$

In compact form this can be written as:

$$H\vec{s} = \vec{z} \tag{D.8}$$

H is a matrix of dimension (N-1)×M and $\vec{z}$ is a vector of length N-1. As a result a unique solution for $\vec{s}$ only exists if N-1 = M (where it is assumed that the M-1 equations are not inconsistent or dependent).

Case C (N < M+1)

In most practical cases the number of points N will be much smaller than the dimension of the space M+1 (recall that N is the number of valve characteristics). In that case the Eqs. (D.7,8) form an underdetermined system that cannot be solved in a strict sense, since infinitely many solutions exist for $\vec{s}$. If additional constraints are applied, however, a unique solution can be found. A reasonable constraint that makes sense is to require that the function f(·) has minimal variation. Since

$$\vec{s} = (\vec{\nabla} f)^n = \left(\left.\frac{\partial f}{\partial x_1}\right|_{\vec{r}=\vec{r}^n}, \left.\frac{\partial f}{\partial x_2}\right|_{\vec{r}=\vec{r}^n}, \cdots, \left.\frac{\partial f}{\partial x_M}\right|_{\vec{r}=\vec{r}^n} \right)^T \tag{D.9}$$

this means that of all the admissable $\vec{s}$ the one with the minimal norm must be taken.

This leads to the minimization of a cost function J, defined by

$$J(\vec{s}) = \tfrac{1}{2}\|\vec{s}\|^2 = \vec{s}^T\vec{s} = \tfrac{1}{2}\sum_{m=1}^{M}(s_m)^2 \qquad \text{(D.10)}$$

under the restrictions of Eq. (D.8).

The solution of this problem is:

$$\vec{s} = H^T(HH^T)^{-1}\vec{z} \qquad \text{(D.11)}$$

For details on the solution procedure see e.g. Tarantola (1987) or Maybeck (1979).

Note It is easily seen that the expression found for $\vec{s}$ does not depend on the choice of the 'origin' $\vec{r}^n$. This means that the same plane will be found if instead of Eq.(4), f(·) is initialized by $f(\vec{r}) = \xi^k + \vec{s}\cdot(\vec{r} - \vec{r}^k)$ for some k, $k \neq n$ and $1 \leq k \leq N$.

Example The normal vector $\vec{s}$ is determined for the case that N=2 valve characteristics are available, $(\vec{r}^1, \xi^1)$ and $(\vec{r}^2, \xi^2)$. It is then easily seen that $\vec{z}$ is a scalar, $z=\xi^2-\xi^1$, H is the $1\times M$ matrix $(\vec{r}^2 - \vec{r}^1)^T$, and $HH^T = \|\vec{r}^2 - \vec{r}^1\|^2$. As a result:

$$\vec{s} = \frac{\xi^2 - \xi^1}{\|\vec{r}^2 - \vec{r}^1\|^2}(\vec{r}^2 - \vec{r}^1) \qquad \text{(D.12)}$$

D.4 Dependent systems, stochastic environment

The procedure of the preceding section requires that the N-1 vectors

$$\left\{\vec{r}^1 - \vec{r}^n\ ,\ \vec{r}^2 - \vec{r}^n\ ,\ \vec{r}^3 - \vec{r}^n\ ,\ \cdots,\ \vec{r}^{n-1} - \vec{r}^n\ ,\ \vec{r}^{n+1} - \vec{r}^n,\ \cdots,\ \vec{r}^N - \vec{r}^n\right\} \qquad \text{(D.13)}$$

are independent. In that case the square $(N-1)\times(N-1)$ matrix HH^T is not singular.

If the vectors are dependent two alternative approaches are feasible:

- Reduce the data set of Eq. (D.2) until N' samples are found (hereby $N' < N$, while N' is as large as possible) for which the corresponding vectors $\{\vec{r}^j - \vec{r}^n \mid 1 \leq j \leq N'\ ,\ j \neq n\}$ are independent. This approach may lead to loss

of information and should be avoided if possible.

- Generalize the present approach where the valve characteristics of Eq. (D.2) are embedded in a stochastic environment. The latter approach and its consequences for the solution of the vector $\vec{s}$ are summarized in the next.

In section D.3 the calculation of the normal vector $\vec{s}$ is considered for the non-degenerated case that the N-1 vectors of Eq. (D.13) are independent. If this is not the case the procedure must be generalized. This can be done by embedding the valve characteristics $\xi^n = f(\vec{r}^n)$ in a stochastic environment. This approach is not new and is quite commonly used in linear estimation theory. The technique, and the result for the estimate of the vector $\vec{s}$ are summarized below.

The basic idea is that the loss coefficient ξ^n is considered as a random variable. The n-th valve characteristic then has the form of a *stochastic linear equation*:

$$\xi^n = f(\vec{r}^n) + \epsilon^n \qquad \textbf{(D.14)}$$

In Eq.(D.14) ϵ^n is a random noise with zero mean and standard deviation q^n.

Embedding the original deterministic equations in a stochastic environment offers many advantages. Two of these are:

- With the addition of random terms it is possible to account for *measurement and model errors*. This is not of purely academic interest, since in practice usually no perfect models or perfect measurements are available.
- In the stochastic model the Eqs. (D.14) ($1 \le n \le N$) are not dependent or inconsistent as long as the random terms ϵ^n are not omitted (i.e. variance $Var[\epsilon^n] > 0$). This is even true if $N > M$, i.e. when there are more equations than unknown variables. For the original non-stochastic equation dependencies or inconsistencies may easily occur, especially for overdetermined systems.

The random noise ϵ^n in Eq. (D.14) denotes the (model) uncertainty in the loss coefficient. Its standard deviation is denoted by q^n. The standard deviation may be taken proportional to ξ^n: $q^n = \delta \cdot \xi^n$ (e.g. $\delta = 2\frac{1}{2}\%$). Moreover the ϵ^n ($1 \le n \le N$), are assumed to be mutually independent. As a result the covariance matrix of the random vector $\vec{\epsilon}$ is:

$$covar[\vec{\epsilon}] = \mathrm{E}[\vec{\epsilon}\,\vec{\epsilon}^T] = diag[(q^1)^2, (q^2)^2, \cdots, (q^N)^2] \qquad \textbf{(D.15)}$$

Because of the randomness of the ξ^n also the set of linear equations for the normal vector $\vec{s}$ are random, i.e. instead of Eq.(D.8) we must write:

$$H\vec{s} + \vec{e} = \vec{z} \tag{D.16}$$

The $\vec{e}$ in these measurement equations are random vectors of dimension (N-1)×1 with zero mean. From Eqs.(D.7,8,16) it is seen that the relation between $\vec{e}$ and $\vec{\epsilon}$ is as follows:

$$\begin{pmatrix} e^1 \\ e^2 \\ \cdot \\ \cdot \\ e^{n-1} \\ e^n \\ \cdot \\ \cdot \\ e^{N-1} \end{pmatrix} = \begin{pmatrix} \epsilon^1 - \epsilon^n \\ \epsilon^2 - \epsilon^n \\ \cdot \\ \cdot \\ \epsilon^{n-1} - \epsilon^n \\ \epsilon^{n+1} - \epsilon^n \\ \cdot \\ \cdot \\ \epsilon^N - \epsilon^n \end{pmatrix} \tag{D.17}$$

As a result of Eqs. (D.15,17) the covariance matrix Q of $\vec{e}$ is an (N-1)×(N-1) matrix and has the following form:

$$Q = diag\left[(q^1)^2 , (q^2)^2 , (q^3)^2 , \cdots , (q^{n-1})^2 , (q^{n+1})^2 , (q^{n+2})^2, \cdots , (q^N)^2 \right] + (q^n)^2 \cdot \begin{pmatrix} 1 & 1 & 1 & \cdot & \cdot & 1 \\ 1 & 1 & 1 & \cdot & \cdot & 1 \\ 1 & 1 & 1 & \cdot & \cdot & 1 \\ \cdot & \cdot & \cdot & \cdot & \cdot & \cdot \\ 1 & 1 & 1 & \cdot & \cdot & 1 \end{pmatrix} \tag{D.18}$$

In section D.3 it was argued that constraints must be introduced in order to obtain a unique solution for the vector $\vec{s}$. This was done in the form of a minimal norm as expressed by the cost function in Eq. (D.10). It is possible to translate this cost function to the stochastic model by means of the following stochastic linear equation that must be solved in combination with the measurement equations in Eq. (D.16):

$$\vec{s} + \vec{\epsilon}_0 = \vec{0} \tag{D.19}$$

The M×1 vector $\vec{\epsilon}_0$ is a random noise with zero mean and covariance matrix $\mathbf{I}$.

The N-1 stochastic equations of Eq. (D.16) and the M stochastic equations of Eq. (D.19) can be solved in maximum-likelihood sense. The solution $\vec{s}$ minimizes the cost function

$$J = \tfrac{1}{2}\,\vec{s}^{\,T}\vec{s} + \tfrac{1}{2}\,(H\vec{s} - \vec{z})^{T} Q^{-1} (H\vec{s} - \vec{z}) \qquad \textbf{(D.20)}$$

with the following result:

$$\vec{s} = H^{T}(HH^{T} + Q)^{-1}\vec{z} \qquad \textbf{(D.21)}$$

Comparison of Eq. (D.11) and Eq. (D.21) clearly shows the relation of the solutions of this section and the one of section D.3: if Q=0 (i.e. no uncertainty in the loss coefficients), the solution in the stochastic model reduces to the solution in the original deterministic approach, as expected.

The main advantage of Eq. (D.21) is that the matrix $HH^{T} + Q$ is non-singular for any positive definite covariance matrix Q, even if matrix H is singular. Therefore the solution of Eq.(D.21) is preferred for computer implementation.

Summary

The interpolation technique described above can be summarized as follows.

Step 1 : The valve and system parameters x_m ($1 \le m \le M$) are scaled according to Eq. (D.3).

Step 2 : The normal vector $\vec{s}$ is determined on the basis of N known valve characteristics. This vector is prescribed by Eq.(D.11) or Eq.(D.21). The matrix H in these expressions is defined in Eq. (D.7) and (D.8), and the covariance matrix Q is given in Eq. (D.18).

Step 3 : For the combination $\vec{r} := (x_1, x_2, \cdots, x_M)^{T}$ of valve and system parameters, the loss coefficient ξ is determined from Eq. (D.4).

References

Maybeck, P.S., 1979: *Stochastic Models, Estimation and Control*, Vol 1, Academic Press, Orlando, Florida.

Tarantola, A., 1987: *Inverse problem theory, Methods for data fitting and model parameter estimation*, Elsevier, Amsterdam.